Spring 5-23-2019

Proposed New Military Live Load for Highway Bridges in the United States

Walter P. Parker
University of New Orleans, wpparker@uno.edu

Proposed New Military Live Load for Highway Bridges in the United States

A Thesis

Submitted to the Graduate Faculty of the
University of New Orleans
in partial fulfillment of the
requirements for the degree of

Master of Science
in
Engineering
Civil Engineering

by

Walter P. Parker, P.E.

B.S. Clemson University, 1987
M.S. Missouri University of Science and Technology, 2000
Graduate Certificate University of New Orleans, 2017

May, 2019

ACKNOWLEDGMENTS

I would like to express my gratitude to Professors Dr. Norma Jean Mattei, Dr. Malay Ghose Hajra and Dr. Engin Egeseli of my thesis committee. I would also like to thank the following professors: Dr. Alex McCorquodale, Dr. Donald Barbe, Dr. Mysore Nataraj and Dr. Mike Folse. They provided outstanding instruction in their areas of expertise in civil engineering, and provided me with a breadth of understanding of the totality of civil engineering theory and practice.

I am deeply grateful to my wife, daughter and our extended family, for their support and encouragement during my studies in pursuit of this degree.

This thesis is dedicated to my wife Liz and daughter Celia.

TABLE OF CONTENTS

LIST OF FIGURES

LIST OF TABLES

ABSTRACT

This thesis presents the results of a mathematical analysis of various live load combinations on highway bridge spans up to 304.8 meters (1,000 feet) total lengths. The analysis included continuous beams, but only the results for simple beams is presented. The analysis was performed using an independently developed Microsoft EXCEL spreadsheet computation, based on superposition and classical mechanics.

In this thesis, several actual bridge live loadings and several hypothetical live loadings were analyzed and compared to the American Association of State Highway and Transportation Officials Load and Resistance Factor Design method. Also considered was the new bridge design method adopted by the Louisiana Department of Transportation in March 2015. The evolution of bridge design loads is discussed, and the concept of the Military Load Classification is introduced and adapted to the bridge design analysis. The results of the analysis are presented, compared and interpreted for use in future bridge design.

Keywords: National System of Interstate and Defense Highways; Military Load Classification; Alternate Military Loading; Load and Resistance Factor Design; Reliability; Magnification Factors

CHAPTER 1: INTRODUCTION

1.1 SCOPE OF THESIS

This thesis presents the results of a live load analysis for moderate to long span bridge structures using computational methods. Bridge structures were analyzed as both simple beams and multiple span continuous beams with total span lengths of 0-1,000 feet (0-304.8 meters). Only the results from the simple beam analysis are presented for brevity.

Initially, two special loading cases were to be analyzed as possible American Association of State Highway and Transportation Officials (AASHTO) Load and Resistance Factor Design (LRFD) Strength II limit states for specifically designated "critical" bridge structures in the State of Louisiana and elsewhere in the United States of America.

The first special case was to be an assumed "contraflow" forced flow condition ("traffic jam") simulating road conditions during a mandatory hurricane evacuation in the Gulf South region. In this case, all lanes were assumed to be filled with traffic headed in one direction, with laws being enforced to restrict commercial truck traffic to right hand lane and passenger vehicle traffic to left hand lane only. A review of literature revealed that this condition has already been modeled and analyzed by previous researchers.

The second special case was to be a special case where the bridge is assumed to be restricted to one lane, and this lane subjected to a modern-day logistical convoy[1] of military heavy equipment transporters (HET's), each loaded with one main battle tank weighing approximately 140 kips (622.7 kN), as represented by a North Atlantic Treaty Organization (NATO) Standard Agreement (STANAG) Hypothetical Military Load Classification (MLC) 100 wheeled (100W) vehicles.[2] The assumed logistical convoy vehicle spacing is approximately 300

ft (91.4 m) between vehicles, all moving at 55-62.1 miles per hour (mph), or 88.5-100 kilometers per hour (kph) based on current practice in observed logistic operations. This limit state is based on a possible, however unlikely, scenario where the United States military would have to use the highway system for surface movement of heavy combat forces inside the continental United States, in conjunction with or independent of the existing railway transportation system.

Based on the author's experience during overseas logistical and combat operations, the first special case was replaced with contracted civilian logistical convoy in a forced flow condition (stopped on the span), occupying one traffic lane and shoulder, while a logistical convoy of military heavy equipment transporters (HET's) described in the above case uses the other travel lane for movement across the span at specified speed and gap distance. This combined civilian logistical convoy and HET convoy is only analyzed for single span of relatively short length, neglecting the possibility of more than one HET on the span.

Results of analysis are to be plotted as shear and moment bias graphs both based on calculated values, and when normalized to the AASHTO (2007) against Strength I HL-93 limit state. Based on results of analysis, a final recommendation will be made regarding whether changes to the national design guidelines are needed and recommended new design guidance will be presented as appropriate.

1.2 REVIEW OF EXISTING LITERATURE

A review of available literature was conducted to assess whether any studies similar in scope have been conducted by other researchers. One study was found that addressed the first case for assumed "contraflow" forced flow condition[3] and will be discussed further and used with some modification for this study. The primary source material from this study was

reviewed and incorporated into the modeling design and conduct of the analyses of this thesis.[4] Another study addressed the live load of NATO Wheeled Military Trucks on steel bridges; however, it did not include the heavy equipment transport (HET) system analyzed in this thesis.[5] Several other studies addressed the proof testing of actual bridges using loaded military heavy equipment transporters (HET) to validate specific state special permit loads.[6] Another study addressed using analytical methods to determine the impact of increased heavy trucks on the existing highway bridge inventory.[7] The conclusions of the different studies was contradictory and validated the need for the current analysis. Numerous studies addressed various special permit vehicles and the implications of those vehicles on the design of new bridges and the rating and performance of existing bridges.[8] Several of these permit vehicles were incorporated into this study and the rationale for the inclusion of some and not of other permit vehicles will be discussed. Other reviewed literature dealt with the adoption of the AASHTO HL-93 live load and justification for its use to model contemporary live loading on highway bridges.[9] Subsequent to the adoption of the AASHTO HL-93 live load, several reviewed articles focused on calibrating the design code using weight in motion (WIM) and video traffic data collected in previous decades.[10] Other reviewed literature compared the AASHTO HL-93 live load to other design codes that appear to be based on military utility in use in other countries.[11] Finally, the application of the theory of structural reliability to bridge design and the AASHTO HL-93 live load was researched and used to provide the basis of final analysis used in this thesis.[12]

1.3 ORGANIZATION OF DISSERTATION

Chapter 1 of this thesis presents the problem statement, objectives and the scope of the study. This chapter also includes a review of existing literature related to the scope of the thesis.

Chapter 2 discusses the historical development of the ground transportation roads in North America, the genesis and initial development of the Interstate Highway System and the historical evolution of highway bridge design live loads in the United States. This chapter also 3 presents the American Association of State Highway and Transportation Officials (AASHTO) Load and Resistance Factor Design (LRFD) specifications for bridge design, the Louisiana Department of Transportation (LA DOTD) Bridge Design using the Louisiana Special Design Vehicle 2011 (LSDV-11), and various other design codes and special permit vehicles in use across North America.

Chapter 3 describes the concept of the Military Load Classification (MLC) as specified in the North Atlantic Treaty Organization (NATO) Standardization Agreement (STANAG) 2021, with emphasis on the MLC hypothetical tracked and wheeled vehicles and the relationship of these vehicles to the AASHTO HL-93 live loading.

Chapter 4 presents the analysis methodology developed for this thesis and its application to single span simple beams.

Chapter 5 presents the results of the primary analyses and discusses the significant findings for single span simple beams and two equal span continuous beams under various loads.

Chapter 6 presents the reliability procedure used for current bridge design calibration and adapts the results of a previous reliability calibration of an inventory of existing bridges using the results of the completed analysis presented in Chapter 6.

Chapter 7 presents the conclusions drawn from the complete analysis and discusses several recommendations for changes to bridge design methodologies and follow-on research.

Throughout the analyses, the primary calculations were conducted in customary US units commonly used in American (USA) bridge design (feet, kips, etc.), not the internationally

preferred SI units (meters, kilonewtons, etc.) used in Europe and Canada.[13] All values provided in US units in the text and tables are also provided in SI units in parentheses. Derived equations are also provided in SI unit format. Graphical representations of models and analyses results are in customary US units only, and do not include corresponding values in SI units.

1.4 CHAPTER ONE END NOTES

1. See Cotter, D.G. (2003), "The Iron Horse Express"; Dunstan, S.P. (2013), "Examining Decisive Action Sustainment Operations at the Task Force Level"; Keith, T.C. (1998), "Lift Missions in Bosnia"; Kennedy, E. (2000), "Forging An Alliance: Army Transporters in Europe"; and Russell, B.R. and Thrall, A.P. (2013), "Portable and Rapidly Deployable Bridges: Historical Perspective and Recent Technology Developments".

2. See the North Atlantic Treaty Organization (NATO) Standardization Agency (2002), Standardization Agreement (STANAG) 2021, 6th Ed. and U.S. Department of the Army (2002), Military Non-Standard Fixed Bridging (FM 3-34.343).

3. Lutomirska, M. (2009), "Live Load Models for Long Span Bridges". See also Nowak, A.S., Lutomirska, M. and Sheikh Ibrahim, F.I. (2010), "The Development of Live Load for Long Span Bridges" and Nowak, A.S., Kozikowski, M. and Lutomirska, M. (2010), "Risk Mitigation for Highway and Railway Bridges".

4. See ASCE Committee on Loads and Forces on Bridges (1981), "Recommended Design Loads for Bridges"; Buckland, P.G., (1991), "North American and British Long-Span Bridge Loads"; Buckland, P.G., Navin, F.P.D, Zidek, J.V., and McBryde, J.P, (1978), "Traffic loading of long-span bridges"; and Buckland, P.G., Navin, F.P.D, Zidek, J.V., and McBryde, J.P., (1980), "Proposed Vehicle Loading of Long-Span Bridges".

5. Kim, Y.J., Tanovic, R., and Wight, R.G. (2010), "Load Configuration and Lateral Distribution of NATO Wheeled Military Trucks for Steel I-Girder Bridges".

6. See Saraf, V., Sokolik, A.F. and Nowal, A.S. (1996), "Proof Load Testing of Highway Bridges"; Turer, A. and Aktan, A.E. (1999), "Issues in Superload Crossing of Three Steel Stringer Bridges in Toledo, Ohio"; and Nowak, A. S., Eom, J. and Sanli, A. (2000), "Control of Live Load on Bridges".

7. Weissman, J. and Harrison, R. (1998), "Impact of 44 000-kg (97,000-lb) Six-Axle Semitrailer Trucks on Bridges on Rural and Urban U.S. Interstate System".

8. See Sivakumar, B., Moses, F., Fu, G. and Ghosn, M. (2007), "Legal Truck Loads and AASHTO Legal Loads for Posting"; and Zhao, J. and Tabatabai, H. (2012), "Evaluation of a Permit Vehicle Model Using Weigh-in-Motion Truck Records".

9. See Ghosn, M., Sivakumar, B., and Miao, F. (2013), "Development of State-Specific Load and Resistance Factor Rating Method"; Moses, F. and Ghosn, M. (1987), "Discussion Proposed New Truck Weight Limit Formula"; Nowak, A.S. (1993), "Live Load Model for Highway Bridges"; Nowak, A.S. (1994), "Load Model for Bridge Design Code"; Nowak, A.S. and Hong, Y-K. (1991), "Bridge Live Load Models"; and Tobias, D.H. (2011), "Perspectives on AASHTO Load and Resistance Factor Design".

10. See Kwon, O., Kim, E. and Orton, S. (2011), "Calibration of Live-Load Factor in LRFD Bridge Design Specifications Based on State-Specific Traffic Environments"; Nowak, A.S. (1999), "Calibration of LRFD bridge design code"; and Verma, D. and Moses, F. (1989), "Calibration of Bridge-Strength Evaluation Code".

11. See Agrawal, A., Sreyashrao S, and Dawair, B.M. (2011), "Simplification for train loading on bridges" and Shreedhar, R. and Mamadapur, S. (2012), "Analysis of T-beam Bridge Using Finite Element Method".

12. See Chapter Six End Notes.

13. See McCormac, J. and Elling, R.E., (1998), *Structural Analysis A Classical and Matrix Approach*; Nawy, E.G., (2010), *Prestressed Concrete A Fundamental Approach (5th Edition)*; Tonias, D.E. and Zhao, J.J. (2007), *Bridge Engineering (2nd Edition*); and Wright, P.H. and Dixon, K.K., (2004), *Highway Engineering (7th Edition)*.

CHAPTER 2: DICUSSION OF CURRENT BRIDGE DESIGN

2.1 INTRODUCTION

The development of the bridge design procedures and anticipated loads that needed to be safely carried by these structures begin in earnest with the introduction of modern building materials (steel and reinforced concrete) and have continued to the present day. The focus of this thesis is on the bridges of the national interstate highway system created with the passage of the Federal-Aid Highway Act of 1956. The development of the Interstate Highway System was a turning point in the evolution of the nation's surface transportation network. It has resulted in impressive economic growth across the country. Originally called the "National System of Interstate and Defense Highways", the system was named the "Dwight D. Eisenhower System of Interstate and Defense Highways" in acknowledgement of the 34th President's key role in supporting the realization of the road network.[1] Several key factors led to President Eisenhower's keen interest in seeing the interstate highway system created and in the historical development of the live loads used for design of bridges and roads in this system. These issues will be identified and discussed in this chapter.

Also discussed in this chapter is the current bridge design specification in use, which is the American Association of State Highway and Transportation Officials (AASHTO) Load and Resistance Factor Design (LRFD) specification adopted in 1993. The first edition of these specifications was published in 1994, and the current edition is the seventh of 2014. The AASHTO LRFD specifications originated from the determination amongst the members of the AASHTO Subcommittee on Bridges and Structures to develop a more comprehensive specification based on the latest knowledge and research findings in the bridge engineering discipline with a corresponding elimination of gaps and inconsistencies in the Standard

Specifications. The LRFD specification was adopted by AASHTO as an alternative to the AASHTO Standard Specification for Highway Bridges, which allows the use of either the Allowable Stress Design (ASD) or the Load Factor Design (LFD) methodologies. An important goal of the new specification was to achieve a more uniform margin of safety and reliability across a wide range and variety of structures and material construction. During the development of the standard specifications in the LRFD format the variability of the behavior of structural elements was taken into account through the application of statistical methods. The State of Louisiana has further simplified bridge design for highways in the state by adopting the use of magnification factors to account for permitted special vehicles in use within the state.

2.2 DEVELOPMENT OF THE INTERSTATE HIGHWAY SYSTEM

Road networks have traditionally developed to support the economic and military needs of nations and states willing and able to make sufficient investment into their construction. Early examples were the ancient Assyrian and Rome empires, whose road networks supported the rapid movement of military forces throughout each empire, but also allowed the convenient movement and increased communication of people, goods, and products as well.[2] Since the United States is strategically isolated by physical geography due to vast oceans on its east and west borders, it faced internal large scale warfare only once, over the course of the first 200 years of its existence. The development of the national surface transportation network was driven almost exclusively by economic interests.

The earliest roads were often little more than woodland trails and wagon ruts supporting the movement of mounted horses and wagons through the forests, swamps, and prairies of the North American continent. Well-constructed and maintained roads were most likely to be found

in urban areas, and often were built by private commercial interests to support a particular industry.[3] The movement of agricultural produce, raw material, and manufactured goods was accomplished via either coastal or oceanic ship transport or internally along the relatively vast network of waterways and rivers. The first roads linking urban centers were various toll roads, or "turnpikes" created in the northeastern section of the nation such as the Philadelphia and Lancaster Turnpike in Pennsylvania. The toll roads were profit making service enterprises for their builders and owners, and competed directly with surface water transportation, without support from federal government. By the 1830's, the development of steam railroad locomotives began to dominate American surface transportation of goods and services. Interest and investment in road building as lines of communications between population centers diminished significantly. By time the transcontinental railroad network was completed after the American Civil War, interstate road construction was virtually nonexistent.

Fifty years after the first transcontinental railroad was completed, the young officer, Dwight D. Eisenhower, volunteered to participate in the U. S. Army Motor Transport Corps' Coast-to-Coast Motor Transport Train, a truck and automobile convoy commandeered by Lieutenant Colonel Charles W. McClure.[4] The convoy took place during the summer of 1919, beginning in Washington, D.C. and ending in San Francisco, California. Road construction and serviceability rapidly deteriorated as the convoy moved west, and away from the urbanized northeast. Once in the plains of the American Midwest and continuing through the desert west, the existing road network was woefully inadequate for the movement of the modest number of vehicles of the convoy. Eisenhower's experiences on this road march made a lasting impression that would be sharpened during combat operations in Europe during World War II.

During the interwar years, Germany began construction of a network of paved, high speed roads known as the Reischautobahn.[5] Although the numbers of privately owned vehicles in Germany during this period was significantly less than the number of vehicles in America, the German government embarked on this construction for both strategic reasons and to increase German workforce participation during the on-going global economic depression. Unlike the interstate system that would be constructed several decades later in America, the Reischautobahn network was primary built away from urban centers, and as such, survived the Allied bombing of German population centers during the war. Ironically, the arguably greater strategic use of the autobahn network was to facilitate the rapid advance of western Allied ground forces into Germany, routing the last remaining resistance as the Soviet Red army advanced from the east. The Supreme Allied Commander in charge of these operations was General Dwight D. Eisenhower. Following the German unconditional surrender and occupation of the country by Allied forces, Eisenhower took special interest in the survey, inspection, and detailed study of the autobahn network. Later in life, Eisenhower would explain that "after seeing the autobahns of modern Germany and knowing the asset those highways were to the Germans, I decided, as President, to put an emphasis on this kind of road building. ... The old (1919) convoy had started me thinking about good, two-lane highways, but Germany had made me see the wisdom of broader ribbons across the land."[6]

During the Depression, the administration of Franklin D. Roosevelt had proposed the creation of a national federal road construction program as part of the New Deal. Occurring after the successful implementation of earlier work programs, this proposal was not implemented.[7] During World War II, American industrial output and movement to ports of embarkation for deployment overseas demonstrated the need for a national highway system (NHS). The national

highway system was critical for the movement of war material; however, one of the major stumbling blocks was the lack of a uniform design criterion, which had been left up to the individual states prior to the war.[8] In response, the U.S. Congress passed the Federal-Aid Highway Act of 1944 which called for a national standard for highway design criteria but did not extend the states' mandate of building and maintaining the national highway system. Roosevelt's successor, Harry Truman, was also unable to implement polices or programs to dramatically improve America's road network. Although the Truman administration was able to achieve the passage of the Federal-Aid Highway Act of 1952, it would not be until Eisenhower was elected that America would embark on a road building program to rival the German autobahn.[9]

In a speech before the Governor's Conference in July 1954, Vice President Richard Nixon on behalf of President Eisenhower, asked the assembled state officials to assist the Federal government in developing an overarching plan for upgrading the nation's highways. The vice president listed the problems that the administration believed needed to be solved by this upgrade of the national infrastructure: safety, congestion, economy, and defense. The stated goal of the defensive aspect was to meet "the appalling inadequacies" in the case of natural catastrophe or war.[10]

One significant task was the establishment of road design standards, including both bridge and pavement designs. This requirement had been anticipated by the American Association State Highway Officials (AASHO) who had earlier devised a large scale road test and test site in Ottawa, Illinois.[11] This test subsequently became known as the Ottawa Road Test (ORT). The environmental conditions along with the geological subgrade were typical and representative of much of the nation. Multiple agencies both public and private, funded the road

test and participated in its conduct. The test track consisted of six loops, each two miles long, totaling 14 miles (22.5 km) of travel lanes. Various pavement designs were incorporated into the test loops, each varying either material, thicknesses, or both. The test track also included 16 test bridges. Loop 1 carried no traffic and served as the control segment. The other 5 loops each carried different types of traffic, from light truck with 2 kips (8.9 kN) single axle loads, up to heavy trucks with 48 kips (213.5 kN) tandem axle loads.[12] It should be noted that the truck fleet was provided by the U.S. Army's Transportation Corps,[13] the significance of which will be discussed later. Testing began in October 1958, with vehicles operating 18 hours per day. Eventually, the schedule was expanded and the vehicle traffic was increased in order to meet the specified goal of subjecting every design and test feature to one million axle loads in the allotted two year period. The test ended in November 1960 and has not been duplicated in terms of scale and effort again. Refinement of design codes since the ORT have relied new technologies, including weigh-in-motion (WIM) data collection and numerical modeling and analysis.

2.3 DEVELOPMENT OF HIGHWAY BRIDGE DESIGN LOADS

As with roads in general in the early United States, well-constructed and maintained bridges tended to be found in urban areas, and tended to only span modest gaps. The theory and practice of both material science and classical mechanics were still being developed by the great physicists of the era, and bridge construction followed the best practices passed down from master masons and carpenters to their successors in the skilled trades. For wide wet gap crossings of streams and rivers, the surface transport of that era relied on ferry and raft crossings. Outside of the skilled trades of masonry and carpentry, the other public officials skilled and experienced in large construction efforts were military engineers. Practical requirements of

military engineering included road construction, river crossings, and the construction of stone, concrete, and earthen fortifications. Also, the centers of higher education that focused on the sciences related to nascent road and bridge construction were the military academies or military style agricultural and mechanical colleges. As with the surface road network, the development of the railroad and the subsequent development and use of steel in construction pioneered the development of structural analysis and the expansion of the classical physics and material sciences to practical application.

The first major organization in the US to consider live loads for design of new bridges was the railroad industry. Railway bridge engineers initially designed bridges to control allowable deflection, in order to ensure safe operation of the locomotives. In this case, serviceability was of primary importance and strength secondary. Therefore, structures were over-designed by today's standards. As the fabrication and production of construction materials improved, and competition for steel grew as it was adapted to construction, strength as well as serviceability began to control the design allowing the amount and cost of construction materials to be reduced.

Based on available historical material, the first commonly used highway bridge live loading design guides were presented by John Alexander Low Waddell in 1884.[14] Dr. Waddell was an early advocate of the professional licensure of civil engineering practice, and the creation and legal empowerment of state and local bridge engineers and inspectors to protect the life and safety of the public. As an accomplished civil engineer and railroad bridge engineer, the highway bridge live load design specifications proposed by Dr. Waddell grew out of his experience in designing both railroad bridges and dual use railroad and highway traffic bridges. In Dr. Waddell specifications, highway bridges were divided into three classes: Class A, which

included those for cities and their suburbs subjected to the continued application of heavy loads; Class B, which included those for cities and their suburbs, or manufacturing districts, that were subjected to the occasional application of heavy loads; and Class C, which included those country roads, where the traffic is lighter." The live load specifications for bridges of the different classes were provided in the following table.

SPAN IN FEET.	MOVING LOAD PER SQUARE FOOT OF FLOOR.	
	Classes A and B.	Class C.
0 to 50	100 pounds	80 pounds
50 to 150	90 pounds	80 pounds
150 to 200	80 pounds	70 pounds
200 to 300	70 pounds	60 pounds
300 to 400	60 pounds	50 pounds

Figure 2-1: Waddell's Highway Bridge Design Specifications (1884)[15]

As can be seen, the live load is expected to decrease with span length. These specifications also illustrate the bias towards an urban concentration of industry and heavier bridge loadings, typical of the early urbanization and industrialization of America in the late 19th and early 20th centuries. Dr. Waddell's design specifications were focused on truss bridges, which were the state of the art of longer spans at that time. The recommended bridge design specifications set allowable working stresses for different truss members, also based on the Class A, B, and C categories. Allowable design working stresses were lowest for Class A and higher for both Class B and C. This difference in specified working stresses added an increase in the factor of safety of Class A urban bridges which was additive to the higher specified live loads recommended for these bridges as earlier descirbed. Dr. Waddell further refined his bridge

design specifications in subsequent publications, with increasing emphasis placed on the use of engineering judgment to ensure the most economical cost of construction using material available in the early 1920's.[16]

The first professional society in the United States to propose a standard bridge design specification was the American Association of State Highways Officials (AASHO). The earliest known provision was published in 1925 without an edition number.[17] This edition specified three different truck live loads (H20, H15, and H10), where the "H" indicated highway loading and the following number indicated the live load in short tons. Also, five classes of bridges were specified, AA, A, B, C, and D, and loads were assigned to each of these bridge type.

One year earlier, the American Society of Civil Engineers (ASCE) had convened a Special Committee on Specifications for Bridge Design and Construction, bringing together a joint group of highway and railroad bridges designers.[18] The final report of this committee was presented at the spring meeting of ASCE on April 9, 1924, and subsequently published in the 1924 transactions of the ASCE publication.

The first official edition of the AASHO Standard Specification for Highway Design was published in 1931, and was based in part on the ASCE 1924 committee report and represented a refinement of the 1925 specification, based on the results of the ASCE conference. The second edition published in 1935 continued the use of "H" truck live loads, and reduced the classes of highway bridges to three: AA, A, and B.[19] In a refinement of previous provisions, the live load was specified as either a truck train of the appropriate design type, or an applied uniform lane load of 0.60 kip/ft with a concentrated load of 28 kips acting at the critical location on the span. If using the truck train live load, the assumed loading was one truck live load centered between

additional vehicles over the remainder of the span, with an applied factor of 0.75 to all except the center truck axle loads.

A third and fourth edition were published in 1941 and 1944 respectively[20]. In the 1941 edition, the "H-S" loading was introduced to address the semi-trailer truck configurations. The heaviest of the new design vehicles was the H20-S16. The first number designated the weight of the tractor in tons and the second number designated the weight of the trailer also in tons. For the design load, a uniform load of 0.64 kips per foot (9.3 kN/m) was maintained, however the concentrated loads were either 32 kips (142.3 kN) for moment and 40 kips (177.9 kN) for shear. This loading represented a H20-S16 tractor-trailer combination surrounded by H15 trucks evenly spaced. In the 1944 edition, the "H-S" loads were changed to the "Hxx-Szz-44" with 44 designating the year of this edition publication. In this edition the H20-S16 truck was now specified to have 14-30 ft (4.3-9.1 m) spacing between the middle and rear axles to account for the new, longer semi-trailers then being introduced. Therefore, this edition is the origin of the HS20-44 truck still in use today. For this specification the design moments were specified to be the larger of either a single HS20-44 truck with minimum axle spacing or the previously specified uniform lane load of 0.64 kips/ft (9.3 kN/m). The HS20-44 vehicle was not intended to model a specified tractor-trailer combination, but it does adequately represent the group of vehicles later known as the AASHTO 36 kips (160.1 kN) "3S2" rating vehicle, corresponding to the interstate commercial tractor-trailer, the "18 wheeler", in common use.

The AASHO sixth edition was published in 1953, three years prior to the start of the Interstate Highway era.[21] With the passage of the Federal-Aid Highway Act in 1956, the United States Congress also passed legislation specifying the maximum axle load, gross vehicle weight, and width limits for trucks that would be operating on the new Interstate highway system. These

limits were based on recommendations provided in 1946 by AASHO, including 18 kips (80.1 kN) on a single axle, 32 kips (142.3 kN) on a tandem axle, and 73.28 kips (326 kN) gross weight. This legislation allowed states to permit the operation of heavier trucks on the Interstate highways, provided such operation was legal on these states' road networks prior to July 1, 1956. This "grandfather right" prevented a rollback of legal vehicle weights in such states, while using the AASHO standard as the upper limit on weights otherwise allowable.

In 1973, AASHO re-named itself the American Association of State Highway and Transportation Officials (AASHTO). In the 1976 Interim AASHTO Standard Specifications, a new Alternate Military Loading (AML) was added.[22] This consisted of two 24 kip (106.8 kN) axles spaced 4 ft (1.22 m) apart, totaling 48 kips (213.5 kN), becoming known as the "design tandem". The author of this paper theorizes that this loading was added to the design specifications upon reconsideration of the maximum weight vehicles described earlier as taking part in the Ottawa Road Test (ORT).[23] At that time, it is probable that the heaviest vehicle used in the ORT was the U.S. Army's M25 Tank Transporter Truck-Trailer. In use since late in the Second World War, this tractor-trailer combination was capable of a maximum trailer pay load of 40 tons (80 kips; 355.8 kN), with a maximum fifth wheel load of 55 kips (244.6 kN).[24] The second and third axles of the tractor were approximately 4 ft (1.2 m) apart, with the fifth wheel centered between them (corresponding to the king pin of the trailer unit). Therefore, each axle would effectively carry 27.5 kips (122.3 kN) on the four wheels of each axle. It is theorized that the heavy trucks used for the ORT were loaded to less than maximum in order to minimize breakdown and maintenance for vehicles participating in the test. It is considered likely that the AML was added both to account for military use of the Interstate highway system and to

conform the bridge design to the AASHO pavement design specifications which were also developed from the ORT vehicle data.[25]

Throughout the late 1970s and early 1980s, many states observed an increase in both volume and weight of truck traffic compared to earlier decades. In response, many adopted the so-called "HS25" load, which consisted of a 90 kips (400.3 kN) truck with the same axle spacing and weight proportions as the HS20-44 truck and an increase of 25% for the lane loading resulting in 0.8 kips/ft (11.7 kN/m). The adoption and use of the increased HS25 load was often a result of the state's adoption of the load factor design methodology. The increased design load was a means of maintaining a reserve of strength capacity similar to the reserve provided by the allowable stress design methodology with a specified factor of safety. This reserve was used to allow for overload permit loads and for a increase measure of safety for bridge rating.[26]

In 1982, Congress passed additional legislature requiring all states to allow 20 kips (89 kN) on single axles, 34 kips (151.2 kN) on tandem axles, and 80 kips (355.8 kN) total (gross) weight vehicles on the Interstate highways under their authority, and to enforce the Federal Bridge Formula (FBF).[27] The FBF limits the gross weight on any group of axles to a value determined by the number of axles and the distance between them. As before, states with grandfathered bridge formula in effect before 1975 were exempt from enforcing the FBF. The FBF is intended to limit the weight of shorter trucks to levels which will limit the extreme stresses on well-maintained bridges designed with the HS20 loading (including the lane load) to approximately 3%, and to well-maintained bridges designed to the HS15 loading to around 30%. If the FBF is applied to the HS20-44 design truck, the calculated results require a minimum length of 48 ft (14.6 m) from front to rear axle. The design truck length is 28 ft (8.5 m) from front to rear axle, and is out of compliance with the FBF.

As the Interstate era continued, it became increasing apparent to the bridge design community that the HS design loading did not represent a practical relationship to the actual live loads encountered on the road system.[28] Also, the community was becoming increasingly inclined to adopt a more probability based design methodology. This would lead to the development and adoption by AASHTO of the Load and Resistance Factor Design (LRFD) specification. The objective of adopting this type of design methodology was to produce a more uniform and consistent factor of safety for a bridge under design, based on the probability of the variety of live load combinations encountered and variation in strength due to actual construction. The uncertainties in load and resistance can then be quantified as a bias ratio and a coefficient of variation for each load and resistance combination. Due to the wide discrepancies of the HS design load to actual live load combinations expected for existing and future highway usage, a new live load would be needed in order to calibrate the new LRFD design specification.

The AASHTO Highway Subcommittee on Bridges and Structures authorized the development of an updated bridge design specification.[29] Five candidate notional loads were identified as possible new live load combinations:

1. A single six axle vehicle, called the Highway Truck Load (HTL)-57, weighing a total of 114 kips (507.1 kN), with a fixed wheel base, fixed axle spacing, and axle loadings as shown on Figure 2-2.

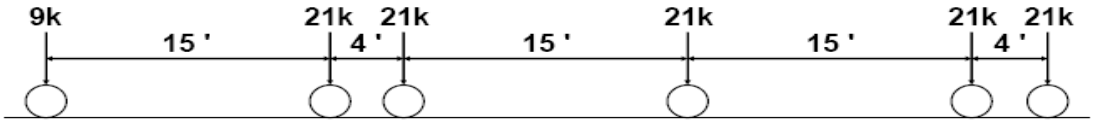

Figure 2-2: Highway Truck Load (HTL)-57 Design Truck Load (114 kips)[30]

2. A combination of three different loads, consisting of a design tandem load (increased to 25 kips (111.2 kN) per axle)[31], a four axle single truck with three rear axles totaling 82 kips (364.7 kN) with a total length of 20 ft (6.1 m) corresponding to heavy hauling short trucks, and a 3-S-2 axle load configuration of 133 kips (591.6 kN) with a total length of 50 ft (15.2 m) with a applied preceding and following uniform lane load of 0.5 kips/ft (7.3 kN/m). These three load combinations are shown in Figure 2-3.
3. A design family of live loads called the Highway Load (HL)-93, consisting of the AML design tandem, or HS20-44 design truck combined with a superimposed HS design lane load of 0.64 kips/ft (9.3 kN/m). Also included is a special case of 90% of two HS20-44 design truck loads with 14 ft (4.3 m) wheel bases and 90% of the uniform lane load for the calculation of negative moments near supports and the interior reactions of any continuous beam over 50 ft (15.2 m) in total length. These load combinations are shown in Figure 2-4.

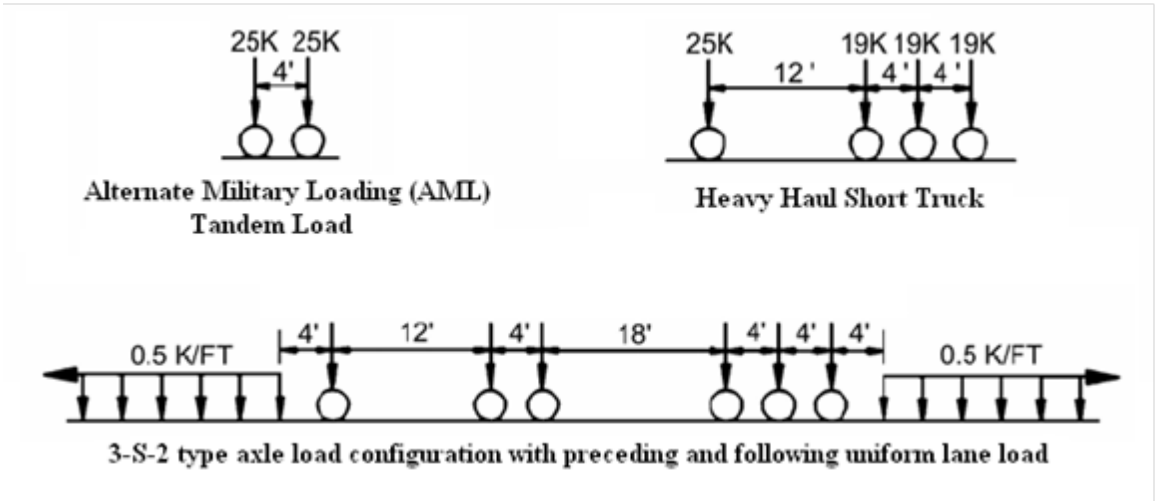

Figure 2-3: Second Possible LRFD Design Live Loads[32]

4. A design family of live loads called the Highway Load (HL)-93, consisting of the AML design tandem, or HS20-44 design truck combined with a superimposed HS design lane load of 0.64 kips/ft (9.3 kN/m). Also included is a special case of 90% of two HS20-44 design truck loads with 14 ft (4.3 m) wheel bases and 90% of the uniform lane load for the calculation of negative moments near supports and the interior reactions of any continuous beam over 50 ft (15.2 m) in total length. These load combinations are shown in Figure 2-4.
5. An equivalent uniform load in kips/ft required to produce the same force effect for a variety of various grandfathered exclusion vehicles, as compiled by the subcommittee.
6. A "HS25" design truck load weighing 90 kips (400.3 kN) with 14 ft (4.3 m) wheel base preceded and followed by a uniform lane load of 0.48 kips/ft (7.0 kN/m).

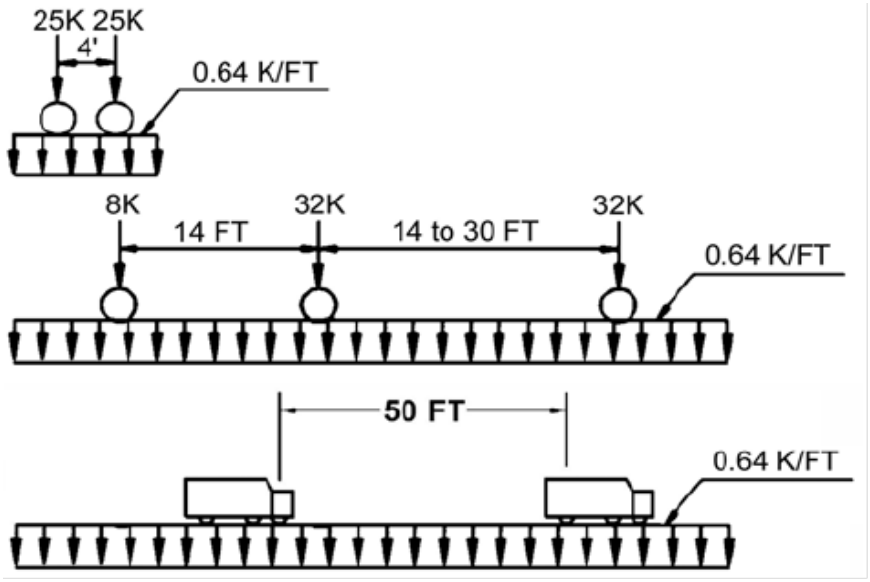

Figure 2-4: Highway Load (HL)-93 Design Live Loads[33]

The candidate live loads were evaluated using influence line analysis. According to the AASHTO subcommittee researchers, the AML tandem axle load along with the uniform lane

loads, or the HS20-44 design truck load along with the uniform lane loads, produced the best fit to the compilation of exclusion vehicles.[34] Thus the combination of the AML tandem load or the HS20-44 design truck load combined with the HS20 uniform lane load was determined to be the preferred basis for a new notional design load in the LRFD specifications. In addition, based on the uncertainty of determining dynamic load effects, the AASHTO subcommittee researchers recommended that the dynamic impact factor of all span lengths be set at 33%.[35] This was subsequently adopted in the LRFD design specifications.

The subcommittee researchers initially considered the HTL-57 truck load for the LRFD design load due to the previous work of Canadian researchers on the Ontario Highway Bridge Design Code (OBDC) that produced a desirable reliability bias for all span lengths. However, the researchers realized the potential political ramifications for specifying a new super-legal design load, and therefore chose to use the superposition of pre-existing sub-legal loads consisting of the HS20-44 design truck load along with the HS uniform lane load to produce the super legal load effects corresponding to a variety of state super-legal exclusion vehicles. The researchers determined that the moments and shears due to the HL-93 live load and the HTL-57 design truck load were comparable for all span lengths. In addition, the HL-93 notional design load has been shown to be a reasonable fit for statistically projected and actually encountered live loads on the bridges of the Interstate Highway System.[36]

2.4 LOAD AND RESISTANCE FACTOR DESIGN (LRFD)[37]

As specified in Article 3.5.1 (A3.5.1) of the AASHTO LRFD specification, dead loads are permanent loads on the bridge structure that include the weight of all components of the structure, appurtenances and utilities attached to the structure. Dead loads also include earth

cover, wearing surfaces, future overlays and any planned widenings or structures anticipated over the life of the structure. For the purposes of this analysis, the dead load on a bridge is assumed to be constant across the various live loads considered, and is neglected in the various analyses.

Live loads are specified in Article 3.6.1 (A3.6.1) of the AASHTO LRFD. Live loads are considered to consist of gravity loads (vehicular live loads, rail transit loads and pedestrian loads), the dynamic load allowance (wheel load impact), vehicular collision forces, centrifugal forces and braking forces. Live loads of interest for this analysis are the vehicular live loads and specified loadings for live load deflection evaluation, with dynamic load allowance included as appropriate. Live loads are considered to be transient loads applied to the bridge throughout its service life, and include any dynamic load allowance, multiple presence factors, and distribution factors as applicable.

The basic design vehicular live load in the LRFD specification is designated as the HL-93 as discussed earlier, and consists of a combination of either a design truck or tandem, plus a design lane load within each design lane.

The design truck, specified in Article 3.6.1.2.2, is composed of “an 8-kip lead axle spaced 14 feet from the closer of two 32-kip rear axles, which have a variable axle spacing of 14 feet to 30 feet, and a transverse wheel spacing of 6 feet. The design truck occupies a 10 foot lane width and is positioned within the design lane to produce the maximum force effects, but may be no closer than 2 feet from the edge of the design lane, except for the design of the deck overhang. For the purpose of maximum loading, in practice the axles are assumed to be 14 feet apart with a total vehicle axle length of 28 feet.”

The design tandem, specified in Article 3.6.1.2.3, is composed of "a pair of 25-kip axles spaced 4 feet apart, again with the transverse wheel spacing of 6 feet. As discussed earlier, this is said to represent the Alternative Military Tandem (AMT). The design lane load is specified in Article 3.6.1.2.4 and has a magnitude of 640 lbs per linear foot or 0.64 kips per linear foot (klf) uniformly distributed in the longitudinal direction. In the transverse direction, the load occupies a 10 foot width."

As stated in the AASHTO LRFD specification, the live-load models are not intended to represent a particular truck, but rather they are representative of the moments and shears produced by vehicles currently using the national highway system. These models were calibrated using selected weigh-in-motion data, truck weight studies, the Ontario Highway Bridge Design Code live-load model, and statistical projections of 75-year vehicles, when scaled by appropriate load factors.

As specified in Article 3.6.2 of the AASHTO LRFD specification, "a 33 percent dynamic load allowance (or impact factor) is applied only to the design truck or tandem portion of the HL-93 design live load or to the truck portion of the special negative-moment loading for both strength limit state and live-load deflection checks. The dynamic load allowance is not applied to the design lane load."

Multiple Presence Factors are specified in Article 3.6.1.1.2 of the AASHTO LRFD specification. These factors account for the probability of multiple lanes on the bridge being loaded simultaneously. These factors are specified for various numbers of loaded lanes in Table 3.6.1.1.2-1 of the specifications. Based on the assumptions discussed later, multiple presence factors are not used in this analysis.

The various load combinations are presented in Table 3.4.1-1 of the AASHTO LRFD specification and are shown on Table 2-1. The STRENGTH I load combination is used for checking the strength of a member or component under normal use in the absence of wind. The basic STRENGTH I load combination is 1.25 times the permanent load of member components plus 1.5 times the load due to any non-integral wearing surfaces and utilities plus 1.75 times the design live load discussed above. The STRENGTH II load combination is used to check the strength of the bridge member or component under special permit loadings in the absence of wind. The STRENGTH II load combination is the same as the STRENGTH I load combination except the live-load load factor is reduced from 1.75 to 1.35. The STRENGTH II load combination is specified by the various state departments of transportation and no standard STRENGTH II load combination is specified in the AASHTO LRFD specification.

2.5 LOUISIANA DESIGN LIVE LOAD VEHICLE 2011 (LADV-11)[38]

The Louisiana Department of Transportation (LA DOTD) policy prior to the publication of the new Bridge Design and Evaluation Manual (BDEM) in March 2015, required the use of the HL-93 live load as the STRENGTH I load combination for all new bridges. In addition, designers were required to use the eight (8) Louisiana design vehicles (LASDVs) as the STRENGTH II load combinations with applicable load factors. The eight LASDV and applicable load factors are shown on Figure 2-5.

This complicated process required significant design effort and often resulted in a new bridge not meeting the minimum load rating criteria. To simplify the design process, the LA DOTD developed a new load model that envelops the Louisiana special design vehicles design load effects and meets minimum load rating criteria. As specified in Article 3.6.2 of the 2015

LA DOTD BDEM, all bridges in Louisiana shall be designed for Louisiana Design Vehicle Live Load 2011 (LADV-11). LADV-11 is essentially a magnified HL-93 load model that is representative of current routine truck traffic in Louisiana.

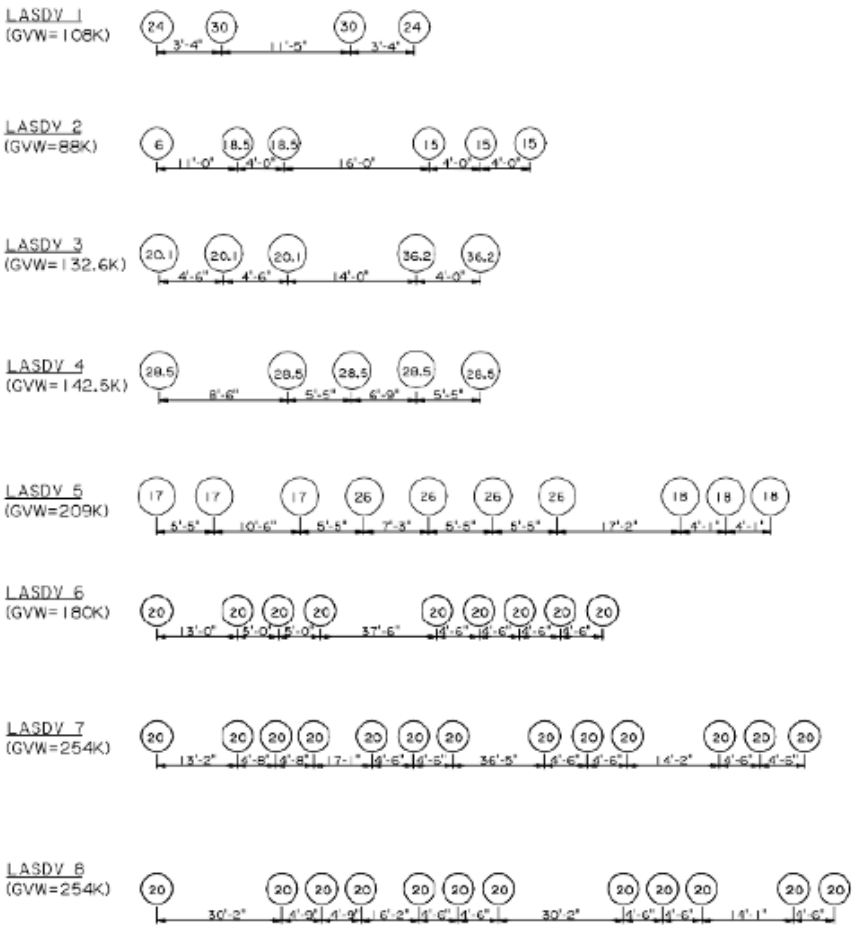

Figure 2-5: Louisiana Special Design Vehicles[39]

Use of the LADV-11 shall be indicated on the General Notes plan sheet under "Design Criteria" for all new bridge design and construction in the State of Louisiana. The LADV-11 is the product of the force effects produced by HL-93, as specified in A3.6.1.2 and a magnification factor (MF) listed on Table 2-2 (Table 1.3.1-1 in the 2015 LA DOTD BDEM). The LADV-11

Table 3.4.1-1—Load Combinations and Load Factors

Load Combination Limit State	DC DD DW EH EV ES EL PS CR SH	LL IM CE BR PL LS	WA	WS	WL	FR	TU	TG	SE	Use One of These at a Time				SC[1]
										EQ	IC	CT	CV	
Strength-I	γ_p	1.75	1.00	-	-	1.00	0.50/1.20	γ_{TG}	γ_{SE}	-	-	-	-	-
Strength-II	γ_p	1.35	1.00	-	-	1.00	0.50/1.20	γ_{TG}	γ_{SE}	-	-	-	-	-
Strength-III	γ_p	-	1.00	1.40	-	1.00	0.50/1.20	γ_{TG}	γ_{SE}		-	-	-	-
Strength-IV	γ_p	-	1.00	-	-	1.00	0.50/1.20	-	-	-	-	-	-	-
Strength-V	γ_p	1.35	1.00	0.40	1.00	1.00	0.50/1.20	γ_{TG}	γ_{SE}	-	-	-	-	-
Extreme Event-I	1.00	**0.25[2]**	1.00	-	-	1.00		-	-	1.00	-	-	-	
Extreme Event-II	γ_p	0.50	1.00	-	-	1.00	-	-	-	-	1.00	1.00	1.00	-
Extreme Event-III[1]	**γ_p**	**1.75**	**1.00**	**0.30**	-	**1.00**	-	**γ_{TG}**	**γ_{SE}**	-	-	-	-	**1.00**
Extreme Event-IV[1]	**γ_p**	-	**1.00**	**1.40**	-	**1.00**	-	**γ_{TG}**	**γ_{SE}**	-	-	-	-	**0.70**
Extreme Event-V[1]	**γ_p**	-	**1.00**	-	-	**1.00**	-	-	-	-	**1.00**	**1.00**	**1.00**	**0.60**
Extreme Event-VI[1]	**γ_p**	-	**1.00**	-	-	**1.00**	-	-	-	**1.00**	-	-	-	**0.25**
Service-I	1.00	1.00	1.00	0.30	1.00	1.00	1.00/1.20	γ_{TG}	γ_{SE}	-	-	-		-
Service-II	1.00	1.30	1.00	-	-	1.00	1.00/1.20	-	-	-	-	-		-
Service-III	1.00	**1.00[3]**	1.00	-	-	1.00	1.00/1.20	γ_{TG}	γ_{SE}	-	-	-		-
Service-IV	1.00	-	1.00	0.70	-	1.00	1.00/1.20	-	1.00	-	-	-		-
Fatigue- I LL, IM & CE only	-	1.50	-	-	-	-	-	-	-	-	-	-	-	-
Fatigue- II LL, IM & CE only	-	0.75	-	-	-	-	-	-	-	-	-	-	-	-

1. SC (Scour) is the total scour depth determined by Bridge Hydraulic Engineer in accordance with *HEC-18*. Scour is not a load, but an extreme event that alters geometry of the foundation, possibly causing structural collapse or amplification of applied load effects. Adopted factors for SC are based on NCHRP Report 489, *Design of Highway Bridges for Extreme Events*, and modified for Louisiana practice.
2. NCHRP Report 489 has shown that the commonly used live load factor of 0.50 in combination with earthquake effects is conservative and a reduced live load factor of 0.25 will provide an adequate safety level. Since probability of a major earthquake occurring in Louisiana is generally very low, it is reasonable to use a live load factor of 0.25.

Table 2-1: AASHTO Load and Resistance Factor Design Combinations and Factors[40]

was developed to provide a live load model that is representative of routine permit vehicles in the State of Louisiana. Bridges designed using LADV-11 will meet the minimum service and strength requirements for these vehicles and satisfy load rating and evaluation criteria.

Table 1.3.1-1: Load Factors for Design Loading and LASDV

Loading Vehicle		Load Factor
Design Loading	HL-93	1.750
LA Special Design Vehicles (LASDVs)	LASDV1	1.720
	LASDV2	1.800
	LASDV3	1.474
	LASDV4	1.375
	LASDV5	1.300
	LASDV6	1.300
	LASDV7	1.300
	LASDV8	1.300

Table 2-2: Louisiana Load Factors for use with Special Design Vehicles[41]

The 2015 LA DOTD BDEM specifies that a magnification factor (MF) shall be applied to all bridge elements and limit states that are subject to design vehicular live load. The magnification factors were developed through rigorous analysis of the load effects of the aforementioned permit vehicles and HL-93 load model on simple and continuous span bridges with varying span lengths. The value of MF varies and is a function of span length as shown on Table 2-3. A MF of 1.0 shall be used for vehicular live load applied to decks, deck systems, and the top slab of box culverts per A3.6.1.3.3 of the 2015 LA DOTD BDEM.

It is inferred from the commentary provided in the 2015 LA DOTD BDEM that the LADV-11 with applicable span based MF is to be used in lieu of the HL-93 live load in the STRENGTH I and SERVICE load combinations, thereby removing the need for a separate calculation using a permit vehicle (one of the eight LASDV) as the live load in the STRENGTH II load combination. It is also inferred that the MF is applied to the total HL-93 live load (a combination of either a design truck or tandem, plus a design lane load within each design lane) versus simply a factor applied to the design truck or tandem. In other words, the MF is applied to the contribution of the uniform 0.64 kips/ft (9.3 kN/m) lane load to the design live load as well as the design truck or tandem load. Other states continue to use "grandfathered" permit vehicle as the live load in the STRENGTH II load combination. The use of some of these permit vehicles for further analysis is discussed below in more detail.

2.6 OTHER BRIDGE DESIGN LOADS USED FOR COMPARISON

A theoretical loading developed as part of a civil engineering doctoral dissertation[42] was used both for comparison and as a basis for a design methodology for the proposed logistical convoy live load. Several other design loads were considered for this analysis, as well as several existing and proposed state permit vehicles.

A theoretical loading was developed by Dr. Marta Lutomirska as part of her doctorate dissertation at the University of Nebraska, Lincoln in 2009.[43] Dr. Lutomirska analyzed forced flow traffic condition on long span bridges which corresponds to the contraflow traffic condition during a mandatory hurricane evacuation in the Gulf South region. Dr. Lutomirska proposed a live loading consisting of a train of AASHTO Type 3-3 vehicles distributed in accordance with the assumptions used to develop the AASHTO uniform lane load. Vehicle clear distance

LADV-11 Magnification Factor Table

Load Effect	Range of Applicability	Magnification Factor (MF)
M^+, V	$L \leq 240$	1.30
	$240 < L < 600$	1.30-0.00083(L-240)
	$L \geq 600$	1.00
M^-	$L \leq 100$	1.30
	$100 < L < 240$	1.30-0.00214(L-100)
	$L \geq 240$	1.00
R_B	All Span Lengths	1.60
R_F	$L_1 + L_2 \leq 100$	1.30
	$100 < L_1 + L_2 < 240$	1.30-0.00214(L_1+L_2-100)
	$L_1 + L_2 \geq 240$	1.00
R_S	$L_1 + L_2 \leq 100$	1.55
	$100 < L_1 + L_2 < 600$	1.55-0.00110(L_1+L_2-100)
	$L_1 + L_2 \geq 600$	1.00

L = Span Length taken as center of bearing to center of bearing length, feet (use the shortest span length for unequal continuous spans)

$L_1 + L_2$ = Sum of Span 1 Length and Span 2 Length on either side of the support, feet (for end bents use the approach slab length as L_1 and the span length as L_2)

M^+ = Positive Moment (use for design of superstructure elements only)

M^- = Negative Moment (use for design of superstructure elements only)

V = Shear (use for design of superstructure elements only)

R_B = Bearing Reaction (use for design of bearings only)

R_F = Factored Support Reaction (use for design of all substructure elements and determination of factored pile/shaft loads)

R_S = Service Support Reaction (use for determination of service pile/shaft loads only)

* Equations are linear interpolations between the upper and lower values of the MFs.

Table 2-3: Louisiana Special Design Vehicle (2011) Magnification Factors[44]

(spacing) was varied between 10 to 15 ft (3.0 to 4.6 m), corresponding to a spacing 20-25 ft (6.1-7.6 m) between the last axle of one truck and first axle of the following truck. The Gross Vehicle Weight (GVW) of a Type 3-3 unit is 80 kips (355.8 kN) and total length of a Type 3-3 unit is 54 ft (16.5 m).

Therefore the proposed live loading consisted of:

80 kips / (54+25) ft = 1.01 kips/ft (14.7 kN/m) for clearance distance of 15 ft (4.6 m)

80 kips / (54+20) ft = 1.08 kips/ft (15.8 kN/m) for clearance distance of 10 ft (3.0 m)

Since the value obtained in this way is based on heavy trucks and is very conservative, its value can be multiplied by factor 0.75. This approach derives from basic philosophy used to develop lane load of 0.64 kip/ft.

The adjusted live loads are:

0.75 x 1.01 kips/ft (14.7 kN/m) = 0.76 kip/ft (11.1 kN/m) for 15 ft (4.6 m) spacing

0.75 x 1.08 kips/ft (15.8 kN/m) = 0.81 kip/ft (11.8 kN/m) for 10 ft (3.0 m) spacing

The graphical representation of these proposed loadings are shown on Figure 2-6.

The other design loads used for comparative analysis were the Ontario Highway Bridge Design (OHBD) Code and the Canadian Highway Bridge Design Code CL-W loading.

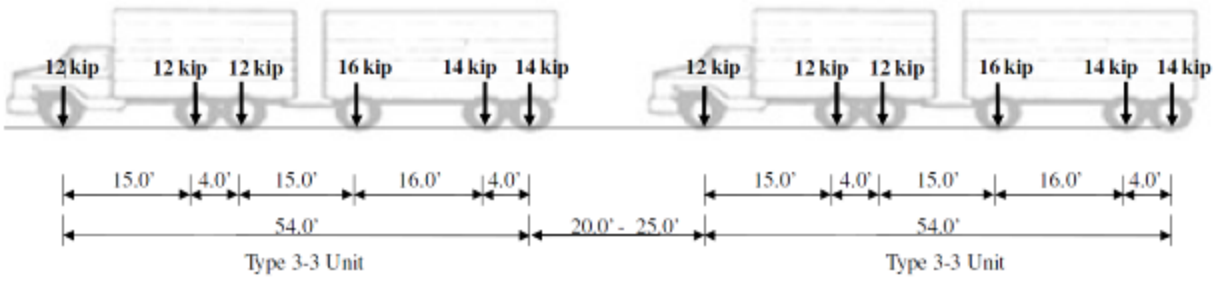

Figure 2-6: AASHTO Type 3-3 vehicle train, proposed by Lutomirska (2009)[45]

The Ontario Highway Bridge Design (OHBD) code specifies a live load of either a truck load or a combination of truck and lane load, as shown in Figure 2-7. These loads are either:

1) The OHBD Truck, which is a 5-axle truck, or

2) The OHBD Lane Load consists of an OHBD Truck with each axle reduced to 70%, and superimposed centrally within the width of a 3.0 m (10 ft) wide uniformly distributed load of 10.0 kN/m (0.685 kip/ft).

The Canadian Highway Bridge Design Code, also known as the CAN/CSA-S6-00, applies the CL-W loading, which consists of the truck or the lane load, as shown in Figure 2-8. These loadings are:

1) The CL-W Truck is a 5-axle truck. The number "W" indicates the gross load of the truck in kilonewtons (kN). For the design of a national highway network, loading not less than CL-625 (140.5 kips) shall be used, or

2) The CL-W Lane Load consists of CL-W Truck with each axle reduced by 80% (~500 kN; 112.5 kips) and a superimposed uniformly distributed lane load of 9.0 kN/m (0.617 kip/ft), that is 3.0 m (10 ft) wide.

Finally, two permit vehicles from other areas of the United States were used for comparison against both the various design codes and for evaluation of the proposed new military live load.

The first permit vehicle to be considered was the Washington State Type 03 (WA-03) live load, shown in Figure 2-9. The maximum shear and moment loadings for this vehicle were used for the adaptation of analysis results to the reliability assessment presented in Chapter 6. The second permit vehicle considered was the Wisconsin Special Permit Vehicle (Wis-SPV) as

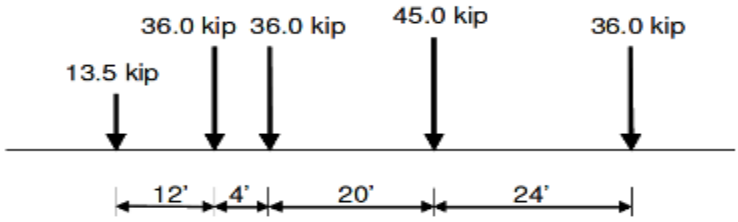

OHBD Live Loading [1991]. OHBD Truck.

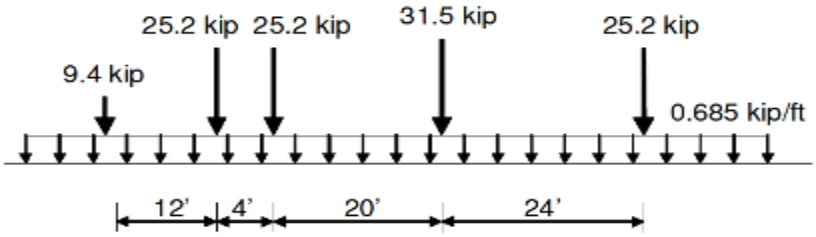

OHBD Live Loading [1991]. OHBD Truck and Lane Load.

Figure 2-7: Ontario Highway Bridge Design Code (OBDC), 3rd Edition (1991)[46]

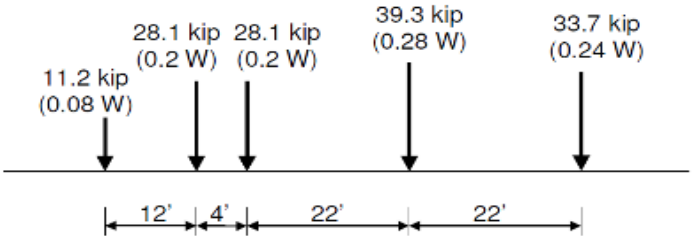

CAN/CSA-S6-00 Live Loading [2000]. CL-W Truck

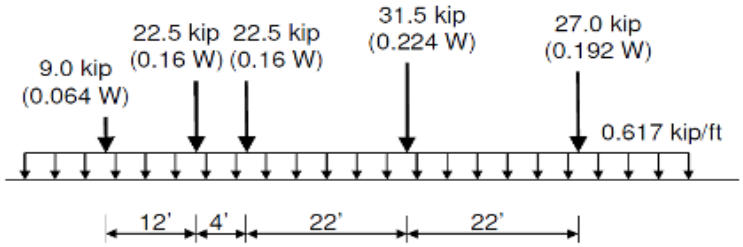

CAN/CSA-S6-00 Live Loading [2000]. CL-W Lane Load

Figure 2-8: Canadian Highway Bridge Design Code CL-W, CAN/CSA-S6-00 (2000)[47]

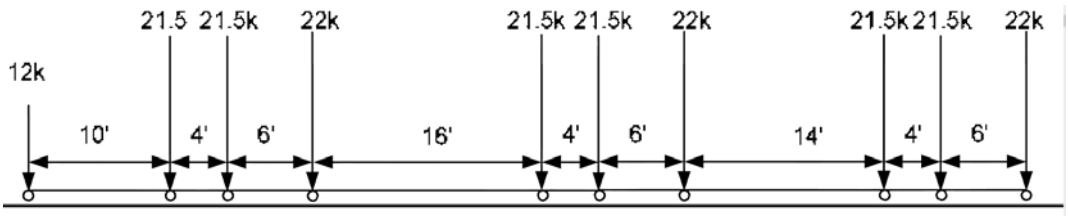

Figure 2-9: Washington State Type 03 (WA-03)[48]

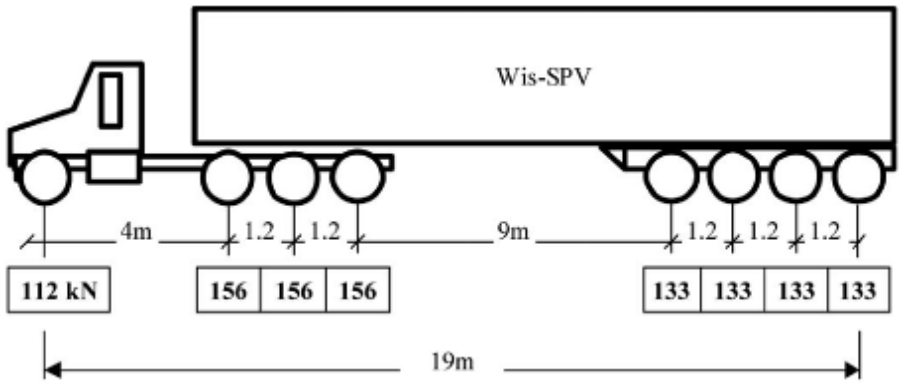

Figure 2-10: Wisconsin Special Permit Vehicle[49]

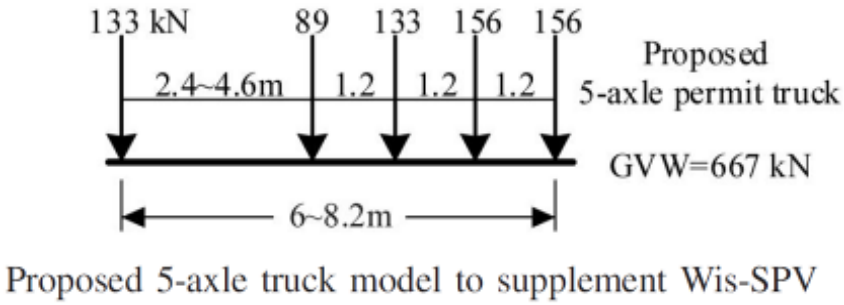

Figure 2-11: Hypothetical Permit Vehicle, proposed by Zhao and Tabatabai (2012)[50]

well as a hypothetical 5-axle permit vehicle, proposed as an adjunct to the Wis-SPV to account for the high loads on short spans caused by heavier, shorter vehicles. Both Wis-SPV (Figure 2-10) and the proposed 5-axle permit truck (Figure 2-11) were used for comparison with the design codes and the proposed military live loading for all span lengths.

Two other potential special permit vehicles identified in the literature were considered but not analyzed.[51] These permit trucks (the Delaware DE 3 and Connecticut Construction Vehicle T4 vehicles) were identified as calibration trucks for exclusion vehicles, also referred to as "governing non-Formula B special heavy vehicles (SHV)". The proposed 5-axle permit truck (Figure 2-11) and the military loading discussed in the next chapter are inclusive of these governing non-Formula B SHV since the rear axle groups of both proposed 5-axle permit truck and the proposed military heavy equipment transporter (HET) produce greater end shear and maximum moments for considered span lengths.

2.7 CHAPTER TWO END NOTES

1. Bhide, S., Culmo, M., Ma, J., Martin, B. and Russell, H. (2006), "The Interstate Highway System and the Development of Prestressed Concrete Bridges, page 51.
2. Parker, W.P. (2001) "Infantry assault engineers: An old (world) approach for engineer close combat support", page 32.
3. Bhide et al. (2006), page 50.
4. Bhide et al. (2006), page 51. See also Weingroff, R.F. (2003), "The Man Who Changed America, Part I", pages 4-8.
5. Weingroff, R.F. (2014); "A Vast System of Interconnected Highways", pages 170-182. See also Weingroff, R.F. (2003), "The Man Who Changed America, Part I", pages 8-10. See also Part II of series for a complete history of the development of the Interstate Highway System.
6. Bhide et al. (2006), page 51.

7. Walther, R.A. and Chase, S.B. (2006), "Condition Assessment of Highway Structures", page 68. See also Weingroff (2014), "A Vast System of Interconnected Highways", pages 164-169.

8. Weingroff (2014), "A Vast System of Interconnected Highways", page 323

9. Weingroff (2003), "The Man Who Changed America, Part I", page 10.

10. Weingroff, R.F. (2006), "Essential to the National Interest", page 3.

11. Lewis, S. (2006), "Industry's Largest R&D Effort Founded Interstate Construction", page 32. See also Fisher, J., Hall, D., McCabe, R., Price, K., Seim, C. and Woods, S. (2006), "Steel Bridges in the United States", page 36.

12. Lippert, D.L. (2008), "Illinois DOT - From the AASHO Road Test To 20 Years of Mechanistic Pavement Experience and Counting", page (slide) 5

13. Lewis (2006), "Industry's Largest R&D Effort Founded Interstate Construction ", page 32

14. Fisher et al. (2006), "Steel Bridges in the United States", page 33.

15. Waddell, J.A.L. (1884), *The Designing of Ordinary Iron Highway Bridges*, , page 5. See also Fisher et al., "Steel Bridges in the United States", page 33.

16. Waddell, J.A.L. (1921), *Economics of Bridgework A Sequel to Bridge Engineering*.

17. Fisher et al. (2006), "Steel Bridges in the United States", page 33.

18. Kulicki, J.M. and Metz, D. (2006), "Evolution of Vehicular Live Load Models During the Interstate Design Era and Beyond", page 7.

19. Fisher et al. (2006), "Steel Bridges in the United States", page 34.

20. Kulicki and Metz (2006), "Evolution of Vehicular Live Load Models During the Interstate Design Era and Beyond", page 2. See also Fisher et al. (2006), "Steel Bridges in the United States", pages 34-35.

21. Kulicki and Metz (2006), page 3

22. Kulicki and Metz (2006), page 7.

23. Lewis (2006), page 32. See also Lippert (2008), page (slide) 5

24. U.S. War Department (1944), Technical Manual (TM) 9-767, 40-Ton Tank Transporter, Tractor-Trailer M25, page 14.

25. Lippert (2008), page (slide) 24.

26. Kulicki and Metz (2006), page 7.

27. Kulicki and Metz (2006), page 7.

28. Kulicki and Metz (2006), page 8.

29. Kulicki and Metz (2006), page 30.

30. Metz, D.R. (2009b), "The HL-93 Notional Live Load Model: What Nature of Truck Does It Represent", page 52. See also Kulicki and Metz (2006), Figure 12, page 19

31. Metz, D.R. (2009a), "Development of the HL-93 Notional Live Load Model", page 52. See also Miller, L. and Durham, S., (2008), "Comparison of Standard Load and Load and Resistance Factor Bridge Design Specifications for Buried Concrete Structures", page 83.

32. Kulicki and Metz (2006), Figure 13, page 19

33. Kulicki and Metz (2006), Figure 14, page 19.

34. Metz, D.R. (2009b), page 52.

35. Metz, D.R. (2010), "The HL-93 Live Load Model Dynamic Load Allowance", page 56

36. Metz, D.R. (2009b), page 52

37. American Association of State Highway and Transportation Officials (AASHTO) (2010), Load Resistance Factor Design (LRFD) Bridge Design Specifications, 5th Edition.

38. Louisiana Department of Transportation and Development (LA DOTD) (2015), Bridge Design and Evaluation Manual (BDEM).

39. LA DOTD (2015), Figure 1.2.2-1, Page IV.Ch1-2

40. LA DOTD (2015), Table 3.4.1-1, Page II.V1-Ch3-2

41. LA DOTD (2015), Table 1.3.1-1, Page IV.Ch1-4

42. Lutomirska, M. (2009), "Live Load Models for Long Span Bridges".

43. Lutomirska (2009), pages 61-66

44. LA DOTD (2015), Page II.V1-Ch3-6

45. Lutomirska (2009), Figure 5.7, page 65

46. Lutomirska (2009), Figures 2.4 and 2.5, page 13-14. See also Ontario Highway Bridge Design Code (OHBDC), 1979, 1983 and 1993

47. Lutomirska (2009), Figures 2.6 and 2.7, page 15. See also Canadian Standards Association. (2006), "Canadian highway bridge design code" and Nowak, A.S. (1994) "Load Model for Bridge Design Code".

48. Mlynarski, M., Wassef, W., and Nowak, A.S. (2011), “A Comparison of AASHTO Bridge Load Rating Methods”, page 14.

49. Zhao, J. and Tabatabai, H. (2012), “Evaluation of a Permit Vehicle Model Using Weigh-in-Motion Truck Records”, page 390.

50. Zhao and Tabatabai (2012), page 392.

51. Sivakumar, B., Moses, F., Fu, G. and Ghosn, M. (2007), “Legal Truck Loads and AASHTO Legal Loads for Posting”, National Cooperative Highway Research Program (NCHRP) Report 575, page 62.

CHAPTER 3: DISCUSSION OF MILITARY LOAD CLASSIFICATION

3.1 INTRODUCTION

The estimation and calculation of the load carrying capacity of bridges and other gap crossing structures is of critical importance to the planning and execution of military logistical operation using surface transportation. Before allowing a bridge or other gap crossing structure or device to be used for military traffic, military engineers must first determine if the structure or device can safely support all vehicles that may use the crossing structure. For this purpose, the United States (U.S.) and other North Atlantic Treaty Organization (NATO) member nations use a military load classification (MLC) system as defined in the NATO Standardization Agreement (STANAG) 2021.[1]

The aim of this agreement is to standardize for all NATO forces a method of computing the MLC of bridges, ferries, and rafts (including their landing stages) and vehicles. Based on the criticality of bridging in support of plans to defend Western Europe during the Cold War, the member nations of NATO agreed to establish a common, standardized method of computing the military load classification (MLC) of bridges, ferries, rafts and vehicles. Under exceptional operational circumstances, the prohibition of crossing a higher MLC vehicle over a lower MLC rated bridge, ferry, or raft may be lifted on special decision of the senior ranking military commander in the operational zone, or on the authority of civilian authorities in control of designated areas.

The NATO participating nations agreed that military forces would use the MLC for military planning only. These countries also agreed that the MLC are not intended to govern existing or future civil bridge design or construction, within the national borders of the NATO

member countries. The methodology agreed upon in the STANAG and refined and expanded in U.S. Army Field Manual (FM) 3-34.343 provides a standard process to determine the MLC of any bridge, ferry, or raft.[2] The determination allows the MLC number of the bridge, ferry, or raft to be compared to the MLC of the particular vehicle in a given scenario. If the MLC of the bridge, ferry, or raft is greater than the MLC of the vehicle under consideration, then in this scenario the vehicle may safely cross the bridge or be embarked on the ferry of raft. Otherwise (in the case where the vehicle MLC exceeds the bridge, ferry, or raft MLC), the vehicle must be diverted to avoid bridge damage or failure, or flooding and sinking of a ferry or raft, and more importantly, the loss of military personnel, equipment, and combat power. However, the diversion of the surface transportation of combat forces or logistical material has the potential to negatively impact overall operational success by delaying the arrival of forces or supplies, and also increasing usage and traffic on the more robust links of the surface transportation system.

3.2 HYPOTHETICAL VEHICLES

All military vehicles, both tracked and wheeled, are assigned a MLC number to represent the loading effect of that vehicle on bridges and roadways. The MLC does not represent the actual total weight or axle loads and spacing of a particular vehicle. Rather, it represents a combination of factors that include gross vehicle weight, vehicle axle spacing and load distribution, and speed of the vehicle acting on a bridge or roadway.

The agreed MLC categories consist of 32 hypothetical vehicles, 16 tracked vehicles and 16 wheeled vehicles. The tracked vehicles are represented as the total vehicle weight acting over a given area, representing the hypothetical track surface in contact with the ground or road surface. The wheeled vehicles have various axle and wheel configurations, but generally

approximate a tractor and trailer type vehicle configuration. These 32 hypothetical vehicles are shown on the Tables 3-1 through 3-4 which have been taken from U.S. Army publication FM 3-34.343.

Hypothetical Vehicles for Classification of Actual Vehicles and Bridges			
1	2	3	4
Class	Tracked Vehicles	Wheeled Vehicles	
		Axle Loads and Spacing	Maximum Single-Axle Load (in Short Tons)
4	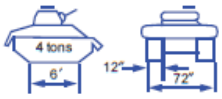	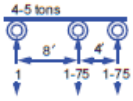	
8	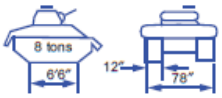	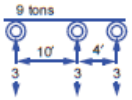	
12	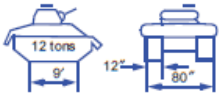	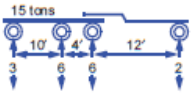	
16	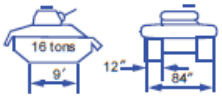	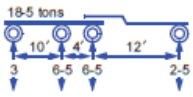	
20	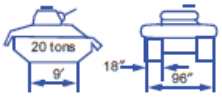	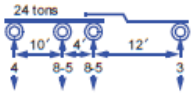	
24	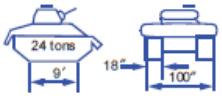	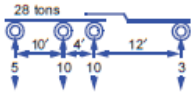	
30	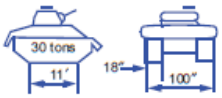	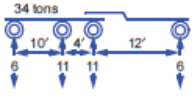	
40	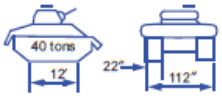	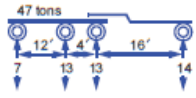	

NOTES:
1. The single-axle tire sizes shown in Columns 5, 6, and 7 refer to the maximum single-axle loads given in Column 4.
2. The bogie-axle tire sizes shown in Columns 5, 6, and 7 refer to the maximum bogie-axle loads shown on the diagrams in Column 3.
3. The maximum tire pressure for all tires shown in Column 8 should be taken as 75 psi. The first dimension of tire size refers to the overall width of the tire and the second dimension is the rim diameter of the tire.

Table 3-1: Standard Classes of Hypothetical Vehicles, Class 4 - 40[3]

Hypothetical Vehicles for Classification of Actual Vehicles and Bridges				
1	5	6	7	8
Class	Wheeled Vehicles			
	Minimum Wheel Spacing and Tire Sizes of Critical Axles			Maximum Tire Load and Minimum Tire Size
4	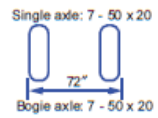	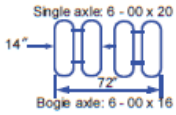		 2,500 lb on 7 - 50 x 20
8	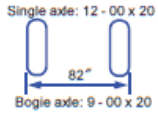	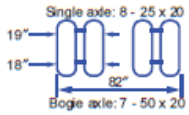		 5,500 lb on 12 - 00 x 20
12	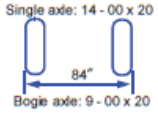	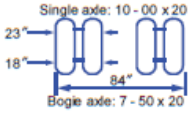		 8,000 lb on 14 - 00 x 20
16	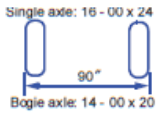	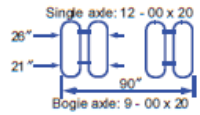		 10,000 lb on 16 - 00 x 24
20	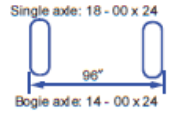	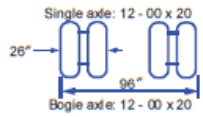	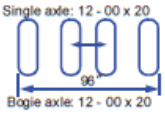	 11,000 lb on 18 - 00 x 24
24	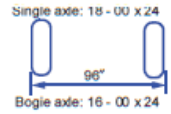	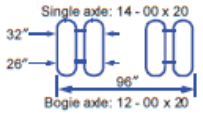	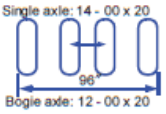	 12,000 lb on 18 - 00 x 24
30	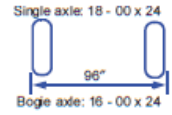	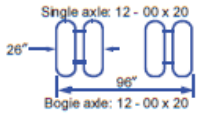	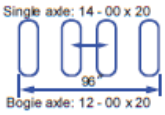	 13,500 lb on 18 - 00 x 24
40	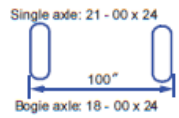	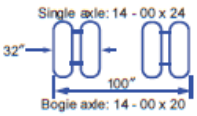	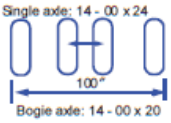	 17,000 lb on 21 - 00 x 24

NOTES:
1. The single-axle tire sizes shown in Columns 5, 6, and 7 refer to the maximum single-axle loads given in Column 4.
2. The bogie-axle tire sizes shown in Columns 5, 6, and 7 refer to the maximum bogie-axle loads shown on the diagrams in Column 3.
3. The maximum tire pressure for all tires shown in Column 8 should be taken as 75 psi. The first dimension of tire size refers to the overall width of the tire and the second dimension is the rim diameter of the tire.

Table 3-2: Standard Classes of Hypothetical Vehicles, Class 4 - 40 (continued)[4]

Hypothetical Vehicles for Classification of Actual Vehicles and Bridges			
1	2	3	4
Class	Tracked Vehicles	Wheeled Vehicles Axle Loads and Spacing	Maximum Single-Axle Load (in Short Tons)
50	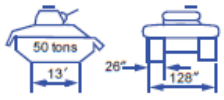	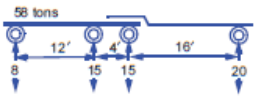	
60	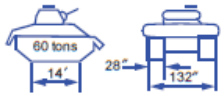	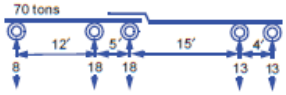	
70	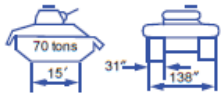	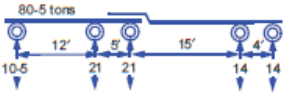	
80	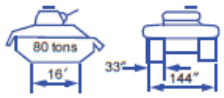	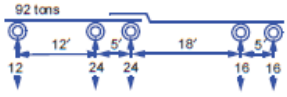	
90	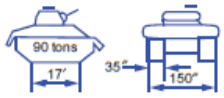	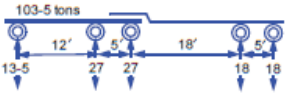	
100	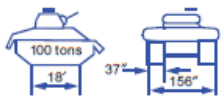	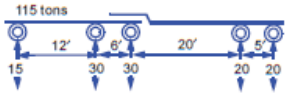	
120	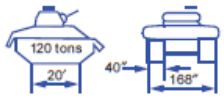	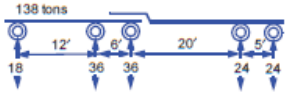	
150	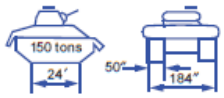	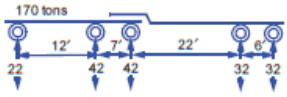	

NOTES:
1. The single-axle tire sizes shown in Columns 5, 6, and 7 refer to the maximum single-axle loads given in Column 4.
2. The bogie-axle tire sizes shown in Columns 5, 6, and 7 refer to the maximum bogie-axle loads shown on the diagrams in Column 3.
3. The maximum tire pressure for all tires shown in Column 8 should be taken as 75 psi. The first dimension of tire size refers to the overall width of the tire and the second dimension is the rim diameter of the tire.

Table 3-3: Standard Classes of Hypothetical Vehicles, Class 50 – 150[5]

Hypothetical Vehicles for Classification of Actual Vehicles and Bridges				
1	5	6	7	8
Class	Wheeled Vehicles			
	Minimum Wheel Spacing and Tire Sizes of Critical Axles			Maximum Tire Load and Minimum Tire Size
50	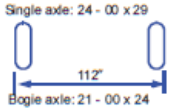	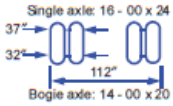		
60		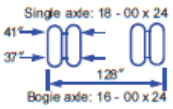	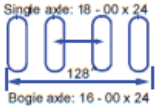	
70		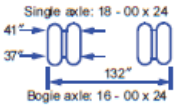	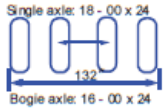	
80			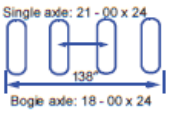	
90		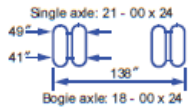	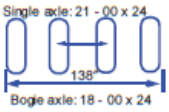	
100		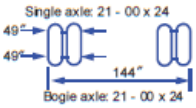	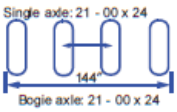	
120			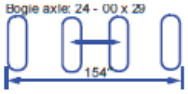	
150				

NOTES:
1. The single-axle tire sizes shown in Columns 5, 6, and 7 refer to the maximum single-axle loads given in Column 4.
2. The bogie-axle tire sizes shown in Columns 5, 6, and 7 refer to the maximum bogie-axle loads shown on the diagrams in Column 3.
3. The maximum tire pressure for all tires shown in Column 8 should be taken as 75 psi. The first dimension of tire size refers to the overall width of the tire and the second dimension is the rim diameter of the tire.

Table 3-4: Standard Classes of Hypothetical Vehicles, Class 50 – 150 (continued)[6]

These 16 tracked and 16 wheeled hypothetical vehicles create 16 standard MLC categories or classes, from MLC 4 to MLC 150 inclusive. These classification numbers were

originally developed from studies of hypothetical vehicles having the same load characteristics as actual military vehicles in use by NATO prior to STANAG adoption. As can be seen from these tables, the weight of the specific tracked vehicle in US short ton units represented the MLC of that vehicle. However, the weight of the corresponding MLC wheeled vehicle is larger, typically by a factor of 10-15%. In addition, a maximum single axle load, minimum wheel spacing and tire size for the critical axles, and a maximum tire load and minimum tire size are also provided for each MLC hypothetical wheeled vehicle.

3.3 HYPOTHETICAL VEHICLE LIVE LOADS

The maximum bending moments and shear forces generated by the hypothetical vehicles on a simple span or by the maximum single-axle loads on spans from 1-100 m (3.3- 328 ft) were calculated and provided as stated values in the STANAG. Once tabulated, the values were divided by the span length to create unit bending moment and unit shear forces, in order to simplify the plotting of the various MLC curves in the STANAG. For the U.S. military, these values were converted from SI to US customary units and tabulated for spans from 4-300 ft (1.2-91.4 m) in FM 3-34.343. Tabulated values for shear and bending moment were plotted as the actual values versus span length on Figures 3-1 to 3-4.

The AASHTO HL-93 live load moment and shear with dynamic impact curve is also plotted on each family of curves to show the comparison between these two systems.

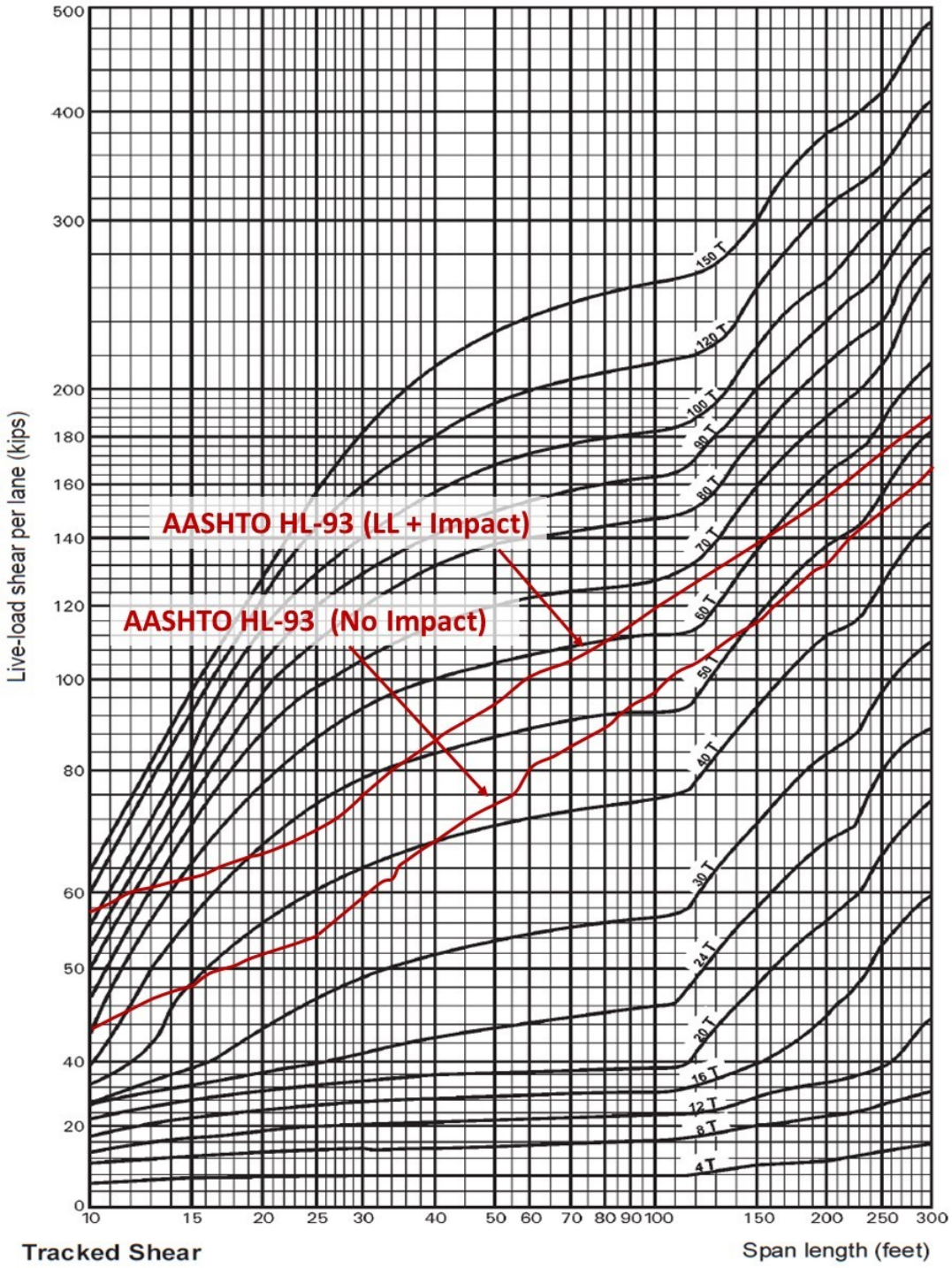

Figure 3-1: Hypothetical Tracked Vehicle Military Load Class Shear Curves with Superimposed AASHTO HL-93 Live Load Shear Curves[7]

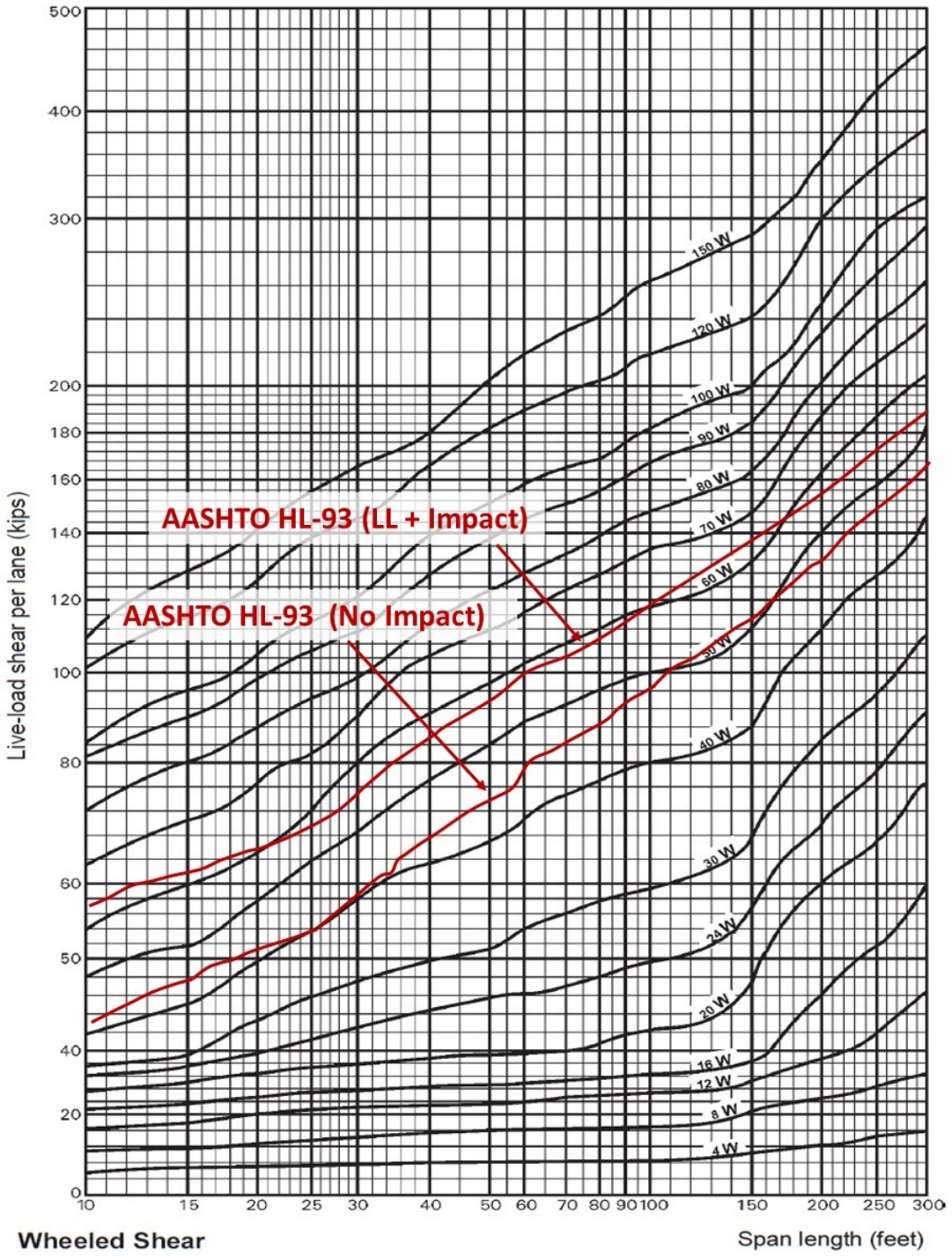

Figure 3-2: Hypothetical Wheeled Vehicle Military Load Class Shear Curves with Superimposed AASHTO HL-93 Live Load Shear Curves[8]

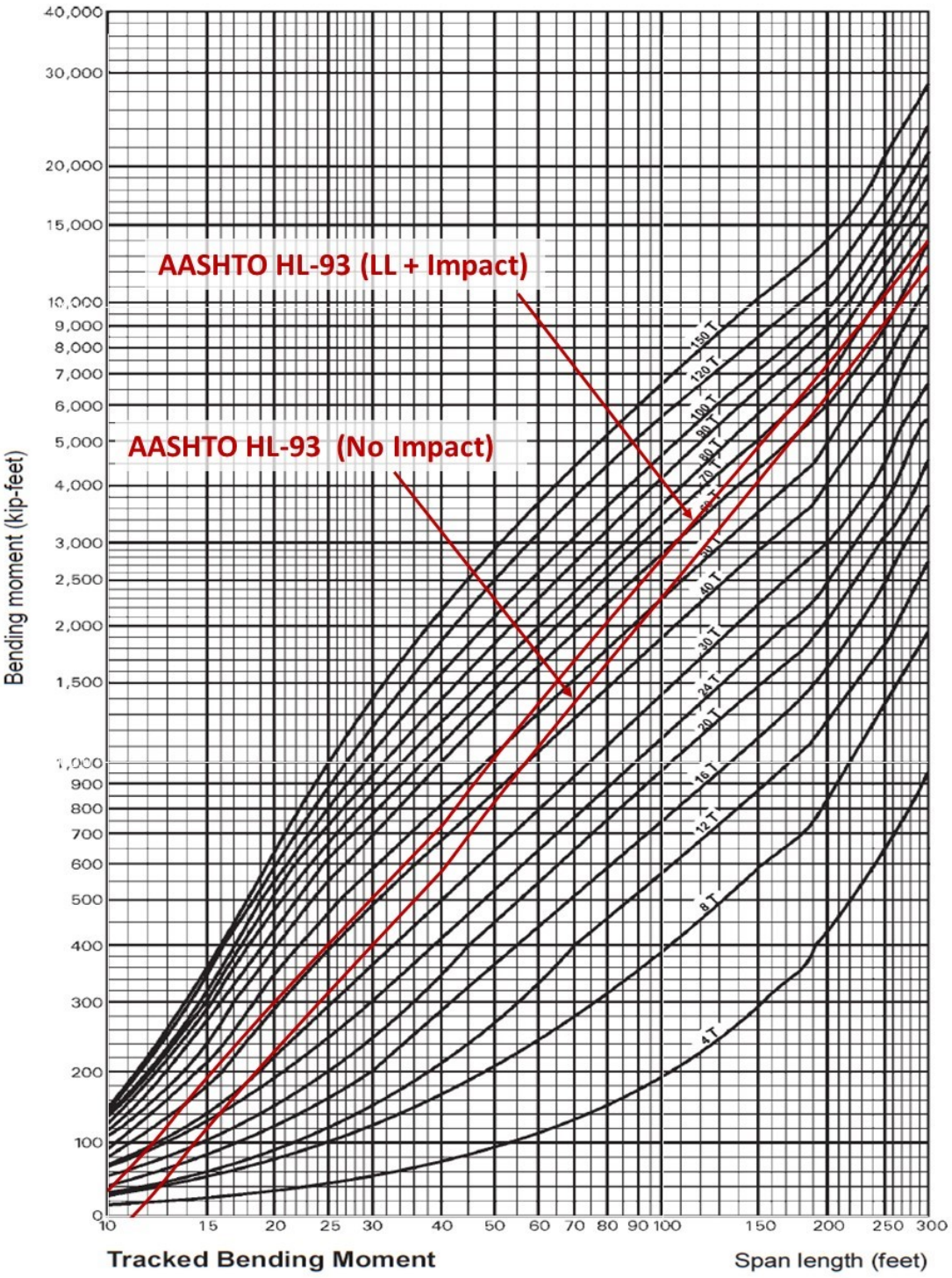

Figure 3-3: Hypothetical Tracked Vehicle Military Load Class Moment Curves with Superimposed AASHTO HL-93 Live Load Moment Curves[9]

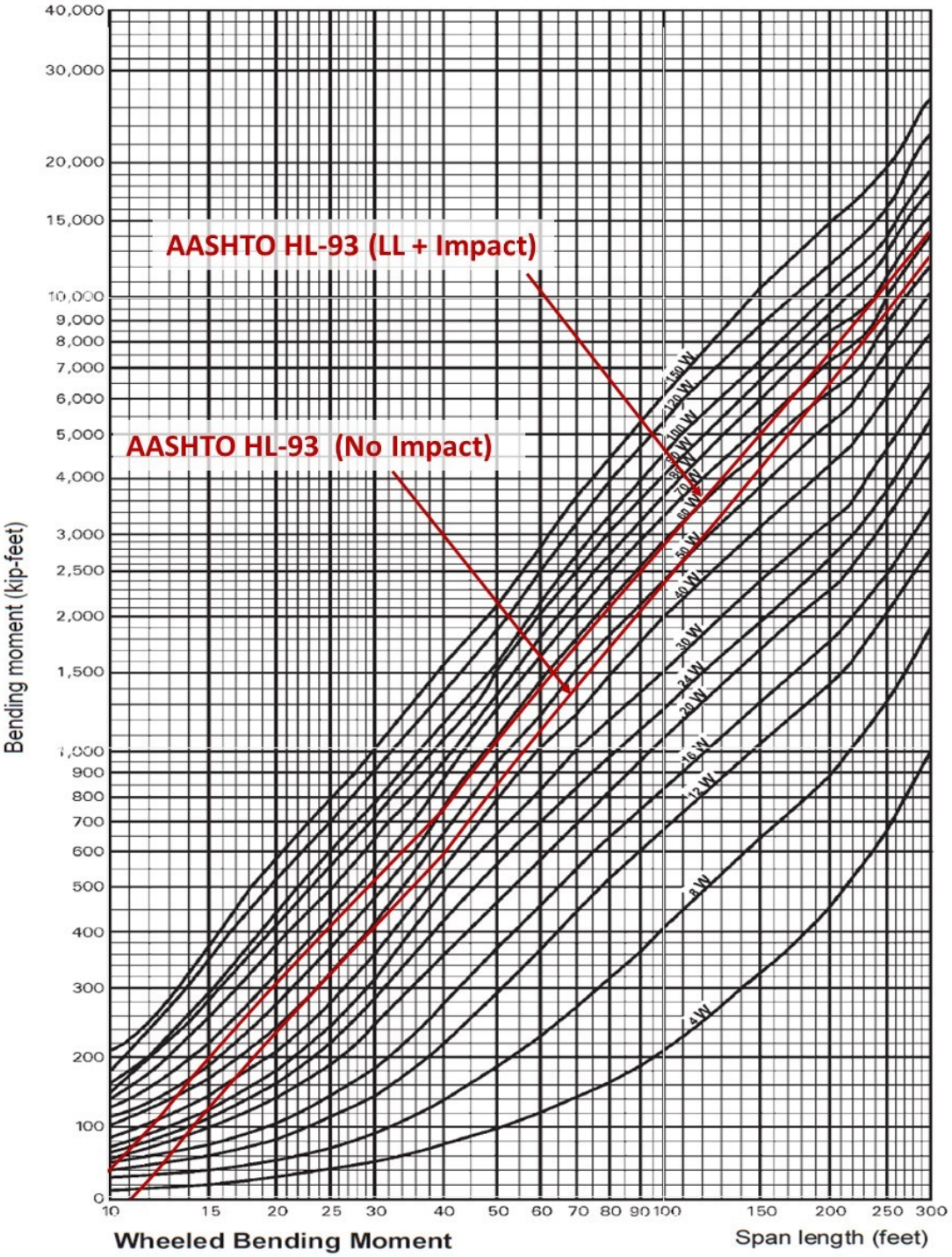

Figure 3-4: Hypothetical Wheeled Vehicle Military Load Class Moment Curves with Superimposed AASHTO HL- Live Load Moment Curves[10]

3.4 DISCUSSION OF MECHANICS USED FOR MLC DETERMINATIONS

According to the analytical methodology provided in FM 3-34.343, the superstructure is considered to be the controlling feature in bridge classification. The rationale is that since the superstructure must span large distances, the superstructure elements are designed and constructed to be as lightweight as possible. In other words, it is assumed that all bridge designs are optimized for material costs. It is further assumed that this design optimization is uniformly conducted for superstructure loadings since these are inherently more predictable. Substructures, on the other hand, must be more conservative and therefore less efficient in design because of various unpredictable or extreme loadings (stream and ice flow, barge impact) and unknown soil conditions. FM 3-34.343 does not requires the inspection of the substructure unless it appears to be significantly deteriorated or unstable due to scour or settlement, or is improperly designed or constructed. Per FM 3-34.343, the deck structure is generally stronger than its supporting superstructure; therefore, it is not considered in most classifications. Also, the FM assumes that bridge connections are also stronger than the superstructure beams; therefore, they do not have to be considered in most classifications.

For bending-moment calculations on bridge superstructures, the mid-span location is considered to be the controlling location for maximum moment. In general, shear is not considered to govern design or classification; although FM 3-34.343 provides simplified calculations for determining allowable shear loading.

Finally, vehicle loads are assumed to be the only live load acting on the bridge. The standard hypothetical vehicles discussed above are the vehicle live loads used for bridge design or classification. It is assumed both in FM 3-34.343 and STANAG 2021 that a standard military convoy would use the bridge, with a uniform spacing of 100 ft (30.5 m) between vehicles.

Because of this large spacing, it is assumed that only one vehicle will be on any single span of the bridge at a time. No allowance is made for other vehicular traffic on the bridge. The only other allowed live load is a line load of 75 pounds per ft (0.334 kN/m), each over a 1 ft (0.3 m) width, to account for refugees and dismounted military pedestrian traffic. Finally an impact factor of 1.15 (live loads increased by 15 percent) is required for all bridge types and span lengths except for timber-stringer or floating bridges. The impact on these bridges is zero. This low impact factor compared to civilian highway bridge design is based on the assumption that the military convoy using the bridge is traveling at relatively slow speeds compared to normal highway traffic.

3.5 USE OF MLC FOR BRIDGE DESIGN AND CONSTRUCTION

According to FM 3-34.343, military engineers using the MLC method design nonstandard fixed bridges to match specific conditions of a particular site when standard fixed bridges are not available. Available structural materials, site details, proposed traffic, and time will influence the design. The design of military nonstandard fixed bridges is similar to that of civilian fixed bridges; however, several simplifications and assumptions about the loads to be carried are typically required.

In the methodology specified in FM 3-34.343, bridge design engineers establish the desired MLC and then determine the required size and quantity of bridge components to meet that MLC. Simply supported stringer bridges are recommended since they are easy to design and construct. Per the FM, bridge design is a two-phase process, first involving the determination of the design loads and their effects in terms of moment and shear forces. The second phase involves selecting members that have sufficient strength to resist the effects of the intended loads

on the bridge. Before considering the design process complete, the failure modes (lateral buckling, excessive deflection, end bearing, and so forth) as well as moment and shear must be checked. Further detail regarding the recommended design process is contained in Part Three of FM 3-34.343 and will not be reiterated in this thesis.

3.6 USE OF MLC FOR RATING OF EXISTING BRIDGES

As stated in FM 3-34.343, a "highly mobile Army will make use of existing bridges. Before using a bridge for military traffic, engineers must first determine if the bridge can safely support the loadings. For this purpose, the Army uses the MLC system. Several methods exist for determining a bridge's MLC, each with different degrees of complexity and accuracy."

A temporary MLC can be determined by the "direct correlation between known civilian design loads and an equivalent MLC, by equating the respective design criteria and the vehicle's load effects." For bridges within the United States, FM 3-34.343 provides the correlation curves shown in Figure 3-5. A plot of the AASHTO HL-93 live load moment and shear with dynamic impact values is superimposed on the FM 3-34.343 correlation curves for additional comparison.

Section IV of Chapter 3 of FM 3-34.343 provides detailed guidance on determining a permanent MLC. As stated in the FM, the analytical classification method is basically the reverse of the design method. The analytical classification is based on classical methods of engineering analysis, and the difficulty of analytical bridge classification varies with the bridge type. The FM states that only qualified engineers should make permanent classifications. See Chapter 3 of the U.S. Army publication FM 3-34.343 for more detail on the analytical method.

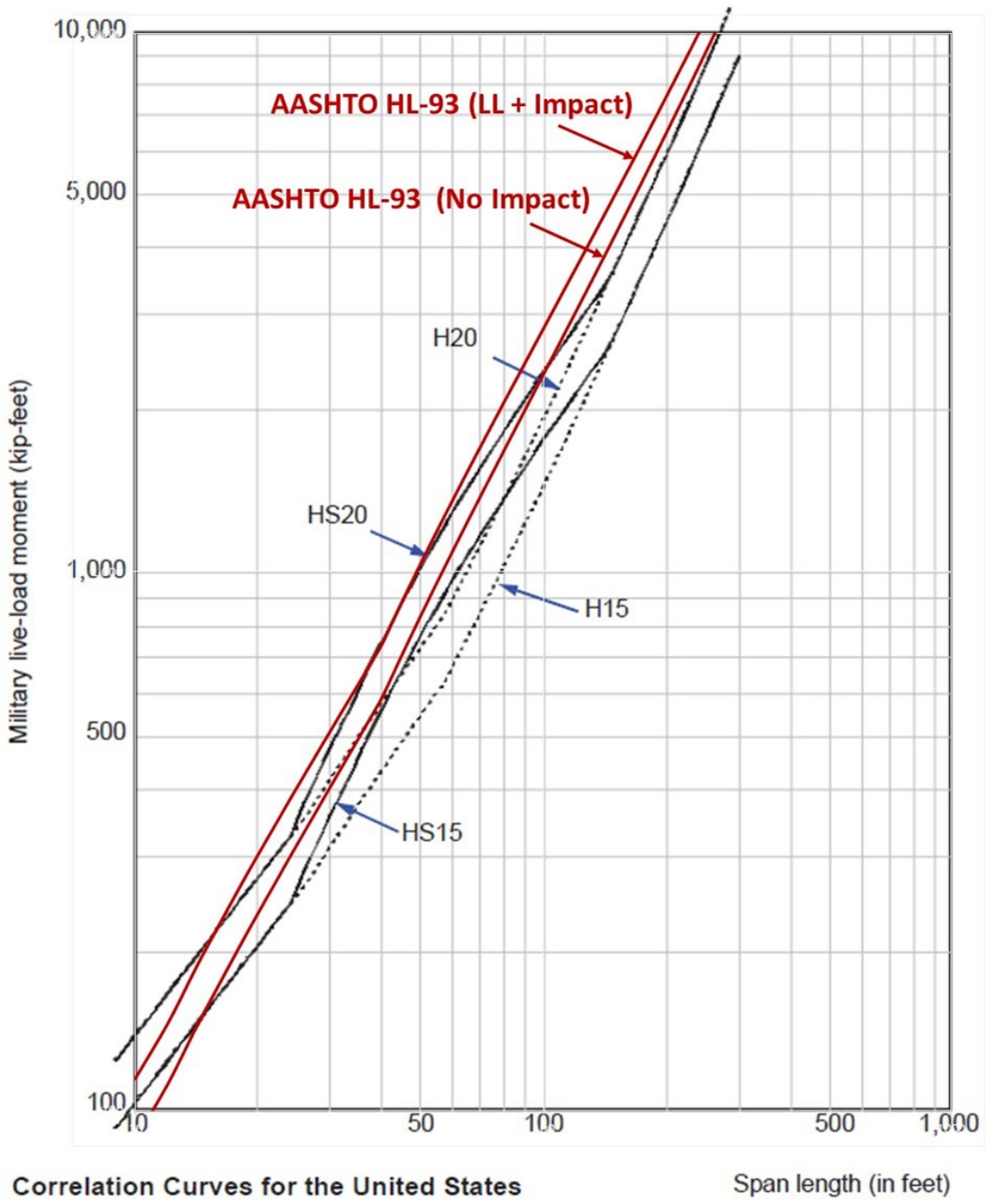

Figure 3-5: FM 3-34.343 Correlation Curves For United States Highway Bridges with Superimposed AASHTO HL-93 Live Load Moment Curves[11]

3.7 CHAPTER THREE END NOTES

1. North Atlantic Treaty Organization (NATO) Standardization Agency (2002), Standardization Agreement (STANAG) 2021, 6th Ed., Brussels, Belgium.

2. U.S. Department of the Army (2002), Military Non-Standard Fixed Bridging (FM3-34.343), Washington, DC.

3. U.S. Department of the Army (2002), page B-2.

4. U.S. Department of the Army (2002), page B-3.

5. U.S. Department of the Army (2002), page B-4.

6. U.S. Department of the Army (2002), page B-5.

7. U.S. Department of the Army (2002), page B-18.

8. U.S. Department of the Army (2002), page B-17.

9. U.S. Department of the Army (2002), page B-16.

10. U.S. Department of the Army (2002), page B-15.

11. U.S. Department of the Army (2002), page 3-4.

CHAPTER 4: ANALYSIS DESIGN AND DEVELOPMENT

4.1 PROBLEM STATEMENT

The initial task of the analysis was the determination of the assumptions and equations available to solve the stated problem. Once the assumptions and equations were identified, the methods by which the equations would be solved were established for both single span simple beams and a specific type of a continuous beam.

4.2 DEVELOPMENT OF ANALYSIS METHODOLOGY

Several programs have been established and approved for use by various agencies for the determination of AASHTO HL-93 loadings. For example in the State of Louisiana, the computer programs approved for bridge design are shown on Table 4-1.

None of these programs were available to the author; therefore, an independent, original method of calculation was developed to allow for the numerical solution of analytical models, versus hand calculations for each condition to be examined. Based on computational methods available, it was determined to develop a Microsoft Excel (subsequently referred to as MS EXCEL) spreadsheet to perform the required numerical calculations based on classical mechanics and the principle of superposition. Influence line analysis has been extensively used by other researchers and is discussed in several of the references.[1] The classical mechanics method was used for this study to mitigate the difficulties determining load factor ratios based on superposition of influence lines, as the analysis model was expanded to include an large number of axle loads.

Software Name	Developer
AGi32	Lighting Analysts, Inc.
Brass-Culvert	Wyoming Dept. of Transportation
Bridge Design	AASHTOware
Bridge Rating	AASHTOware
ConSpan	Bentley LEAP
CSiBridge/SAP2000/CSiCOL	Computers and Structures, Inc.
FB-Multipier	BSI/Univ. of Florida
LEAP Bridge Enterprise	Bentley LEAP
L-Pile	ENSOFT, INC.
LUSAS	LUSAS
MDX	MDX
Midas Civil	MIDASoft
PCA Column	PCA/Structure Point
RC-Pier	Bentley LEAP
SABRE	Univ. of Maryland
Smart Bridge Suites	SDR
SolidWorks	MLC CAD Systems
STAAD	Bentley
STAAD Sectionwizard	Bentley
STAAD.Beava	Bentley
Visual	Acuity Brands Lighting

Table 4-1: Approved Software for Use in Bridge Design in Louisiana[2]

The development of the superposition composite model began by complying and verifying the classic solutions for individual load cases from various sources. All of the load cases for single spans were reduced to a simply supported beam with a combination of a uniform load and multiple concentrated loads acting on the span. The uniform load applied represented the continuous lane loading created by an evenly spaced train of specified standard vehicles. Multiple concentrated loads represented the specified axles of a design vehicle which was either actual or hypothetical. These concentrated loads were spaced at set distances corresponding to the specified design vehicle. The key aspect of the development of an independent, original

method was the determination of the maximum moments acting on the simply supported beam based on the load configuration. This classical method was used by the author instead of an influence line analysis due to the ease of the developing the calculation spreadsheets using this methodology. The author determined that for this analysis, the use of explicit equations along with the principle of superposition and the use of graphical methods using basic mechanics would provide the most supportable, and robust methodology for developing a Microsoft EXCEL spreadsheet platform for numerical computation.

The classical explicit, derived solutions for a simple beam with a uniform distributed load and concentrated load acting at any point along the span are shown on Figures 4-1 and 4-2.

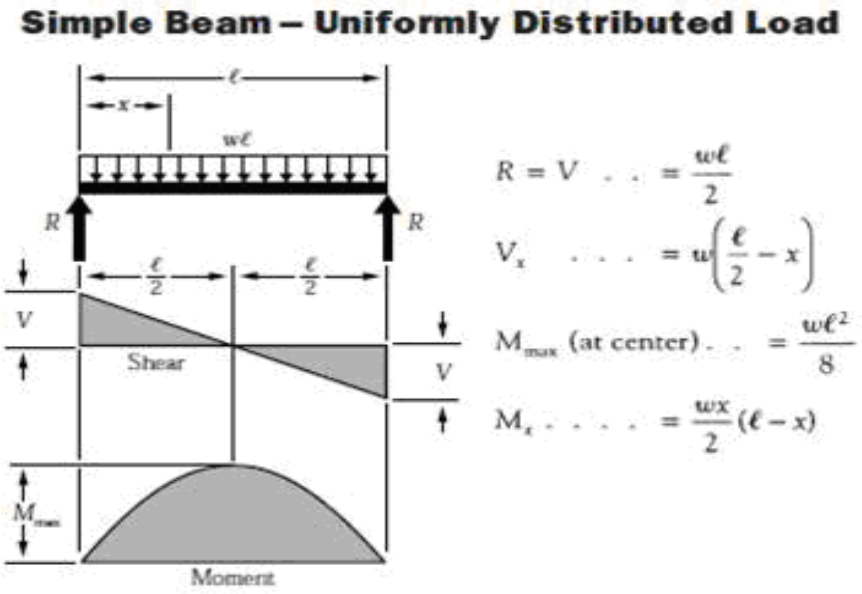

Figure 4-1: Explicit Solutions for Uniformly Distributed (Lane) Loading on a Simple Beam[3]

The axle spacing, along with the uniformly distributed lane load, and the loadings per axle, are set by the specified design load conditions, therefore the only variables for the proposed simple beam analysis were the span (beam) length and the position of the design axle loads along

the span. The vehicular position for maximum bending moment was assumed to be unknown and therefore was determined by independent calculation. The determined location was then compared to confirmed, tabulated AASHTO HL-93 maximum design moments. The determined location was also compared to the location sometimes specified as a theoretical maximum moment location derived from classical mechanics.[4]

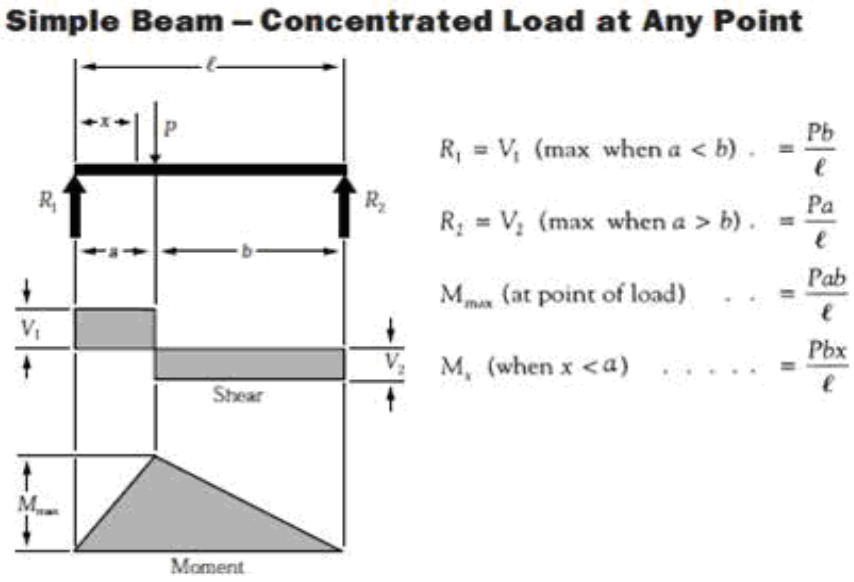

Figure 4-2: Explicit Solutions for a Concentrated (Axle) Load on a Simple Beam[5]

The methodology of the independently developed numerical method uses the principle of superposition to determine the maximum moment for various loadings on a single span simple beam. The independently developed numerical method for maximum moment along the span is illustrated with the following example utilizing a combination of a uniform lane loading with three concentrated axle loads to represent a hypothetical vehicle loading on a simply supported single span as shown in the Figure 4-3. The vehicle load will be advanced along the span

length in order to compare the changes in calculated shear and moment based on different vehicle locations along the span.

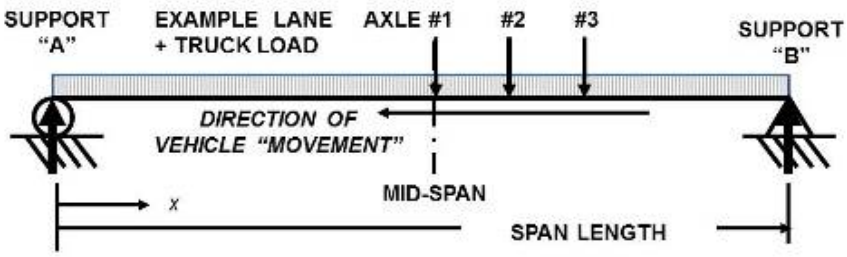

Figure 4-3: Illustration of Loading Used for Explicit Maximum Moment Calculation

The methodology used for the analysis involved three steps. The first step was to determine the shear at each end support using static equilibrium equations. The second step was to determine the maximum and minimum shear at each discrete axle locations by applying the uniform loading and the axle concentrated according to classical mechanics. The final step consisted of using the calculated shear values and the known distance from each end support for each axle to calculate the moment areas along the span. Moments at the various discrete axle locations were calculated by summation of the calculated moment areas along the span to that discrete location. The calculated shears and moments were considered correct if the results balanced; in other words if the calculated moments at each end support summed to zero.

The hypothetical lane loading and the concentrated loads representing the hypothetical vehicle axle loads were separated into individual discrete loadings and solved using explicit equations for both shear and moment, and combined using superposition.

The case of maximum shear can be solved using elementary mechanical analysis. In most cases, the rear axle or combination of rear axles of a hypothetical vehicle is greater than or equal to the front axle or combination of front axles. Therefore, the maximum shear will be

obtained when the hypothetical vehicle or design truck load is positioned so that the entire vehicle load is acting on the beam and the rear axle is acting at one end support.

4.3 METHODOLOGY FOR SINGLE SPAN SIMPLE BEAMS

As stated in the introduction, the analysis included the application of the independently developed numerical method to an equal span continuous beams, but only the results for simple beams is presented for brevity in this study.

The first simple beam analysis conducted was for the AASHTO HL-93 loading, both with and without dynamic loading. Although none of the approved AASHTO HL-93 programs were available to the author, tabulated design values were provided by the California Department of Transportation (CALTRANS) on-line, and these CALTRANS maximum shear and moment values were used to validate the analysis methodology using the MS EXCEL spreadsheet platform for numerical computation. The analysis included five possible vehicle positions near mid-span and the maximum shear vehicle position on a simple span. These five positions near mid-span were used to determine the location of the vehicle relative to mid-span that would result in the maximum mid-span moment and the maximum absolute moment on a simple beam for the HL-93 live loading. For the analysis, the term "xR" refers to the distance between the calculated resultant of the design truck load and the nearest axle, which for the AASHTO HL-93 design truck load is the middle (#2) axle as shown in Figure 4-4.

For the determination of the vehicle position along the span which results in the maximum moment, HL-93 live loading and all subsequent hypothetical vehicle and other design loadings were analyzed using a span length of 100 ft. In most cases, the determined vehicle position was verified with follow-on calculations for span lengths up to 1,000 ft.

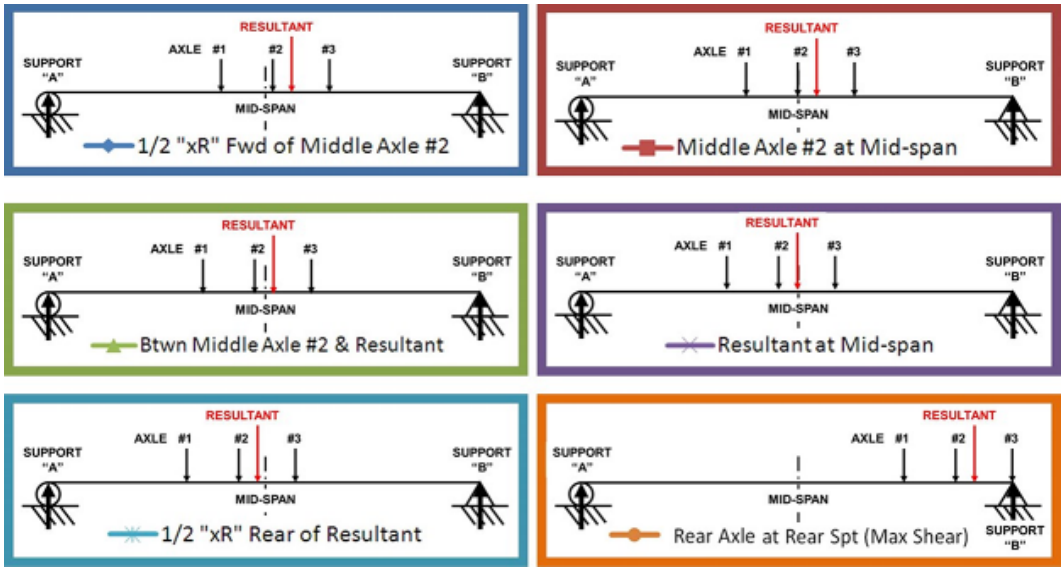

Figure 4-4: Possible Loadings for Determining Maximum Moment and Shear for AASHTO HL-93 Live Load

The intent of the next phase of the analysis was to verify the tabulated values provided in the STANAG/FM for Military Load Class (MLC) hypothetical tracked and wheeled vehicles. STANAG tabulated MLC Tracked (MLC-T) shear and moment values were calculated using explicit equations for uniformly distributed load of a discrete length (less than total span length) partially distributed on a simply supported beam, as shown below. For maximum moment, this uniform distributed load is centered at mid-span, as shown in Figure 4-5. The maximum shear was calculated using the full length of the uniformly discrete distributed loading located at one end of the beam (c = 0 for the free body diagram shown on Figure 4-5).

For the STANAG/FM tabulated MLC Wheeled (MLC-W) values, the focus of the analysis was on military vehicles of greater live load than civilian vehicles, particularly the maximum legal load of 80 kips (355.8 kN). Therefore, the analysis neglected vehicles of a load classes lower than MLC 40 and greater than MLC 120. The MLC 150 hypothetical tracked and

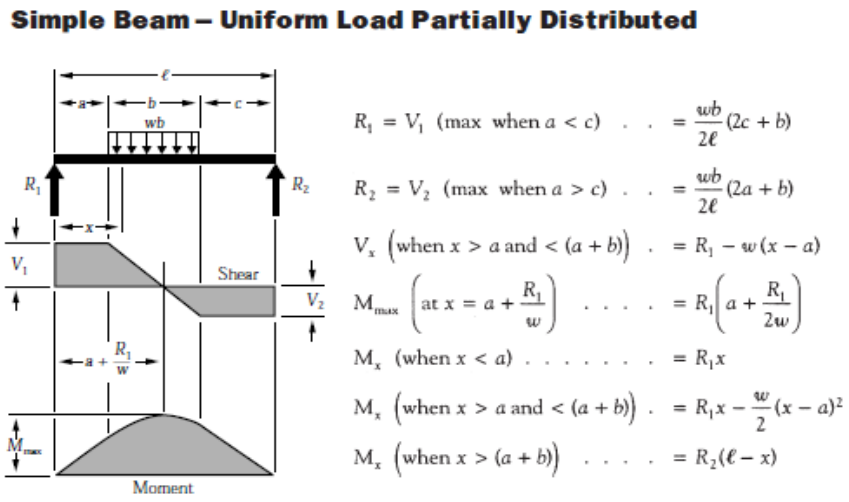

Figure 4-5: Explicit solution for moment and shear for MLC Tracked vehicles[6]

wheeled vehicles were neglected for this analysis since this class vehicle would not be expected to be moved over long distances using surface transportation on the national highway system. The MLC 120 hypothetical tracked and wheeled vehicles were included to provide an upper boundary for comparison over MLC 100; however, these vehicles are also considered unlikely to be traveling on the national highway system for a significant distance.

Similar to the earlier HL-93 analysis, an analysis conducted was to determine and verify the vehicle position along the span for maximum moment. Again, five possible vehicle positions near mid-span were used to determine the location of the vehicle relative to mid-span that would result in the maximum mid-span moment and the maximum absolute moment on a simple beam. The free body diagrams used for the hypothetical MLC vehicles are depicted on Figure 4-6. For the determination of the vehicle position along the span which results in the maximum moment, all hypothetical vehicles were first analyzed using a span length of 100 ft (30.5 m). The maximum shear was calculated based on the vehicle being positioned with the heaviest end axle over the left support. For the four axle MLC hypothetical vehicles (MLC 40-50W), the five

possible vehicle locations for maximum moment and maximum shear are shown of Figure 4-7. For the five axle MLC hypothetical vehicles (MLC 60 - 120W), the five possible vehicle locations for maximum moment and maximum shear are shown of Figure 4-8. The colors used for the various different vehicle locations on Figures 4-7 and 4-8 correspond to similar color schemes for the graphical results presented in the Microsoft EXCEL analysis solutions.

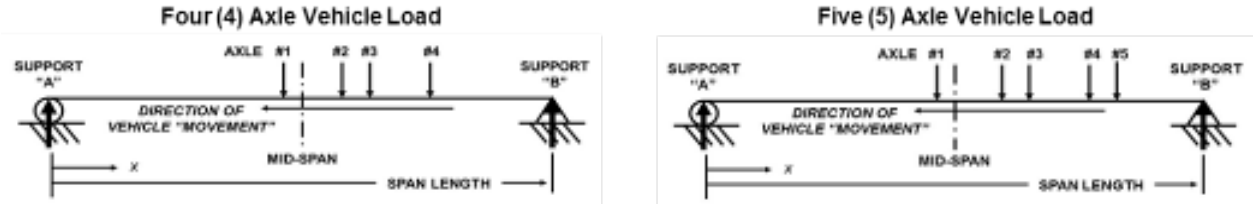

Figure 4-6: Free Body Diagrams for 4 and 5 Axle Hypothetical Vehicles

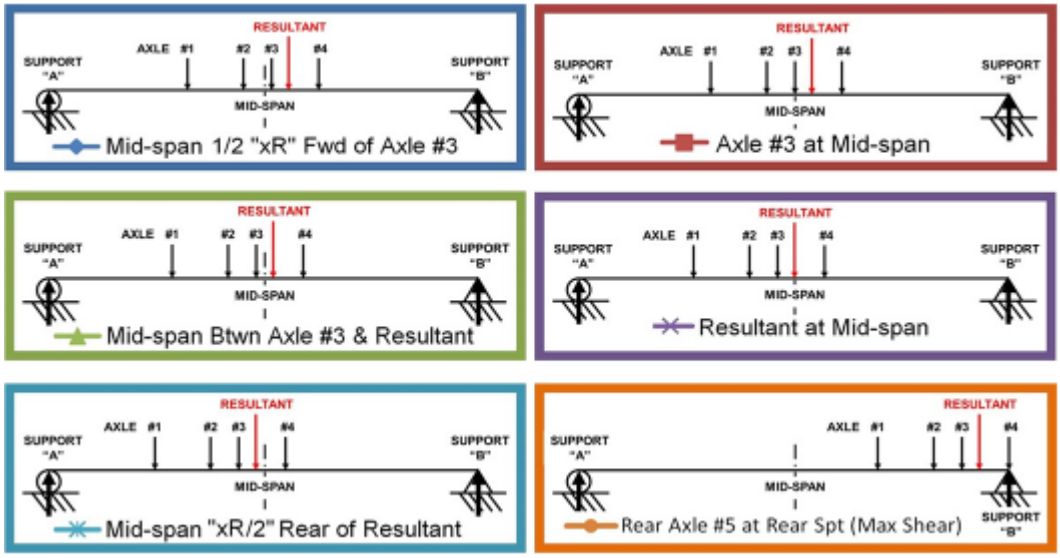

Figure 4-7: Possible Maximum Moment and Shear Locations, 4 Axle Vehicles

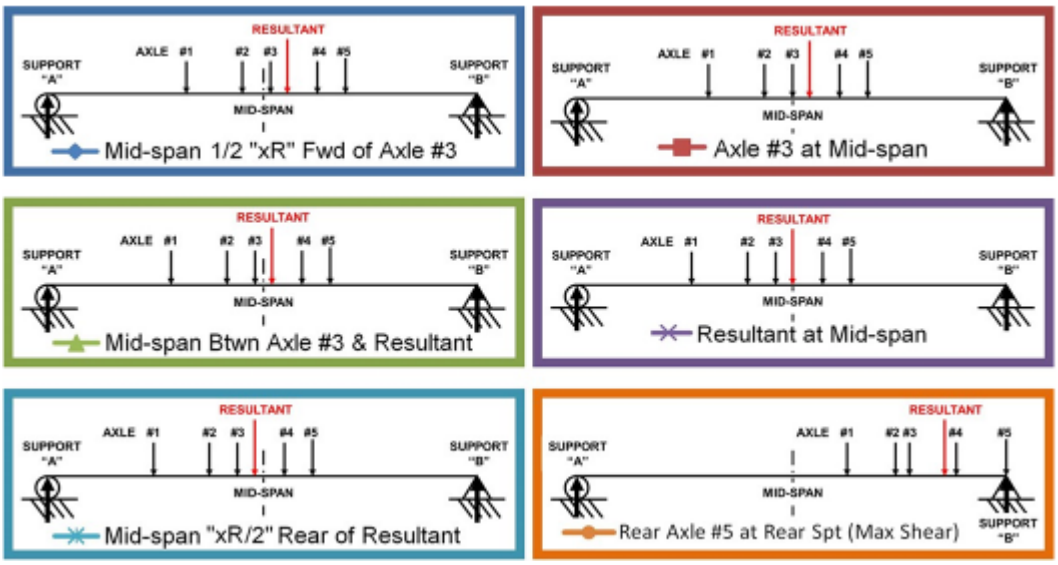

Figure 4-8: Possible Maximum Moment and Shear Locations, 5 Axle Vehicles

In addition to the determination of maximum moment and maximum mid-span moment for AASHTO HL-93 live load and the STANAG/FM hypothetical MLC Wheeled (MLC-W) vehicles, the two five axle Canadian Bridge Design Codes, the Ontario Highway Bridge Design (OHBD) and the Canadian Highway Bridge Design Code, CAN/CSA-S5-06, condition CL-W, were also analyzed to verify vehicle load positioning for maximum moment and maximum mid-span moment. The five axle free body diagram and possible vehicle locations were used for these analyses. The hypothetical 5-axle permit vehicle, proposed by Zhao and Tabatabai (2012) as an adjunct to the Wisconsin Special Permit Vehicle (Wis-SPV), was also analyzed using the five axle free body diagram and possible vehicle locations.

In order to validate the use of the hypothetical MLC 100W vehicle as the baseline for this analysis, two known and one proposed nine axle heavy military equipment transporters corresponding to real world MLC 100W class vehicles were also analyzed. All three vehicles consisted of a four axle tractor and a five axle trailer tractor and trailer combination, for a total of

nine axles. The increased axles required the development of an expanded numerical spreadsheet from five to nine axles, resulting in more numerical complexity of the shear and moment calculations using classical mechanics.

The first known nine axle vehicle combination was the U.S. Army Heavy Equipment Transporter (HET) provided in Annex E of STANAG 2021 Edition 6.[7] The vehicle combination consists of the M-1070 tractor and M-1000 semi-trailer, and is shown in Figure 4-9. For this vehicle load, the overall combined axle weights and positions are (taken from the standard NATO agreement, or STANAG): axle loads of 9.389 metric tonne (t) (20.7 kips; 92.1 kN) on the forward axle, followed by axles of 10.384 t (22.9 kips; 101.8 kN), 9.768 t (21.5 kips; 95.8 kN), 9.045 t (19.9 kips; 88.7 kN), 12.773 t (28.2 kips; 125.3 kN), 12.519 t (27.6 kips; 122.8 kN), 12.519 t (27.6 kips; 122.8 kN), 14.016 t (30.9 kips; 137.4 kN), and 13.925 t (30.7 kips; 136.6 kN) on rear axle, with corresponding axle spacings of 3.962 m, 1.537 m, 1.549 m, 4.547 m, 1.842 m, 1.829 m, 1.829 m, 1.842 m (13 ft, 2 x 5 ft, 15 ft, 4 x 6 ft). The vehicle width is specified as 3.66 m (12 ft).

Figure 4-9: STANAG 2021 U.S. Army Heavy Equipment Transporter

The next known nine axle vehicle combination considered was the U.S. Army HET specified in the Kansas Department of Transportation (KS DOT) Bridge Design manual[8] which is shown on Figure 4-10. A simplified HET vehicle loading was developed using axle loads totaling 230 kips (1,023 kN) using only axle loads of 20 or 30 kips (89 or 133.4 kN), as shown on Figure 4-11.

All three vehicles required confirmation of the positioning of the vehicle along the span length for maximum moment. In this case, because the length of the vehicles is greater than half the span lengths for a 100 ft (30.5 m) span, the analysis to determine the location of the maximum moment was conducted on a span length of 300 ft (91.4 m). The maximum shear was calculated with the rear axle located over the left support.

All three vehicles required confirmation of the positioning of the vehicle along the span length for maximum moment. In this case, because the length of the vehicles is greater than half the span lengths for a 100 ft (30.5 m) span, the analysis to determine the location of the maximum moment was conducted on a span length of 300 ft (91.4 m). The maximum shear was calculated with the rear axle located over the left support.

Following the expansion of the numerical analysis for nine axle vehicle combinations, the numerical spreadsheet was further expanded for ten and fifteen axle vehicles. The intent of the ten axle spreadsheet was used to conduct an analysis of the Louisiana Department of

Transportation (LA DOTD) Special Design Vehicle No. 5 (LASDV-5) shown on Figure 4-12.[9] The LASDV-5 is the LA DOTD permit vehicle most closely corresponding to the U.S. Army HET. Following the determination of vehicle positioning of the span for maximum moment, the maximum shear and moment for the LASDV-5 was calculated for span lengths of

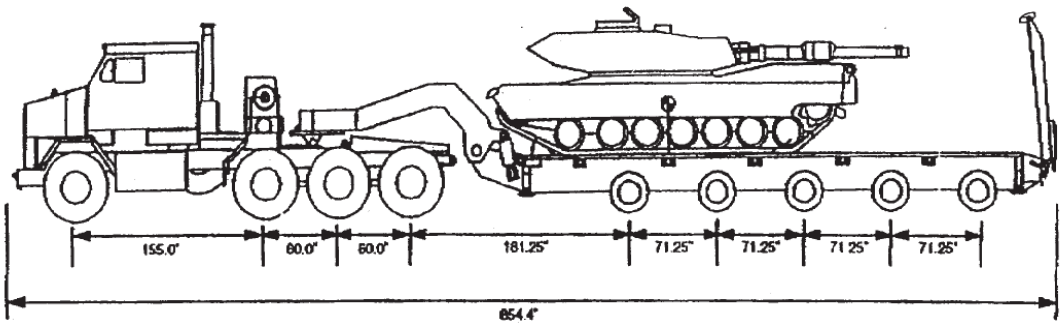

AXLE NUMBER:	1	2	3	4	5	6	7	8	9	TOTAL
TIRES PER AXLE: 2/	2	2	2	2	8	8	8	8	8	48
EMPTY LOAD: 3/ (pounds (tons))	19,450 (9.7)	10,750 (5.4)	10,175 (5.1)	10,075 (5.1)	6,450 (3.2)	6,550 (3.3)	6,250 (3.1)	10,650 (5.3)	10,450 (5.2)	90,800 (45.4)
64.5-TON LOAD: 4/ (pounds (tons))	21,477 (10.7)	21,346 (10.7)	21,163 (10.6)	19,128 (9.6)	25,385 (12.7)	27,835 (13.9)	26,291 (13.1)	27,420 (13.7)	29,754 (14.9)	219,800 (109.9)

	M1070 Truck Tractor	M1000 Semitrailer	M1A1 / M1A2 Tank
WIDTH	102"	144"	144" / 144"
HEIGHT	144.16"	43" (cargo bed) 143.14" (overall)	113.7" / 121.1 (trailer with tank: 156.7" / 164.1)

NOTES:
1/ The axle loads are approximations. The only accurate way to determine axle loads is to measure the system.
2/ M1070 Tire size - 16.00R20XZLT LRM
Cross country - 55psi
Highway - 75 psi
M1000 Tire size - 215/75R 17.5xXTA(135J)LRH - 95 psi
3/ Axle loads are based on measured data.
4/ Axle loads are based on calculated data.

M1070/M1000 HEAVY EQUIPMENT TRANSPORTER WITH M1A1/M1A2 TANK 1/

Figure 4-10: Kansas DOT U.S. Army Heavy Equipment Transporter

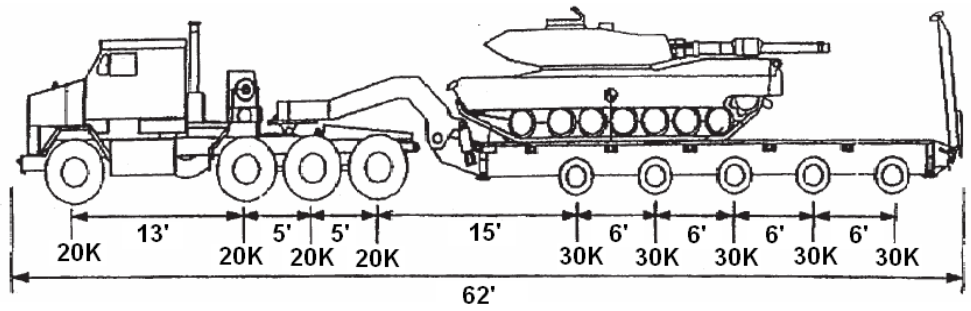

Figure 4-11: Proposed simplified U.S. Army Heavy Equipment Transporter

100-1,000 ft (30.5-304.8 m). This analysis was conducted but has been superseded by the new Louisiana Design Vehicle Live Load 2011 (LADV-11) of the LA DOTD Bridge Design and Evaluation Manual (BDEM) of March 2015, previously discussed in Chapter 3.

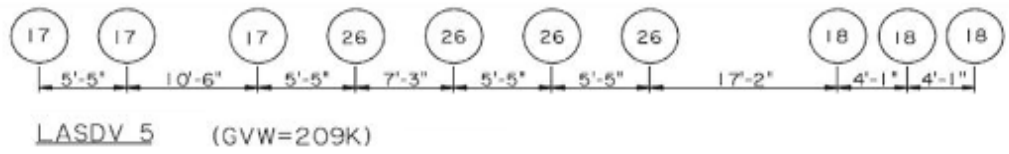

Figure 4-12: Louisiana Special Design Vehicle Type Five (LASDV-5)

The second use of the ten axle analysis was to calculate the maximum moment and shear for two five axle MLC-100W vehicles on span lengths of 386 - 1,000 ft (118 – 304.8 m). A span length of 386 ft (118.0 m) corresponds to the minimum span length two MLC-100W vehicles occupy at the same time assuming a vehicle spacing of 300 ft (91.4 m) between the rear axle of the first vehicle and the front axle of the second vehicle.

The numerical analysis was expanded to fifteen axles to account for three MLC-100W vehicles on very long spans of 730 - 1,000 ft (222.5 – 304.8 m), although simple spans of these span lengths are not applicable to the North American highway bridge existing inventory or new construction based on the review of existing literature. As with the two MLC-100W vehicle analysis, the minimum span length for three MLC-100W separated by interval of 300 ft (91.4 m) between rear and front axles is 730 ft (222.5 m).

In addition to the various design live loadings and vehicle axel loads, two saturated flow conditions were also analyzed. One case utilized the saturated flow, or the so-called traffic jam condition, derived by Lutomirksa.[10] The other case utilized an independently derived uniform saturated flow condition corresponding to logistic convoy conditions witnessed during military operations.

The Lutomirksa saturated flow condition is based on a truck train of AASHTO LRFD legal load trucks, Type 3-3 Units, placed in a lane with the clearance distance of 10 to 15 ft (3.0 to 4.6 m). The saturated flow is also called the forced flow condition and represents vehicles moving at crawl speeds with intermittent halts and pauses. Therefore, the distance between the last axle of one truck and first axle of the following truck was assumed to be 20-25 ft (6.1-7.6 m) as shown is Figure 4-13.

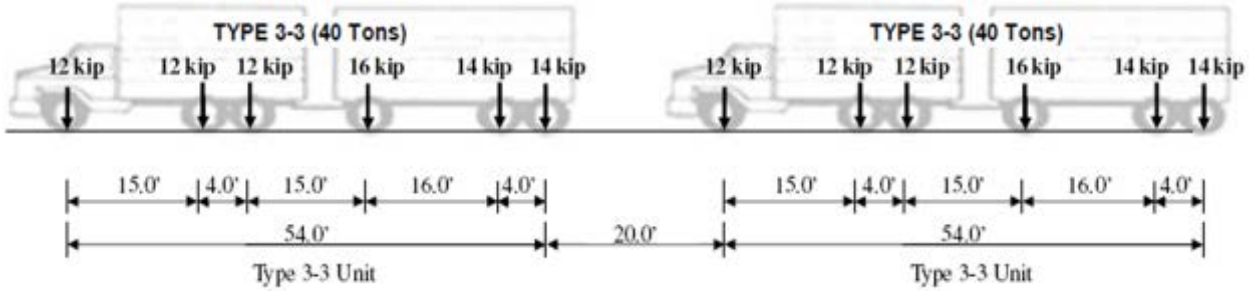

Figure 4-13: Saturated Traffic Flow Condition

For the worst case scenario, the uniform loading for the truck train is equal to:

80 kips / (54+20) ft = 1.08 kip/ft (15.8 kN/m) for clearance distance of 10 ft (3.0 m)

Since the value obtained in this way is based on heavy trucks and is very conservative, a factor of 75% is applied to this uniform loading and conforms to the basic philosophy used to develop the AASHTO HL-93 lane load of 0.64 kip/ft (9.3 kN/m).

Therefore: 0.75 x 1.08 kip/ft = 0.81 kip/ft (11.8 kN/m)

It is important to note that the vehicle spacing was confirmed by Dr. Lutomirksa using an analysis of various Weight-in-Motion (WIM) survey data for traffic flow at reduced speeds.

The (stopped) saturated flow condition observed for contracted host nation civilian convoys during logistical operations in Kuwait and Iraq more closely correspond to a truck train of AASHTO LRFD Type 3S2 trucks placed in a lane with the clearance distance between the last axle of one truck and first axle of the following truck of 15 ft (4.6 m) shown in Figure 4-14. This close spacing was due to observed tendency of truck drivers to narrow the gaps between vehicles to prevent non-convoy vehicle drivers from attempting to merge into the convoy formation.

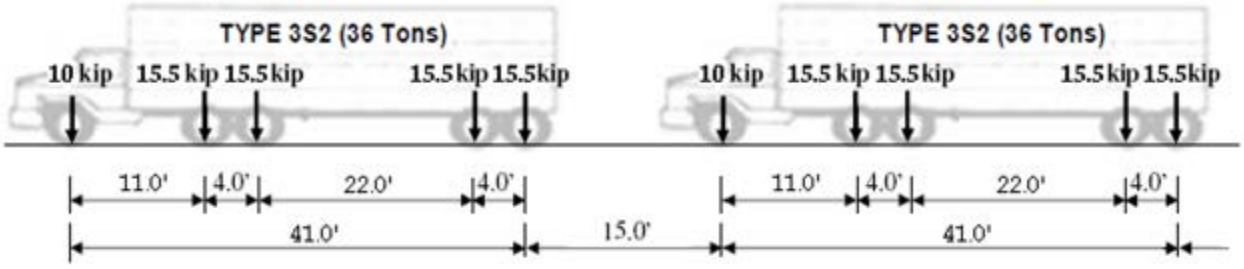

Figure 4-14: Observed Military Logistical Convoys Saturated Flow Condition

The GVW of an AASHTO LRFD legal load Type 3S2 truck is 72 kips (320.3 kN) and the total length is 41 ft (12.5 m), therefore the equivalent uniform loading for the truck train is:

72 kips / (41+15) ft = 1.286 kip/ft (18.8 kN/m)

Again applying a factor of 75% based on the basic philosophy used to develop AASHTO HL-93 lane load of 0.64 kip/ft, yields

0.75 x 1.286 kip/ft = 0.965 kip/ft (14.1 kN/m)

These calculations complete the calculations for simply supported, single spans.

4.4 CHAPTER FOUR END NOTES

1. Turer, A. and Aktan, A.E. (1999), "Issues in Superload Crossing of Three Steel Stringer Bridges in Toledo, Ohio", Pages 775-779 and Vigh, A. and Kollar, L.P. (2007), "Routing and Permitting Techniques of Overweight Vehicles", page 92.

2. Louisiana Department of Transportation and Development, Bridge Design Section, Pre-Approved Software List, Updated: September 7, 2016 (URL http://wwwsp.dotd.la.gov/Inside_LaDOTD/Divisions/Engineering/Bridge_Design/QCQA/Pre-Approved%20Software%20List.pdf, last accessed April 29, 2018). See also Louisiana Department of Transportation and Development (LADOTD) (2015), Bridge Design and Evaluation Manual (BDEM), page I.Ch3-7.

3. American Forest and Paper Association (2007), Beam Design Formulas with Shear and Moment Diagrams, Figure 1, page 4.

4. Tonias, D.E. and Zhao, J.J. (2007), *Bridge Engineering (2nd Edition)*, Figure 3.32, page 174.

5. American Forest and Paper Association (2007), Figure 8, page 7.

6. American Forest and Paper Association (2007), Figure 2, page 4.

7. North Atlantic Treaty Organization (NATO) Standardization Agreement (STANAG) 2021, 6th Ed., Brussels, Belgium, Annex E, page 3/7.

8. Kansas Department of Transportation (2011), Design Manual, Volume III US (LRFD) Bridge Section, Topeka, KS, page 3-3-7.

9. Louisiana Department of Transportation and Development (LA DOTD) (2015), Bridge Design and Evaluation Manual (BDEM), Figure 1.2.2-1, page IV.Ch1-2.

10. Lutomirska, M. (2009), "Live Load Models for Long Span Bridges", Figure 5.7, page 65.

CHAPTER 5: RESULTS AND DISCUSSION OF PRIMARY ANALYSES

5.1 OVERVIEW

The development of the computational spreadsheets used in this study will be discussed in this chapter, along with the various modifications added to the computations during the progress of analyses. The results of the analyses will be used to assess the validity of using a new alternate military live loading for highway bridges. Some results of the analyses are presented in tabular form, however the bulk of the results are presented in graphical form to summarize the large amount of data being presented. The actual calculation spreadsheets are included as appendices to this report and are available upon request in either electronic or printed versions. These spreadsheets were developed from 2012 to the present. Therefore the calculations, tabulated results and figures shown in this thesis are not contained in a single file, nor follow a linear progression within a single or multiple files. The name designations of the files used as the source data for the various tables and figures in this and subsequent chapters of this study are provided in appendix. Printed results for all analyses are available upon request.

5.2 VERIFICATION OF AASHTO HL-93 LIVE LOADING

After an initial spreadsheet was developed, the first objective of the analyses was to validate the calculated results using the methodology described in the previous chapter against known values. Validation was accomplished using the bridge design guides produced by the California Department of Transportation (CALTRANS) that provided tabulated values for the HL-93 maximum moment and shear both with and without dynamic load allowance (hereafter referred to as the CALTRANS values). Span lengths of 30-300 ft (9.1–91.4 m) were calculated using the spreadsheet and compared to the CALTRANS provided design values. Excerpts from

the CALTRANS bridge design guides are shown on Figure 5-1 and 5-2, with no dynamic impact load allowance and with the AASHTO specified 33% dynamic impact load allowance respectively. Representative span lengths of 100 ft (30.5 m) and 200 (61.0 m) ft will be used for comparison with the calculated results.

LRFD

BRIDGE DESIGN AIDS • FEBRUARY 2008

Table of Maximum Moments, Shears, and Reactions Simple Spans, One Lane **Without** Dynamic Load Allowance (cont.)

Span(ft)		Moment (k-ft)		End Shear and End Reaction (k)		Span(ft)		Moment (k-ft)		End Shear and End Reaction (k)	
42	———	617.1	a	69.4	a	100	———	2320.0	a	97.3	a
44	———	666.9	a	70.8	a	110	———	2668.0	a	101.1	a
46	———	717.3	a	72.1	a	120	———	3032.0	a	104.8	a
48	———	768.3	a	73.4	a	130	———	3412.0	a	108.4	a
50	———	820.0	a	74.6	a	140	———	3808.0	a	112.0	a
52	———	872.3	a	75.7	a	150	———	4220.0	a	115.5	a
54	———	925.3	a	76.8	a	160	———	4648.0	a	119.0	a
56	———	978.9	a	77.9	a	170	———	5092.0	a	122.4	a
58	———	1033.1	a	79.0	a	180	———	5552.0	a	125.9	a
60	———	1088.0	a	80.0	a	190	———	6028.0	a	129.3	a
62	———	1143.5	a	81.0	a	200	———	6520.0	a	132.6	a
64	———	1199.7	a	82.0	a	220	———	7552.0	a	139.3	a
66	———	1256.5	a	82.9	a	240	———	8648.0	a	146.0	a
68	———	1313.9	a	83.9	a	260	———	9808.0	a	152.6	a

Figure 5-1: California Department of Transportation Bridge Design Aid (2008), Tabulated HL-93 Values without Dynamic Load Allowance[1]

Table of Maximum Moments, Shears, and Reactions Simple Spans, One Lane **With** Dynamic Load Allowance (cont.)

Span(ft)		Moment (k-ft)		End Shear and End Reaction (k)		Span(ft)		Moment (k-ft)		End Shear and End Reaction (k)	
42	————	774.2	a	87.9	a	100	————	2821.6	a	118.8	a
44	————	835.8	a	89.5	a	110	————	3229.0	a	122.8	a
46	————	898.1	a	91.1	a	120	————	3652.4	a	126.7	a
48	————	961.0	a	92.5	a	130	————	4091.8	a	130.5	a
50	————	1024.6	a	93.9	a	140	————	4547.2	a	134.2	a
52	————	1088.8	a	95.2	a	150	————	5018.6	a	137.8	a
54	————	1153.6	a	96.5	a	160	————	5506.0	a	141.4	a
56	————	1219.1	a	97.7	a	170	————	6009.4	a	144.9	a
58	————	1285.2	a	98.9	a	180	————	6528.8	a	148.4	a
60	————	1352.0	a	100.1	a	190	————	7064.2	a	151.9	a
62	————	1419.4	a	101.2	a	200	————	7615.6	a	155.3	a
64	————	1487.4	a	102.3	a	220	————	8766.4	a	162.1	a
66	————	1556.1	a	103.3	a	240	————	9981.2	a	168.8	a

Figure 5-2: California Department of Transportation Bridge Design Aid (2008), Tabulated HL-93 Values with Dynamic Load Allowance[2]

Maximum shear and moments for the HL-93 design truck and lane load were calculated using the developed spreadsheets for span lengths of 387. The maximum moments for the HL-93 design truck positioned at different possible locations near mid-span were calculated for the span lengths. The results are shown on Table 5-1. The CALTRANS design values are also included. The analysis results for the two representative span lengths of 100 ft (30.5 m) and 200

ft (61.0 m) maximum moments are shown of Figure 5-3 through 5-6, without and with dynamic impact respectively.

Maximum Moments for AASHTO HL-93 Design Truck and Lane Load, with Impact					
Span Length L, ft (m)	CALTRANS Design Values Mmax, ft-kips	Calculated Maximum Mid-span Moment Mmax, ft-kips (kN-m)	Calculated Absolute Maximum Moment on Span Mmax, ft-kips (kN-m)	Location of Calculated Absolute Maximum Moment on Span ft (m)	Calculated Mid-span Moment for Max Absolute Moment Condition Mmax, ft-kips (kN-m)
50 (15.2)	1,024.6 (1,389.2)	1,024.6 (1,389.2)	1,033.3 (1,401.0)	22.667 (6.909)	1,012.2 (1,372.4)
100 (30.5)	2,821.6 (3,825.6)	2,821.6 (3,825.6)	2,825.1 (3,830.3)	47.667 (14.529)	2,809.2 (3,808.7)
200 (61.0)	7,615.6 (10,325.3)	7,615.6 (10,325.3)	7,616.5 (10,326.4)	97.667 (29.769)	7,603.2 (10,308.4)
300 (91.4)	14,009.6 (18,994.2)	14,009.6 (18,994.2)	14,009.6 (18,994.2)	147.667 (45.009)	13,997.2 (18,977.4)
400 (121.9)		22,003.6 (29,832.5)	22,003.2 (29,831.9)	197.667 (60.250)	21,991.2 (29,815.7)
500 (152.4)		31,597.6 (42,840.1)	31,596.9 (42,839.1)	247.667 (75.490)	31,585.2 (42,823.2)
600 (182.9)		42,791.6 (58,016.9)	42,790.7 (58,015.7)	297.667 (90.730)	42,779.2 (58,000.1)
700 (213.4)		55,585.6 (75,363.0)	55,584.6 (75,361.6)	347.667 (105.970)	55,573.2 (75,346.2)
800 (243.8)		69,979.6 (94,878.4)	69,978.5 (94,876.9)	397.667 (121.210)	69,967.2 (94,861.5)
900 (274.3)		85,973.6 (116,563.0)	85,972.5 (116,561.5)	447.667 (136.451)	85,961.2 (116,546.2)
1,000 (304.8)		103,567.6 (140,417.0)	103,566.4 (140,415.3)	497.667 (151.691)	103,555.2 (140,400.2)

Table 5-1: Maximum Moments for AASHTO HL-93 Design Truck and Lane Load

As noted earlier, the maximum shear occurs when the last axle of the heavier end of the design truck load is directly over an end support of the simple beam. The maximum moment occurs when the design truck is positioned near the middle of the simple span. According to structural analysis theory, the maximum moment occurs when the design truck load is positioned

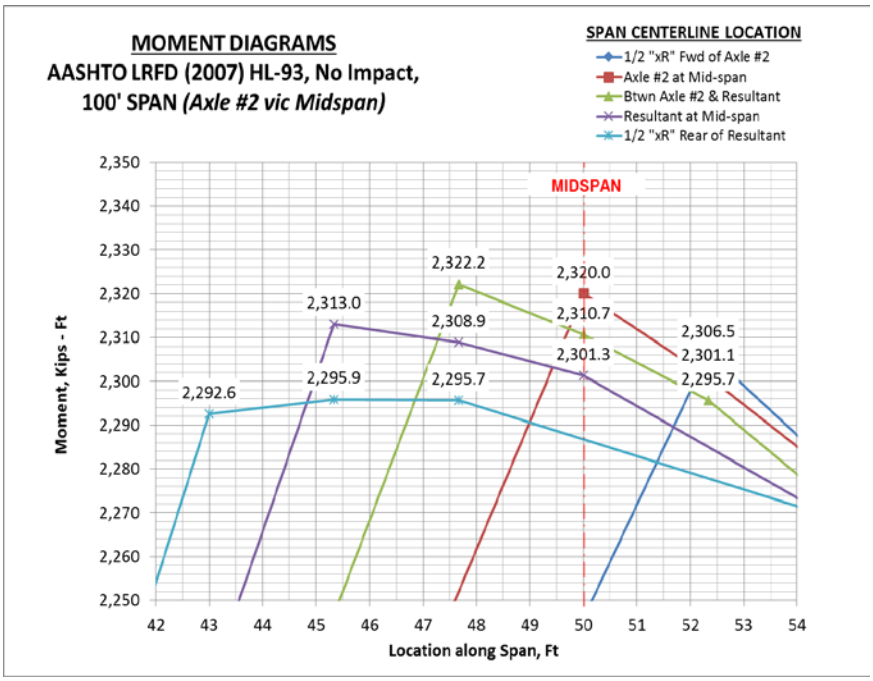

Figure 5-3: Calculated Moments for HL-93 Live Loading on a 100 ft (30.5 m) Simple Beam, Without Dynamic Load Allowance

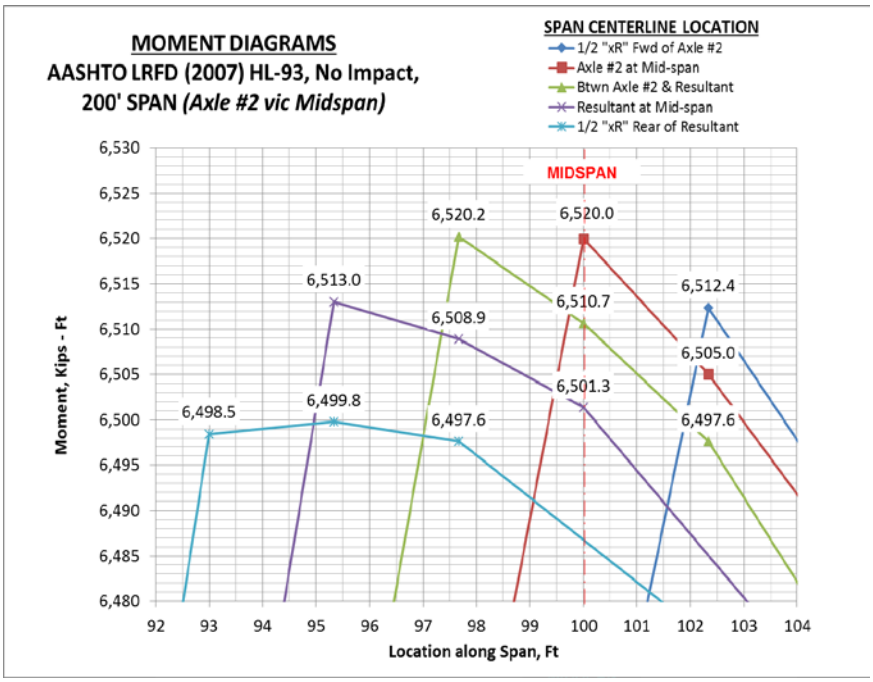

Figure 5-4: Calculated Moments for HL-93 Design Truck and Lane Load on a 200 ft (61.0 m) Simple Beam, without Dynamic Load Allowance

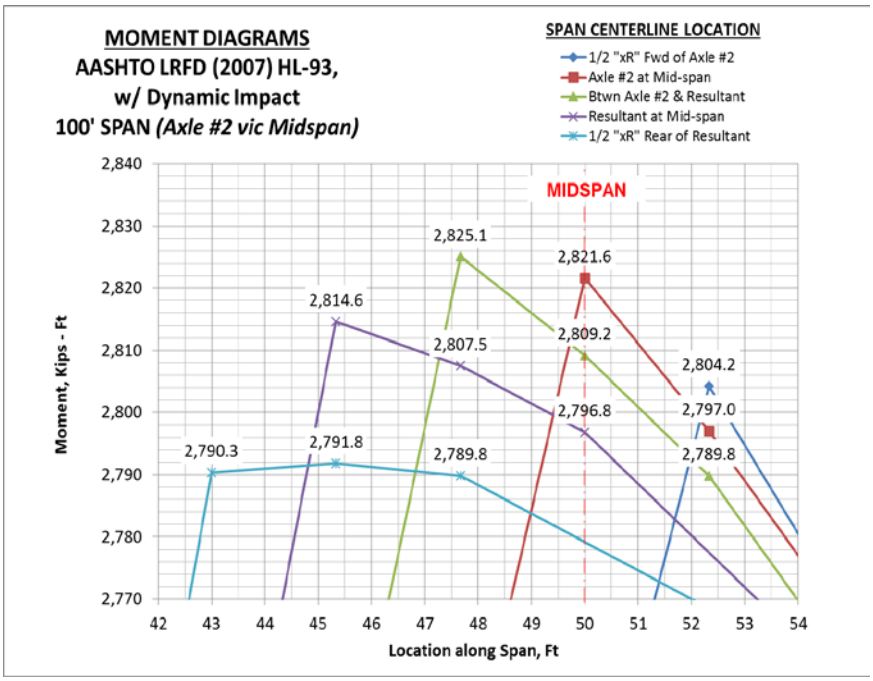

Figure 5-5: Calculated Moments for HL-93 Design Truck and Lane Load on a 100 ft (30.5 m) Simple Beam, with Dynamic Load Allowance

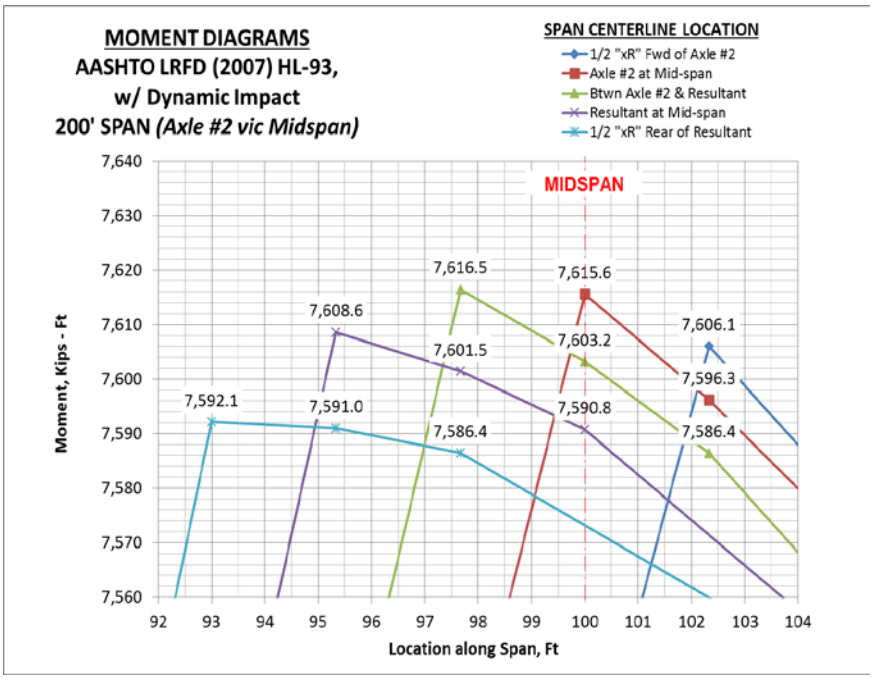

Figure 5-6: Calculated Moments for HL-93 Design Truck and Lane Load on a 200 ft (61.0 m) Simple Beam, with Dynamic Load Allowance

such that the resultant of the truck axle loads and the nearest axle are equidistant from the simple beam's mid-span.[3] This represents the maximum absolute moment, but not the maximum mid-span moment. The maximum mid-span moment must occur when the axle is positioned at the mid-span location, which is expected for a concentrated load on a simple beam.

Maximum End Shear (Vmax, kips)				Maximum Mid-Span Moment (Mmax, ft-kips)			
Span Length L, ft (m)	AASHTO HL-93 Design Truck and Lane Load, No Impact Vmax, kips (kN)	AASHTO HL-93 Design Truck and Lane Load, with Impact Vmax, kips (kN)	AASHTO Alternative Military Tandem (AMT) and Lane Load, with Impact Vmax, kips (kN)	Span Length L, ft (m)	AASHTO HL-93 Design Truck and Lane Load, No Impact Mmax, ft-kips (kN-m)	AASHTO HL-93 Design Truck and Lane Load, with Impact Mmax, ft-kips (kN-m)	AASHTO Alternative Military Tandem (AMT) and Lane Load, with Impact Mmax, ft-kips (kN-m)
50 (15.2)	74.6 (331.6)	93.9 (417.6)	49.3 (219.1)	50 (15.2)	820.0 (1,111.8)	1,024.6 (1,389.2)	964.8 (1,308.0)
100 (30.5)	97.3 (432.7)	118.8 (528.5)	65.3 (290.2)	100 (30.5)	2,320.0 (3,145.5)	2,821.6 (3,825.6)	2,396.0 (3,248.5)
200 (61.0)	132.6 (590.0)	155.3 (690.7)	97.3 (432.6)	200 (61.0)	6,520.0 (8,839.8)	7,615.6 (10,325.3)	6,458.5 (8,756.4)
300 (91.4)	165.8 (737.3)	188.8 (839.7)	129.3 (574.9)	300 (91.4)	12,320.0 (16,703.5)	14,009.6 (18,994.2)	12,121.0 (16,433.7)
400 (121.9)	198.3 (882.1)	221.5 (985.3)	161.3 (717.2)	400 (121.9)	19,720.0 (26,736.4)	22,003.6 (29,832.5)	19,383.5 (26,280.1)
500 (152.4)	230.7 (1,026.0)	254.0 (1,129.7)	193.3 (859.6)	500 (152.4)	28,720.0 (38,938.6)	31,597.6 (42,840.1)	28,246.0 (38,295.9)
600 (182.9)	262.9 (1,169.3)	286.3 (1,273.3)	225.3 (1,001.9)	600 (182.9)	39,320.0 (53,310.1)	42,791.6 (58,016.9)	38,708.5 (52,481.0)
700 (213.4)	295.0 (1,312.3)	318.5 (1,416.6)	257.3 (1,144.2)	700 (213.4)	51,520.0 (69,850.8)	55,585.6 (75,363.0)	50,771.0 (68,835.3)
800 (243.8)	327.2 (1,455.2)	350.6 (1,559.7)	289.3 (1,286.6)	800 (243.8)	65,320.0 (88,560.9)	69,979.6 (94,878.4)	64,433.5 (87,358.9)
900 (274.3)	359.3 (1,598.0)	382.8 (1,702.5)	321.3 (1,428.9)	900 (274.3)	80,720.0 (109,440.2)	85,973.6 (116,563.0)	79,696.0 (108,051.8)
1,000 (304.8)	391.3 (1,740.6)	414.9 (1,845.3)	353.3 (1,571.3)	1,000 (304.8)	97,720.0 (132,488.8)	103,567.6 (140,417.0)	96,558.5 (130,914.0)

Table 5-2: Maximum End Shear and Mid-span Moment for AASHTO HL-93 Design Truck and Lane Load of Span Lengths for Various Span Lengths

The CALTRANS design moments correspond exactly to the maximum mid-span moment calculated using the developed spreadsheet. Based on the agreement in maximum moments, the spreadsheet calculations were validated as accurate. The maximum calculated shear and mid-span moments for the HL-93 design truck and lane loading for the simple beam of 50 - 1,000 feet (15.2 – 304.8 m) with and without dynamic load allowance of 33% are provided on Table 5-2.

Variations in Maximum Moments for AASHTO HL-93 Design Truck and Lane Load			
Span Length	Difference in Span Length between the Location of Maximum Absolute and Mid-span Moments	Percent (%) Difference between Maximum Mid-span and Absolute Moment, No Impact	Percent (%) Difference between Max Mid-span and Absolute Moment, with Dynamic Impact
ft (m)	%	%	%
50 (15.2)	9.332%	-0.738%	-0.840%
100 (30.5)	4.666%	-0.094%	-0.123%
200 (61.0)	2.333%	-0.003%	-0.011%
300 (91.4)	1.555%	0.004%	0.000%
400 (121.9)	1.167%	0.004%	0.002%
500 (152.4)	0.933%	0.003%	0.002%
600 (182.9)	0.778%	0.003%	0.002%
700 (213.4)	0.667%	0.002%	0.002%
800 (243.8)	0.583%	0.002%	0.002%
900 (274.3)	0.518%	0.002%	0.001%
1,000 (304.8)	0.467%	0.001%	0.001%

Table 5-3: Variations in Maximum Moment Magnitude and Location for AASHTO HL-93 Design Truck and Lane Load for Various Span Lengths

From these results, the variation between the absolute maximum moment and the maximum mid-span moment was determined to be less than 1% in all cases and transitions from a negative to a positive value between 200 ft (61.0 m) and 300 ft (91.4 m) span lengths for the HL93 design truck and lane loading, both with and without dynamic impact. The variations are shown on Table 5-3 and graphically portrayed in Figures 5-7 and 5-8.

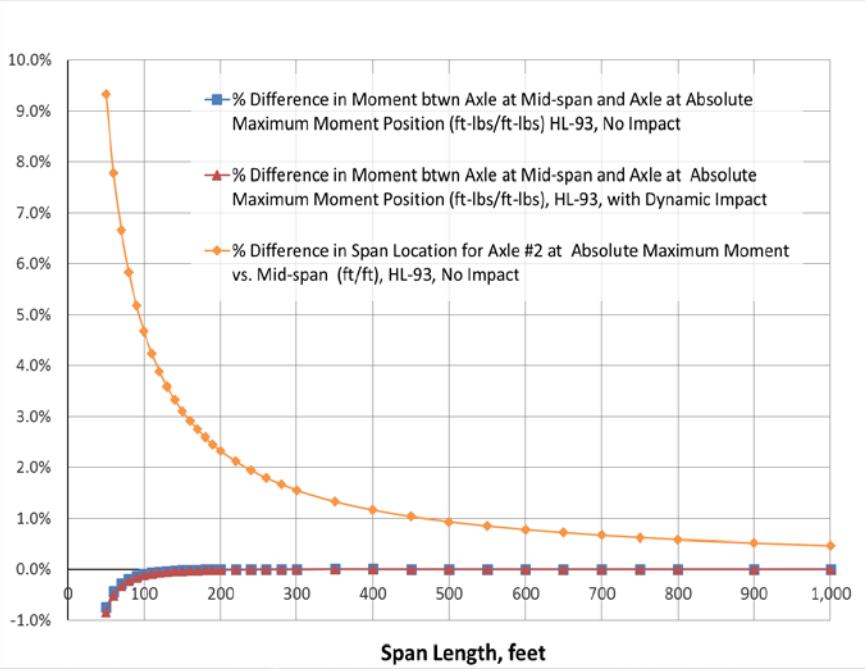

Figure 5-7: Comparison of Maximum Absolute and Mid-span Moments for HL-93 Design Truck and Lane Loading for Various Span Lengths

The span lengths where the variation between the maximum absolute moment and the maximum mid-span moment transitions from a negative to positive value indicates the transition from the condition where the absolute maximum moment is greater than the mid-span moment (negative difference) to the condition where the mid-span moment is greater than the absolute maximum moment (positive difference). The transition indicates the approximate location where the uniform lane loading of the HL93 specification begins to dominate the beam response (causing greater mid-span moment for longer spans) versus the dominance of the design truck live load, which is dominant for shorter spans.

Also shown on Table 5-3 and Figure 5-7 is the observation that the difference in span length between the middle axle location where the truck load generates the absolute maximum

moment and the mid-span for the 50 - 1,000 feet (15.2 – 304.8 m) span lengths decreases from less than 10% for the shortest span length (50 ft; 15.2 m) to less than 1% for longer span lengths (> 500 ft; > 152 m)).

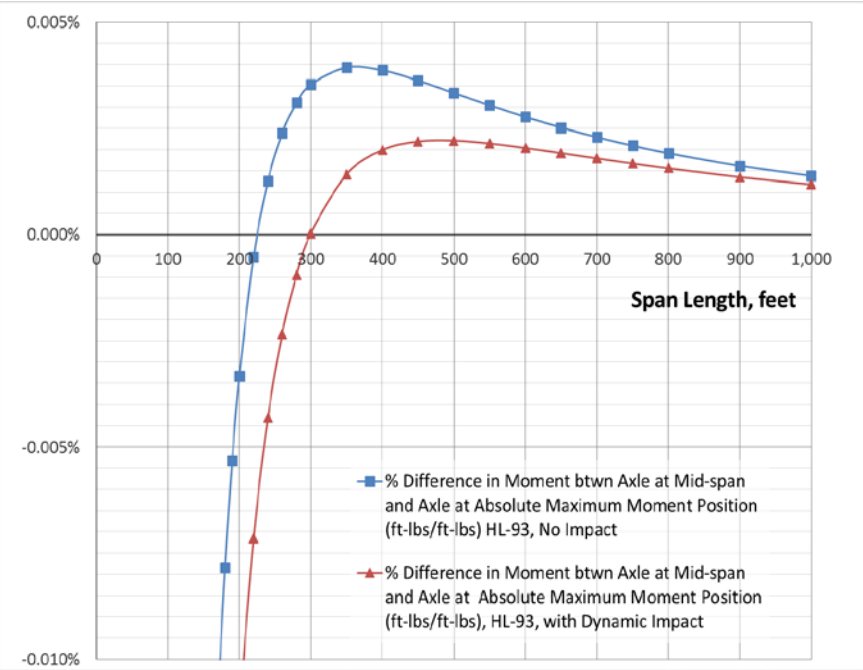

Figure 5-8: Inflection of the Difference between the Maximum Absolute and Maximum Mid-span Moment for HL-93 Live Loading for Various Span Lengths

5.3 VERIFICATION OF STANAG/FM TABULATED RESULTS

Following confirmation that the spreadsheet calculations produced accurate and validated results for the AASHTO HL-93 live loading, an analysis was conducted to compare calculated maximum shear and moment values against the tabulated values for MLC 40 to 120 hypothetical vehicles (hereafter referred as the FM values).[4] The spreadsheet calculations did not include any dynamic load allowance, or impact load factor, since it is not known if a dynamic allowance was

used in the original STANAG calculations although the commentary on the FM indicates that an impact factor of 15% was included in the tabulated values.[5]

The maximum shear and mid-span moment values for the hypothetical tracked vehicles were calculated using the explicit solution for a partially distributed uniform load. The maximum shear values for the hypothetical wheeled vehicles were calculated with the vehicle positioned such that the last (end) axle of the heavier end of the vehicle is directly over an end support. The maximum moments for the hypothetical wheeled vehicles were calculated by varying the position of the hypothetical MLC vehicle such that the resultant and middle axle translated over the mid-span location. The MLC 50W and 100W hypothetical wheeled vehicles were assumed to be representative of three and four axle hypothetical vehicles. The calculated moment values for these two representative hypothetical vehicles were calculated with the axle load closest to the resultant positioned at different possible locations near mid-span. The moments were calculated for a span length of 100 ft (30.5 m) and are plotted on Figures 5-9 and 5-10 respectively. The calculated moments exhibited the same behavior as discussed in the previous section.

Figures 5-9 and 5-10 show the possible maximum moments in the vicinity of mid-span for the two representative hypothetical vehicles. The calculated maximum absolute and mid-span moments do not exactly correspond to the FM values. This finding was also confirmed for the other hypothetical wheeled vehicles considered for this analysis. Therefore, an analysis to compare the FM 3 values versus the calculated maximum absolute and mid-span moment for both tracked and wheeled hypothetical vehicles was conducted.

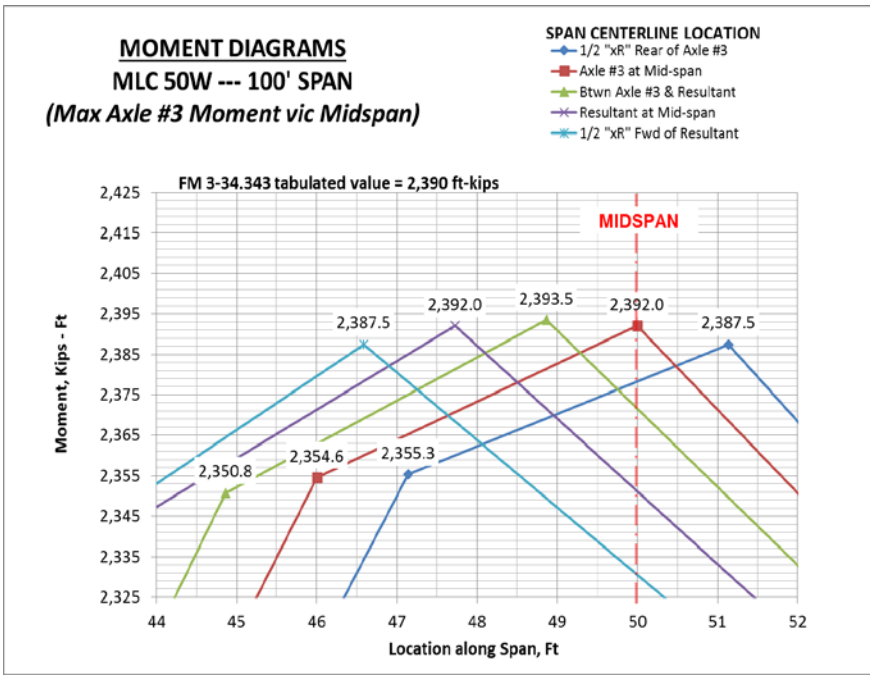

Figure 5-9: Calculated Moments for MLC 50W Hypothetical Vehicle Live Loading on a 100 ft (30.5 m) Simple Beam, with no Dynamic Load Allowance

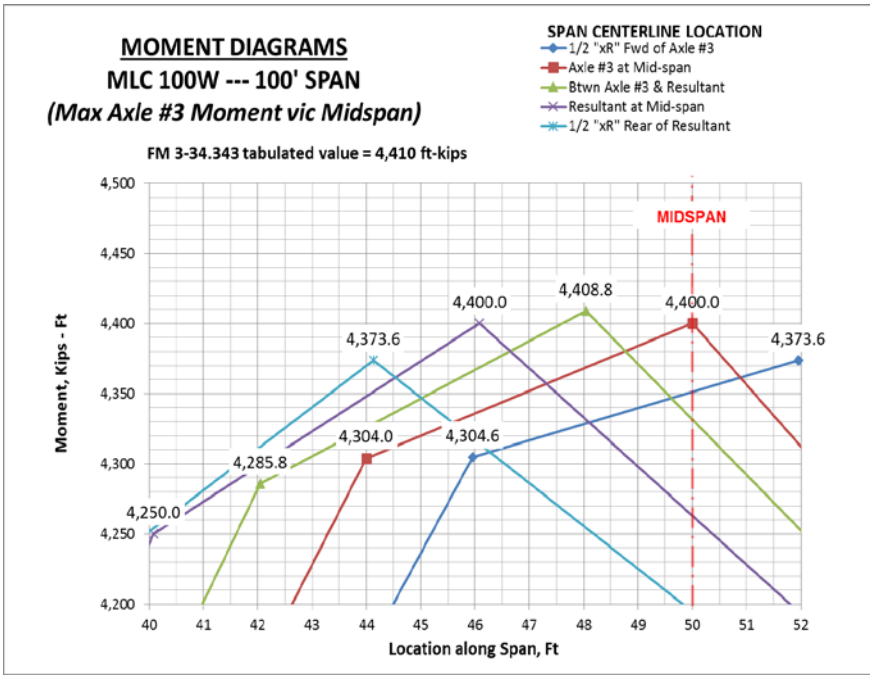

Figure 5-10: Calculated Moments for MLC 100W Hypothetical Vehicle Live Loading on a 100 ft (30.5 m) Simple Beam, with no Dynamic Load Allowance

The calculations were performed for only the MLC 40 to MLC 120 tracked and wheeled hypothetical vehicles. A range of span lengths was chosen to allow for the greatest number of calculations to be performed using the tabulated span lengths using separation distance of 100 ft (30.5 m) as stipulated for military vehicle convoys traveling at normal speeds.[6] The span lengths were selected to ensure that only one vehicle would be acting on the span and that the entire track width or all axles would be acting on the span for the hypothetical tracked and wheeled vehicles respectively. Therefore, the range of span lengths of 30-100 ft (9.1-30.5 m) was chosen for tracked hypothetical vehicles and 45-130 ft (13.7-39.6 m) for wheeled hypothetical vehicles. The results of these analyses are shown of Figures 5-11 through 5-15.

The results of this analysis indicate that there is general agreement between the FM values and the calculated values. There appears to be several anomalous data points that are potentially due to transcription or conversion errors from the metric values provided in STANAG 21. The maximum moments for the hypothetical wheeled vehicles provided in the FM are more closely aligned to the absolute maximum moment, not the maximum mid-span moment as shown on Figures 5-14 and 5-15. And there is an unknown error that appears to be systematic for the wheeled vehicle shear values for shorter span lengths.

A comparison of the absolute maximum moment versus the maximum mid-span moment was conducted for the range of MLC hypothetical wheeled vehicles, similar to the analysis conducted for the HL-93 design truck and lane load. As was the case with the HL93 live load, Figure 5-16 shows that the variation between the absolute maximum moment and the maximum mid-span moment is less than 2% for all of the MLC hypothetical wheeled vehicles for the

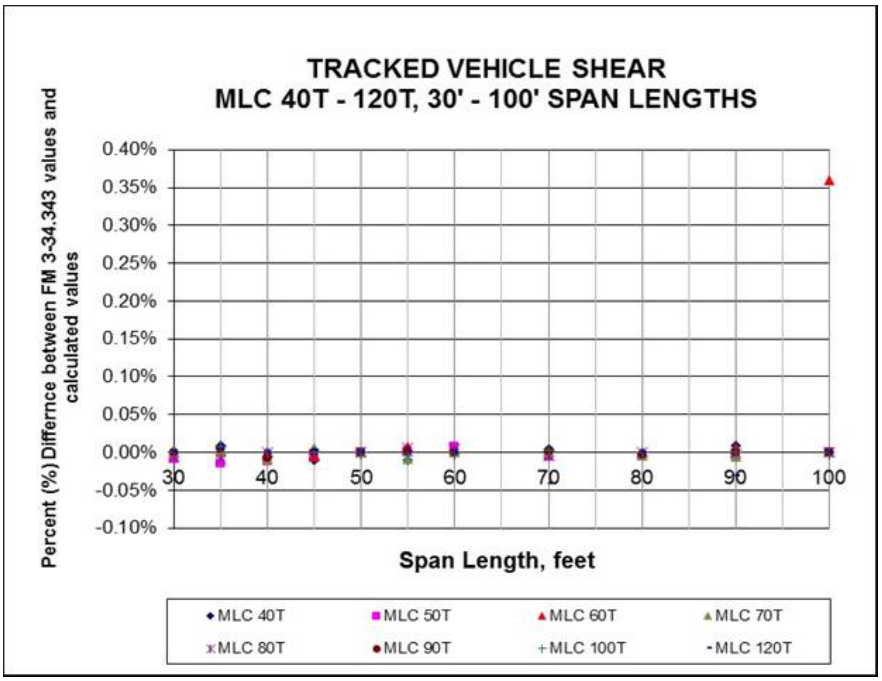

Figure 5-11: Comparison of the FM 3-34.343 Tabulated Shear Values versus Calculated Maximum Shear for Hypothetical MLC 40T – 120T Tracked Vehicles

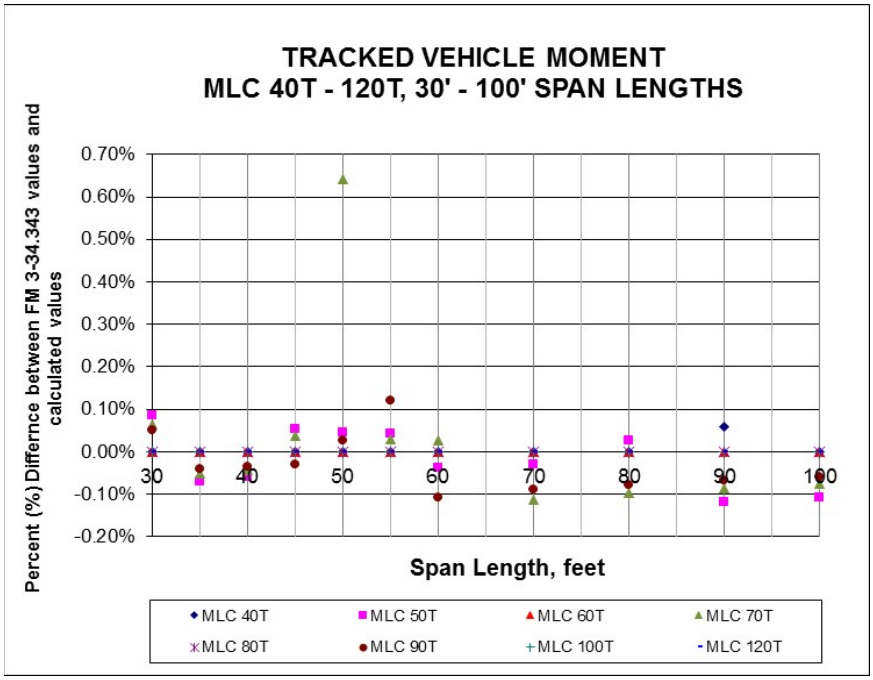

Figure 5-12: Comparison of the FM 3-34.343 Tabulated Values versus Calculated Absolute Maximum Moments (at Mid-span) for Hypothetical MLC 40T – 120T Tracked Vehicles

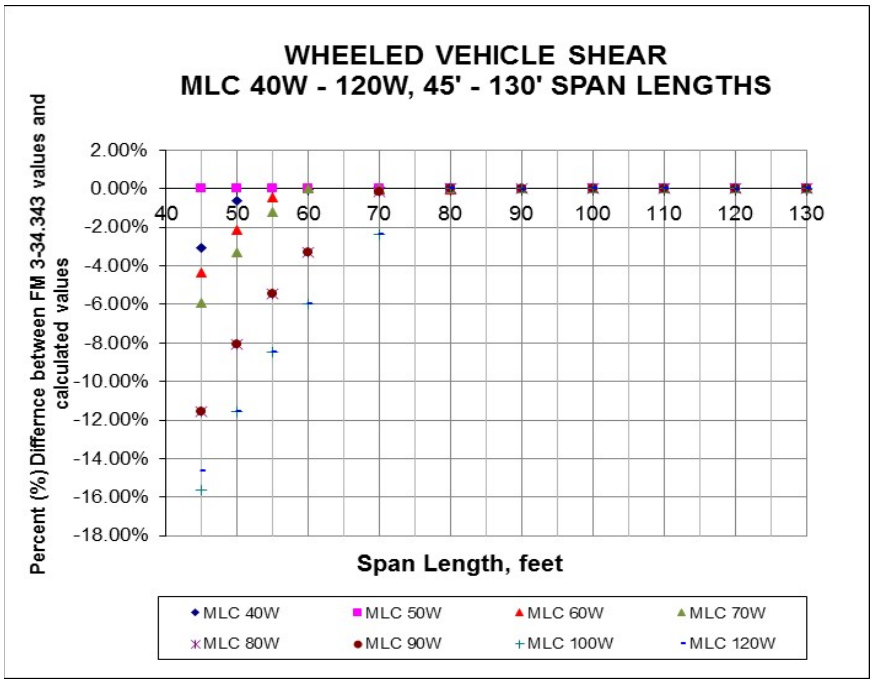

Figure 5-13: Comparison of the FM 3-34.343 Tabulated Shear Values versus Calculated Maximum Shear for Hypothetical MLC 40W – 120W Wheeled Vehicles

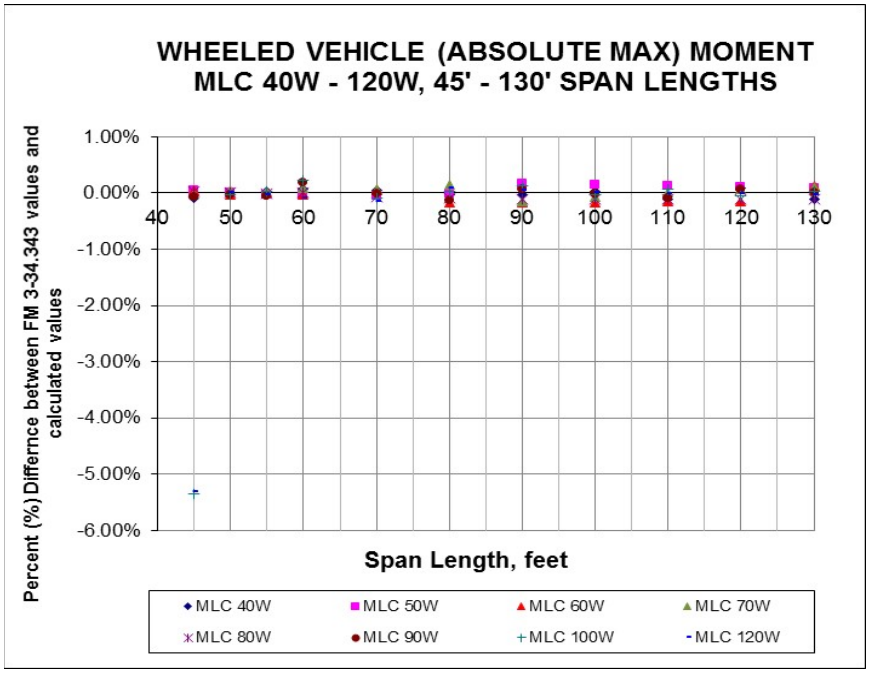

Figure 5-14: Comparison of the FM 3-34.343 Tabulated Values versus Calculated Absolute Maximum Moments for MLC Hypothetical Wheeled Vehicles

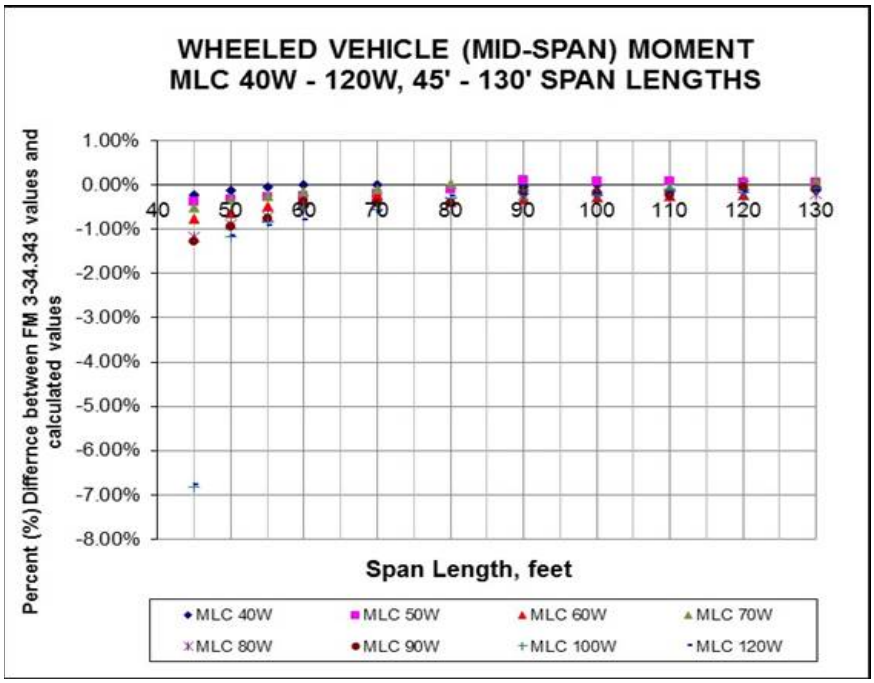

Figure 5-15: Comparison of the FM 3-34.343 Tabulated Values versus Calculated Maximum Mid-span Moments for MLC Hypothetical Wheeled Vehicles

considered span lengths. Figure 5-17 illustrates that the difference between the axle location nearest the resultant where the hypothetical vehicle produces the absolute maximum moment and the mid-span decreases with span length, with greater variation for heavier vehicles.

Based on these results, the spreadsheet calculations were considered validated for use in all subsequent calculations for the various live loads and design codes considered in this analysis. The maximum shear and mid-span moments were calculated for the MLC 40 to 120 hypothetical tracked and wheeled vehicles transiting a simple beam of 50 - 1,000 feet (15.2 – 304.8 m) span

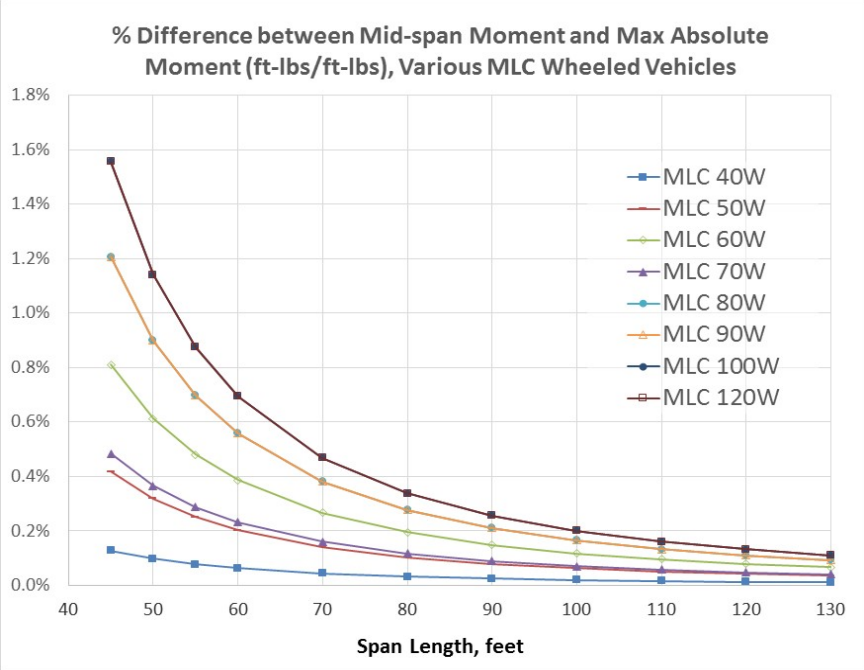

Figure 5-16: Comparison of Maximum Absolute and Mid-span Moments for MLC 40W – 120W Hypothetical Wheeled Vehicles for Various Span Lengths

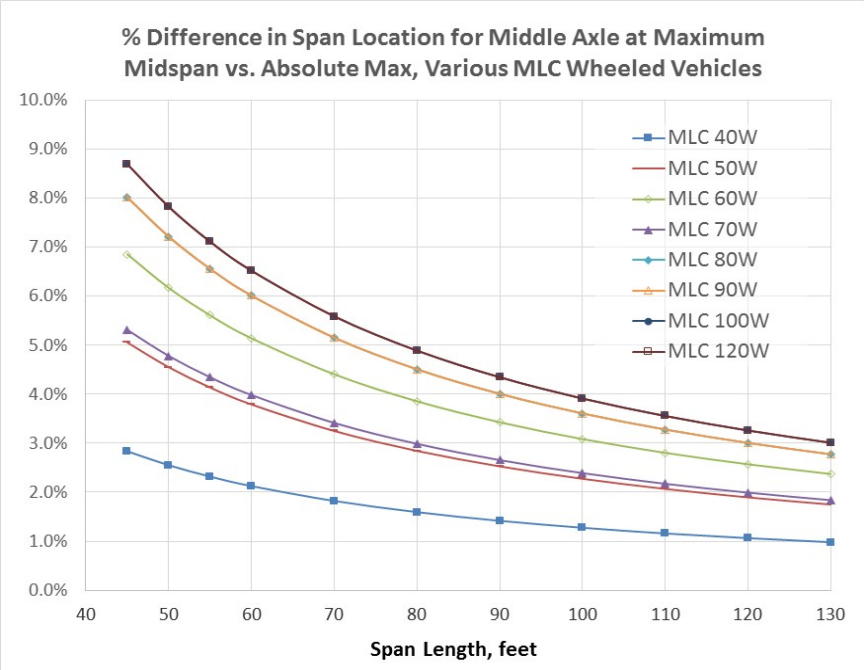

Figure 5-17: Comparison of Span Location for the Maximum Absolute versus Maximum Mid-span Moment, for MLC Hypothetical Wheeled Vehicles

length. These maximum shears and mid-span moments are shown on Table 5-4 and Figure 5-5 respectively. The maximum shear and mid-span moments for the MLC 40 to 120 hypothetical tracked and wheeled vehicles were plotted with the AASHTO HL-93 design truck and lane live loading maximum shears and mid-span moments on Figure 5-18 and 5-19 respectively. For these calculations, no dynamic allowance or impact was applied to either the HL-93 design truck live loading or the hypothetical vehicle live loading in order to present the general comparison of load conditions.

The maximum shear and mid-span moment generated by the MLC 40 to 120 hypothetical tracked and wheeled vehicle live loading are presented as normalized to the maximum shear and mid-span moment for the HL-93 design truck and lane live loading, as shown on Figures 5-20 and 5-21. The normalized curves highlight the contrast between the maximum shear and mid-span moments generated by the different live loadings for shorter span lengths.

The normalized maximum shear and mid-span moment curves show that as the span length increases, the AASHTO HL-93 lane live load increasingly dominates the live load applied to the simple beam. As a result, the HL-93 design truck and lane loading approximates the loading for MLC 40W hypothetical vehicle at short spans, and produces a load effect greater than the MLC 100W hypothetical vehicle at a span length of approximately 500 ft (152.4 m).

The large normalized value (> 2.0) of maximum shear and mid-span moment for short spans indicate that the MLC 100W hypothetical vehicle is a valid candidate for an alternate military live load for bridge design as a new AASHTO Strength II load condition, to replace the current AASHTO HL-93 alternative military tandem (AMT) and lane load currently used with the design truck and lane load as a Strength I condition. The basic premise of this thesis was considered validated and subsequent analyses considered the possible design implications.

Maximum End Shear (Vmax, kips)								
Span Length L, ft (m)	MLC 40T Vmax, kips (kN)	MLC 50T Vmax, kips (kN)	MLC 60T Vmax, kips (kN)	MLC 70T Vmax, kips (kN)	MLC 80T Vmax, kips (kN)	MLC 90T Vmax, kips (kN)	MLC 100T Vmax, kips (kN)	MLC 120T Vmax, kips (kN)
50 (15.2)	70.4 (313.1)	87.0 (387.0)	103.2 (459.0)	119.0 (529.3)	134.4 (597.8)	149.4 (664.5)	164.0 (729.5)	192.0 (854.0)
100 (30.5)	75.2 (334.5)	93.5 (415.9)	111.6 (496.4)	129.5 (576.0)	147.2 (654.7)	164.7 (732.6)	182.0 (809.5)	216.0 (960.8)
200 (61.0)	77.6 (345.2)	96.8 (430.3)	115.8 (515.1)	134.8 (599.4)	153.6 (683.2)	172.4 (766.6)	191.0 (849.6)	228.0 (1,014.1)
300 (91.4)	78.4 (348.7)	97.8 (435.2)	117.2 (521.3)	136.5 (607.2)	155.7 (692.7)	174.9 (778.0)	194.0 (862.9)	232.0 (1,031.9)
400 (121.9)	78.8 (350.5)	98.4 (437.6)	117.9 (524.4)	137.4 (611.0)	156.8 (697.4)	176.2 (783.6)	195.5 (869.6)	234.0 (1,040.8)
500 (152.4)	79.0 (351.6)	98.7 (439.0)	118.3 (526.3)	137.9 (613.4)	157.4 (700.3)	176.9 (787.0)	196.4 (873.6)	235.2 (1,046.2)
600 (182.9)	79.2 (352.3)	98.9 (440.0)	118.6 (527.5)	138.3 (614.9)	157.9 (702.2)	177.5 (789.3)	197.0 (876.3)	236.0 (1,049.7)
700 (213.4)	79.3 (352.8)	99.1 (440.7)	118.8 (528.4)	138.5 (616.0)	158.2 (703.5)	177.8 (790.9)	197.4 (878.2)	236.6 (1,052.3)
800 (243.8)	79.4 (353.2)	99.2 (441.2)	119.0 (529.1)	138.7 (616.9)	158.4 (704.6)	178.1 (792.1)	197.8 (879.6)	237.0 (1,054.2)
900 (274.3)	79.5 (353.5)	99.3 (441.6)	119.1 (529.6)	138.8 (617.5)	158.6 (705.4)	178.3 (793.1)	198.0 (880.7)	237.3 (1,055.7)
1,000 (304.8)	79.5 (353.7)	99.4 (441.9)	119.2 (530.0)	139.0 (618.0)	158.7 (706.0)	178.5 (793.8)	198.2 (881.6)	237.6 (1,056.8)
Span Length L, ft (m)	MLC 40W Vmax, kips (kN)	MLC 50W Vmax, kips (kN)	MLC 60W Vmax, kips (kN)	MLC 70W Vmax, kips (kN)	MLC 80W Vmax, kips (kN)	MLC 90W Vmax, kips (kN)	MLC 100W Vmax, kips (kN)	MLC 120W Vmax, kips (kN)
50 (15.2)	66.3 (295.0)	84.2 (374.3)	95.4 (424.5)	107.5 (478.2)	112.6 (501.0)	126.7 (563.7)	133.0 (591.6)	159.6 (709.9)
100 (30.5)	80.2 (356.6)	100.1 (445.2)	117.7 (523.6)	134.3 (597.2)	148.3 (659.7)	166.9 (742.2)	181.5 (807.3)	217.8 (968.8)
200 (61.0)	87.1 (387.3)	108.0 (480.6)	128.9 (573.2)	147.6 (656.7)	166.2 (739.1)	186.9 (831.5)	205.8 (915.2)	246.9 (1,098.2)
300 (91.4)	89.4 (397.6)	110.7 (492.4)	132.6 (589.7)	152.1 (676.5)	172.1 (765.5)	193.6 (861.2)	213.8 (951.1)	256.6 (1,141.4)
400 (121.9)	90.5 (402.7)	112.0 (498.3)	134.4 (597.9)	154.3 (686.4)	175.1 (778.8)	197.0 (876.1)	217.9 (969.1)	261.5 (1,162.9)
500 (152.4)	91.2 (405.8)	112.8 (501.8)	135.5 (602.9)	155.7 (692.3)	176.9 (786.7)	199.0 (885.0)	220.3 (979.9)	264.4 (1,175.9)
600 (182.9)	91.7 (407.9)	113.3 (504.2)	136.3 (606.2)	156.5 (696.3)	178.1 (792.0)	200.3 (891.0)	221.9 (987.1)	266.3 (1,184.5)
700 (213.4)	92.0 (409.3)	113.7 (505.9)	136.8 (608.6)	157.2 (699.1)	178.9 (795.8)	201.3 (895.2)	223.1 (992.2)	267.7 (1,190.7)
800 (243.8)	92.3 (410.4)	114.0 (507.1)	137.2 (610.3)	157.7 (701.3)	179.5 (798.6)	202.0 (898.4)	223.9 (996.1)	268.7 (1,195.3)
900 (274.3)	92.5 (411.3)	114.2 (508.1)	137.5 (611.7)	158.0 (702.9)	180.0 (800.8)	202.5 (900.9)	224.6 (999.1)	269.5 (1,198.9)
1,000 (304.8)	92.6 (412.0)	114.4 (508.9)	137.8 (612.8)	158.3 (704.2)	180.4 (802.6)	203.0 (902.9)	225.2 (1,001.5)	270.2 (1,201.8)

Table 5-4: Maximum End Shear for MLC 40 to 120 Hypothetical Wheeled and Tracked Vehicles on 50 to 1,000 ft (15.2 – 304.8 m) Spans

Maximum Mid-Span Moment (Mmax, ft-kips)								
Span Length L, ft (m)	MLC 40T Mmax, ft-kips (kN-m)	MLC 50T Mmax, ft-kips (kN-m)	MLC 60T Mmax, ft-kips (kN-m)	MLC 70T Mmax, ft-kips (kN-m)	MLC 80T Mmax, ft-kips (kN-m)	MLC 90T Mmax, ft-kips (kN-m)	MLC 100T Mmax, ft-kips (kN-m)	MLC 120T Mmax, ft-kips (kN-m)
50 (15.2)	880.0 (1,193.1)	1,087.5 (1,474.4)	1,290.0 (1,749.0)	1,487.5 (2,016.8)	1,680.0 (2,277.7)	1,867.5 (2,532.0)	2,050.0 (2,779.4)	2,400.0 (3,253.9)
100 (30.5)	1,880.0 (2,548.9)	2,337.5 (3,169.2)	2,790.0 (3,782.7)	3,237.5 (4,389.4)	3,680.0 (4,989.3)	4,117.5 (5,582.5)	4,550.0 (6,168.9)	5,400.0 (7,321.3)
200 (61.0)	3,880.0 (5,260.5)	4,837.5 (6,558.7)	5,790.0 (7,850.1)	6,737.5 (9,134.7)	7,680.0 (10,412.5)	8,617.5 (11,683.6)	9,550.0 (12,947.9)	11,400.0 (15,456.1)
300 (91.4)	5,880.0 (7,972.1)	7,337.5 (9,948.2)	8,790.0 (11,917.5)	10,237.5 (13,880.0)	11,680.0 (15,835.7)	13,117.5 (17,784.7)	14,550.0 (19,726.9)	17,400.0 (23,590.9)
400 (121.9)	7,880.0 (10,683.7)	9,837.5 (13,337.7)	11,790.0 (15,984.9)	13,737.5 (18,625.3)	15,680.0 (21,258.9)	17,617.5 (23,885.8)	19,550.0 (26,505.9)	23,400.0 (31,725.7)
500 (152.4)	9,880.0 (13,395.3)	12,337.5 (16,727.2)	14,790.0 (20,052.3)	17,237.5 (23,370.6)	19,680.0 (26,682.1)	22,117.5 (29,986.9)	24,550.0 (33,284.9)	29,400.0 (39,860.5)
600 (182.9)	11,880.0 (16,106.9)	14,837.5 (20,116.7)	17,790.0 (24,119.7)	20,737.5 (28,115.9)	23,680.0 (32,105.3)	26,617.5 (36,088.0)	29,550.0 (40,063.9)	35,400.0 (47,995.3)
700 (213.4)	13,880.0 (18,818.5)	17,337.5 (23,506.2)	20,790.0 (28,187.1)	24,237.5 (32,861.2)	27,680.0 (37,528.5)	31,117.5 (42,189.1)	34,550.0 (46,842.9)	41,400.0 (56,130.1)
800 (243.8)	15,880.0 (21,530.1)	19,837.5 (26,895.7)	23,790.0 (32,254.5)	27,737.5 (37,606.5)	31,680.0 (42,951.7)	35,617.5 (48,290.2)	39,550.0 (53,621.9)	47,400.0 (64,264.9)
900 (274.3)	17,880.0 (24,241.7)	22,337.5 (30,285.2)	26,790.0 (36,321.9)	31,237.5 (42,351.8)	35,680.0 (48,374.9)	40,117.5 (54,391.3)	44,550.0 (60,400.9)	53,400.0 (72,399.7)
1,000 (304.8)	19,880.0 (26,953.3)	24,837.5 (33,674.7)	29,790.0 (40,389.3)	34,737.5 (47,097.1)	39,680.0 (53,798.1)	44,617.5 (60,492.4)	49,550.0 (67,179.9)	59,400.0 (80,534.5)
Span Length L, ft (m)	MLC 40W Mmax, ft-kips (kN-m)	MLC 50W Mmax, ft-kips (kN-m)	MLC 60W Mmax, ft-kips (kN-m)	MLC 70W Mmax, ft-kips (kN-m)	MLC 80W Mmax, ft-kips (kN-m)	MLC 90W Mmax, ft-kips (kN-m)	MLC 100W Mmax, ft-kips (kN-m)	MLC 120W Mmax, ft-kips (kN-m)
50 (15.2)	787.0 (1,067.0)	942.0 (1,277.2)	1,082.0 (1,467.0)	1,253.0 (1,698.8)	1,320.0 (1,789.7)	1,485.0 (2,013.4)	1,525.0 (2,067.6)	1,830.0 (2,481.1)
100 (30.5)	1,962.0 (2,660.1)	2,392.0 (3,243.1)	2,832.0 (3,839.6)	3,265.5 (4,427.4)	3,620.0 (4,908.0)	4,072.5 (5,521.5)	4,400.0 (5,965.5)	5,280.0 (7,158.6)
200 (61.0)	4,312.0 (5,846.2)	5,292.0 (7,174.9)	6,332.0 (8,584.9)	7,290.5 (9,884.5)	8,220.0 (11,144.7)	9,247.5 (12,537.8)	10,150.0 (13,761.4)	12,180.0 (16,513.6)
300 (91.4)	6,662.0 (9,032.3)	8,192.0 (11,106.7)	9,832.0 (13,330.2)	11,315.5 (15,341.6)	12,820.0 (17,381.4)	14,422.5 (19,554.0)	15,900.0 (21,557.2)	19,080.0 (25,868.7)
400 (121.9)	9,012.0 (12,218.5)	11,092.0 (15,038.5)	13,332.0 (18,075.5)	15,340.5 (20,798.6)	17,420.0 (23,618.0)	19,597.5 (26,570.3)	21,650.0 (29,353.1)	25,980.0 (35,223.7)
500 (152.4)	11,362.0 (15,404.6)	13,992.0 (18,970.4)	16,832.0 (22,820.8)	19,365.5 (26,255.7)	22,020.0 (29,854.7)	24,772.5 (33,586.6)	27,400.0 (37,148.9)	32,880.0 (44,578.7)
600 (182.9)	13,712.0 (18,590.7)	16,892.0 (22,902.2)	20,332.0 (27,566.1)	23,390.5 (31,712.8)	26,620.0 (36,091.4)	29,947.5 (40,602.8)	33,150.0 (44,944.8)	39,780.0 (53,933.7)
700 (213.4)	16,062.0 (21,776.9)	19,792.0 (26,834.0)	23,832.0 (32,311.4)	27,415.5 (37,169.9)	31,220.0 (42,328.1)	35,122.5 (47,619.1)	38,900.0 (52,740.6)	46,680.0 (63,288.7)
800 (243.8)	18,412.0 (24,963.0)	22,692.0 (30,765.8)	27,332.0 (37,056.7)	31,440.5 (42,627.0)	35,820.0 (48,564.8)	40,297.5 (54,635.4)	44,650.0 (60,536.5)	53,580.0 (72,643.8)
900 (274.3)	20,762.0 (28,149.1)	25,592.0 (34,697.6)	30,832.0 (41,802.0)	35,465.5 (48,084.1)	40,420.0 (54,801.4)	45,472.5 (61,651.6)	50,400.0 (68,332.3)	60,480.0 (81,998.8)
1,000 (304.8)	23,112.0 (31,335.2)	28,492.0 (38,629.5)	34,332.0 (46,547.3)	39,490.5 (53,541.2)	45,020.0 (61,038.1)	50,647.5 (68,667.9)	56,150.0 (76,128.2)	67,380.0 (91,353.8)

Table 5-5: Maximum Mid-span Moments for MLC 40 to 120 Hypothetical Wheeled and Tracked Vehicles on 50 to 1,000 ft (15.2 – 304.8 m) Spans

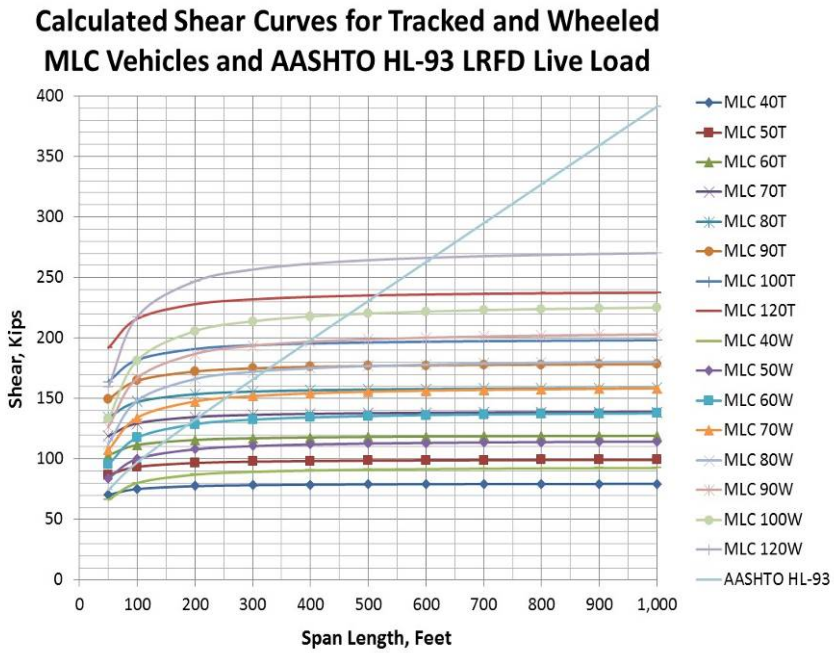

Figure 5-18: Maximum End Shear for MLC Hypothetical Vehicle Classes and the AASHTO HL-93 Design Truck and Lane Load, Various Span Lengths

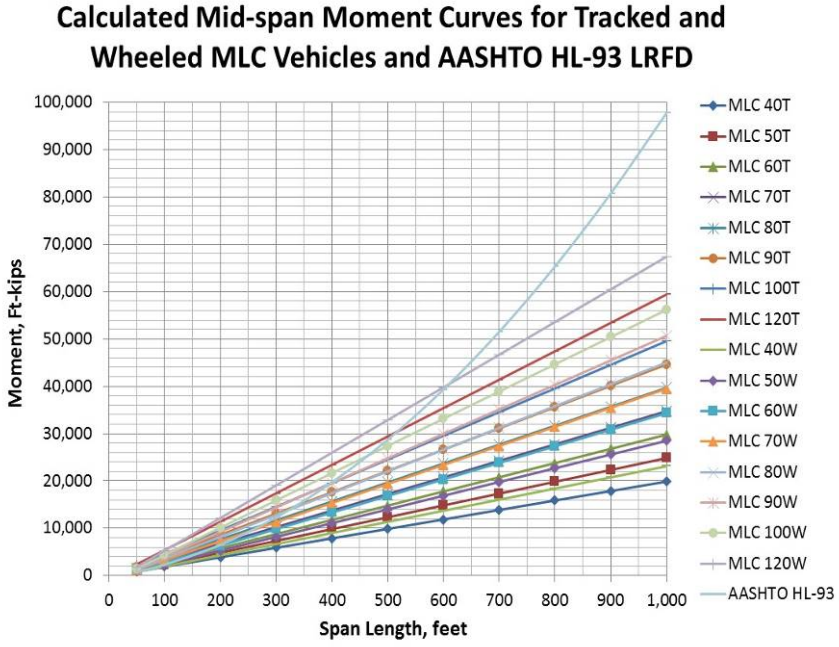

Figure 5-19: Maximum Mid-span Moment for MLC Hypothetical Vehicle Classes and the AASHTO HL-93 Design Truck and Lane Load, Various Span Lengths

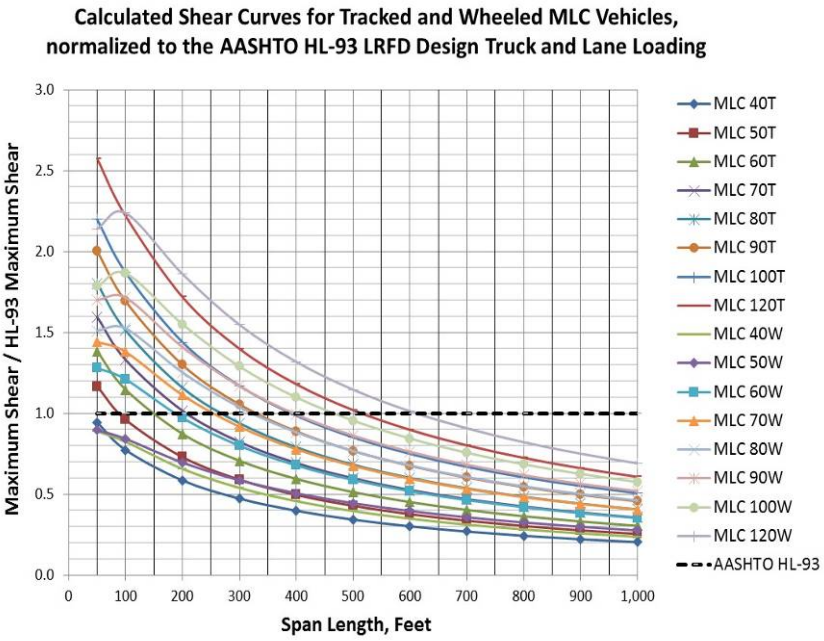

Figure 5-20: Maximum End Shear for MLC Hypothetical Vehicle Classes and AASHTO HL-93, Various Span Lengths, Normalized to HL-93 Values

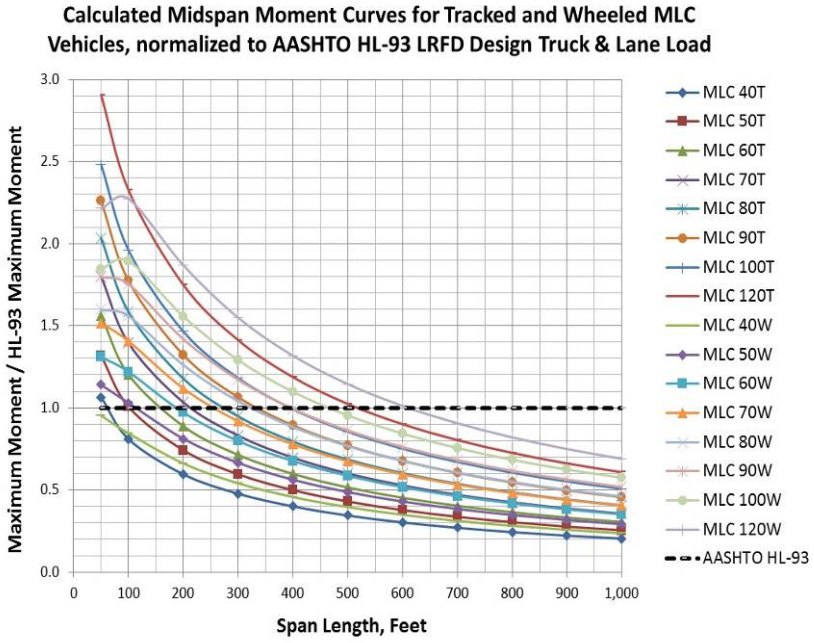

Figure 5-21: Maximum Mid-span Moment for MLC Hypothetical Vehicle Classes and AASHTO HL-93, Various Span Lengths, Normalized to HL-93 Values

5.4 COMPARISON OF MLC-100W VEHICLES

The next step of this study was to confirm that MLC 100W hypothetical vehicle live load produces maximum shear and mid-span moments equal to or greater than the maximum shear and mid-span moment created by actual military heavy equipment transport (HET) systems.

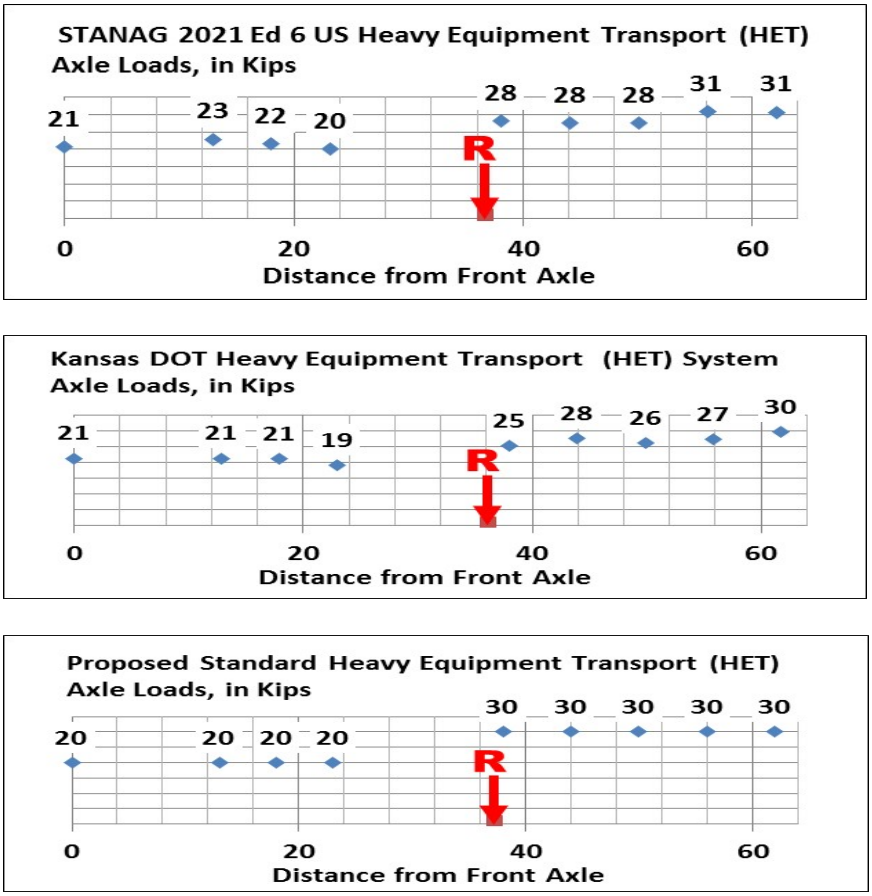

Figure 5-22: Heavy Equipment Transportation (HET) Systems Considered

The three systems described in Chapter 5 were analyzed using a calculation spreadsheet expanded to allow for nine axle concentrated loads acting on a simple beam of a specified span length.

The resultant for each of the three HET systems considered are shown in Figure 5-22. These diagrams are taken from the nine axle calculation spreadsheet used for the analysis, and show that for all three cases, the axle nearest the resultant location is the number five (#5) axle. As stated earlier, structural analysis theory dictates that the maximum moment occurs when the concentrated loads are positioned such that the resultant of the loads and the nearest concentrated load are equidistant from mid-span of the simple beam under consideration. This will be shown to be not true for these live load conditions.

The determination of maximum mid-span moment for all three cases reveals that the maximum absolute moment occurs when the mid-span is located equidistant from the resultant and number six (#6) axle, not equidistant from the resultant and the number five (#5) axle, as shown on Figures 5-23, 5-24, and 5-25.

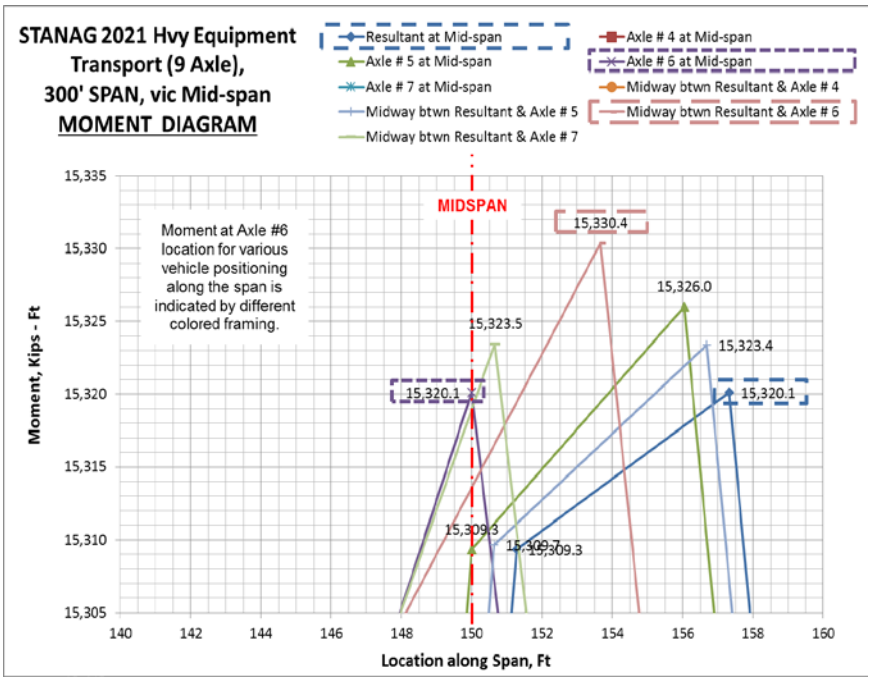

Figure 5-23: STANAG 2021 Typical MLC 100W Vehicle Maximum Moments

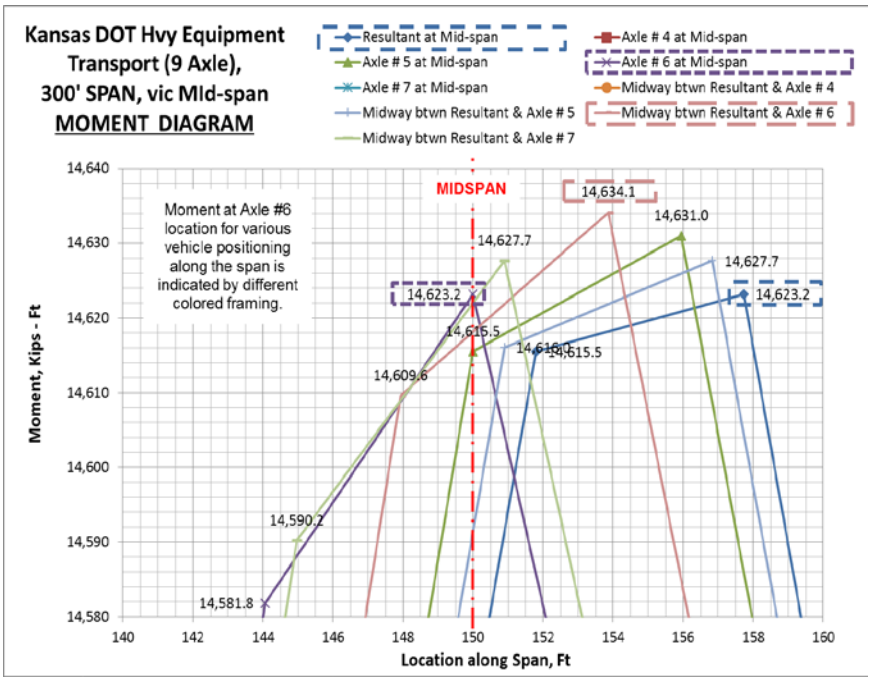

Figure 5-24: Kansas Department of Transportation (DOT) U.S. Army Heavy Equipment Transporter (HET) Live Load Maximum Moment Determination

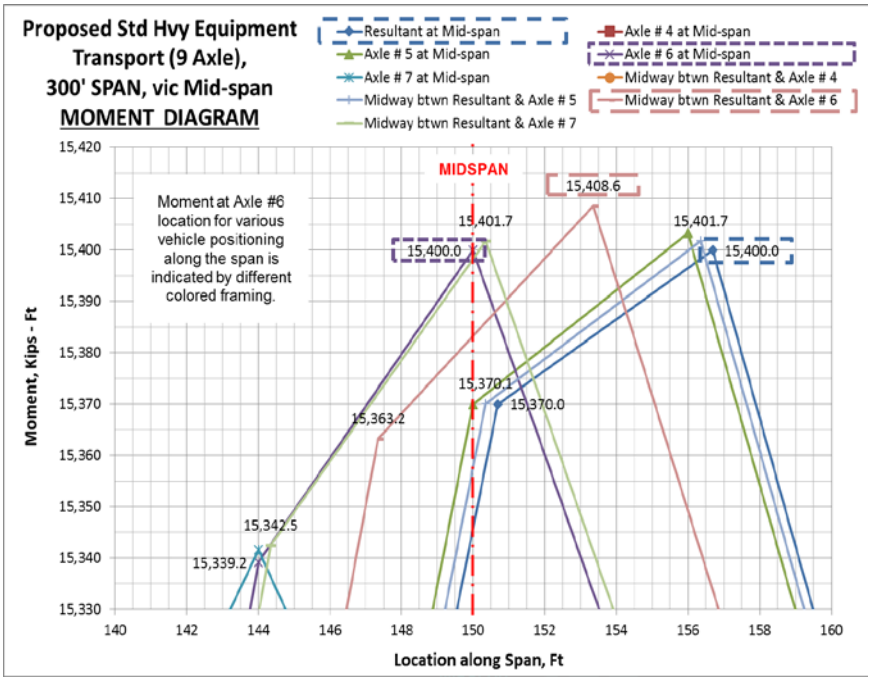

Figure 5-25: Proposed Standardized (Simplified) 230K Heavy Equipment Transport (HET) Live Load Maximum Moment Determination

Based on the analysis for these vehicles, the maximum mid-span moment is created when number six (#6) axle is located at the mid-span and the magnitude is equal to the maximum mid-span moment generated when the resultant is located at the mid-span as shown on Figures 5-23, 5-24 and 5-25.

As in previous cases, the relative differences between the absolute maximum and the maximum mid-span moment for the three HET systems were plotted as a percentage versus span length. These values along with the percentages for the MLC hypothetical wheeled vehicles are shown on Figure 5-26.

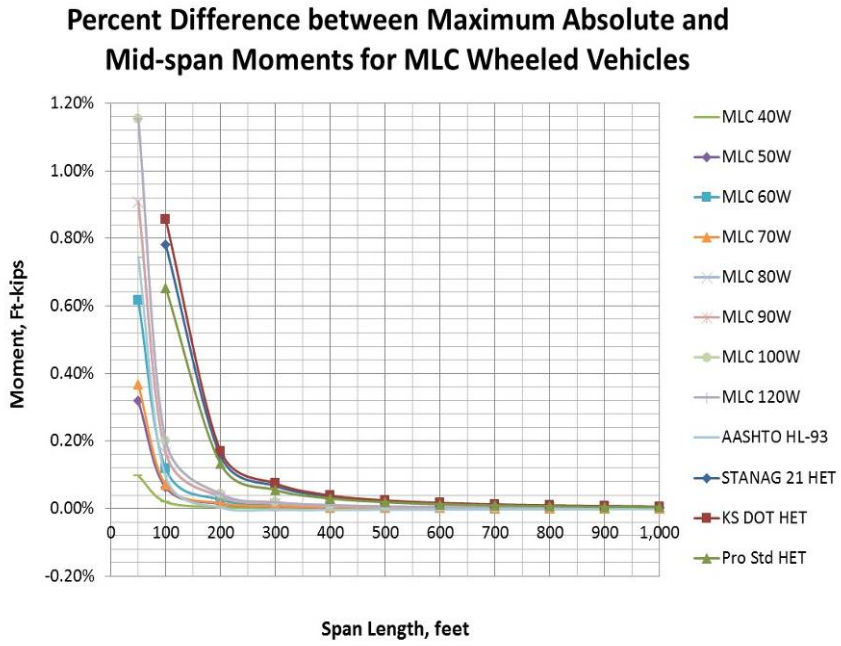

Figure 5-26: Comparison of Maximum Absolute and Mid-span Moments for MLC Hypothetical Wheeled Vehicles and HET Systems

From these results, three related observations were concluded from the results for a closely spaced group (length "a") of concentrated loads acting on a simple beam of a span length (length "L") greater than the group length (L > a).

1. The magnitude of the maximum mid-span moment can be calculated by positioning the resultant at mid-span and identifying the maximum moment at a concentrated load. This maximum moment will occur some distance from the middle of the span. The concentrated load at which the maximum moment occurs may or may not be the axle closest to the resultant positon.
2. The absolute maximum moment occurs when the load group is positioned such that the resultant and the concentrated load where the maximum mid-span moment occurs are positioned equidistant from the mid-span. This maximum absolute moment does not occur at mid span. The magnitude of the mid-span moment generated when the loads are positioned to produce the maximum absolute moment will always be less than the magnitude of the mid-span moment when the resultant is at mid-span.
3. The difference in magnitude of the maximum absolute moment and the maximum mid-span moment is negligible for spans relatively longer than the group length ($L > 3a$).

These observations will be validated in subsequent calculations for other live loadings analyzed later in this chapter, specifically the design codes and the special permit vehicles.

After the position of the HET system along the span that creates the maximum mid-span moment was established, the maximum shear and mid-span moment were calculated for each HET system transiting a simple beam of 50 - 1,000 feet (15.2 – 304.8 m) span length. The maximum shear and mid-span moment for the HET systems and a MLC100W hypothetical vehicle are shown on Table 5-6 and plotted on Figures 5-27 and 5-28 respectively. A dynamic load allowance or impact was not applied to either the HET systems or the MLC100W hypothetical vehicle live loadings (either a group of five concentrated loads for the MLC 100W

vehicle or a group of nine concentrated loads for the three HET systems). The maximum shear and moment for the three HET systems were less than the maximum shear and moment produced by the MLC 100W hypothetical vehicle for all span lengths.

Based on these results, the MLC 100W hypothetical vehicle was validated as an appropriate live load to serve as an alternative military live load for civilian bridge design. Therefore, the MLC 100W hypothetical will be used as the basis for further calculations, using the existing five axle (or five concentrated point loads) calculation spreadsheet and two new spreadsheets for ten axle and fifteen axle (or concentrated point loads) for two and three vehicles on span lengths up to 1,000 ft (304.8 m).

Using the ten axle calculation spreadsheet, spans lengths of 387 - 1,000 ft (118.0 - 304.8 m) were analyzed for the condition of two MLC 100W hypothetical vehicles on the span. The lower limit of 387 ft (118.0 m) corresponds to two MLC 100W vehicles each 43 ft (13.1 m) in length (from front to rear axle) separated by 300 ft (91.4 m) from the rear axle of the first vehicle to front axle of the second vehicle. Representative results of the analysis for possible maximum moments based on the position of the vehicles along the span are shown on Figures 5-29 and 5-30. An interesting observed phenomena is that for some span lengths, the plot of the possible moment curves corresponding to different vehicle positioning along the span demonstrated a double peaked profile as shown on Figures 5-29 and 5-30. This effect is characterized by the moment diagram curve intersecting a common point at mid-span corresponding to a maximum moment created when the vehicles are positioned such that the resultant of both vehicles (i.e. the total live loading on the span) is at mid-span.

Maximum End Shear (Vmax, kips)				
Span Length	MLC 100W Hypothetical Wheeled Vehicle	Kansas DOT (US Army) Heavy Equipment Transporter (HET)	STANAG 21 (US Army) Heavy Equipment Transporter (HET)	Proposed Standard Heavy Equipment Transporter (HET)
L, ft (m)	Vmax, kips (kN)	Vmax, kips (kN)	Vmax, kips (kN)	Vmax, kips (kN)
50 (15.2)	133.0 (591.6)			
100 (30.5)	181.5 (807.3)	163.6 (727.9)	171.7 (763.7)	173.2 (770.4)
200 (61.0)	205.8 (915.2)	191.7 (852.8)	200.9 (893.4)	201.6 (896.7)
300 (91.4)	213.8 (951.1)	201.1 (894.4)	210.6 (936.7)	211.1 (938.8)
400 (121.9)	217.9 (969.1)	205.8 (915.2)	215.4 (958.3)	215.8 (959.9)
500 (152.4)	220.3 (979.9)	208.6 (927.7)	218.4 (971.3)	218.6 (972.5)
600 (182.9)	221.9 (987.1)	210.4 (936.0)	220.3 (979.9)	220.5 (980.9)
700 (213.4)	223.1 (992.2)	211.8 (942.0)	221.7 (986.1)	221.9 (986.9)
800 (243.8)	223.9 (996.1)	212.8 (946.4)	222.7 (990.7)	222.9 (991.5)
900 (274.3)	224.6 (999.1)	213.6 (949.9)	223.5 (994.3)	223.7 (995.0)
1,000 (304.8)	225.2 (1,001.5)	214.2 (952.7)	224.2 (997.2)	224.3 (997.8)

Maximum Mid-Span Moment (Mmax, ft-kips)				
Span Length	MLC 100W Hypothetical Wheeled Vehicle	Kansas DOT (US Army) Heavy Equipment Transporter (HET)	STANAG 21 (US Army) Heavy Equipment Transporter (HET)	Proposed Standard Heavy Equipment Transporter (HET)
L, ft (m)	Mmax, ft-kips (kN-m)	Mmax, ft-kips (kN-m)	Mmax, ft-kips (kN-m)	Mmax, ft-kips (kN-m)
50 (15.2)	1,525.0 (2,067.6)			
100 (30.5)	4,400.0 (5,965.5)	3,633.2 (4,925.9)	3,818.9 (5,177.6)	3,900.0 (5,287.6)
200 (61.0)	10,150.0 (13,761.4)	9,128.2 (12,376.0)	9,569.5 (12,974.3)	9,650.0 (13,083.5)
300 (91.4)	15,900.0 (21,557.2)	14,623.2 (19,826.1)	15,320.1 (20,771.0)	15,400.0 (20,879.3)
400 (121.9)	21,650.0 (29,353.1)	20,118.2 (27,276.2)	21,070.8 (28,567.8)	21,150.0 (28,675.2)
500 (152.4)	27,400.0 (37,148.9)	25,613.2 (34,726.3)	26,821.4 (36,364.5)	26,900.0 (36,471.0)
600 (182.9)	33,150.0 (44,944.8)	31,108.2 (42,176.5)	32,572.1 (44,161.2)	32,650.0 (44,266.9)
700 (213.4)	38,900.0 (52,740.6)	36,603.2 (49,626.6)	38,322.7 (51,957.9)	38,400.0 (52,062.7)
800 (243.8)	44,650.0 (60,536.5)	42,098.2 (57,076.7)	44,073.3 (59,754.6)	44,150.0 (59,858.6)
900 (274.3)	50,400.0 (68,332.3)	47,593.2 (64,526.8)	49,824.0 (67,551.4)	49,900.0 (67,654.4)
1,000 (304.8)	56,150.0 (76,128.2)	53,088.2 (71,976.9)	55,574.6 (75,348.1)	55,650.0 (75,450.3)

Table 5-6: Maximum End Shear and Mid-span Moments for HET systems and Single MLC100W Hypothetical Wheeled Vehicle, Various Span Lengths

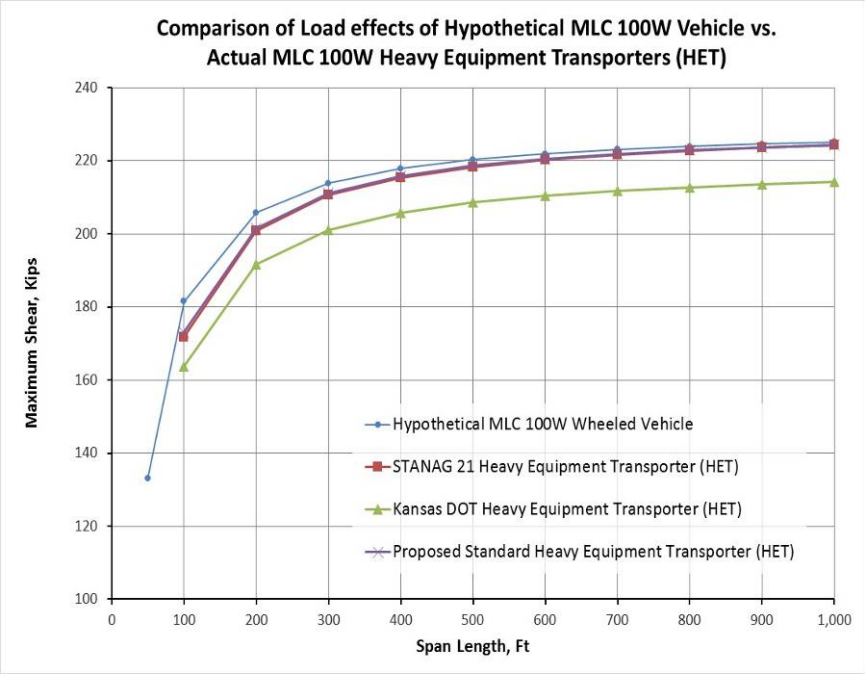

Figure 5-27: Maximum End Shear for MLC 100W Hypothetical Vehicle and Heavy Equipment Transport Systems, Various Span Lengths

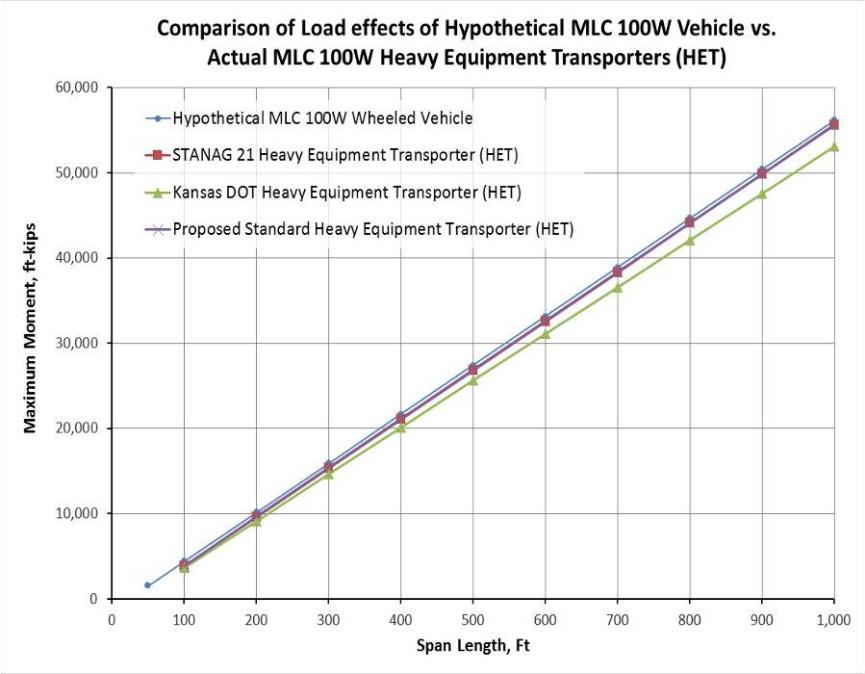

Figure 5-28: Maximum Moments for MLC 100W Hypothetical Vehicle and Heavy Equipment Transport Systems, Various Span Lengths

The calculated maximum moments shown on Figures 5-29, 5-30 and 5-31 include the AASHTO dynamic load allowance increase, or impact of 33%, in order to allow for the comparison of these results to the maximum AASHTO HL-93 design truck and lane loading with impact and the single MLC 100W hypothetical vehicles live loading with impact on a span of the same length.

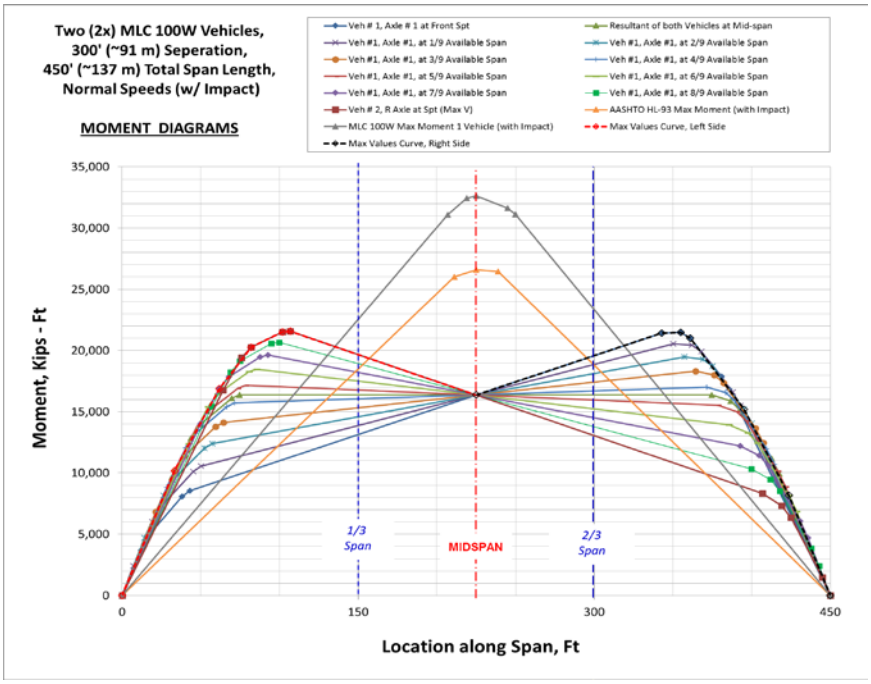

Figure 5-29: Maximum Moments for Two MLC 100W Vehicles on a 450 ft (137.2 m) Span

Following the analysis of two vehicles on span, a fifteen axle calculation spreadsheet was developed and used to analyze the condition of three MLC 100W hypothetical vehicles on the span, for spans of 730 - 1,000 ft (222.5 – 304.8 m). The lower limit of 730 ft (222.5 m) corresponds to three MLC 100W vehicles each 43 ft (13.1 m) in length (from front to rear axle)

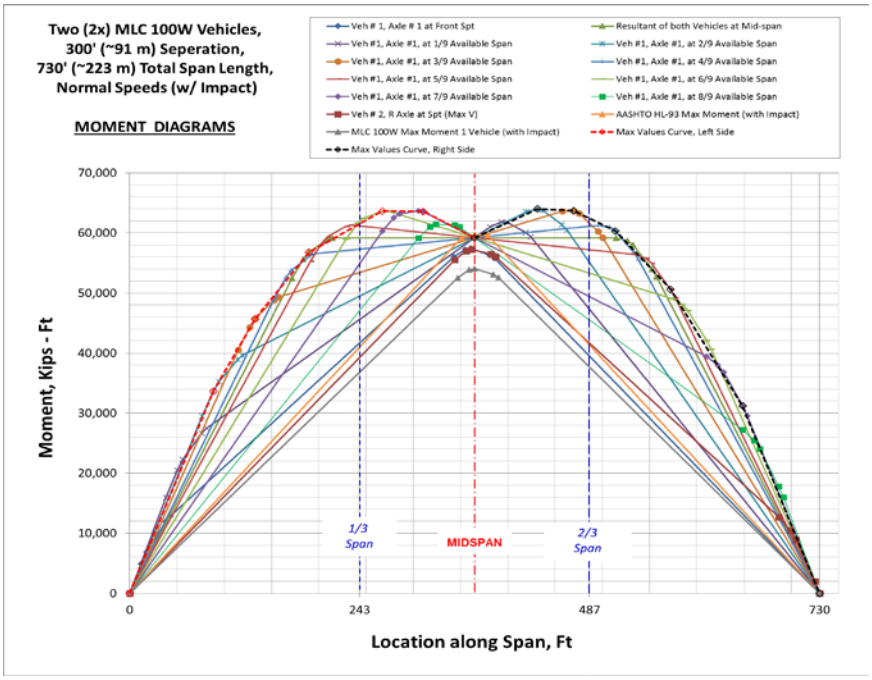

Figure 5-30: Maximum Moments for Two MLC 100W Vehicles on a 730 ft (222.5 m) Span

separated by 300 ft (91.4 m) between rear axle of leading vehicle to front axle of following vehicle, resulting in two separation distances of 300 ft (91.4 m) between three hypothetical vehicles. A representative plot of the moment diagram based on possible vehicle positioning along the span is shown on Figure 5-31. It is interesting to note that the possible moment curve for the two MLC 100W hypothetical vehicle loading resulted in significantly higher moment magnitudes at span lengths less than mid-span than the corresponding maximum moment at the same span location for three MLC 100W hypothetical vehicles on the span.

The individual and combined maximum end shear and mid-span moment profiles for one, two and three MLC 100W vehicles on simple beams of spans 50 - 1,000 feet (15.2 – 304.8 m) are plotted on Figure 5-32 and 5-33 and shown on Table 5-7 and 5-8 respectively. Note that these values include the 33% dynamic load allowance or impact increase.

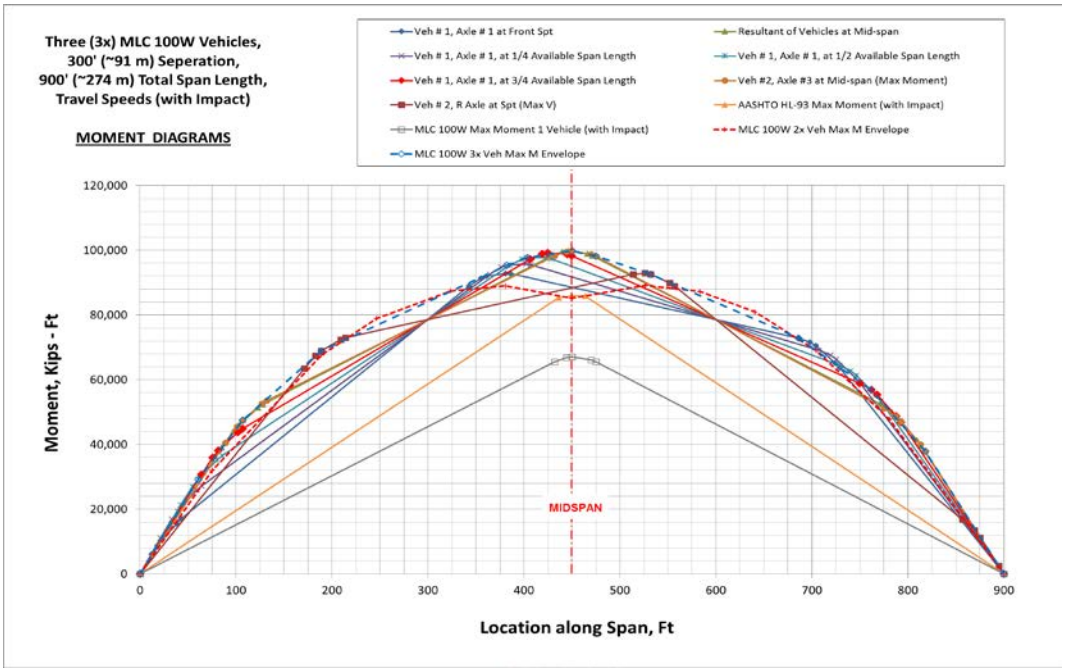

Figure 5-31: Maximum Moments for Three MLC 100W Vehicles, 900 ft (274.3 m) Span

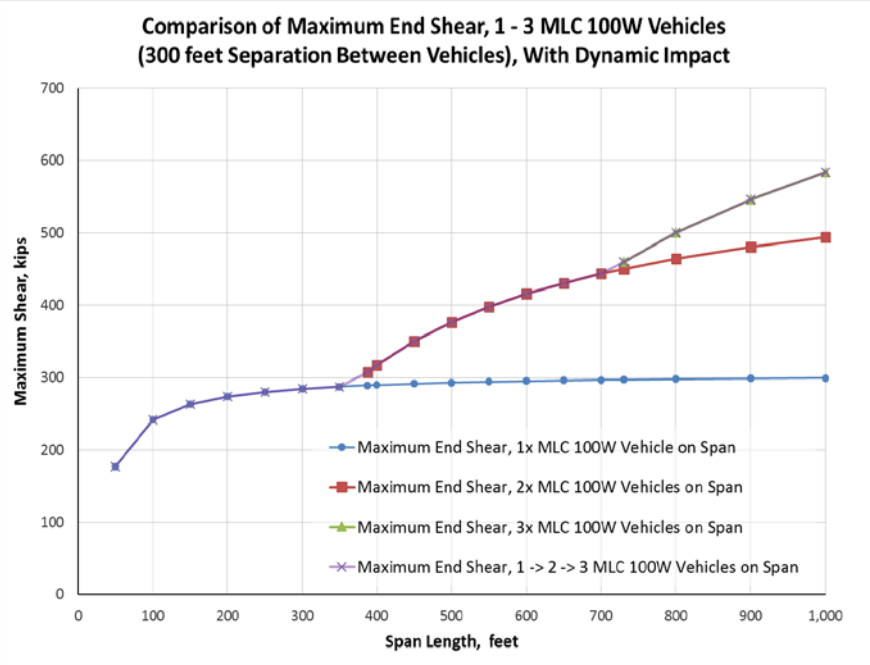

Figure 5-32: Maximum End Shears for 1-3 MLC100W Hypothetical Vehicles

Maximum End Shear (Vmax, kips), with Dynamic Load Allowance (Impact)				
Span Length	MLC 100W, 1 Vehicle	MLC 100W, 2 Vehicle, 300' separation	MLC 100W, 3 Vehicle, 300' separation	Multiple MLC 100W Vehicles on span, with Impact
L, ft (m)	Vmax, kips (kN)	Vmax, kips (kN)	Vmax, kips (kN)	Vmax, kips (kN)
50 (15.2)	176.9 (786.8)			176.9 (786.8)
100 (30.5)	241.4 (1,073.7)			241.4 (1,073.7)
150 (45.7)	262.9 (1,169.4)			262.9 (1,169.4)
200 (61.0)	273.6 (1,217.2)			273.6 (1,217.2)
250 (76.2)	280.1 (1,245.9)			280.1 (1,245.9)
300 (91.4)	284.4 (1,265.0)			284.4 (1,265.0)
350 (106.7)	287.5 (1,278.7)			287.5 (1,278.7)
387 (118.0)	289.2 (1,286.5)	307.3 (1,367.1)		307.3 (1,367.1)
400 (121.9)	289.8 (1,288.9)	317.2 (1,411.1)		317.2 (1,411.1)
450 (137.2)	291.6 (1,296.9)	350.0 (1,556.7)		350.0 (1,556.7)
500 (152.4)	293.0 (1,303.3)	376.2 (1,673.1)		376.2 (1,673.1)
550 (167.6)	294.2 (1,308.5)	397.6 (1,768.4)		397.6 (1,768.4)
600 (182.9)	295.1 (1,312.8)	415.4 (1,847.8)		415.4 (1,847.8)
650 (198.1)	296.0 (1,316.5)	430.5 (1,915.0)		430.5 (1,915.0)
700 (213.4)	296.7 (1,319.7)	443.5 (1,972.6)		443.5 (1,972.6)
730 (222.5)	297.1 (1,321.3)	450.4 (2,003.4)	460.0 (2,046.1)	460.0 (2,046.1)
800 (243.8)	297.8 (1,324.8)	464.5 (2,066.2)	500.0 (2,224.2)	500.0 (2,224.2)
900 (274.3)	298.7 (1,328.8)	480.9 (2,139.0)	546.5 (2,430.6)	546.5 (2,430.6)
1,000 (304.8)	299.4 (1,332.0)	494.0 (2,197.2)	583.6 (2,595.8)	583.6 (2,595.8)

Table 5-7: Maximum End Shears for 1-3 MLC100W Hypothetical Vehicles

In order to compare the multiple MLC 100W hypothetical vehicle loading with the AASHTO HL-93 live load specification, the maximum shear and moment profiles were normalized to the AASHTO HL-93 design truck and lane load, and plotted along with the

AASHTO alternative military tandem and lane load, with dynamic load allowance (impact), on Figures 5-34 and 5-35. On these and subsequent normalized figures, the ratio of the live load factors for AASHTO Strength I to Strength II design conditions is plotted to indicate the relative comparison between the proposed military loading as a permit load and the standard specification. This ratio is equal to the Strength I design condition load factor of 1.75 divided by the Strength II design condition load factor, resulting in a ratio of 1.296. The proposed multiple MLC 100W hypothetical vehicle loading would be an AASHTO Strength II design condition, therefore the 1.75:1.35 ratio allows for comparison between these two design conditions.

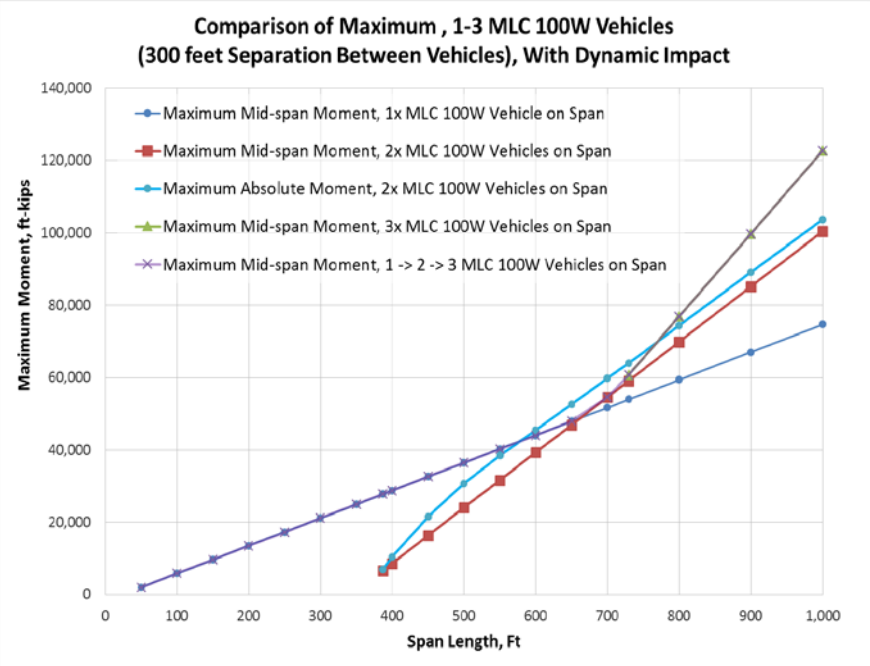

Figure 5-33: Maximum Moments for 1-3 MLC100W Hypothetical Vehicles, with Impact

Maximum Mid-Span / Absolute Moment (Mmax, ft-kips), with Dynamic Load Allowance (Impact)					
Span Length	Maximum Mid-span Moment, 1x MLC 100W Vehicles	Maximum Mid-span Moment, 2x MLC 100W Vehicles	Maximum Absolute Moment, 2x MLC 100W Vehicles	Maximum Mid-span Moment, 3x MLC 100W Vehicles	Maximum Possible Moment, 1-3x MLC 100W Vehicles
L, ft (m)	Mmax, ft-kips (kN-m)	Mmax, ft-kips (kN-m)	Mmax, ft-kips (kN-m)	Mmax, ft-kips (kN-m)	Mmax, ft-kips (kN-m)
50 (15.2)	2,028.3 (2,749.9)				2,028.3 (2,749.9)
100 (30.5)	5,852.0 (7,934.1)				5,852.0 (7,934.1)
150 (45.7)	9,675.8 (13,118.4)				9,675.8 (13,118.4)
200 (61.0)	13,499.5 (18,302.6)				13,499.5 (18,302.6)
250 (76.2)	17,323.3 (23,486.9)				17,323.3 (23,486.9)
300 (91.4)	21,147.0 (28,671.1)				21,147.0 (28,671.1)
350 (106.7)	24,970.8 (33,855.3)				24,970.8 (33,855.3)
387 (118.0)	27,800.3 (37,691.7)	6,729.8 (9,124.3)	6,945.6 (9,416.8)		27,800.3 (37,691.7)
400 (121.9)	28,794.5 (39,039.6)	8,718.2 (11,820.1)	10,339.5 (14,018.3)		28,794.5 (39,039.6)
450 (137.2)	32,618.3 (44,223.8)	16,365.7 (22,188.5)	21,565.6 (29,238.6)		32,618.3 (44,223.8)
500 (152.4)	36,442.0 (49,408.1)	24,013.2 (32,557.0)	30,804.5 (41,764.8)		36,442.0 (49,408.1)
550 (167.6)	40,265.8 (54,592.3)	31,660.7 (42,925.5)	38,442.2 (52,119.9)		40,265.8 (54,592.3)
600 (182.9)	44,089.5 (59,776.5)	39,308.2 (53,294.0)	45,481.2 (61,663.4)		44,089.5 (59,776.5)
650 (198.1)	47,913.3 (64,960.8)	46,955.7 (63,662.5)	52,562.5 (71,264.2)		47,913.3 (64,960.8)
700 (213.4)	51,737.0 (70,145.0)	54,603.2 (74,031.0)	59,797.8 (81,073.9)		54,603.2 (74,031.0)
730 (222.5)	54,031.3 (73,255.6)	59,191.7 (80,252.0)	64,010.9 (86,786.0)	60,764.5 (82,384.5)	60,764.5 (82,384.5)
800 (243.8)	59,384.5 (80,513.5)	69,898.2 (94,767.9)	74,297.4 (100,732.4)	76,820.8 (104,153.6)	76,820.8 (104,153.6)
900 (274.3)	67,032.0 (90,882.0)	85,193.2 (115,504.9)	89,138.1 (120,853.5)	99,763.3 (135,259.1)	99,763.3 (135,259.1)
1,000 (304.8)	74,679.5 (101,250.5)	100,488.2 (136,241.8)	103,729.9 (140,636.9)	122,705.8 (166,364.5)	122,705.8 (166,364.5)

Table 5-8: Maximum Moments for 1-3 MLC100W Hypothetical Vehicles

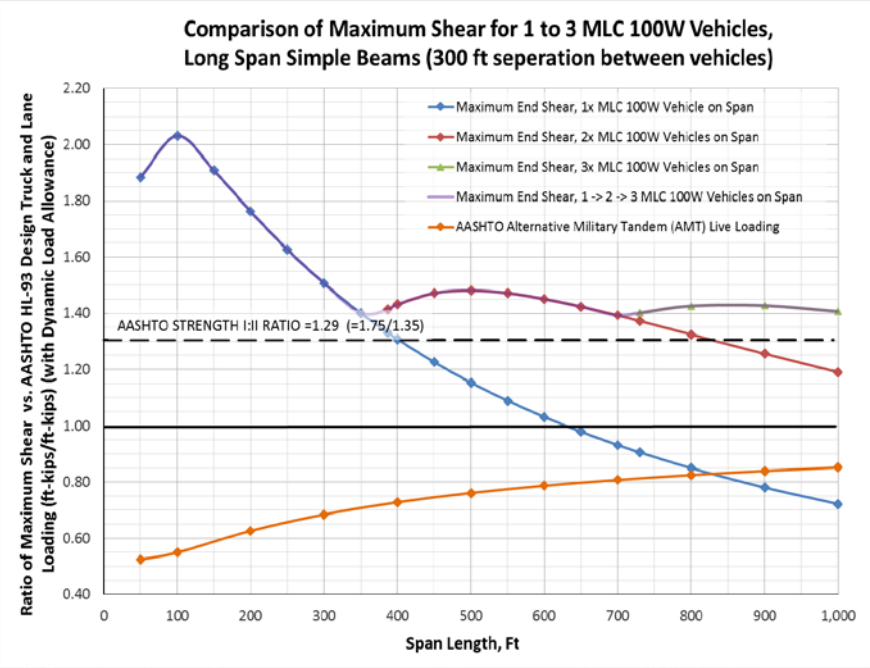

Figure 5-34: Maximum End Shear for Multiple MLC 100W Hypothetical Vehicles, Normalized to HL-93 Design Truck and Lane Live Load

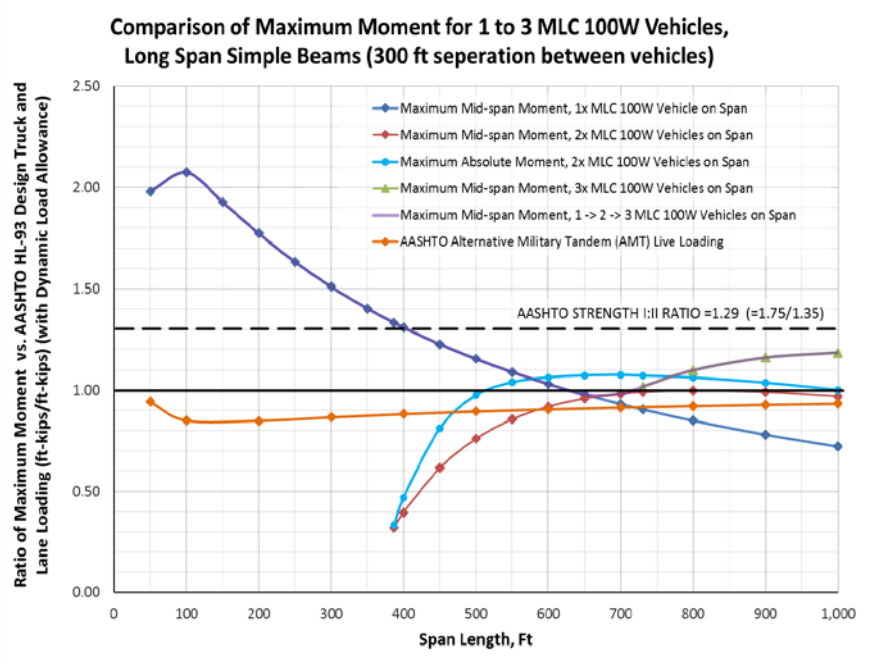

Figure 5-35: Maximum Moments for Multiple MLC 100W Hypothetical Vehicles, Normalized to HL-93 Design Truck and Lane Live Load

5.5 COMPARISON TO OTHER DESIGN CODES AND LOADINGS

The MLC 100W hypothetical vehicle live load was also compared to the various other bridge live loadings described in Chapter 3 to confirm its validity as an appropriate alternative military live load for civilian bridge design. The two broad categories considered were loadings of primarily uniform lane loads and permit loads representing state specific heavy vehicles operating on the national highway system.

For the uniform lane loads, the two Canadian standard loadings (the Ontario Highway Bridge Design and the Canadian CL-W truck loading) and the saturated flow condition[7] loading described in Chapter 3 and the proposed logistic truck convoy described in the previous chapter were compared to the results from the AASHTO HL-93 design truck and lane live load and the maximum shear and mid-span moment for 1-3 MLC 100W hypothetical wheeled vehicles on a span of 50 - 1,000 feet (15.2 – 304.8 m). The maximum shear and mid-span moment for the selected uniform lane loads are shown on Table 5-9, plotted on Figures 5-36 and 5-37 respectively, and plotted as normalized to the AASHTO HL-93 design truck and lane live load on Figures 5-38 and 5-39. For these loadings, no dynamic load allowance was applied to either the end shear or the maximum mid-span moment since impact does not apply to uniform, or steady state, applied live loadings.

As shown on the Figures 5-38 and 5-39, the proposed MLC 100W live load produces greater shear and moment at shorter spans (< 300 ft; < 91.4 m) compared to the various other design codes. In the case of mid-span moment, the two Canadian loadings produce greater moment at very short spans (< 100 ft; < 30.5 m). This is because these two loadings incorporate a truck load that corresponds to a heavy permit truck load similar to the American permit truck loads that will be analyzed in the following paragraphs. The normalized curves plotted on

Figures 5-38 and 5-39 show that the proposed MLC 100W live load exceeds the AASHTO Strength I:II ratio of 1.296 for span lengths of 100 - 300 ft (30.5 – 91.4 m).

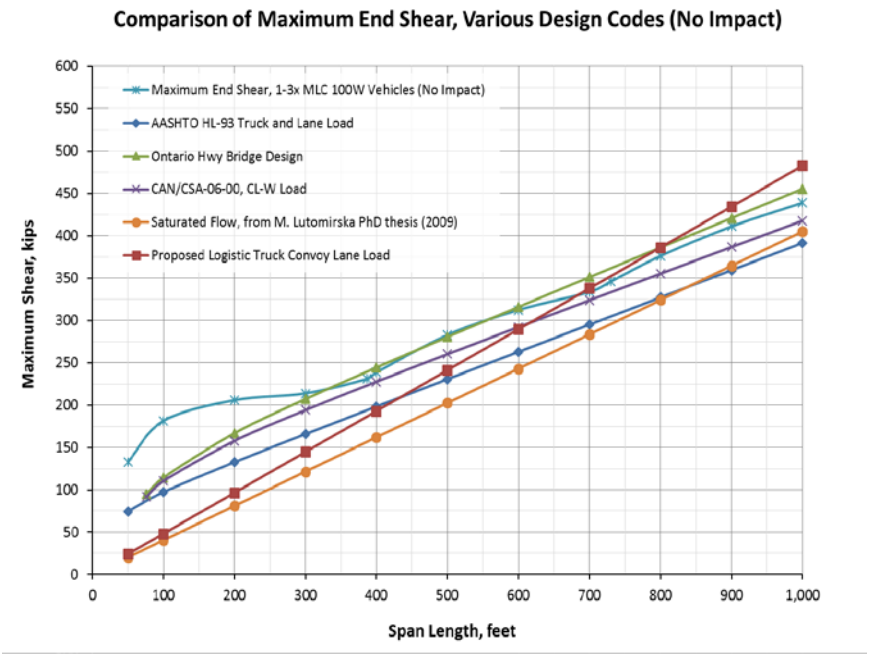

Figure 5-36: Comparison of Maximum End Shear for Various Other Considered Design Codes and Proposed Live Loads

For the selected non-Louisiana permit loads, the vehicles considered were the Washington State Permit Vehicle Type 3 (WA-03)[8], the Wisconsin Special Permit Vehicle (Wis-SPV)[9], and a proposed hypothetical 5 axle permit vehicle[10]. The AASHTO dynamic load allowance factor was applied to these permit loads to allow for comparison to the AASHTO HL-93 design truck and lane load as the dynamic condition. The maximum shears and mid-span moments for the selected permit vehicles are shown on Table 5-10 and plotted normalized to the AASHTO HL-93 truck and land load on Figures 5-40 and 5-41.

Maximum End Shear (Vmax, kips), No Impact					
Span Length L, ft (m)	Maximum Mid-span Moment, 1-3x MLC 100W Vehicles Vmax, kips (kN)	Ontario Hwy Bridge Design Vmax, kips (kN)	CAN/CSA-06-00, CL-W Load Vmax, kips (kN)	Saturated Flow (Lutomirska, 2009 Vmax, kips (kN)	Proposed Logistic Truck Convoy Lane Load Vmax, kips (kN)
50 (15.2)	133.0 (591.6)	94.7 (421.0)	91.6 (407.4)	20.3 (90.1)	24.1 (107.3)
100 (30.5)	181.5 (807.3)	114.4 (508.7)	110.3 (490.7)	40.5 (180.1)	48.3 (214.6)
200 (61.0)	205.8 (915.2)	166.8 (742.0)	157.7 (701.4)	81.0 (360.3)	96.5 (429.2)
300 (91.4)	213.8 (951.1)	207.1 (921.3)	194.0 (863.1)	121.5 (540.4)	144.8 (643.8)
400 (121.9)	238.5 (1,061.0)	244.4 (1,087.1)	227.6 (1,012.6)	162.0 (720.6)	193.0 (858.5)
500 (152.4)	282.8 (1,258.0)	280.5 (1,247.5)	260.1 (1,157.1)	202.5 (900.7)	241.3 (1,073.1)
600 (182.9)	312.4 (1,389.3)	315.9 (1,405.3)	292.1 (1,299.2)	243.0 (1,080.9)	289.5 (1,287.7)
700 (213.4)	333.4 (1,483.2)	351.1 (1,561.5)	323.7 (1,440.0)	283.5 (1,261.0)	337.8 (1,502.3)
800 (243.8)	376.0 (1,672.3)	386.0 (1,716.7)	355.2 (1,579.8)	324.0 (1,441.2)	386.0 (1,716.9)
900 (274.3)	410.9 (1,827.5)	420.7 (1,871.3)	386.5 (1,719.1)	364.5 (1,621.3)	434.3 (1,931.5)
1,000 (304.8)	438.8 (1,951.7)	455.4 (2,025.4)	417.7 (1,857.9)	405.0 (1,801.4)	482.5 (2,146.2)

Maximum Mid-Span Moment (Mmax, ft-kips), No Impact					
Span Length L, ft (m)	Maximum Mid-span Moment, 1-3x MLC 100W Vehicles Mmax, ft-kips (kN-m)	Ontario Hwy Bridge Design Mmax, ft-kips (kN-m)	CAN/CSA-06-00, CL-W Load Mmax, ft-kips (kN-m)	Saturated Flow (Lutomirska, 2009 Mmax, ft-kips (kN-m)	Proposed Logistic Truck Convoy Lane Load Mmax, ft-kips (kN-m)
50 (15.2)	1,525.0 (2,067.6)	1,761.6 (2,388.4)	1,551.3 (2,103.3)	253.1 (343.2)	301.6 (408.9)
100 (30.5)	4,400.0 (5,965.5)	2,807.3 (3,806.1)	2,586.8 (3,507.2)	1,012.5 (1,372.7)	1,206.3 (1,635.4)
200 (61.0)	10,150.0 (13,761.4)	8,264.8 (11,205.4)	7,705.4 (10,447.0)	4,050.0 (5,491.0)	4,825.0 (6,541.7)
300 (91.4)	15,900.0 (21,557.2)	15,450.6 (20,947.9)	14,371.7 (19,485.1)	9,112.5 (12,354.7)	10,856.3 (14,718.9)
400 (121.9)	21,650.0 (29,353.1)	24,352.9 (33,017.7)	22,581.6 (30,616.2)	16,200.0 (21,964.0)	19,300.0 (26,166.9)
500 (152.4)	27,400.0 (37,148.9)	34,969.3 (47,411.4)	32,334.6 (43,839.3)	25,312.5 (34,318.7)	30,156.3 (40,885.8)
600 (182.9)	34,199.5 (46,367.7)	47,299.0 (64,127.9)	43,630.4 (59,154.0)	36,450.0 (49,418.9)	43,425.0 (58,875.6)
700 (213.4)	44,984.6 (60,990.1)	61,341.6 (83,166.9)	56,468.7 (76,560.3)	49,612.5 (67,264.6)	59,106.3 (80,136.3)
800 (243.8)	57,763.3 (78,315.5)	77,097.0 (104,528.1)	70,849.7 (96,058.1)	64,800.0 (87,855.8)	77,200.0 (104,667.8)
900 (274.3)	75,012.9 (101,702.5)	94,565.1 (128,211.3)	86,773.3 (117,647.2)	82,012.5 (111,192.5)	97,706.3 (132,470.1)
1,000 (304.8)	92,262.6 (125,089.7)	113,745.8 (154,216.5)	104,239.3 (141,327.7)	101,250.0 (137,274.8)	120,625.0 (163,543.4)

Table 5-9: Maximum End Shear and Mid-span Moments for Various Uniform Loads and 1-3 MLC100W Hypothetical Wheeled Vehicles, Various Span Lengths

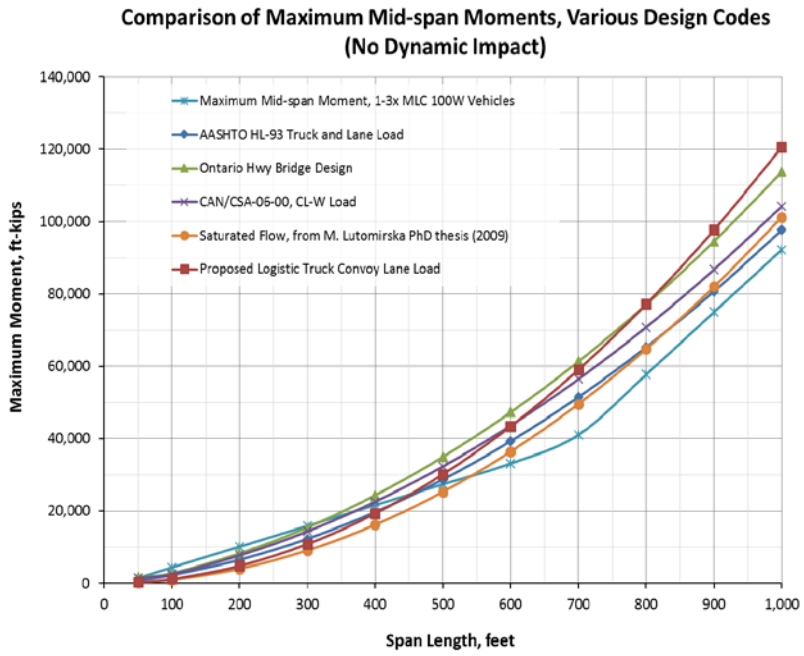

Figure 5-37: Comparison of Maximum Mid-span Moment for Various Other Considered Design Codes and Proposed Live Loads

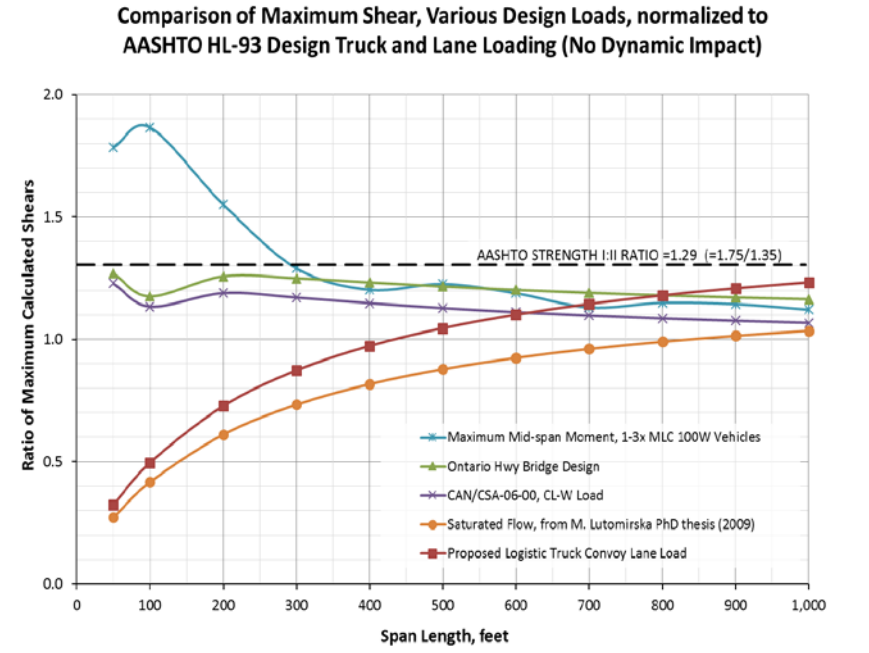

Figure 5-38: Comparison of Maximum End Shear for Various Other Considered Design Codes and Proposed Live Loads, Normalized to AASHTO HL-93

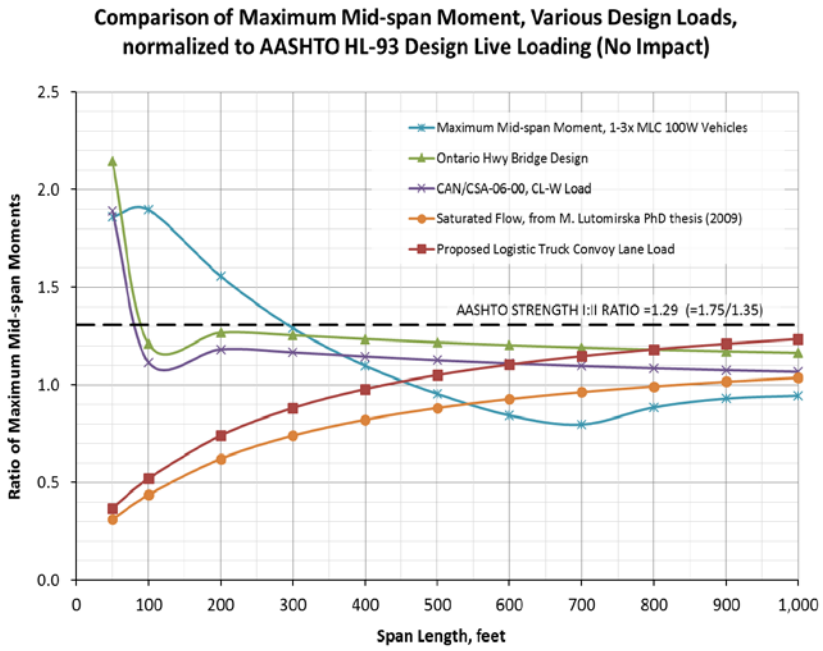

Figure 5-39: Comparison of Maximum Mid-span Moment for Various Other Considered Design Codes and Proposed Live Loads, Normalized to AASHTO HL-93

For bridge design in the State of Louisiana, the Strength II condition requires the use of a design envelope as discussed previously in Chapter 3. Accordingly, the MLC 100W multiple vehicle loading was plotted with the Louisiana Design Vehicle Live Load 2011 (LADV-11) design criteria envelope, along with the Louisiana Special Design Vehicle Type 5 (LASDV-5) and one MLC 70T hypothetical tracked vehicle on span, which represents a single main battle tank crossing the span in a controlled crossing. The LASDV-5 was used due to its similarity to selected non-Louisiana permit loads and the military heavy equipment transport (HET) systems discussed earlier. The single MLC 70T hypothetical tracked vehicle on span condition was included to analyze the possibility of a tracked vehicle crossing the bridge in extreme circumstances.

Dynamic impact was included in the comparison of the various permit truck loadings to allow for normalization to the AASHTO HL-93 design truck and lane loading with impact as shown on Figures 5-40 and 5-41. If needed, the dynamic impact can be factored out of all values shown on Table 5-10 due to the absence of a uniform lane load in any load condition. The dynamic load allowance factor was included for a single MLC 70T hypothetical tracked vehicle on span since this crossing would cause significant vibrational loading to all bridge structures.

The comparison of the LADV-11 design procedure to the MLC 100W multiple vehicle loading and the LASDV-5 loading was accomplished using a LADV-11 design criteria envelope based on the AASHTO Strength I to Strength II condition ratio described previously. Assuming that the LADV-11 is used as an AASHTO Strength I condition and using the MF listed on Table 3-3, the upper limit of the MF magnified Strength I to Strength II condition ratio is equal to 1.69 (=1.3 x 1.75/1.35). This ratio is applied to the normalized maximum shear and moments for span lengths less 240 ft (73.2 m). For span lengths equal to or greater than 600 ft (182.9 m), the previously described Strength I to Strength II ratio of 1.296 is applied to the normalized values. Between these span lengths (240 - 600 ft; 73.2 - 182.9 m), the Strength I to Strength II condition ratio decreases linearly from 1.69 to 1.296. The linear segments of the LADV-11 design criteria envelope are plotted with the normalized maximum shear and moments on Figures 5-42 and 5-43.

In comparison to the state permit loads, the MLC 100W multiple vehicle loading produces approximately equal shear compared to the considered permit trucks and the hypothetical 5 axle permit vehicle. The MLC 100W multiple vehicle loading develops greater mid-span moment for the two permit trucks but less mid-span moment than the hypothetical 5 axle permit vehicle for very short span lengths (< 100 ft; < 30.5 m).

Maximum End Shear (Vmax, kips), with Dynamic Impact				
Span Length L, ft (m)	Maximum Mid-span Moment, 1-3x MLC 100W Vehicles Vmax, kips (kN)	Washington State Permit Veh Type 3 (WA-03) Vmax, kips (kN)	Wisconsin Special Permit Vehicle (Wis-SPV) Vmax, kips (kN)	Hypothetical 5-axle permit vehicle (Zhao Tabatabai, 2012) Vmax, kips (kN)
50 (15.2)	176.9 (786.8)			189.7 (843.8)
100 (30.5)	241.4 (1,073.7)	248.0 (1,102.9)	238.8 (1,062.3)	194.6 (865.5)
200 (61.0)	273.6 (1,217.2)	307.1 (1,365.8)	285.7 (1,270.6)	197.0 (876.3)
300 (91.4)	284.4 (1,265.0)	326.8 (1,453.4)	301.3 (1,340.0)	197.8 (879.9)
400 (121.9)	317.2 (1,411.1)	336.6 (1,497.3)	309.1 (1,374.7)	198.2 (881.7)
500 (152.4)	376.2 (1,673.1)	342.5 (1,523.5)	313.8 (1,395.6)	198.5 (882.7)
600 (182.9)	415.4 (1,847.8)	346.5 (1,541.1)	316.9 (1,409.5)	198.6 (883.5)
700 (213.4)	443.5 (1,972.6)	349.3 (1,553.6)	319.1 (1,419.4)	198.7 (884.0)
800 (243.8)	500.0 (2,224.2)	351.4 (1,563.0)	320.8 (1,426.8)	198.8 (884.4)
900 (274.3)	546.5 (2,430.6)	353.0 (1,570.3)	322.1 (1,432.6)	198.9 (884.7)
1,000 (304.8)	583.6 (2,595.8)	354.3 (1,576.1)	323.1 (1,437.2)	198.9 (884.9)

Maximum Mid-Span Moment (Mmax, ft-kips), with Dynamic Impact				
Span Length L, ft (m)	Maximum Mid-span Moment, 1-3x MLC 100W Vehicles Mmax, ft-kips (kN-m)	Washington State Permit Veh Type 3 (WA-03) Vmax, kips (kN-m)	Wisconsin Special Permit Vehicle (Wis-SPV) Vmax, kips (kN-m)	Hypothetical 5-axle permit vehicle (Zhao Tabatabai, 2012) Vmax, kips (kN-m)
50 (15.2)	2,028.3 (2,749.9)			2,321.4 (3,147.3)
100 (30.5)	5,852.0 (7,934.1)	5,667.0 (7,683.3)	5,010.6 (6,793.4)	4,814.2 (6,527.2)
200 (61.0)	13,499.5 (18,302.6)	14,818.7 (20,091.2)	13,250.5 (17,965.0)	9,800.0 (13,286.8)
300 (91.4)	21,147.0 (28,671.1)	23,972.0 (32,501.2)	21,538.6 (29,202.0)	14,785.8 (20,046.5)
400 (121.9)	28,794.5 (39,039.6)	33,125.6 (44,911.7)	29,838.6 (40,455.2)	19,771.5 (26,806.2)
500 (152.4)	36,442.0 (49,408.1)	42,279.4 (57,322.5)	38,143.6 (51,715.0)	24,757.3 (33,565.9)
600 (182.9)	45,485.3 (61,669.0)	51,433.3 (69,733.3)	46,450.9 (62,978.1)	29,743.0 (40,325.6)
700 (213.4)	59,829.5 (81,116.9)	60,587.3 (82,144.2)	54,759.6 (74,243.0)	34,728.8 (47,085.3)
800 (243.8)	76,825.2 (104,159.6)	69,741.2 (94,555.2)	63,069.1 (85,509.1)	39,714.6 (53,845.0)
900 (274.3)	99,767.2 (135,264.4)	78,895.2 (106,966.2)	71,379.2 (96,776.0)	44,700.3 (60,604.7)
1,000 (304.8)	122,709.3 (166,369.3)	88,049.2 (119,377.2)	79,689.7 (108,043.4)	49,686.1 (67,364.4)

Table 5-10 Maximum Shear and Mid-span Moments for State Permit Vehicles and 1-3 MLC100W Hypothetical Wheeled Vehicles on 50 to 1,000 ft (15.2 – 304.8 m) Span Length Simple Beams

Maximum End Shear (Vmax, kips), With Dynamic Impact				
Span Length	AASHTO HL-93 Design Truck and Lane Load	Maximum Mid-span Moment, 1-3x MLC 100W Vehicles	Louisiana Special Design Veh Type 5 (LASDV-5)	One MLC 70T Hypothetical Tracked Vehicle
L, ft (m)	Vmax, kips (kN)	Vmax, kips (kN)	Vmax, kips (kN)	Vmax, kips (kN)
50 (15.2)	93.9 (417.6)	176.9 (786.8)		210.5 (936.3)
100 (30.5)	118.8 (528.5)	241.4 (1,073.7)	189.0 (840.8)	229.1 (1,018.9)
200 (61.0)	155.3 (690.7)	273.6 (1,217.2)	233.5 (1,038.6)	238.4 (1,060.2)
300 (91.4)	188.8 (839.7)	284.4 (1,265.0)	248.3 (1,104.5)	241.5 (1,074.0)
400 (121.9)	221.5 (985.3)	317.2 (1,411.1)	255.7 (1,137.5)	243.0 (1,080.9)
500 (152.4)	254.0 (1,129.7)	376.2 (1,673.1)	260.2 (1,157.3)	243.9 (1,085.0)
600 (182.9)	286.3 (1,273.3)	415.4 (1,847.8)	263.1 (1,170.5)	244.6 (1,087.8)
700 (213.4)	318.5 (1,416.6)	443.5 (1,972.6)	265.3 (1,179.9)	245.0 (1,089.7)
800 (243.8)	350.6 (1,559.7)	500.0 (2,224.2)	266.9 (1,187.0)	245.3 (1,091.2)
900 (274.3)	382.8 (1,702.5)	546.5 (2,430.6)	268.1 (1,192.5)	245.6 (1,092.3)
1,000 (304.8)	414.9 (1,845.3)	583.6 (2,595.8)	269.1 (1,196.8)	245.8 (1,093.3)

Maximum Mid-Span Moment (Mmax, ft-kips), With Dynamic Impact				
Span Length	AASHTO HL-93 Design Truck and Lane Load	Maximum Mid-span Moment, 1-3x MLC 100W Vehicles	Louisiana Special Design Veh Type 5 (LASDV-5)	One MLC 70T Hypothetical Tracked Vehicle
L, ft (m)	Mmax, ft-kips (kN-m)	Mmax, ft-kips (kN-m)	Mmax, ft-kips (kN-m)	Mmax, ft-kips (kN-m)
50 (15.2)	1,024.6 (1,389.2)	2,028.3 (2,749.9)		1,978.4 (2,682.3)
100 (30.5)	2,821.6 (3,825.6)	5,852.0 (7,934.1)	4,674.5 (6,337.7)	4,305.9 (5,837.9)
200 (61.0)	7,615.6 (10,325.3)	13,499.5 (18,302.6)	11,623.2 (15,758.7)	8,960.9 (12,149.2)
300 (91.4)	14,009.6 (18,994.2)	21,147.0 (28,671.1)	18,572.3 (25,180.3)	13,615.9 (18,460.4)
400 (121.9)	22,003.6 (29,832.5)	28,794.5 (39,039.6)	25,521.4 (34,601.9)	18,270.9 (24,771.7)
500 (152.4)	31,597.6 (42,840.1)	36,442.0 (49,408.1)	32,470.6 (44,023.7)	22,925.9 (31,082.9)
600 (182.9)	42,791.6 (58,016.9)	45,485.3 (61,669.0)	39,419.8 (53,445.4)	27,580.9 (37,394.2)
700 (213.4)	55,585.6 (75,363.0)	59,829.5 (81,116.9)	46,369.1 (62,867.2)	32,235.9 (43,705.4)
800 (243.8)	69,979.6 (94,878.4)	76,825.2 (104,159.6)	53,318.3 (72,288.9)	36,890.9 (50,016.6)
900 (274.3)	85,973.6 (116,563.0)	99,767.2 (135,264.4)	60,267.5 (81,710.7)	41,545.9 (56,327.9)
1,000 (304.8)	103,567.6 (140,417.0)	122,709.3 (166,369.3)	67,216.8 (91,132.5)	46,200.9 (62,639.1)

Table 5-11 Maximum Shear and Mid-span Moments per Louisiana DOTD BDEM and 1-3 MLC100W Hypothetical Wheeled Vehicles on 50 to 1,000 ft (15.2 – 304.8 m) Span Length Simple Beams

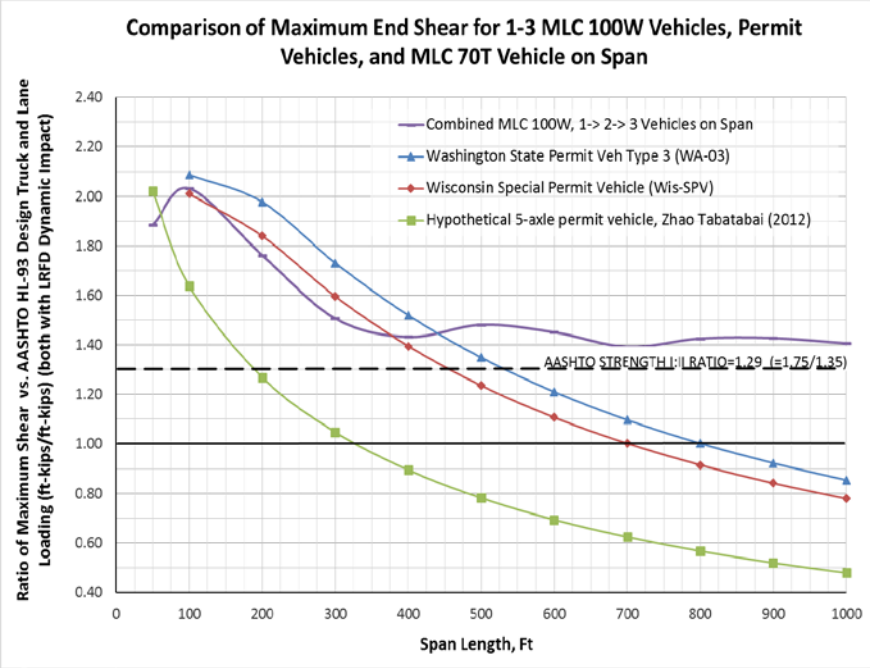

Figure 5-40: Comparison of Maximum Shear for Various (Non State of Louisiana) Permit Loads, Normalized to AASHTO HL-93

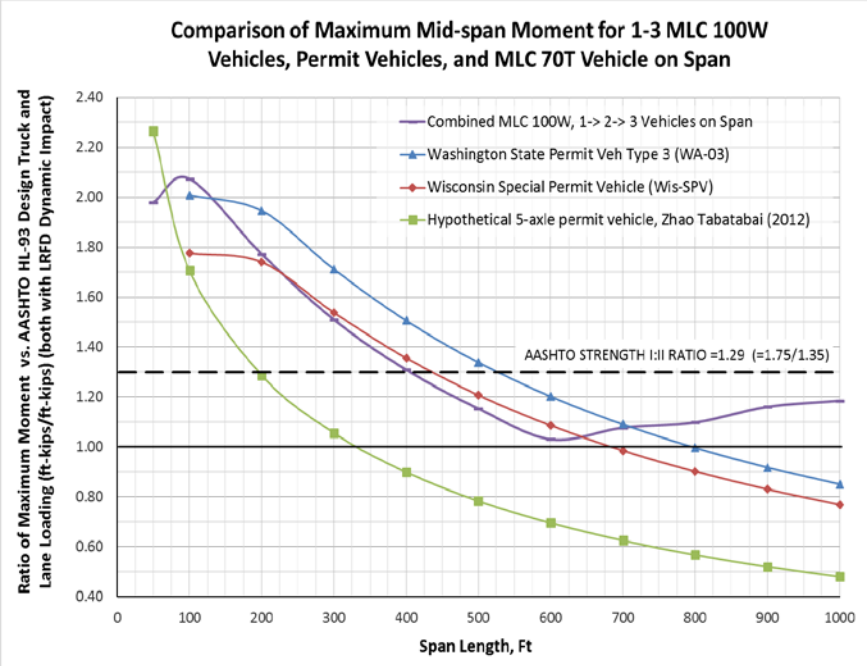

Figure 5-41: Comparison of Maximum Mid-span Moment for Various (Non State of Louisiana) Permit Loads, Normalized to AASHTO HL-93

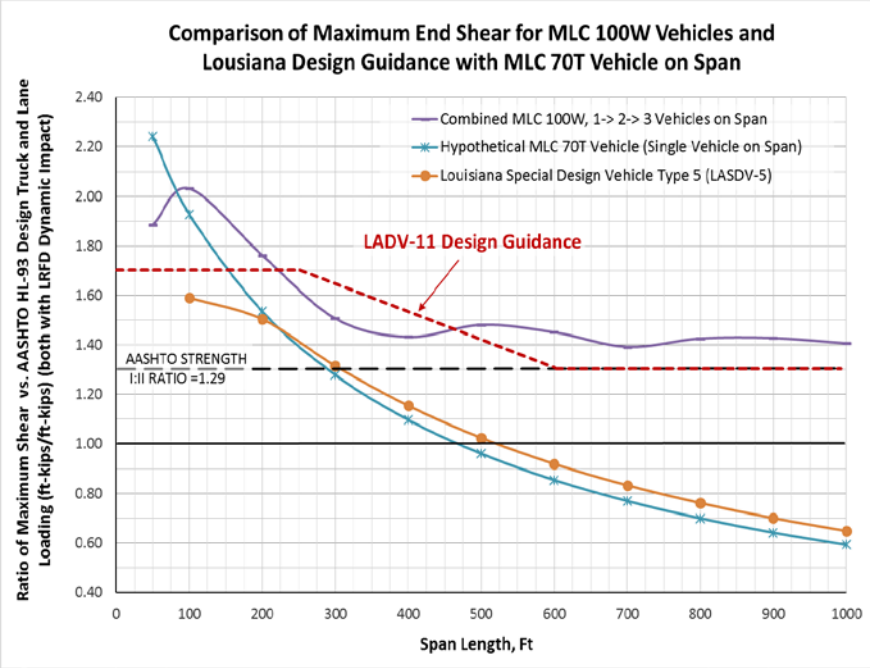

Figure 5-42: Comparison of Maximum Shear for Louisiana Bridge Design Guidance and Hypothetical MLC 70 Tracked Vehicle on Span, Normalized[11]

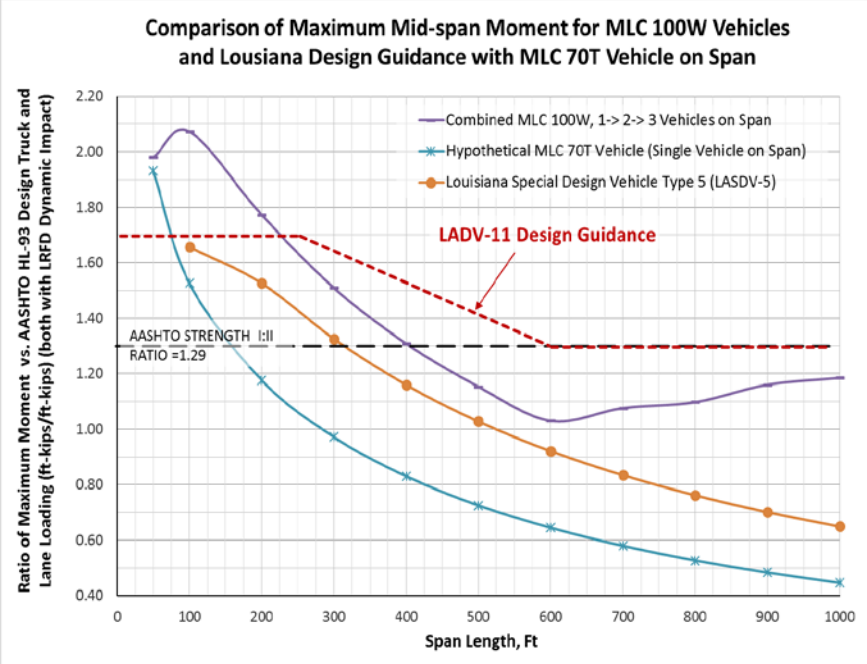

Figure 5-43: Comparison of Maximum Mid-span Moment for Louisiana Bridge Design Guidance and Hypothetical MLC 70 Tracked Vehicle on Span, Normalized[12]

For bridge design in the State of Louisiana, the proposed MLC 100W live load plots outside of the LADV-11 design envelope for shorter spans (< 200 ft; < 61.0 m). Therefore, the proposed MLC 100W live load would result in greater shear and mid-span moments than the current Louisiana design criteria for short spans of 200 ft (61.0 m) or less.

5.6 CHAPTER FIVE END NOTES

1. California Department of Transportation (CALTRANS) (2008), Bridge Design Aids, HL-93 Loading, page 2.
2. California Department of Transportation (2008), page 4.
3. Tonias, D.E. and Zhao, J.J. (2007), *Bridge Engineering (2nd Edition)*, page 176. See also McCormac, J. and Elling, R.E. (1998), *Structural Analysis: A Classical and Matrix Approach*, page 183.
4. U.S. Department of the Army (2002), Military Non-Standard Fixed Bridging (FM3-34.343), pages B-6 - B-13.
5. U.S. Department of the Army (2002), page 3-13. See also Ray and Seda-Sanabria, Technical Commentary on FM3-34.343, page 6.
6. U.S. Department of the Army (2002), pages 3-13. See also STANAG 2021, 6th Edition, page 9/16.
7. Lutomirska, M. (2009), "Live Load Models for Long Span Bridges", page 65.
8. Mlynarski, M., Wassef, W., and Nowak, A.S. (2011), "A Comparison of AASHTO Bridge Load Rating Methods", page 14.
9. Zhao, J. and Tabatabai, H. (2012), "Evaluation of a Permit Vehicle Model Using Weigh-in-Motion Truck Records", page 390.
10. Zhao, J. and Tabatabai, H. (2012), page 392.
11. Compare to Louisiana Department of Transportation and Development (LA DOTD) (2015), Bridge Design and Evaluation Manual (BDEM), Figure 1.3.2-3, page IV.Ch1-9.
12. Compare to LA DOTD (2015), Figures 1.3.2-1 and 1.3.2-2, pages IV.Ch1-6 and IV.Ch1-8.

CHAPTER 6: RELIABILITY ANALYSIS FOR SELECT BRIDGES

6.1 INTRODUCTION

The final analysis determined the impact of adopting the MLC-100W hypothetical vehicle loading as the alternative military live load for a subset of existing bridges in the United States national highway system using reliability analysis.[1]

Over the last several decades, a reliability based assessment of strength of existing bridges and bridge design has been developed, both to calibrate the AASHTO LRFD design criteria based on observed vehicle weight-in-motion (WIM) data and to provide the capability to perform a statistical assessment of the potential for failure of specified inventory of existing bridge structures. In this chapter, previous reliability analyses will be used to assess the implications of using the proposed new Strength II design condition on a set of existing bridges that are assumed to represent existing bridges in the U.S.

6.2 BASIC CONCEPTS OF STRUCTURAL RELIABILITY[2]

The aim of structural reliability theory is to account for load and resistance uncertainties encountered or predicted when evaluating the safety of structural systems. The uncertainties associated with predicting the load carrying capacity of a structure, the intensities of the loads expected to be applied, and the effects of these loads as well as the capacity of structural members are represented by random variables.

The value that a random variable can take is described by a probability distribution function. That is, a random variable may take a specific value with a certain probability and the set of a larger sample at these values and their probabilities can be described by the probability

distribution function. The most important characteristics of a random variable are its mean value or average, and the standard deviation that gives a measure of dispersion or a measure of the uncertainty in estimating the variable. The standard deviation of a random variable R is normally represented by σ_R. A dimensionless measure of the uncertainty is the coefficient of variation (COV) which is the ratio of the standard deviation divided by the mean value. For example the COV of the random variable R is represented by V_R using Equation 6.1.

$$V_R = \frac{\sigma_R}{\overline{R}}$$

Equation 6.1

Design values of random variables of load and resistance must be conservative, i.e., loads overestimated (Figure 6-1) and load carrying capacity (resistance) underestimated (Figure 6-2), in order to provide an adequate safety level according to reliability theory. Therefore, load and resistance factors represent partial safety margins.

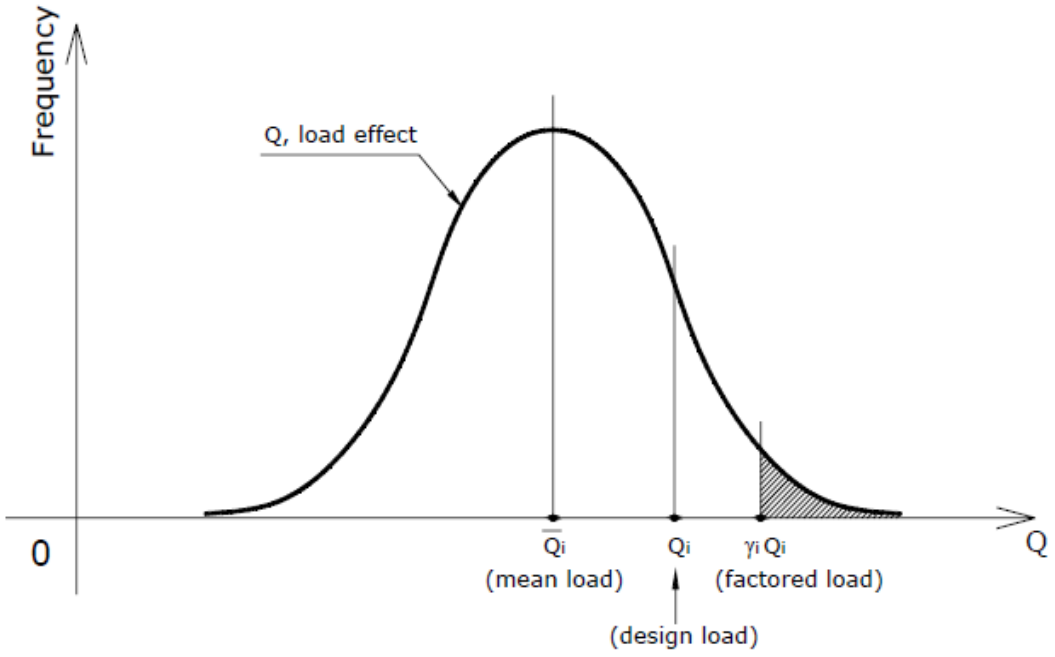

Figure 6-1: Mean, Design (Nominal) and Factored Load[3]

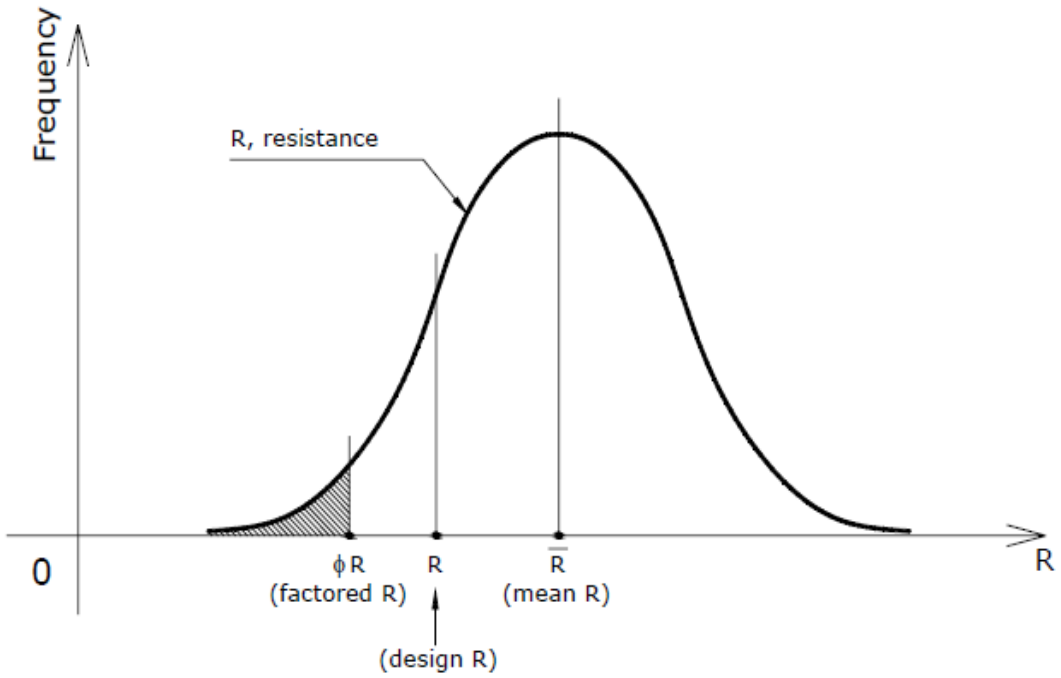

Figure 6-2: Mean, Design (Nominal) and Factored Resistance[4]

Design codes, including the AASHTO LRFD, establish load and resistance factors to ensure that the reliability of structural components is at the acceptable level (target reliability). This involves the development of reliability analysis procedure, selection of the target reliability level, and implementation (i.e. selection of the load and resistance factors). For AASHTO LRFD, the format of basic design formula is: $\gamma D \times (DL) + \gamma L \times (LL + IL) \leq \varphi R$ (1), where γD = dead load factor, γL = live load factor, φ = resistance factor, DL, LL and IL are nominal values of load components, and R = nominal value of resistance.[5]

The limit state function is a mathematical representation of the acceptability criterion. In the basic design case the limit state function is: $g = R - (DL + LL + IL) = 0$, where R, DL, LL and IL are random variables representing resistance and load components. If $g \geq 0$, the structural component is safe, and if $g < 0$, the component fails. The boundary between the safe and unsafe

domain is represented by g = 0. This corresponds to the case of total load being equal to resistance.

The random variable of load is represented as Q, and sometimes represented as S in literature. If the random variable of resistance R and random variable of load S (or Q) follow independent normal (Gaussian) distributions, then the probability of failure can be obtained based on the mean of Z and its standard deviation which can be calculated from the mean of R and S and their standard deviations using Equation 6.2 where Φ is the log normal probability function that gives the probability that the normalized random variable is below a given value.[6]

$$P_f = \Phi\left(\frac{0-\overline{Z}}{\sigma_Z}\right) = \Phi\left(-\frac{\overline{R}-\overline{S}}{\sqrt{\sigma_R^2+\sigma_S^2}}\right)$$

Equation 6.2

The reliability index, β, which is used as a measure of structural safety, indicates the number of standard deviations that the mean margin of safety falls on the safe side of the expected operating environment as represented in Figure 6-3.

The reliability index, β, is defined by the equation: $P_f = \Phi(-\beta)$. Therefore, substituting terms, Equation 6.2 can be re-written as Equation 6.3:

$$\beta = \frac{\overline{R}-\overline{S}}{\sqrt{\sigma_R^2+\sigma_S^2}}$$

Equation 6.3

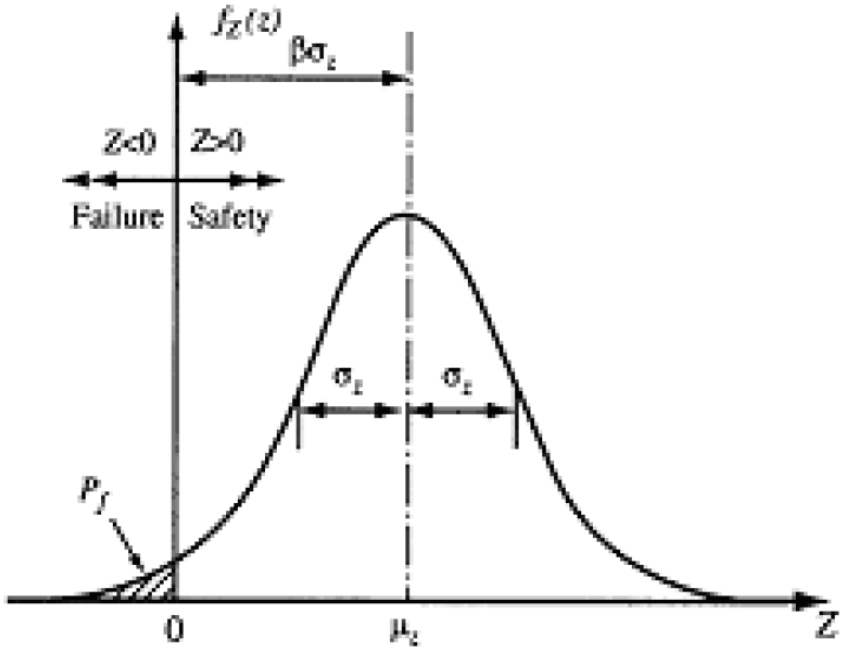

Figure 6-3: Graphical Representation of Reliability Index[7]

The reliability index of β = 3.0 is defined in literature as the target reliability index of the AASHTO LRFD design code and was developed using observed weight-in-motion (WIM) traffic data. It has been subsequently validated with subsequent calibrations using additional WIM collected data.[8] The probability of failure for a reliability index of 3.0 is 0.135%, meaning a bridge with a β = 3.0 is predicted to be approximately 99.9% reliable. A plot of reliability index β versus the probability of failure is shown on Figure 6.4.

The reliability index, β, defined in Equations 6.3 provides an exact evaluation of risk (failure probability) if R and S follow normal distributions. Although β was originally developed for normal distributions, similar calculations can be made if R and S are lognormally distributed (i.e. when the logarithms of the basic variables follow normal distributions). In this case, the reliability index can be calculated using in Equations 6.4.

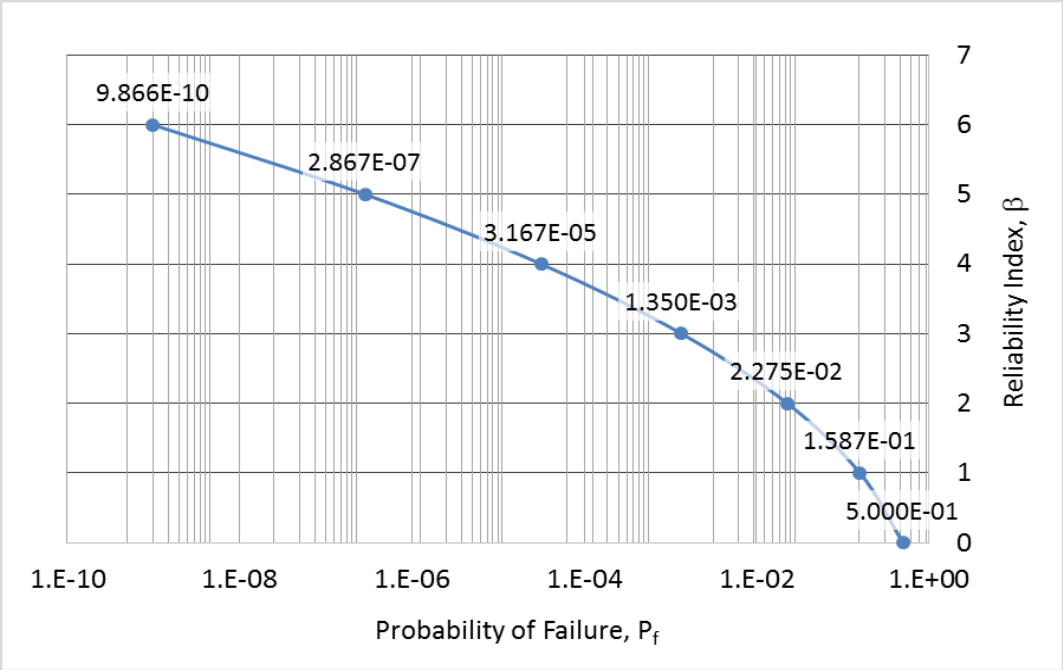

Figure 6-4: Plot of Reliability Index β versus Probability of Failure, P_f

$$\beta = \frac{\ln\left(\frac{\overline{R}}{\overline{S}}\frac{\sqrt{1+V_S^2}}{\sqrt{1+V_R^2}}\right)}{\sqrt{\ln\left[\left(1+V_R^2\right)\left(1+V_S^2\right)\right]}}$$

Equation 6.4

For small values of V_R and V_S, on the order of 20% or less, the reliability index β can be approximated using Equation 6.5.[9]

$$\beta = \frac{\ln\left(\frac{\overline{R}}{\overline{S}}\right)}{\sqrt{V_R^2+V_S^2}}$$

Equation 6.5

Equation 6.5 will be used to analyze a known inventory of bridges from the references to calculate the revised reliability indexes using both the standard heavy equipment transporter proposed in previous chapters and the hypothetical MLC 100W wheeled vehicle as an ASSHTO strength II design condition.

6.3 BRIDGE INVENTORY

For the analysis, it was assumed that coefficients of variation for material and loading, V_R and V_S respectively, can be considered constant for a closed form determination of the reliability index β. The coefficient of variation for the total load on the bridge under consideration, V_S, was assumed to be zero since the calculated loadings are based on precise calculations. The coefficient of variation for the bridge resistance or strength, V_R, was assumed to be 15% for shears and 10% for moments for reinforced concrete slab and pre-stressed I-beam concrete bridges under consideration based on averaged values from the references.[10] Also, the mean or expected value of the distribution of resistance, R, was assumed to be constant for a given bridge under consideration. Based on these assumptions, the change in the reliability index, β, for each bridge under consideration was assumed to be only dependent on the change in the mean or expected value of the distribution of load, Q, due to a change in the applied loading, calculated during the previous analyses.

The bridge set used for a previous calibration of the AASHTO LRFD code[11] was assumed to be representative of the current general condition of existing highway bridges. This "sample bridge database was established during the development of the LRFD specifications under NCHRP 12-33. Approximately 200 representative bridges were selected from various

regions of the United States by requesting sample bridge plans from various states. For bridges selected from within this database, moments and shears were calculated for the dead load components, the live load and the dynamic load allowance. Nominal or design values were calculated using the 1989 edition of the AASHTO Standard Specifications. The statistically projected live load and the notional values of live load force effects were calculated. Resistance was calculated in terms of moment and shear capacity. With respect to the use of the information in this new database, it was assumed that all designs exactly satisfied the requirements of the factored loads in the specifications and were not over-strength for reasons of either designer bias or the possibility that another limit state controlled."[12]

The approximately 200 representative bridges were reduced to the 42 bridges that were either reinforced concrete slab bridges or pre-stressed concrete I-beam and composite slab bridges. The other approximately 158 bridges were not considered because of the significant uncertainties involved in estimating dead loads based on unknown bridge construction, component dimensions and construction materials. The standard I-beam sizes used for dead load calculation are shown on Figure 6-5.

AASHTO Type I (1) girder	35 - 55 ft (10.7 - 16.8 m)
AASHTO Type II (2) girder	45 - 75 ft (13.7 - 22.9 m)
AASHTO Type III (3) girder	65 - 95 ft (19.8 - 29.0 m)
AASHTO Type IV (4) girder	85 - 120 ft (25.9 - 36.6 m)
AASHTO Type V (5) girder	110 - 145 ft (33.5 - 44.2 m)
AASHTO Type VI (6) girder	120 - 160 ft (36.6 - 48.8 m)

Figure 6-5: AASHTO Standard I-Beam Type Girder Sizes[13]

The details of the 42 bridges used for this analysis are listed on Table 6-1. The following caveats apply to the analysis. Since the dead load was not specified in the published literature,

the dead load was estimated using the type of bridge construction and the span length. All bridges were considered to be normal weight concrete with a uniform slab thickness for both slab and composite bridges, and pre-stressed concrete I-beams type based on the recommended sizes for the span length. The weight of reinforcing and pre-stressing steel, wearing (deck) surface, and superimposed dead loads were neglected in the calculation of the bridge dead load.

6.4 RELIABILITY ANALYSIS

Before beginning the reliability analysis, the dead loads and live loads applied to the bridges under consideration were re-calculated for the span lengths of the bridge inventory. The bridge dead loads were calculated assuming a concrete slab thickness of 18 inches (1.5 ft; 45.7 cm) for all of the bridges under consideration, multiplied by the unit weight of normal weight concrete (0.15 kips per cubic ft; 2400 kg per cubic meters), multiplied by the bridge width as shown on Table 6-1. This slab thickness was assumed to be representative of actual highway bridge construction. For the pre-stressed concrete I-beam bridges specified the girders were assumed to be AASHTO standard I-beam type and sizes. The I-beam type and size was assumed to be the type and size recommended per Figure 6-5 based on the span lengths specified on Table 6-1. The number of girders was determined as the integer result of the specified bridge width divided by the specified girder spacing. This calculated number was then multiplied by the standard type size cross sectional area and the unit weight of normal concrete. The girder unit weight was then added to the slab unit weight to obtain a uniform bridge dead load, applied to the bridge as a simple span to obtain maximum dead load shear and mid-span moments.

Bridge	Identifier	Type	Span Length (FT)	Bridge Width, ft	Girder Spacing, ft	Probable AASHTO/ACI Type Girder Based on Span	Year Built	Design Load	Design Method	Beta, based on HL-93 Loading (LRFD Strength I)
Slab #1	MM-Slab-L-01	Reinforced Concrete Slabs	15	31	N/A	N/A	2006 Design	HL-93	LRFD	4.08
Slab #2	MM-Slab-L-02	Reinforced Concrete Slabs	20	31	N/A	N/A	2006 Design	HL-93	LRFD	4.09
Slab #3	MM-Slab-L-03	Reinforced Concrete Slabs	25	31	N/A	N/A	2006 Design	HL-93	LRFD	4.02
Slab #4	MM-Slab-L-04	Reinforced Concrete Slabs	30	31	N/A	N/A	2006 Design	HL-93	LRFD	3.87
Slab #5	MM-Slab-L-05	Reinforced Concrete Slabs	35	31	N/A	N/A	2006 Design	HL-93	LRFD	3.85
Slab #6	MM-Slab-L-06	Reinforced Concrete Slabs	40	31	N/A	N/A	2006 Design	HL-93	LRFD	3.97
Slab #7	MM-Slab-L-07	Reinforced Concrete Slabs	45	31	N/A	N/A	2006 Design	HL-93	LRFD	3.91
Slab #8	MM-Slab-L-08	Reinforced Concrete Slabs	50	31	N/A	N/A	2006 Design	HL-93	LRFD	3.65
Slab #9	MM-Slab-L-09	Reinforced Concrete Slabs	55	31	N/A	N/A	2006 Design	HL-93	LRFD	3.85
P/S I #3	MM-IB-L-01	Prestressed Concrete I-Beams	60	31	7.75	II (2)	2006 Design	HS25	LFD	3.72
P/S I #8	MM-IB-L-12	Prestressed Concrete I-Beams	60	47	11.75	II (2)	2006 Design	HL-93	LRFD	3.93
Slab #10	MM-Slab-L-10	Reinforced Concrete Slabs	60	31	N/A	N/A	2006 Design	HL-93	LRFD	3.41
Slab #11	MM-Slab-L-11	Reinforced Concrete Slabs	65	31	N/A	N/A	2006 Design	HL-93	LRFD	3.40
P/S I #14	MM-IB-L-18	Prestressed Concrete I-Beams	80	31	7.75	III (3)	2006 Design	HL-93	LRFD	3.87
P/S I #19	MM-IB-L-29	Prestressed Concrete I-Beams	80	47	11.75	III (3)	2006 Design	HL-93	LRFD	3.77
P/S I #25	MM-IB-A-1	Prestressed Concrete I-Beams	80	31	7.75	III (3)	2006 Design	HS25	LFD	3.84
P/S I #30	MM-IB-A-12	Prestressed Concrete I-Beams	80	47	11.75	III (3)	2006 Design	HS25	LFD	3.78
P/S I #4	MM-IB-L-02	Prestressed Concrete I-Beams	80	31	7.75	III (3)	2006 Design	HL-93	LRFD	3.77
P/S I #9	MM-IB-L-13	Prestressed Concrete I-Beams	80	47	11.75	III (3)	2006 Design	HL-93	LRFD	3.87
P/S I #10	MM-IB-L-14	Prestressed Concrete I-Beams	100	47	11.75	IV (4)	2006 Design	HL-93	LRFD	3.82
P/S I #15	MM-IB-L-19	Prestressed Concrete I-Beams	100	31	7.75	IV (4)	2006 Design	HL-93	LRFD	3.74
P/S I #20	MM-IB-L-30	Prestressed Concrete I-Beams	100	47	11.75	IV (4)	2006 Design	HL-93	LRFD	3.83
P/S I #26	MM-IB-A-2	Prestressed Concrete I-Beams	100	31	7.75	IV (4)	2006 Design	HS25	LFD	3.80
P/S I #31	MM-IB-A-13	Prestressed Concrete I-Beams	100	47	11.75	IV (4)	2006 Design	HS25	LFD	3.70
P/S I #5	MM-IB-L-03	Prestressed Concrete I-Beams	100	31	7.75	IV (4)	2006 Design	HL-93	LRFD	3.76
P/S I #11	MM-IB-L-15	Prestressed Concrete I-Beams	120	47	11.75	V (5)	2006 Design	HL-93	LRFD	3.83
P/S I #16	MM-IB-L-20	Prestressed Concrete I-Beams	120	31	7.75	V (5)	2006 Design	HL-93	LRFD	3.69
P/S I #21	MM-IB-L-31	Prestressed Concrete I-Beams	120	47	11.75	V (5)	2006 Design	HL-93	LRFD	3.73
P/S I #27	MM-IB-A-3	Prestressed Concrete I-Beams	120	31	7.75	V (5)	2006 Design	HS25	LFD	3.71
P/S I #32	MM-IB-A-14	Prestressed Concrete I-Beams	120	47	11.75	V (5)	2006 Design	HS25	LFD	3.77
P/S I #6	MM-IB-L-04	Prestressed Concrete I-Beams	120	31	7.75	V (5)	2006 Design	HL-93	LRFD	3.65
P/S I #33	MM-IB-A-15	Prestressed Concrete I-Beams	130	47	9.4	V (5)	2006 Design	HS25	LFD	3.67
P/S I #12	MM-IB-L-16	Prestressed Concrete I-Beams	140	47	11.75	V (5)	2006 Design	HL-93	LRFD	3.69
P/S I #17	MM-IB-L-21	Prestressed Concrete I-Beams	140	31	7.75	V (5)	2006 Design	HL-93	LRFD	3.63
P/S I #22	MM-IB-L-32	Prestressed Concrete I-Beams	140	47	11.75	V (5)	2006 Design	HL-93	LRFD	3.72
P/S I #28	MM-IB-A-4	Prestressed Concrete I-Beams	140	31	7.75	V (5)	2006 Design	HS25	LFD	3.59
P/S I #7	MM-IB-L-05	Prestressed Concrete I-Beams	140	31	7.75	V (5)	2006 Design	HL-93	LRFD	3.64
P/S I #13	MM-IB-L-17	Prestressed Concrete I-Beams	160	47	9.4	VI (6)	2006 Design	HL-93	LRFD	3.61
P/S I #18	MM-IB-L-22	Prestressed Concrete I-Beams	160	31	7.75	VI (6)	2006 Design	HL-93	LRFD	3.58
P/S I #23	MM-IB-L-33	Prestressed Concrete I-Beams	160	47	9.4	VI (6)	2006 Design	HL-93	LRFD	3.75
P/S I #29	MM-IB-A-5	Prestressed Concrete I-Beams	160	31	6.2	VI (6)	2006 Design	HS25	LFD	3.49
P/S I #24	MM-IB-L-34	Prestressed Concrete I-Beams	180	47	7.833	VI (6)	2006 Design	HL-93	LRFD	3.61

Table 6-1: Bridge Inventory Used For Reliability Analysis[14]

For the live loads, the AASHTO HL-93 design truck and land loading maximum shear and mid-span moment values were calculated and verified using the values provided in the CALTRANS design guide. The determination of maximum shear and mid-span moment for the AASHTO HL-93 live load only considered a single HS20-44 design truck vehicle on a simple beam. The maximum calculated shears and mid-span moments for the proposed standard (230 kip) heavy equipment transporter (HET) and the hypothetical MLC 100W wheeled vehicle presented in the previous chapter were not applicable to the reliability analysis bridge set due to the very short spans (15 - 180 ft; 4.6 – 54.9 m) under consideration. A substantial number of bridges under consideration were less than the vehicle length (front to rear axle distance), the maximum shear and mid-span moments were re-calculated based on a consideration of all possible axle or adjacent axles combinations acting on a given span length of the vehicle length.

The calculations for the proposed standard HET and MLC 100W hypothetical wheeled vehicles are shown on Figures 6-6 and 6-7 respectively. The maximum shear and mid-span moments were determined based on a comparison of different possible axle loadings for a given span, not just the axle groupings beginning from either the front or rear end of the vehicle. The calculations account for a vehicle traveling over the span length in motion. The maximums were determined based on the maximum for any possible vehicle position on the span.

The maximum shears and mid-span moments created by the estimated dead loads and the various live loads for the bridge span lengths under consideration are shown on Figures 6-8 and 6-9 respectively. The live loads applied for the AASHTO HL-93, proposed standard HET, and the MLC 100W hypothetical vehicle also include a 33% increase due to dynamic impact. Both the civilian traffic forced flow and the proposed logistics convoy, both at crawl speeds, do not include an increase due to dynamic impact. From Figures 6-8 and 6-9, the applied live loads

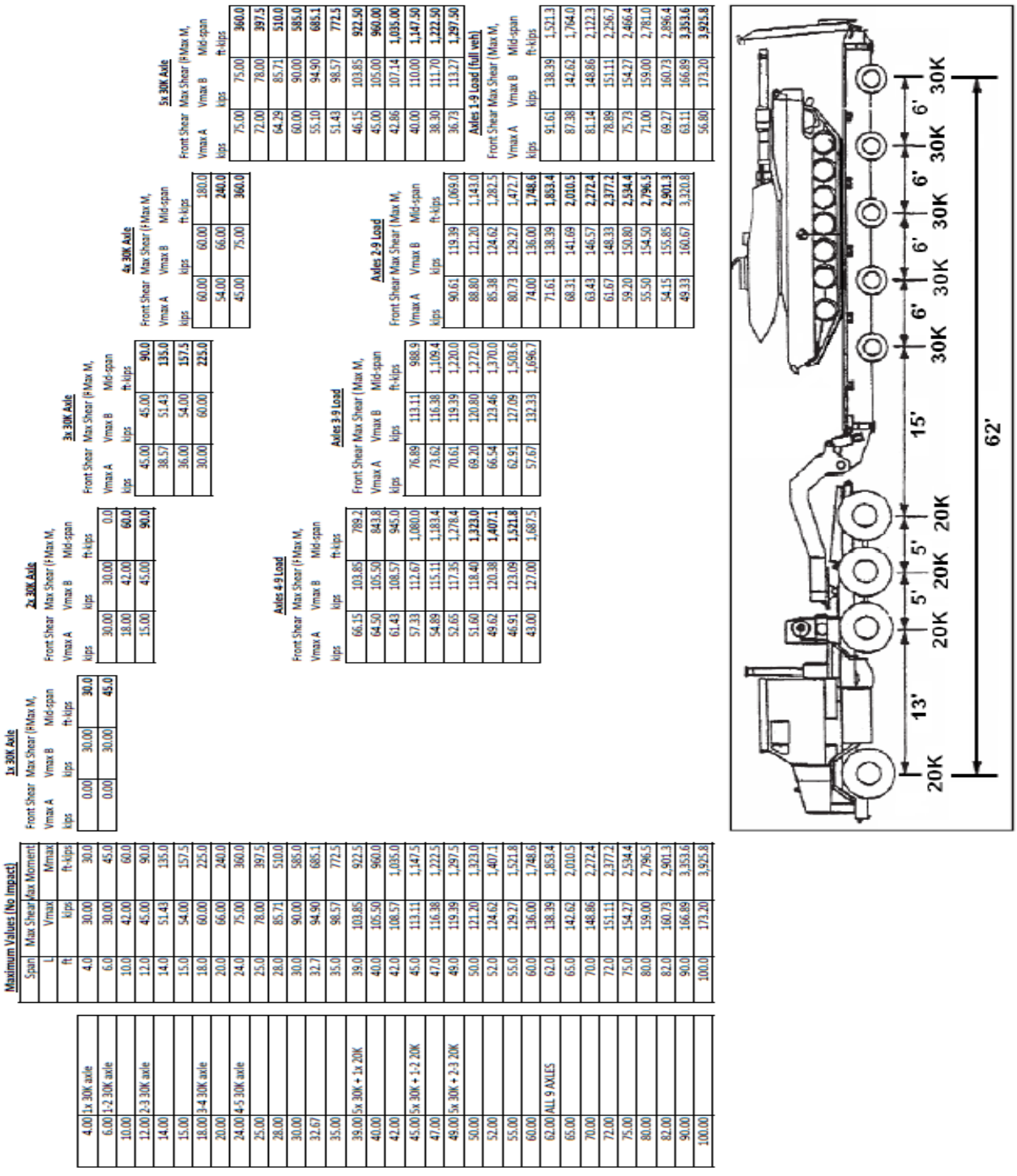

Figure 6-6: Maximum Shear and Moments for Proposed 230K Heavy Equipment Transporter (HET) for Spans Lengths considered during Reliability Analysis

Figure 6-7: Maximum Shear and Moments for MLC 100W Hypothetical Wheeled Vehicle for Spans Lengths considered during Reliability Analysis

with impact dominate the total load for shorter span lengths and the estimated dead load predominates for longer spans. The pre-stressed concrete I-beam bridges show a significant variation in dead load versus span length due to the uncertainty in accurately predicting the I-beam type and size based on span length.

All of the bridges considered were either 31 ft (9.4 m) or 47 ft (14.3 m) wide as shown on Table 6-1. These widths were assumed to indicate two travel lanes. A width of 31 ft (9.4 m) was assumed to represent a two lane highway bridge with traffic in the same direction for both lanes (two 12 ft (3.7 m) wide travel lanes with 7 ft (2.1 m) width combined shoulders). A width of 47 ft (14.3 m) was assumed to represent a two lane highway bridge with traffic in opposite directions for both lanes (two 12 ft wide (3.7 m) travel lanes with 1 ft (0.3 m) median and 11 ft (3.3 m) shoulders on the outside of each travel lane. It was assumed that all of the bridges were designed for AASHTO Strength Condition I HL-93 design truck and lane load for both lanes, with a multiple presence factor of 1.0 applied to the live load for both lanes.[15] This design criteria was also assumed to be the live load condition used to calculate the reliability indices shown on Table 6-1.

Following the determination of the dead and live loadings acting on the bridge span under consideration, the reliability index β shown on Table 6-1 was used to calculate new reliability indices for the increased live loads based on the proposed standard HET and the MLC 100W hypothetical wheeled vehicle. The reliability index β shown on Table 6-1 was assumed to be the result of the AASHTO Strength Condition I applied to the AASHTO HL-93 live load; however it was unclear from the literature whether maximum shear or moment generates the minimum reliability index. Therefore, the revised reliability index β was calculated for both the maximum shear and moment generated by the increased live loads.

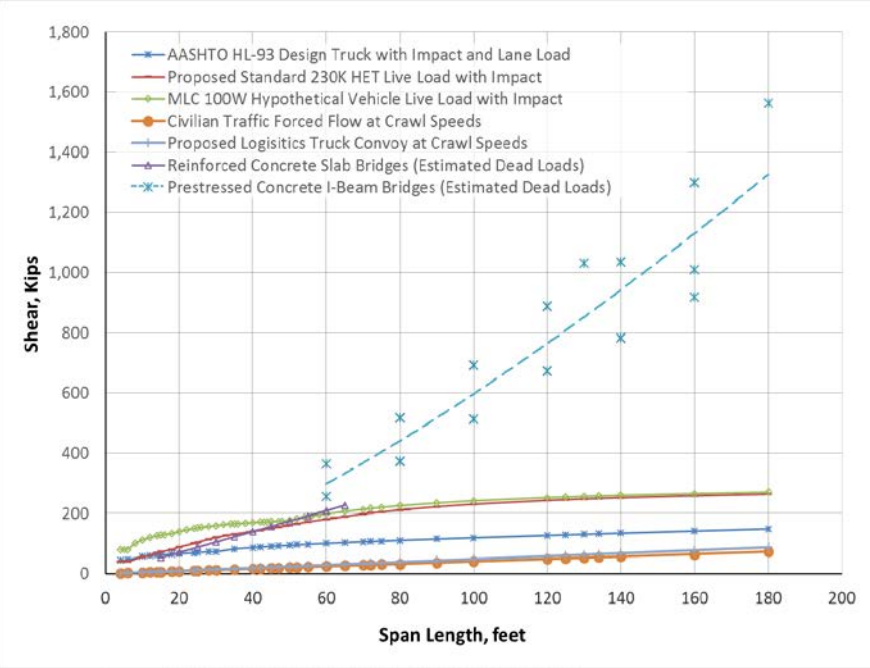

Figure 6-8: Maximum Shears due to Various Live Loads and Estimated Dead Loads

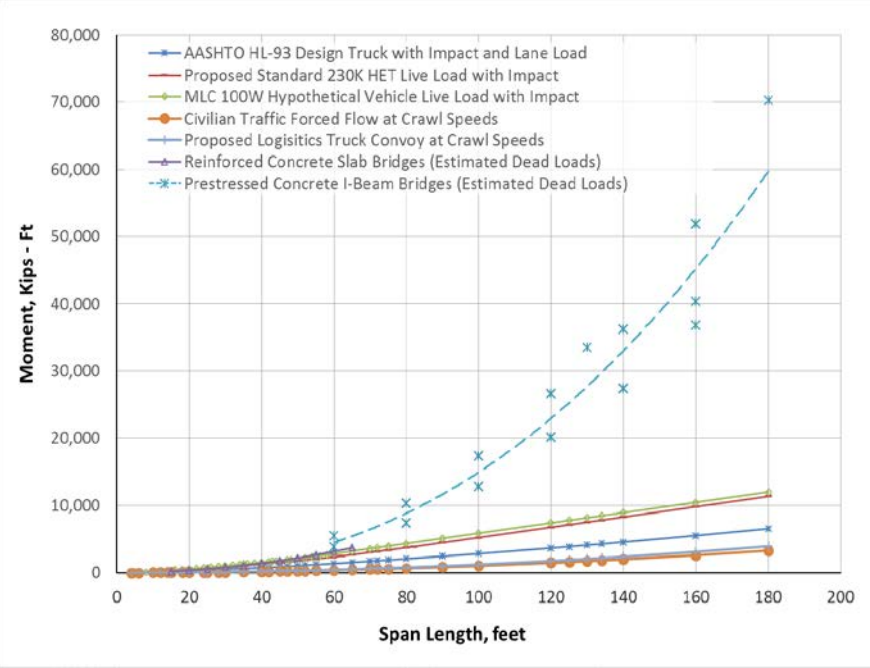

Figure 6-9: Maximum Moments due to Various Live Loads and Estimated Dead Loads

A sample calculation is provided for the bridge identified as "MM-Slab-L-08", span length of 50 ft (~15 m) shown on Table 6-1. The bridge width is 31 ft (~9.5 m) and the reliability index β is 3.65. Based on the calculations described above, the dead load unit weight is:

DL = (0.15 kcf) x 1.5 ft slab thickness x 31 ft bridge width = 6.975 kips/ft (101.8 kN/m)

For an uniformly loaded simple span with ω = 6.975 klf, the maximum shear and moments are: VDL = ωl/2 = 6.975 klf x 50 ft / 2 = 174.4 kips (775.7 kN) and

MDL = $\omega l^2/8$ = 6.975 klf x $(50\text{ ft})^2$ / 8 = 2,179.7 ft-kips (2,955.2 kN-m)

The known maximum shear and mid-span moments for the AASHTO HL-93 design truck and lane live loading with impact for a 50 ft (~15 m) single span are 93.9 kips (417.7 kN) and 1,024.6 ft (1,389.1 kN-m) as shown on Figure 5-2 in the previous chapter.

The resistance of the subject bridge, R, is calculated using Equation 6.5 as previously discussed. Re-arranging Equation 6.5 to provide a closed form solution for resistance, R, yields:

$$\overline{R} = \overline{S}\left(e^{\beta\sqrt{V_R^2 + V_S^2}}\right) \qquad \textbf{Equation 6.6}$$

The nominal resistance, R, for bridge "MM-Slab-L-08" is then re-calculated as:

R_{shear} = e (β x $V_{R,\,shear}$) ((AASHTO Strength I factor x 2 lanes x HL-93 LL+I) + VDL)

= e (3.65×0.15) ((1.75 x 2 x 93.9 kips)+174.4 kips) = 870 kips (3,870 kN)

R_{moment} = e (β x $V_{R,\,moment}$) ((AASHTO Strength I factor x 2 lanes x HL-93 LL+I) + MDL)

= e (3.65×0.1) ((1.75 x 2 x 1,024.6 ft-kips)+2,179.7 ft-kips) = 8,306 ft-kips (11,261 kN-m)

The calculated maximum shear and mid-span moments for the proposed standard HET on a 50 ft (~15 m) span are 121.2 kips (539.1 kN) and 1,323.0 ft-kips (1,793.7 kN-m) as shown on Figure 6-6. Applying the dynamic impact factor of 33% results in a maximum shear and moment with impact of 161.2 kips (717.0 kN) and 1,759.6 ft-kips (2,385.7 kN-m).

The calculated maximum shear and mid-span moments for the MLC 100W hypothetical wheeled vehicle on a 50 ft (~15 m) span are 133.0 kips (591.6 kN) and 1,525.3 ft-kips (2,068.0 kN-m) as shown on Figure 6-7. Applying the dynamic impact factor of 33% results in a maximum shear and moment for the MLC 100W hypothetical wheeled vehicle with impact of 176.9 kips (786.9 kN) and 2,028.6 ft-kips (2,750.3 kN-m).

If the proposed standard HET and the MLC 100W hypothetical wheeled vehicle are allowed to transit the bridge span without other traffic, these heavy live loads with dynamic impact will be carried by the full bridge resistance if the bridge construction effectively distributes the load across all bridge girders. This was considered a reasonable assumption since the vehicle widths (12 ft; 3.7 m) equal a full travel lane width and the vehicle will likely transit along the span centerline, straddling both lanes instead of being forced to remain in a single travel lane.

For this condition of the heavy vehicle crossing the span along the bridge centerline without any other traffic live load, the revised reliability indices β for the proposed standard HET and the MLC 100W hypothetical wheeled vehicle loading with impact (as the AASHTO Strength II condition) can be calculated using Equation 6.5.

The revised reliability indices β for shear and moment are:

$\beta = \ln (R_{shear} / ((\text{AASHTO Strength II factor} \times LL) + VDL)) / 0.15$, for shear

$\beta = \ln (R_{moment} / ((\text{AASHTO Strength II factor} \times LL) + MDL)) / 0.1$, for moment

For the proposed standard HET loading with impact as the AASHTO Strength II condition:

β_{shear} = ln (869.6 kips / ((1.35 x 161.2 kips) + 174.4 kips)) / 0.15 = 5.31

β_{moment} = ln (8,305.7 ft-kips / ((1.35 x 1,759.6 ft-kips) + 2,179.7 ft-kips)) / 0.1 = 6.01

For the MLC 100W hypothetical wheeled vehicle loading with impact as the AASHTO Strength II condition:

β_{shear} = ln (869.6 kips / ((1.35 x 176.9 kips) + 174.4 kips)) / 0.15 = 4.96

β_{moment} = ln (8,305.7 ft-kips / ((1.35 x 2,028.6 ft-kips) + 2,179.7 ft-kips)) / 0.1 = 5.24

Therefore, the reliability estimated for the proposed standard HET and the MLC 100W hypothetical wheeled vehicle crossing the bridge span without other traffic exceeds the reliability of the bridge assumed to be loaded in two lanes with AASHTO HL-93 design truck and lane loading. This condition corresponds to a special permit crossing typical on highway bridges.

If the bridge is assumed to be a worst case military crossing, the proposed standard HET and the MLC 100W hypothetical wheeled vehicle would be crossing the bridge in one lane with civilian traffic or the proposed logistics convoy as defined earlier occupying the other travel lane.

The civilian traffic or the proposed logistics convoy are assumed to be either stopped or moving at crawl speeds.

For these conditions, for the proposed standard HET loading with impact occupying one lane and civilian traffic occupying the other travel lane as the AASHTO Strength II condition:

β_{shear} = ln (869.6 kips/((1.35 x (161.2 kips+20.25 kips))+174.4 kips)) /0.15 = 4.86

β_{moment} = ln (8,305.7 ft-kips/((1.35x(1,759.6 ft-kips+253.1 ft-kips))+2,179.7 ft-kips)) /0.1

= 5.28

Similarly, for the proposed standard HET loading with impact occupying one lane and the proposed logistics convoy occupying the other travel lane as the AASHTO Strength II condition:

β_{shear} = ln (869.6 kips/((1.35 x (161.2 kips+24.13 kips))+174.4 kips)) /0.15 = 4.78

β_{moment} = ln (8,305.7 ft-kips/((1.35x(1,759.6 ft-kips+301.6 ft-kips))+2,179.7 ft-kips)) /0.1

= 5.15

Similar calculations for the MLC 100W hypothetical wheeled vehicle with either civilian traffic or the proposed logistics convoy occupying the other travel lane as the AASHTO Strength II condition result in reliability indices of 4.53, 4.57, 4.46, and 4.44 respectively.

This methodology was applied to all 42 bridges shown on Table 6-1. The revised reliability indices β for the proposed standard HET and the MLC 100W hypothetical wheeled vehicle loading with impact as the AASHTO Strength II condition are plotted versus span length for shear and moment on Figures 6-10 through Figure 6-13 respectively. The reliability indices β from Table 6-1 are also plotted.

Figures 6-10 and 6-11 show the reliability indices for the proposed standard HET and the MLC 100W hypothetical wheeled vehicle crossing the bridge span without other traffic (typical special permit crossing) and Figures 6-12 and 6-13 show the reliability indices for a worst case military crossing with the heavy vehicle crossing the bridge in one lane with other traffic occupying the other travel lane (i.e., half of the bridge width).

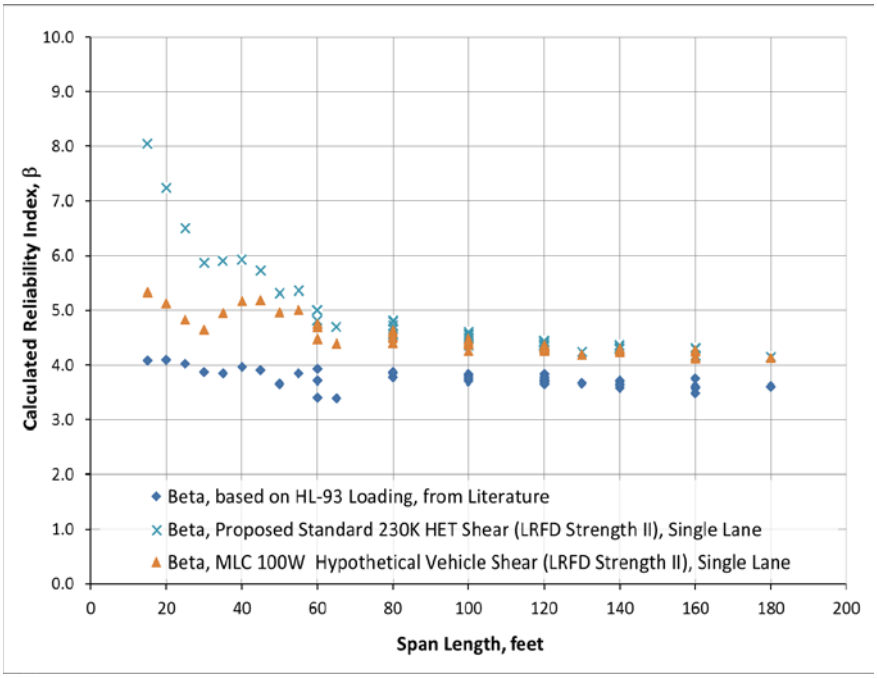

Figure 6-10: Comparison of Reliability Indices β based on Shear, Single Lane

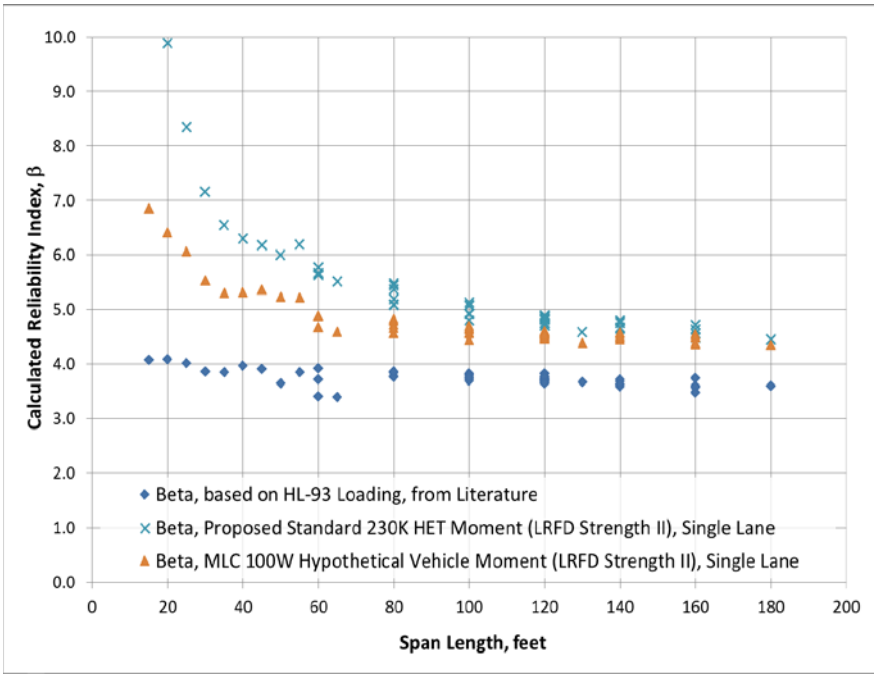

Figure 6-11: Comparison of Reliability Indices β based on Moment, Single Lane

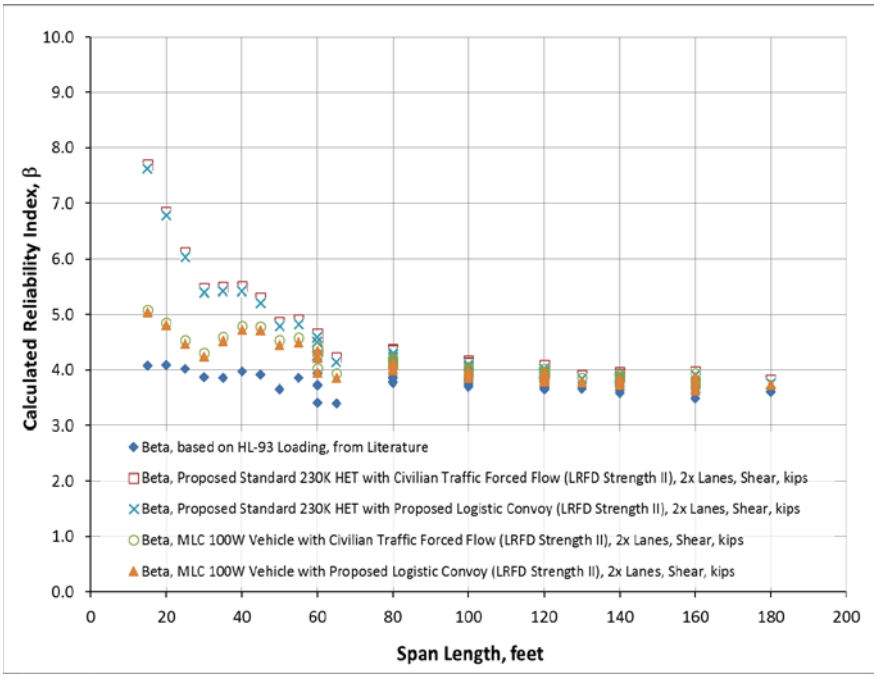

Figure 6-12: Comparison of Reliability Indices β based on Shear for Combined Loads

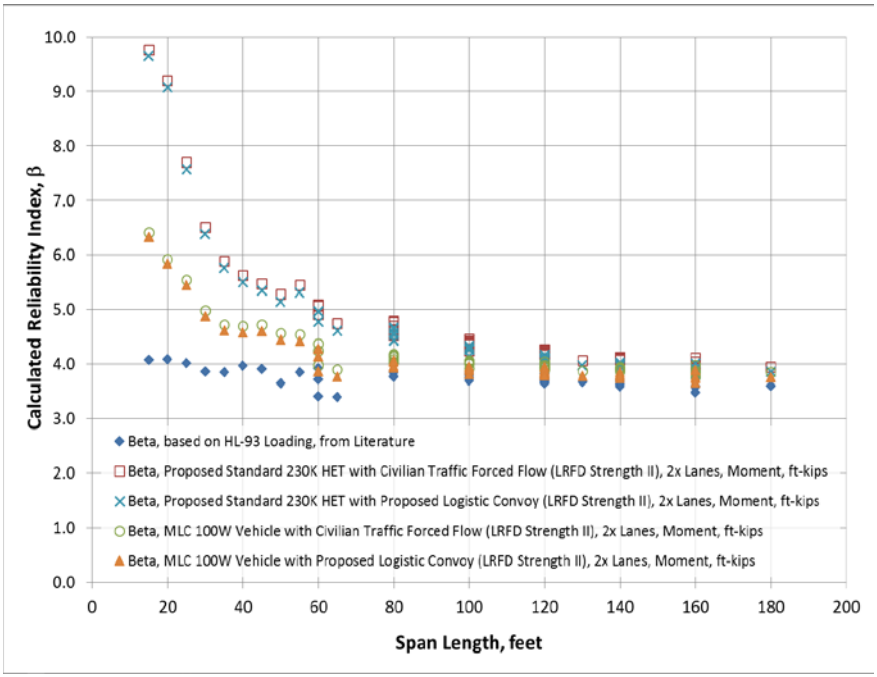

Figure 6-13: Comparison of Reliability Indices β based on Moment for Combined Loads

Considering the uncertainty inherent in this closed form reliability analysis, a more conservative methodology is to remove the AASHTO Strength I and II factors from consideration, and re-calculate the reliability indices for the 42 bridges shown on Table 6-1 using equations 6.4 and 6.5. The nominal bridge resistance for bridge "MM-Slab-L-08" was recalculated to be 626 kips (2,784.4 kN) and 6,092.0 ft-kips (8,259.5 kN-m) for shear and moment respectively. The revised reliability indices for the proposed standard HET and the MLC 100W hypothetical wheeled vehicle crossing the bridge span without other traffic (a typical special permit crossing) are 4.16 and 4.36 for the proposed standard HET (shear and moment respectively) and 3.85 and 3.70 for the MLC 100W hypothetical wheeled vehicle (shear and moment respectively). The condition of the proposed standard HET is crossing the span with either civilian traffic or the proposed logistics convoy occupying the other travel lane results in recalculated reliability indices of 3.77 and 3.70 (shear) and 3.74 and 3.62 (moment) respectively. Recalculated reliability indices for the MLC 100W hypothetical wheeled vehicle with either civilian traffic or the proposed logistics convoy occupying the other travel lane are 3.48 and 3.41 (shear) and 3.11 and 3.01 (moment) respectively.

This new methodology of calculating a closed form approximation of new reliability indices was applied to all 42 bridges shown on Table 6-1 and plotted to allow for comparison with previously determined values using the application of the ASHTO Strength I and II condition factors. These new reliability indices β are shown on Figures 6-14 through 6-17. The scale of the vertical axis showing the calculated reliability index on Figures 6-10 through 6-13 are constant to allow for the direct comparison of results.

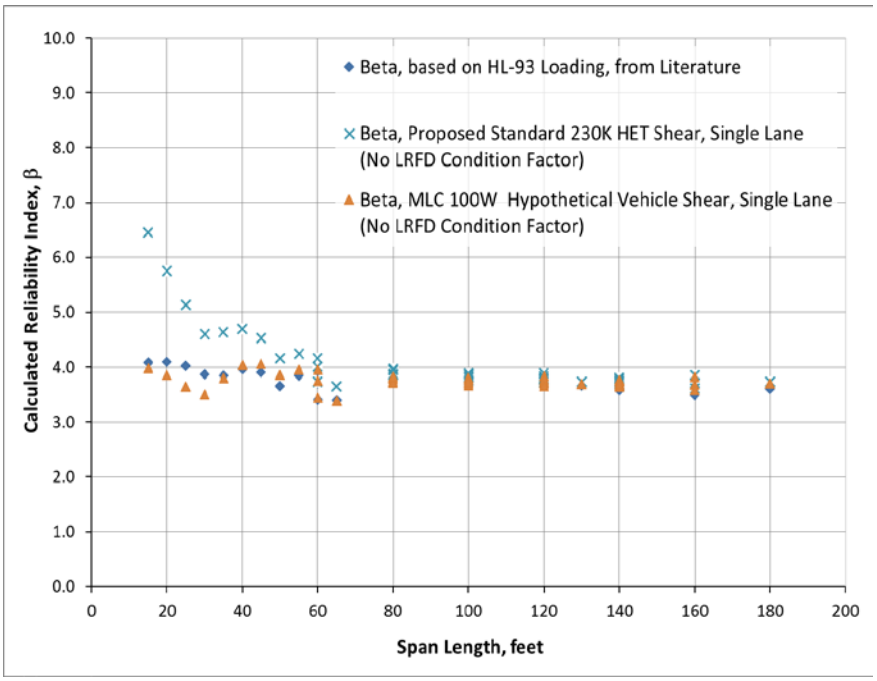

Figure 6-14: Reliability Indices β based on Shear, Single Lane, without AASHTO Strength Condition Factors

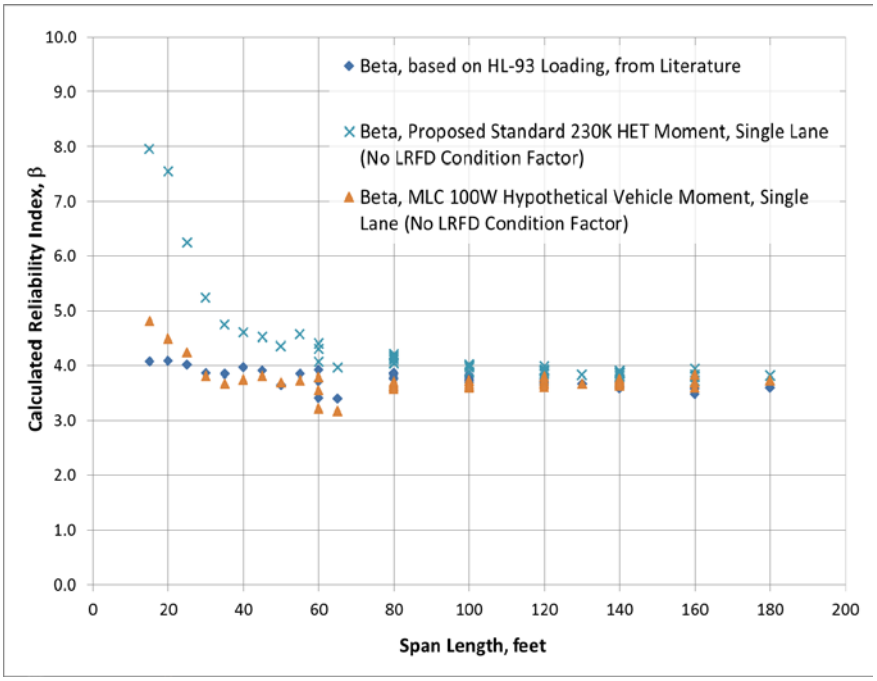

Figure 6-15: Reliability Indices β based on Moment, Single Lane, without AASHTO Strength Condition Factors

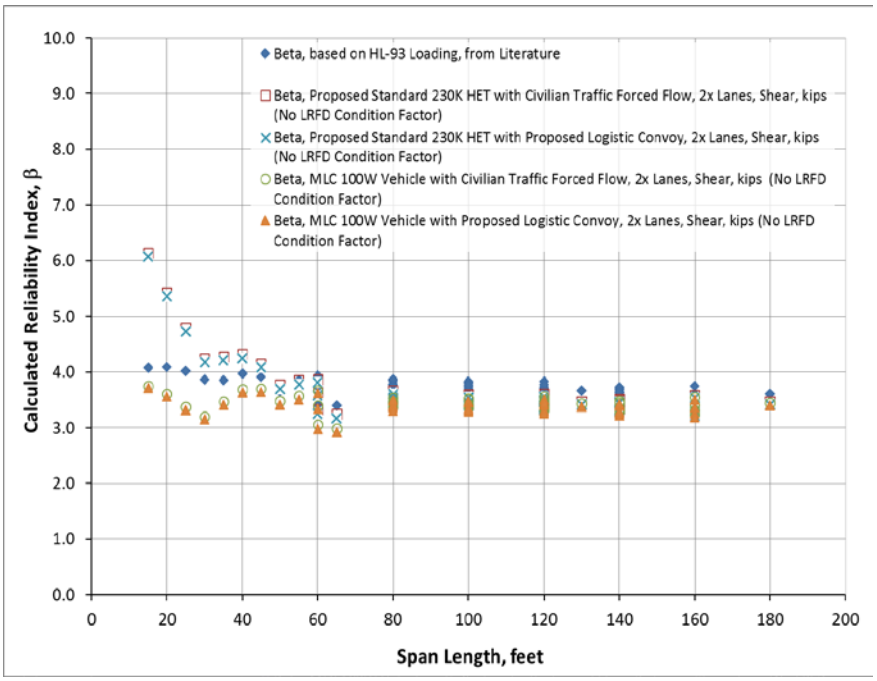

Figure 6-16: Reliability Indices β based on Shear for Combined Loads, without AASHTO Strength Condition Factors

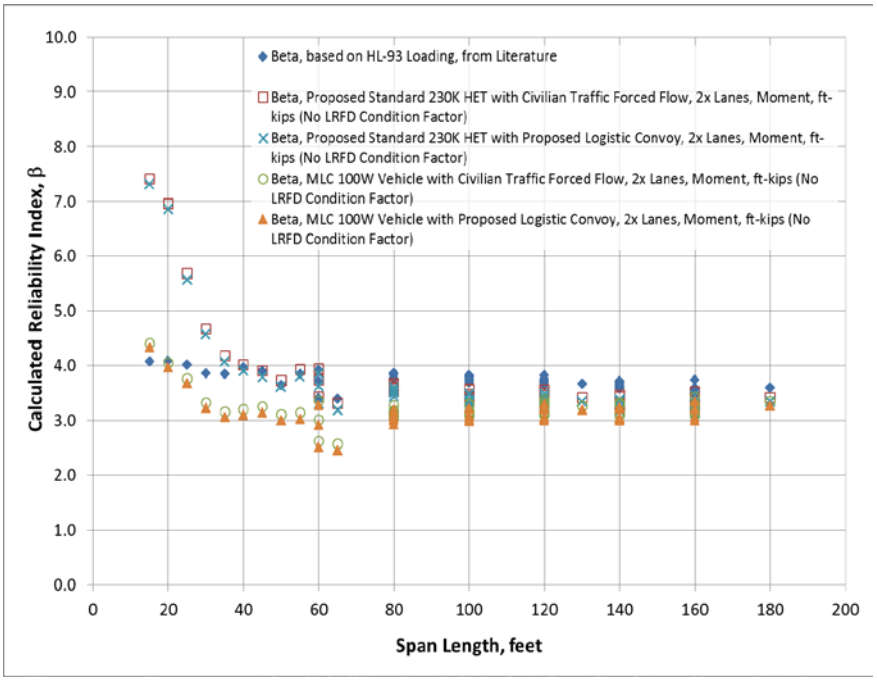

Figure 6-17: Reliability Indices β based on Moment for Combined Loads, without AASHTO Strength Condition Factors

The reliability calculations without the application of the AASHTO Strength I and II condition factors on the determination of the nominal bridge resistance and the live and dead loads allow for the comparison of the reliability based load and resistance factor design (LRFD) with a factor of safety method used in the previously common allowable stress design (ASD) method. Using the nominal bridge resistance calculated without the LRFD strength condition divided by the total load applied to the bridge would provide an approximation of the factor of safety (F.S.) based on the assumption that the stresses developed on the bridge structural members are within the elastic behavior region and manifest in the same locations for both nominal bridge resistance and the total applied loads. Therefore, the resistance (in kips for shear, and ft-kips for moment) was assumed equivalent to the bridge strength (ksi), and the total load effect (again in kips for end shear, and ft-kips for mid-span moment) was assumed similarly equivalent to the shear or bending stresses (ksi) in the bridge at the point of maximum end shear and maximum mid-span moment. The maximum shear and mid-span moment due to the total load was calculated by the simple addition of the maximum shear and mid-span moment resulting from the bridge dead load and the applied live loading, without the application of any factors based on different load conditions.

$$\text{F.S.}_{\text{Approximate}} \cong \frac{\text{Nominal Bridge Resistance}}{\text{Total Load}} \qquad \textbf{Equation 6.7}$$

The approximate F.S. calculated using Equation 6.7 for the 42 bridges shown on Table 6-1 is plotted on Figures 6.18 and 6.19 for shear and moment respectively.

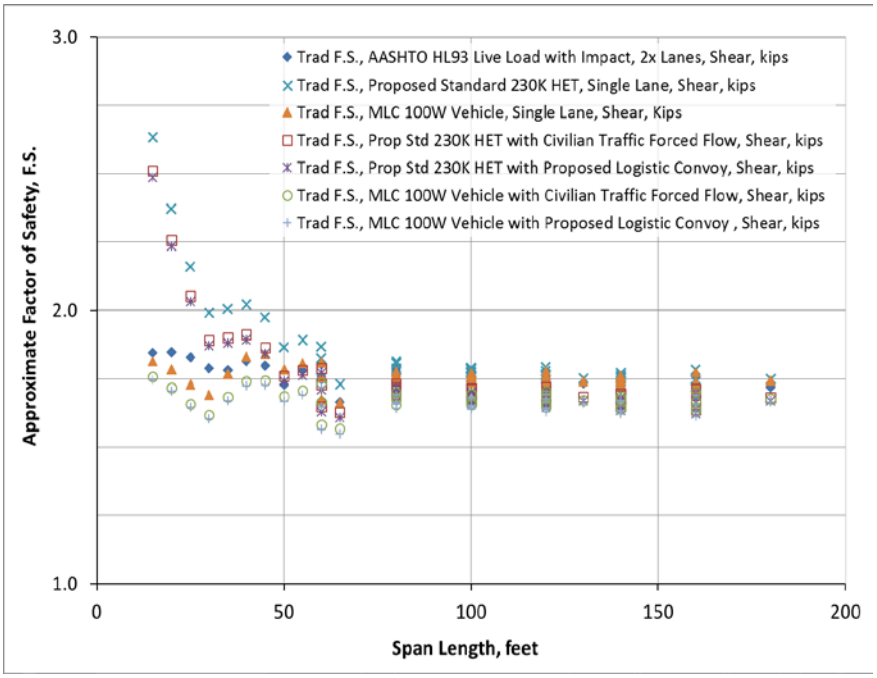

Figure 6-18: Comparison of Approximate Factors of Safety for Maximum Shear

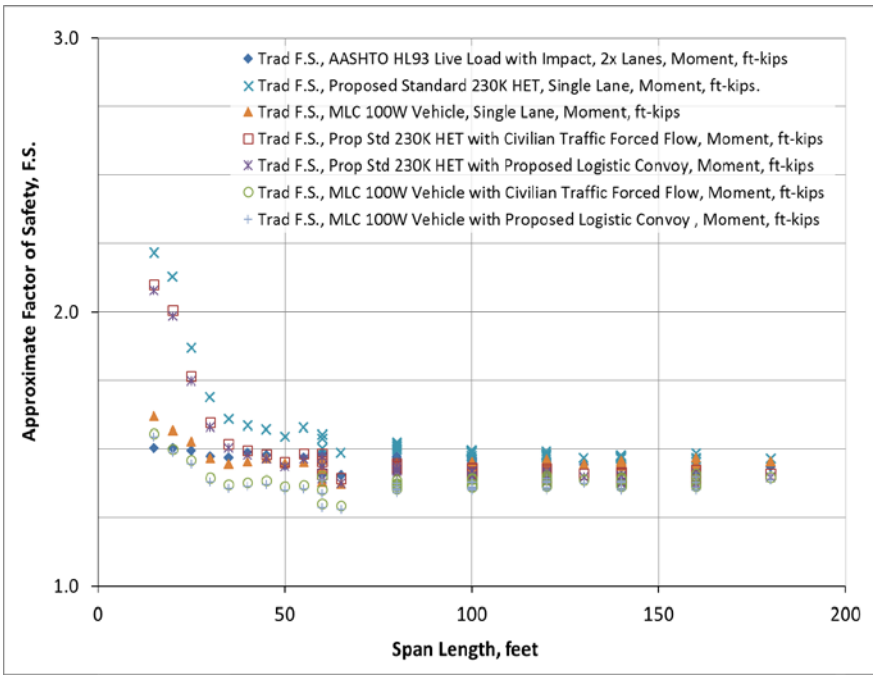

Figure 6-19: Comparison of Approximate Factors of Safety for Maximum Moment

As shown on Figures 6.18 and 6.19 the approximate factors of safety generally are less than 2.0 and between 1.0 and 1.5 for most bridges when based on maximum mid-span moment. In order to determine if any trends could be inferred from these results, the approximate factors of safety and the revised reliability indices for shear and moment for all seven possible loading cases of the 42 bridges are plotted on Figure 6.20. Linear extrapolations of the approximate factor of safety as a function of the reliability index β for both shear and moment were derived from the results and plotted with the bridge inventory data set on Figure 6.20 as well. A representative F.S. of 2.0 from the ASD method results in a predicted reliability index β of 4.5 for shear and 7.0 for mid-span moment. These very low probabilities of failure (less than 0.0003% in each case) illustrates the older bridges designed using the ASM contain greater reservoirs of latent strength compared to the more elegant modern bridges designed using LRFD, but are significantly over-designed.[16]

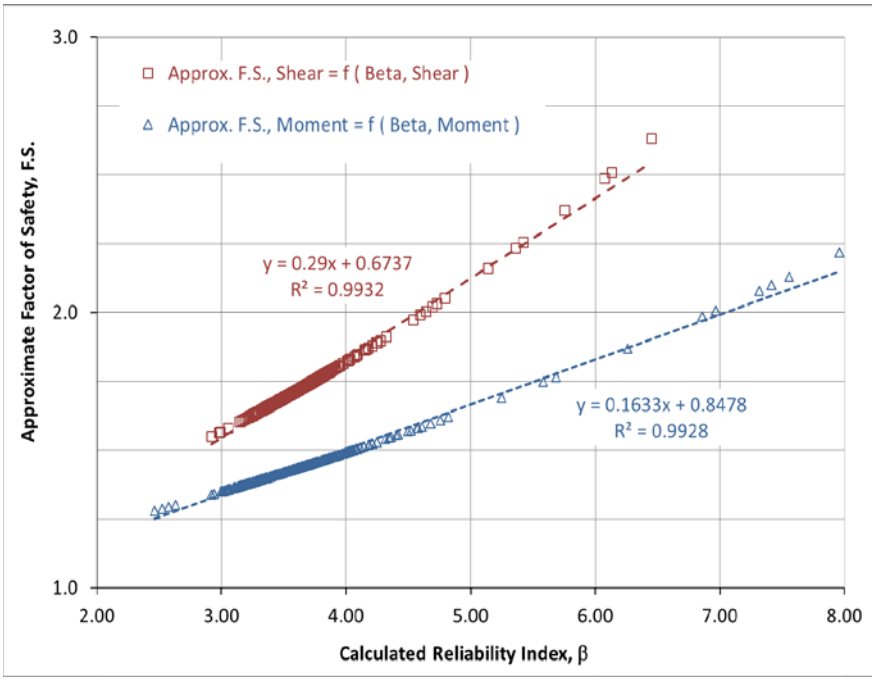

Figure 6-20: Approximate Factor of Safety vs. Reliability Indices β for Bridge Inventory[17]

6.5 FINDINGS

Based on these caveats and assumptions used for the reliability analysis, the results are recognized as only providing a qualitative appreciation of the impacts on bridge design by using the proposed military live loading.

The results of this analysis indicate that the adoption of either the proposed standard HET or the MLC 100W hypothetical wheeled vehicle loading as a new nationwide standard AASHTO Strength II condition would not cause a significant loss of reliability for existing highway bridges. This is true for both special permit crossings (with the heavy vehicle allowed to cross the span without other traffic on the span) and for a worst case military crossing with the heavy vehicle crossing the bridge in one lane with other traffic occupying the other travel lane. The significance inferred from the analysis is that bridges designed for two travel lanes, each loaded with the AASHTO HL-93 design truck and lane load as the Strength I condition, with a multiple lane factor of 1.0 applied to both, results in an equivalent live load representing a single heavy vehicle of 144 kips (= 2 x 72 kips; 640.5 kN) and an applied lane load of 1.28 kips/ft (= 2 x 0.64 kips/ft; 18.7 kN/m), multiplied by a factor of 1.75. Since the Strength II condition factor is 77% of the Strength I factor, the heavier truck (230 kips; 1,023 kN) and a significantly lower uniform load (0.81 kips/ft; 11.8 kN/m and 0.965 kips/ft; 14.1 kN/m for civilian traffic forced flow or the proposed logistics convoy respectively) does not result in reduced reliability for bridges designed as described.

In order to determine an approximate lane loading that would result in a potentially dangerous overloading of a highway bridge for the worst case military crossing with the heavy vehicle crossing the bridge in one lane with other traffic occupying the other travel lane, an analysis was conducted with an uniform lane loading from 0.2 - 5.0 kips/ft (2.9 – 73.0 kN/m)

with either the proposed standard HET and the MLC 100W hypothetical wheeled vehicle on a small number of bridges. The bridges selected for the analysis were the MM-Slab-L-08, MM-IB-L-01 and MM-IB-A-15 as shown on Table 6-1. These bridges are a 50' (15.2 m) span reinforced concrete slab bridge (31'; 9.4 m wide), a 60' (18.3 m) span pre-stressed concrete I-beam composite bridge (31'; 9.4 m wide), and a 130' (39.6 m) span pre-stressed concrete I-beam composite bridge (47'; 14.3 m wide) respectively. The more conservative method of not including the AASHTO Strength I and II condition factors was used for calculating the decrease in reliability for increasing uniform lane loading. The changes in reliability based in maximum mid-span moments are plotted on Figure 6-21.

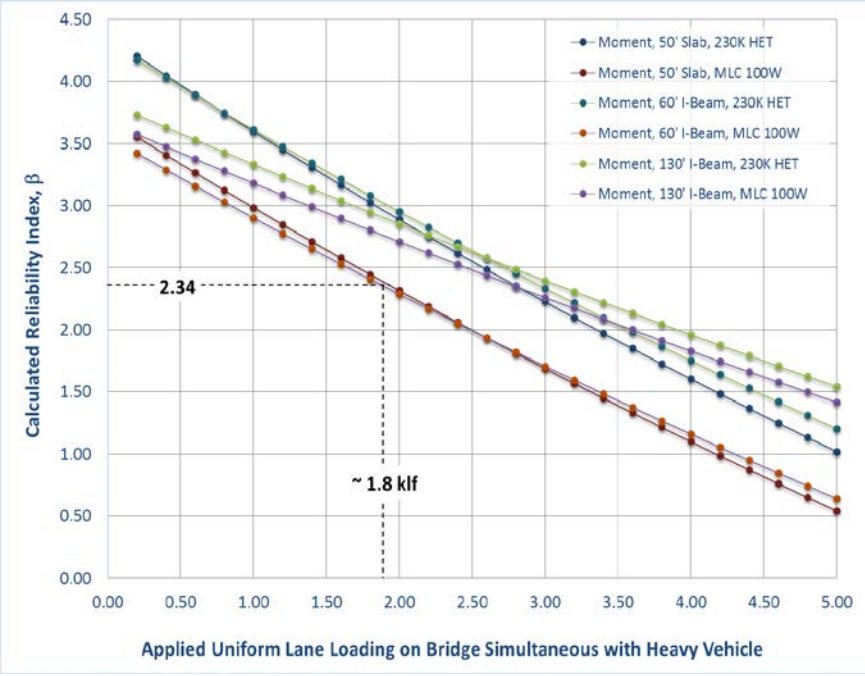

Figure 6-21: Minimum Reliability Indices β for a Factor Applied to Bridge Resistance

Due to the potential rare occurrence of the proposed new military live loading frequently occurring on highway bridges, a reliability index β of 3.0, representing 99.9% reliability was

considered excessive and undesirable. Less than 1% probability of failure was also considered undesirable. Therefore, a target reliability index β for the proposed new military live loading was chosen to be 2.34, which equates to a slightly greater than 99% reliability (or 0.96% probability of failure).

The results of the analysis indicate a rough order of magnitude uniform lane loading of 1.8 kips/ft (approximately 1 US short ton per linear foot; 26.3 kN/m) that combined with the proposed standard HET (special permit vehicle) or the MLC 100W hypothetical wheeled vehicle (both totaling 230 kips; 1,023 kN) result in combined loading that exceeds a bridge designed for two travel lanes, each loaded with the AASHTO HL-93 design truck and lane load as the Strength I condition. This loading represents an AASHTO Strength II condition that results in significantly worse loading effects on highway bridges than the proposed standard HET and the MLC 100W hypothetical wheeled vehicle crossing the bridge span with either civilian traffic forced flow or the proposed logistics convoy, both at crawl speeds, occupying the other travel lane or half of the width of the bridge.

6.6 CHAPTER SIX END NOTES

1. The primary references used for this reliability analysis are Kulicki, J., Prucz, Z., Clancy, C.M., Metz, D.R., and Nowak, A.S. (2007), "Updating the Calibration Report for AASHTO LRFD Code" and Sivakumar, B. and Ghosn, M. (2011), "Recalibration of LRFR Live Load Factors in the AASHTO Manual for Bridge Evaluation". For further discussion on the use and development of reliability based live load modeling and analysis, see also Ghosn, M. (2000), "Development of Truck Weight Regulations Using Bridge Reliability Model"; Ghosn, M. and Moses, F. (2000), "Effect of Changing Truck Weight Regulations on U.S. Bridge Network"; Moses, F. and Ghosn, M. (1987), "Discussion Proposed New Truck Weight Limit Formula"; Novak, A. S. and Collins, K. R. (2000), *Reliability of Structures (1st Edition)*; Nowak, A.S. (1993), "Live Load Model for Highway Bridges"; Nowak, A.S. and Lind, N.D. (1979) "Practical Bridge Code Calibration"; and Verma, D. and Moses, F. (1989), "Calibration of Bridge-Strength Evaluation Code".

2. Sivakumar, B. and Ghosn, M. (2011), "Recalibration of LRFR Live Load Factors in the AASHTO Manual for Bridge Evaluation", page 5-8.

3. Kulicki et al. (2007), page 75.

4. Kulicki et al. (2007), page 76.

5. Kulicki et al. (2007), page 75-77.

6. Sivakumar and Ghosn (2011), page 6.

7. Sivakumar and Ghosn (2011), page 7.

8. See Kwon, O., Kim, E. and Orton, S. (2011), "Calibration of Live-Load Factor in LRFD Bridge Design Specifications Based on State-Specific Traffic Environments"; Ghosn, M., Sivakumar, B., and Miao, F. (2013), "Development of State-Specific Load and Resistance Factor Rating Method"; Nowak, A.S. (1995) "Calibration of LRFD Bridge Code"; and Nowak, A.S. (1999), "Calibration of LRFD bridge design code".

9. Sivakumar and Ghosn (2011), page 7-8.

10. Sivakumar and Ghosn (2011), page 15.

11. Kulicki et al. (2007), page 35-42.

12. Kulicki et al. (2007), page 32.

13. Tonias, D.E. and Zhao, J.J. (2007), *Bridge Engineering (2nd Edition)*, page 77.

14. Derived from 200 bridges provided on pages 35-42 of Kulicki et al. (2007).

15. Fu, G., Liu, L. and Bowman, M.D. (2013), "Multiple Presence Factor for Truck Load on Highway Bridges", Table 1, page 241.

16. See also Ghosn, M. and Moses, F. (1986), "Reliability Calibration of Bridge Design Code".

17. Compare to Fisher, J., Hall, D., McCabe, R., Price, K., Seim, C. and Woods, S. (2006), "Steel Bridges in the United States", Figure 9: Factor of safety versus (LL+I)/DL for WSD, LFD, and LRFD, from page 45.

CHAPTER 7: CONCLUSIONS AND RECOMMENDATIONS

7.1 OVERVIEW

In this study, a new military live loading for long span structures was developed and compared and contrasted to existing bridge design criteria. The new military live load was developed to represent actual military logistic operations during a time of national security emergencies within the continental United States, necessitating the movement of heavy combat vehicles beyond the capacity of the national railway system. The new military live load is recommended to be considered for inclusion in the next update to the American Association of State Highway and Transportation Officials (AASHTO) Load and Resistance Factor Design (LRFD) as a national Strength II for all bridges in the National Highway System (NHS). Further research is recommended to assess the impact of adopting this new bridge design standard, as a National Strength II permit load, for the existing NHS bridge inventory.

7.2 SUMMARY

A preliminary study was performed by reviewing the history of the American interstate highway system and the evolutionary development of bridge design codes for highway bridges in the United States. The current LRFD bridge design methodology was discussed in detail along with the Louisiana Bridge Design and Evaluation Manual's (BDEM) Louisiana Design Vehicle Live Load 2011 (LADV-11). Several other actual and proposed bridge live loads, including two Canadian design codes and several state permit vehicle loads were analyzed. Also analyzed was a theoretical loading developed to represent forced flow which was used in this thesis to represent the contraflow traffic situation condition expected during a mandatory hurricane

evacuation in the Gulf South region. The military load classification (MLC) as defined in the North Atlantic Treaty Organization (NATO) Standardization Agreement (STANAG) 2021 was discussed along with the rationale for using the MLC 100W hypothetical wheeled vehicle as the basis for the subsequent analyses.

The development of a unique analysis method, using independently developed Microsoft EXCEL spreadsheets based on superposition and classical mechanics, developed for each specific analysis, was discussed in detail and the underlying calculations were presented as example analyses. Initially developed and validated for the AASHTO HL-93 design truck and uniform lane live loading, the calculation spreadsheets were expanded to include the MLC vehicles and multi-axle special permit vehicles along with a comparison of actual military heavy equipment transporter (HET) with the MLC 100W hypothetical wheeled vehicle. A theoretical uniform loading was developed to represent saturated flow condition of military logistic convoys. The changes to the computational methodology necessary to calculate maximum positive and negative shear and moments for a two span, equal interior span continuous beam were discussed and explained. Various possible axle positioning for one vehicle on the continuous span was described along with the calculations performed for two vehicles on the continuous span at a specified distance between axles, equidistant from the interior (middle) support.

The first analysis performed was to validate computational spreadsheets using the maximum shear and moment using known values from the California Department of Transportation (CALTRANS) bridge design guide. It was determined that the maximum moment values provided by the CALTRANS bridge design guide were maximum mid-span moment, not the maximum moment as predicted by classical mechanics. The implications were analyzed and discussed. Following the HL-93 calculations, the maximum shear and moment

values for various hypothetical tracked and wheeled vehicles were calculated and compared to the values dictated in from the NATO STANAG 2021 to verify values used in later analyses. The difference between the maximum mid-span and absolute moments for the hypothetical wheeled vehicles was calculated and compared to the previous findings from the AASHTO HL-93 calculations. The spreadsheet was expanded to calculate the maximum shear and moments for several actual HET systems, and other considered bridge design codes and live loadings. The expanded spreadsheet was then used to calculate the shear and moment behavior of two and three MLC 100W hypothetical wheeled vehicles on long spans. The final analysis for a single, simple span considered the Louisiana Bridge Design and Evaluation Manual's (BDEM) Louisiana Design Vehicle Live Load 2011 (LADV-11) and compared the maximum shear and mid-span moments for these vehicles with the AASHTO HL-93 design truck and uniform lane live loading and single and multiple MLC 100W hypothetical wheeled vehicles on long spans. In all cases, the AASHTO HL-93 design truck and uniform lane live loading was evaluated as the Strength I condition, and the special permit vehicles, MLC 100W hypothetical wheeled vehicle, and the various uniform lane loads was evaluated as the Strength II condition.'

The computational spreadsheets were modified and used to determine the maximum positive and negative shear and moments for the AASHO HL-93 design truck and uniform lane live loading and the MLC 100W hypothetical wheeled vehicle on a two span, equal interior span continuous beam. The design truck or vehicle position that produced the maximum positive and negative shear and moments for one vehicle on either interior span was determined for each span length and compared and contrasted with the others. Following this analysis, two vehicles were evaluated on the equal span continuous beam at the specified distances between the front and rear axles of the two vehicles, equidistant from the intermediate support.

Based on the results of the analyses, several interesting and unanticipated discoveries were made regarding the shear and moment behaviors. These were explored and developed to determine what if any new insights presented themselves. These insights included the confirmation of the difference in location (positon along the span) and magnitude of the maximum mid-span moment and absolute maximum moment for the single, simple span. Another insight was the behavior of the maximum moment along the span for multiple vehicles on the single, simple span and the potential application of this finding to bridge design. The continuous beam analyses were expanded to include varying axle distances in order to determine the changes in shear and moment caused by widening or closing of the gap between axles. Finally, the results from the continuous beam analyses, both for a single vehicle and two vehicles equidistant from the intermediate support, were compared to the results from the single, simple beam analyses. Simplified determination of maximum positive and negative shear and moments for the continuous beam were created to create a simplified preliminary assessment criteria for use in bridge design using either the AASHTO HL-93 design truck and uniform lane live loading and the MLC 100W hypothetical wheeled vehicle live loading.

The final analysis was a reliability analysis of a set of known bridges to qualitatively assess the implications of using the proposed new military live loading, either a proposed standard HET that corresponds to several special permit vehicles already in use across the United States and the MLC 100W hypothetical wheeled vehicle, as a new nation-wide standard AASHTO Strength II condition. This analysis began by defining the statistical methodology and demonstrating the calculations by which the revised reliability indices and probabilities of failure were calculated. The completed analysis was used to assess the current reliability and the

recommended design changes necessary on the assumed conditions of current bridge inventory across the United States.

7.3 PROPOSED NEW MILITARY LIVE LOAD FOR DESIGN

Due to the complexity of the two equal span continuous beam analysis results, the author decided to base any recommendation for a new design code using only the simple beam analysis results. It was also recognized that a proposed new live loading should focus on shorter spans since the current design codes adequately account for large design end shear and mid-span moments on longer spans.

The calculated maximum end shear and moments from the reliability analysis of the proposed standard 230 kips (1,023 kN) HET and MLC 100W hypothetical wheeled vehicle live loadings in Chapter 8 were used to develop the proposed new live loading. Additionally, the special case of a MLC 70T hypothetical tracked vehicle live loading was also considered to account for the possible situation where the heavy tracked load (e.g. a main battle tank or an armored bulldozer) is off-loaded from the HET trailer and transverses the span independently of the HET system. The utility of the Louisiana Bridge Design and Evaluation Manual's (BDEM) Louisiana Design Vehicle Live Load 2011 (LADV-11) magnification factor methodology was established by this analysis. A similar methodology was adopted for the development of a proposed new military live loading. The maximum end shear and mid-span moment for these three loadings, normalized to the AASHTO HL-93 design truck and uniform lane live loading, were graphically compared as shown on Figures 7-1 and 7-2. Magnification factors were proposed that accounted for the use of live loadings an AASHTO Strength II condition in comparison to the AASHO HL-93 design truck and uniform lane live loading as an AASHTO

Strength I condition. Also plotted were the Louisiana BDEM LADV-11 magnification factors for end shear and positive mid-span moment as defined previously on Table 3-3. The proposed new military live loading magnifications factors are listed on Table 7-1 in both US and SI convention.

Proposed New Military Live Loading Magnification Factors

Load Effect	Range of Applicability	Magnification Factor (MF)
Maximum End Shear, V	L < = 100 ft (L < = 30.5 m)	1.51
	100 ft < L < 300 ft (30.5 m < L < 91.4 m)	1.51 - (0.36 x (L - 100 ft)) / 200 ft (1.51 - (0.36 x (L - 30.5 m)) / 61 m)
	L > = 300 ft (L > = 91.4 m)	1.15
Maximum Positive Mid-span Moment, M+	L < = 50 ft (L < = 15.2 m)	1.63
	50 ft < L < 400 ft (15.2 m < L < 121.9 m)	1.63 - (0.63 x (L - 50 ft)) / 350 ft (1.63 - (0.63 x (L - 15.2 m)) / 106.7 m)
	L > = 400 ft (L > = 121.9 m)	1.00

Table 7-1: Proposed New Military Live Load Magnification Factors

Although the MLC 100W hypothetical wheeled vehicle live loadings was used for previous analysis for comparison with the AASHO HL-93 design truck and uniform lane live loading, the very large concentrated axle loads, the middle 30 kips (133.4 kN) axles space 6 ft (1.8 m) was less realistic for actual bridge design than the proposed standard 230 kips (1,023 kN) HET. The MLC 100W hypothetical wheeled vehicle live loadings was used for the termination of maximum shear and mid-span moment for multiple vehicles on longer spans.

The maximum end shear for the MLC 70T hypothetical tracked vehicle live loading can be accounted for by creating a magnification factor for the proposed standard 230 kips (1,023 kN) HET for span lengths up to 100 ft (30.5 m) as shown on Figure 7-1. At approximately 400 ft (91.4 m), the maximum end shear for the multiple MLC 100W hypothetical wheeled vehicle

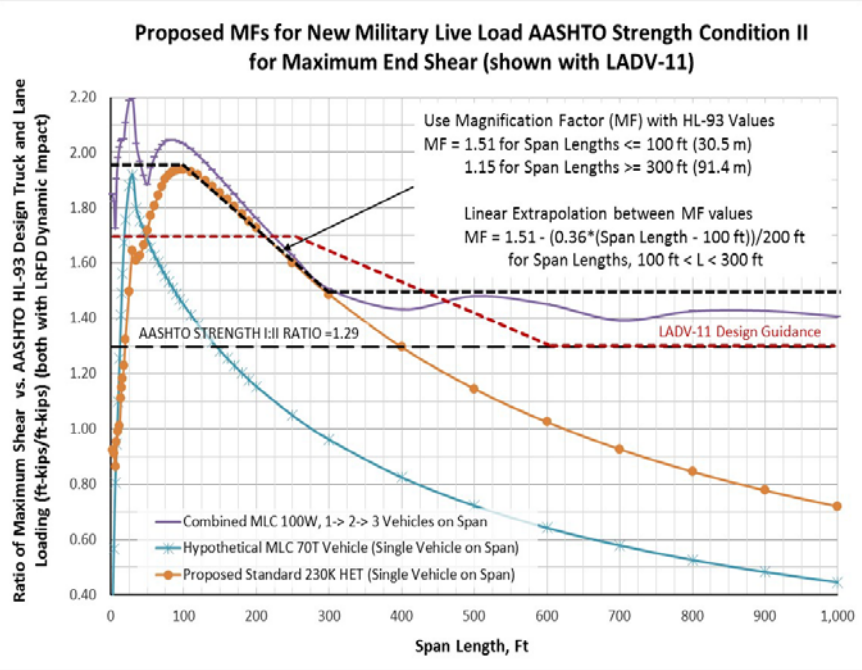

Figure 7-1: Proposed Magnification Factors for New Military Live Load AASHTO Strength Condition II for Maximum End Shear

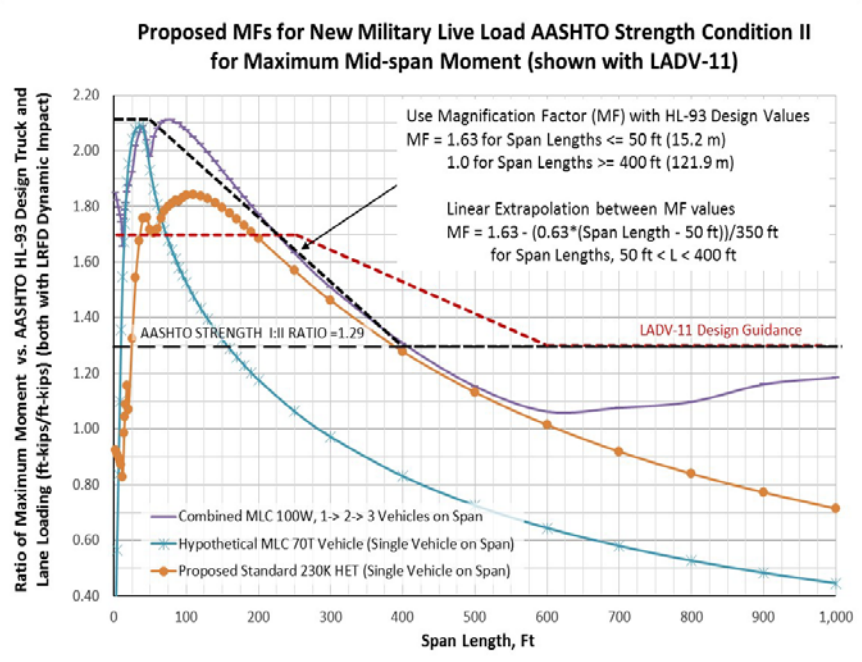

Figure 7-2: Proposed Magnification Factors for New Military Live Load AASHTO Strength Condition II for Maximum Mid-span Moment

live loading is the limiting value. Therefore, the magnification factor of maximum end shear is based on these two limit conditions. The maximum mid-span moment is limited by the MLC 70T hypothetical tracked vehicle live loading as shown on Figure 7-2. It was noted that there are magnification factors dictated by the Louisiana BDEM LADV-11 design guidance that are greater than the proposed new military live loading magnifications factors for span lengths of approximately 220 - 430 ft (67 – 131 m) for maximum end shear and 225 – 600 ft (69 – 183 m) for maximum mid-span moment as shown on Figures 7-1 and 7-2. This was a consequence of the fact that several of the Louisiana special design vehicles shown on Figure 2-1, multiplied by the load factors listed on Table 2-2, produced greater end shear and mid-span moment than the military live loadings considered and would govern bridge design for those span lengths.

Figures 7-3 and 7-4 show a comparison of the proposed new military live loading (MLL) magnification factor at this span length with the other design loads discussed earlier, normalized to the AASHTO HL-93 design truck and uniform lane live loading. As demonstrated on Figure 7-3, the maximum end shear for several of the other design live loads (Washington State WA-03 and Wisconsin Special Permit Vehicle) exceed the proposed magnified loading for spans < 400 ft (< 121.9 m), and are already safe for transit by both the the proposed standard 230 kips (1,023 kN) HET and the MLC 70T hypothetical tracked vehicle live loading as the AASHTO Strength II condition. Figure 7-4 demonstrates that the maximum mid-span moment for the several of the other design live loadings (Ontario Highway Bridge Design and a hypothetical 5 axle permit vehicle) exceed the proposed magnified loading for spans < 100 ft (< 30.5 m). Figures 7-3 and 7-4 also indicate that a number of current state SPV design loads meet or exceed the load effects generated by the proposed new MLL. This result implies that the proposed new MLL could be readily adopted by these same states as an AASHTO Strength II design load.

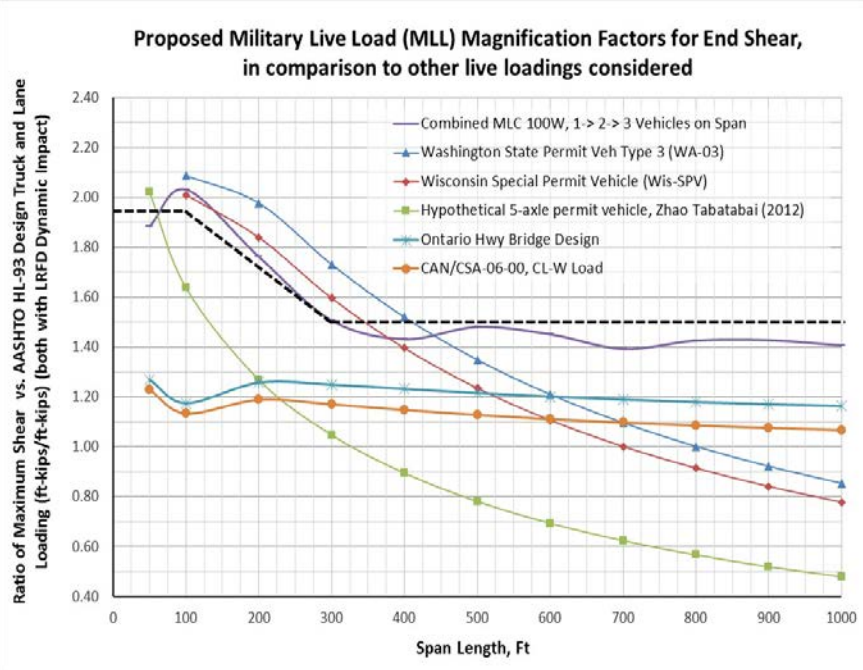

Figure 7-3: Proposed New Military Live Load (MLL) Magnification Factors for End Shear, in comparison to Other Design Codes and Vehicle Loadings

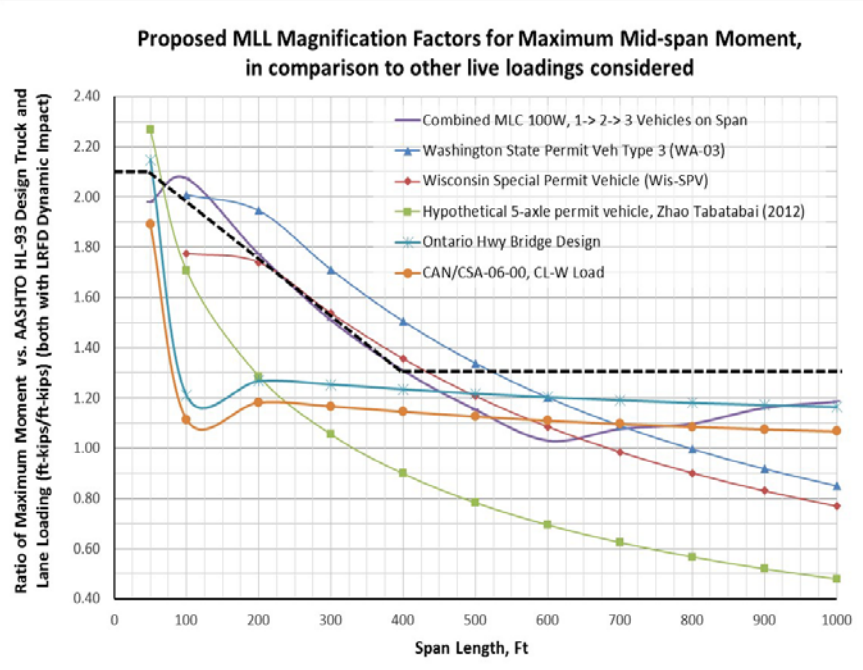

Figure 7-4: Proposed New MLL Magnification Factors for Maximum Mid-span Moment, in comparison to Other Design Codes and Vehicle Loadings

7.4 FINDINGS AND CONCLUSIONS

1. The current AASHTO HL-93 Alternative Military Tandem (AMT) specification is likely based on the original military tank transporter used in the Ottawa Road Test of the late 1950's, and is not a valid representation of potential present and near future military use of interstate highway system.
2. The tabulated values for maximum shear and moment in Appendix B of FM 3-34.343 appear to contain errors.
3. For the AASHTO HL-93 design truck and uniform lane live loading, there is a negligible difference between the maximum mid-span and absolute moment. Structural analysis theory states that the maximum moment of a span under multiple, non-uniform concentrated loads will occur when the group of concentrated loads are positioned such that the resultant of these loads and the nearest concentrated load are equidistant from the simple beam's mid-span. The maximum mid-span moment must occur when a concentrated load is positioned at the mid-span. For most groups of concentrated loads, the resultant will not be exactly co-located with an axle or concentrated load. It was determined that the maximum mid-span moment may or may not occur when the axle closest to the resultant is positioned at mid-span, however, the magnitude of the maximum mid span moment will be equal to the maximum moment at an axle location when the design truck, or group of concentrated loads, are positioned such that the resultant is located at mid-span. Based on these observations, it was determined that for a closely spaced group (length "a") of concentrated loads acting on a simple beam of a span length (length "L") greater than the group length ($L > a$):

a. The magnitude of the maximum mid-span moment can be calculated by positioning the resultant at mid-span and calculating the maximum moment at the location of one of the concentrated loads.

b. The absolute maximum moment occurs when the load group is positioned such that the resultant and the concentrated load that produces the maximum mid-span moment are positioned equidistant from the mid-span. The maximum absolute moment does not occur at mid span.

c. The magnitude of the mid-span moment generated when the loads are positioned to produce the maximum absolute moment will always be less than the magnitude of maximum moment when the resultant is at mid-span.

d. The difference in magnitude of the maximum absolute moment and the maximum mid-span moment is negligible for spans relatively longer than the group length.

4. For the condition where two relatively tightly clustered groups of concentrated loads are positioned along a long span relative to the individual group lengths, the plot of the possible moment curves corresponding to different vehicle positioning along the span demonstrated a double peaked profile and the possible moment diagram curve intersects a common point at mid-span corresponding to a maximum moment created when the vehicles are positioned such that the resultant of both vehicles (i.e. the total live loading on the span) is at mid-span.

5. The proposed new military live load is a better representation of possible military use of the national highway system than the current AASHTO Alternative Military Load (AML). The current AASHTO AML, which is a LRFD Strength I condition of consisting a design tandem axle load of two 25 kips (111.2 kN) concentrated loads spaced 4 ft (1.22 m)

apart) along with the uniform lane load (0.64 kips per foot), produces maximum end shear and mid-span moment that are significantly less than maximum end shear and mid-span moment calculated resulting from the actual movement of combat forces, as shown on Figures 5-34 and 5-35.

7.5 RECOMMENDATIONS

1. The proposed new military live load should be considered for inclusion in the next update to the American Association of State Highway and Transportation Officials (AASHTO) Load and Resistance Factor Design (LRFD) as a national Strength II design condition for all bridges in the National Highway System. The proposed new military live load would supersede various state permit vehicles currently used for the LRFD Strength II condition for select highway bridges in that state.
2. The proposed new military live load consists of the Standard NATO agreement (STANAG) MLC 100W hypothetical wheeled vehicles for longer spans (> 100 ft; > 30.5 m) and the proposed standard heavy equipment transporter (HET) weighing 230K (1,023 kN) for shorter spans. The proposed standard HET consists of a tractor axle load pairs separated by a vehicle width of 12 ft (3.65 m) and the trailer axle loads acting across the full vehicle width. Multiple MLC 100W hypothetical wheeled vehicles separated by 300 ft (91.4 m) between front and rear axles would be used for longer spans. The use of the proposed standard HET, which corresponds to a special permit vehicle already in use in several states, is recommended due to the unrealistically large loads acting on the closely spaced middle tandem axles of the MLC 100W hypothetical wheeled vehicle.

3. A simplified solution recommended for inclusion in future updates of the Louisiana Department of Transportation and Development Bridge Design and Evaluation Manual is the use of the magnification factors shown on Table 7-1 with the HL-93 design values to represent the proposed new military load. Recommended design values with applied magnification factors are provided in Appendix A.
4. The author plans to continue this research and expand the analyses to include the dynamic effects of the proposed new MLL HET vehicle convoy traveling at the specified constant speed and separation on the harmonic resonance of bridge superstructures, particularly cable stayed and/or suspension bridges.
5. The author intends to submit the analysis and findings to the appropriate professional journals and periodicals for publication, in order to share the findings of this analysis with a wider audience in the bridge design community and to nominate the proposed new MLL as a national LRFD Strength II design condition for the next revision of the AASHTO design specification.

REFERENCES

1. American Association of State Highway Officials (1973), Standard Specifications for Highway Bridges, 11th Ed, Washington, DC.

2. American Association of State Highway and Transportation Officials (AASHTO) (2010), Load Resistance Factor Design (LRFD) Bridge Design Specifications, 5th Ed., Washington, DC.

3. American Forest and Paper Association (2007), Beam Design Formulas with Shear and Moment Diagrams, American Wood Council, Washington, DC.

4. Agrawal, A., Sreyashrao S, and Dawair, B.M. (2011), "Simplification for train loading on bridges", Intl. J. Earth Sciences and Eng., 4(6), 744-747.

5. ASCE Committee on Loads and Forces on Bridges (1981), "Recommended Design Loads for Bridges", ASCE J. Structural Eng., 107 (7), 1161-1213.

6. Bhide, S., Culmo, M., Ma, J., Martin, B. and Russell, H. (2006), "The Interstate Highway System and the Development of Prestressed Concrete Bridges", Transportation Research Circular E-C104: 50 Years of Interstate Structures: Past, Present, and Future, Transportation Research Board, Washington, DC, 49-66.

7. Buckland, P.G. (1991), "North American and British Long-Span Bridge Loads", J. Structural Div., 117(10), 2972-2987.

8. Buckland, P.G., Navin, F.P.D, Zidek, J.V., and McBryde, J.P. (1978), "Traffic loading of long-span bridges", Transportation Research Record, 665, 146-154.

9. Buckland, P.G., Navin, F.P.D, Zidek, J.V., and McBryde, J.P. (1980), "Proposed Vehicle Loading of Long-Span Bridges", J. Structural Div., 106(ST4), 915-932.

10. California Department of Transportation (CALTRANS) (2008), Bridge Design Aids, HL-93 Loading, Sacramento, CA.

11. Canadian Standards Association (2006), "Canadian highway bridge design code." CAN/CSA-S6-O6, Toronto, Canada.

12. Cotter, D.G. (2003), "The Iron Horse Express", Army Logistician, September/October, PB 700-03-5, Vol. 35, Issue 5, U.S. Dept. of the Army, Washington, DC (http://www.alu.army.mil/alog/issues/SepOct03/Iron_Horse.htm).

13. Dunstan, S.P. (2013), "Examining Decisive Action Sustainment Operations at the Task Force Level", Army Sustainment, March/April, U.S. Dept. of the Army, Washington, DC, 42-45 (http://www.army.mil/article/97924).

14. Fisher, J., Hall, D., McCabe, R., Price, K., Seim, C. and Woods, S. (2006), “Steel Bridges in the United States”, Transportation Research Circular E-C104: 50 Years of Interstate Structures: Past, Present, and Future”, Transportation Research Board, Washington, DC, 27-48.

15. Fu, G., Liu, L. and Bowman, M.D. (2013), “Multiple Presence Factor for Truck Load on Highway Bridges”, J. Bridge Eng., 18(3), 240-249.

16. Ghosn, M. (2000), “Development of Truck Weight Regulations Using Bridge Reliability Model”, J. Bridge Eng., 5(4), 293-303.

17. Ghosn, M. and Moses, F. (1986), “Reliability Calibration of Bridge Design Code”, J. Struct. Eng., 112(4), 745-763.

18. Ghosn, M. and Moses, F. (2000), “Effect of Changing Truck Weight Regulations on U.S. Bridge Network”, J. Bridge Eng., 5(4), 304-310.

19. Ghosn, M., Sivakumar, B., and Miao, F. (2013), “Development of State-Specific Load and Resistance Factor Rating Method”, J. Bridge Eng., 18(5), 351-361.

20. Hayworth, R. Huo, X.S., and Zheng, L. (2008), “Effects of State Legal Loads on Bridge Rating Results Using the LRFR Procedure”, J. Bridge Eng., 13(6), 565-572.

21. Kansas Department of Transportation (2011), Design Manual, Volume III US (LRFD) Bridge Section, Topeka, KS.

22. Keith, T.C. (1998), “Lift Missions in Bosnia”, Army Logistician, November/December, PB 700-98-6, Vol. 30, Issue 6, U.S. Dept. of the Army, Washington, DC (http://www.alu.army.mil/alog/issues/NovDec98/MS300.htm).

23. Kennedy, E. (2000), “Forging An Alliance: Army Transporters in Europe”, Army Logistician, September/October, PB 700-00-5, Vol. 32, Issue 5, U.S. Dept. of the Army, Washington, DC (http://www.alu.army.mil/alog/issues/SepOct00/MS603.htm).

24. Kim, Y.J., Tanovic, R., and Wight, R.G. (2010), “Load Configuration and Lateral Distribution of NATO Wheeled Military Trucks for Steel I-Girder Bridges”, J. Bridge Eng., 15(6), 740-748.

25. Kulicki, J.M. and Metz, D. (2006), “Evolution of Vehicular Live Load Models During the Interstate Design Era and Beyond”, Transportation Research Circular E-C104: 50 Years of Interstate Structures: Past, Present, and Future, Transportation Research Board, Washington, DC., 1-26.

26. Kulicki, J., Prucz, Z., Clancy, C.M., Metz, D.R., and Nowak, A.S. (2007), “Updating the Calibration Report for AASHTO LRFD Code.” Final Report National Cooperative Highway Research Program (NCHRP) 20-07/186, Transportation Research Board, Washington, DC.

27. Kwon, O., Kim, E. and Orton, S. (2011), “Calibration of Live-Load Factor in LRFD Bridge Design Specifications Based on State-Specific Traffic Environments”, J. Bridge Eng., 16(6), 812-819.

28. Lewis, S. (2006), “Industry’s Largest R&D Effort Founded Interstate Construction “, Engineering News Record (ENR), McGraw-Hill, New York, NY, 32 (accessed at: http://enr.construction.com/features/transportation/archives/060313c.asp).

29. Lippert, D.L. (2008), “Illinois DOT - From the AASHO Road Test To 20 Years of Mechanistic Pavement Experience and Counting“, Transportation Research Board 87th Annual Meeting, Washington, DC.

30. Louisiana Department of Transportation and Development (LADOTD) (2015), Bridge Design and Evaluation Manual (BDEM), Baton Rouge, LA.

31. Lutomirska, M. (2009), “Live Load Models for Long Span Bridges”, Civil Engineering Theses, Dissertations, and Student Research, University of Nebraska-Lincoln, NE.

32. Metz, D.R. (2009a), “Development of the HL-93 Notional Live Load Model “, Aspire The Concrete Bridge Magazine, Chicago, IL, 3(3), 52.

33. Metz, D.R. (2009b), “The HL-93 Notional Live Load Model: What Nature of Truck Does It Represent “, Aspire The Concrete Bridge Magazine, Chicago, IL, 3(4), 52.

34. Metz, D.R. (2010), “The HL-93 Live Load Model Dynamic Load Allowance “, Aspire The Concrete Bridge Magazine, Chicago, IL, 4(4), 56.

35. McCormac, J. and Elling, R.E. (1998), *Structural Analysis A Classical and Matrix Approach*, Harper and Row Publishers, Inc., New York, NY.

36. Miller, L. J. and Durham, S. A. (2008), “Comparison of Standard Load and Load and Resistance Factor Bridge Design Specifications for Buried Concrete Structures”, Transportation Research Record, Volume 2050, Transportation Research Board, Washington, DC, 81-89.

37. Mlynarski, M., Wassef, W., and Nowak, A.S. (2011), “A Comparison of AASHTO Bridge Load Rating Methods”, National Cooperative Highway Research Program (NCHRP) Report 700, Transportation Research Board, Washington, DC.

38. Moses, F. and Ghosn, M. (1987), “Discussion Proposed New Truck Weight Limit Formula”, J. Struct. Eng., 113(11), 2330-2331.

39. Nawy, E.G. (2010), *Prestressed Concrete A Fundamental Approach (5th Edition),* Prentice Hill, Pearson Education, Inc., Upper Saddle River, NY.

40. North Atlantic Treaty Organization (NATO) Standardization Agency, (2002), Standardization Agreement (STANAG) 2021, 6th Ed., Brussels, Belgium.

41. Nowak, A.S. (1993), “Live Load Model for Highway Bridges”, Journal of Structural Safety, Vol. 13, December, pp. 53-66.

42. Nowak, A.S. (1994), “Load Model for Bridge Design Code”, Canadian Journal of Civil Engineering, Vol. 21, pp. 36-49.

43. Nowak, A.S. (1995), “Calibration of LRFD Bridge Code”, ASCE Journal of Structural Engineering, Vol. 121, No. 8, pp. 1245-1251.

44. Nowak, A.S. (1999), “Calibration of LRFD bridge design code” NCHRP Transportation Research Record 368, Transportation Research Board, Washington, DC.

45. Novak, A. S. and Collins, K. R. (2000), *Reliability of Structures (1st Edition),* McGraw-Hill Companies, New York, NY.

46. Nowak, A.S. and Hong, Y-K. (1991), “Bridge Live Load Models”, ASCE Journal of Structural Engineering, Vol. 117, No. 9, Sept. 1991, pp. 2757-2767.

47. Nowak, A.S., and Lind, N.D. (1979), “Practical Bridge Code Calibration,” Journal of Structural Division, ASCE, pp. 2497-2510.

48. Nowak, A. S., Eom, J. and Sanli, A. (2000), “Control of Live Load on Bridges”, Transportation Research Record 1696, Fifth Internatio6al Bridge Engineering Conference, Paper No. 5B0015, Transportation Research Board, Washington, DC, 136-143.

49. Nowak, A.S., Kozikowski, M. and Lutomirska, M. (2010), “Risk Mitigation for Highway and Railway Bridges“, Mid-America Transportation Center, Lincoln, NE.

50. Nowak, A.S., Lutomirska, M. and Sheikh Ibrahim, F.I. (2010), “The Development of Live Load for Long Span Bridges”, Bridge Structures, Vol. 6, pp. 73-79.

51. Nowak, A.S., Nassif, H. and DeFrain, L. (1993), “Effect of Truck Loads on Bridges”, J. Transp. Eng., 119(6), 853-867.

52. Ontario Highway Bridge Design Code (OHBDC), 3rd Edition (1991), Ministry of Transportation, Downsview, Ontario, Canada.

53. Parker, W.P. (2001) “Infantry assault engineers: An old (world) approach for engineer close combat support”, Marine Corps Gazette, Quantico, VA, 85(10), 22-26.

54. Ray, J.C. and Seda-Sanabria, Y. (2002), Technical Commentary on FM3-34.343, "Military Nonstandard Fixed Bridging", U.S. Army Engineer Research and Development Center, Vicksburg, MS.

55. Russell, B.R. and Thrall, A.P. (2013), “Portable and Rapidly Deployable Bridges: Historical Perspective and Recent Technology Developments”, J. Bridge Eng., 18(10), 1074-1085.

56. Saraf, V., Sokolik, A.F. and Nowal, A.S. (1996), “Proof Load Testing of Highway Bridges", Transportation Research Record, Structures, Culverts, and Tunnels,, Transportation Research Board, Washington, DC, 51-57.

57. Shreedhar, R. and Mamadapur, S. (2012), “Analysis of T-beam Bridge Using Finite Element Method”, Intl. J. Eng. And Innovative Tech., 2(3), 340-346.

58. Sivakumar, B., Moses, F., Fu, G. and Ghosn, M. (2007), “Legal Truck Loads and AASHTO Legal Loads for Posting”, National Cooperative Highway Research Program (NCHRP) Report 575, Transportation Research Board, Washington, DC.

59. Sivakumar, B. and Ghosn, M. (2011), “Recalibration of LRFR Live Load Factors in the AASHTO Manual for Bridge Evaluation”, Final Report National Cooperative Highway Research Program (NCHRP) 20-07/285, Transportation Research Board, Washington, DC.

60. Tabsh, S.W. and Tabatabai, M. (2001), “Live Load Distribution in Girder Bridges Subject to Oversized Trucks”, J. Bridge Eng., 6(1), 9-16.

61. Tobias, D.H. (2011), “Perspectives on AASHTO Load and Resistance Factor Design”, J. Bridge Eng., 16(6), 684-692.

62. Tonias, D.E. and Zhao, J.J. (2007), *Bridge Engineering (2nd Edition)*, McGraw-Hill Companies, New York, NY.

63. Turer, A. and Aktan, A.E. (1999), “Issues in Superload Crossing of Three Steel Stringer Bridges in Toledo, Ohio”, Transportation Research Record 1688, Various Bridge Design Issues, Paper No. 99-0385, Transportation Research Board, Washington, DC, 87-96.

64. U.S. Department of the Army (2002), Military Non-Standard Fixed Bridging (FM3-34.343), Washington, DC.

65. U.S. War Department (1944), Technical Manual (TM) 9-767, 40-Ton Tank Transporter, Tractor-Trailer M25, Washington, DC.

66. Verma, D. and Moses, F. (1989), “Calibration of Bridge-Strength Evaluation Code”, J. Struct. Eng., 115(6), 1538-1554.

67. Vigh, A. and Kollar, L.P. (2007), “Routing and Permitting Techniques of Overweight Vehicles”, J. Bridge Eng., 12(6), 774-784.

68. Waddell, J.A.L. (1884*), The Designing of Ordinary Iron Highway Bridges*, John Wiley and Sons, New York, NY.

69. Waddell, J.A.L. (1921), *Economics of Bridgework A Sequel to Bridge Engineering*, John Wiley and Sons, New York, NY.

70. Walther, R.A. and Chase, S.B. (2006), “Condition Assessment of Highway Structures”, Transportation Research Circular E-C104: 50 Years of Interstate Structures: Past, Present, and Future, Transportation Research Board, Washington, DC, 67-78.

71. Weingroff, R.F. (2003). “The Man Who Changed America, Part I”, Public Roads, 66(5), Fed. Hwy. Admin., U. S. Dept. of Trans., Washington, DC.

72. Weingroff, R.F. (2003). “The Man Who Changed America, Part II”, Public Roads, 66(6), Fed. Hwy. Admin., U. S. Dept. of Trans., Washington, DC.

73. Weingroff, R.F. (2006), “Essential to the National Interest”, Public Roads, 69(5), Publication No. FHWA-HRT-2006-003, Fed. Hwy. Admin., U. S. Dept. of Trans., Washington, DC.

74. Weingroff, R.F. (2014); “A Vast System of Interconnected Highways”, Fed. Hwy. Admin., U. S. Dept. of Trans., Washington, DC (http://www.fhwa.dot.gov/highwayhistory/vast.pdf).

75. Weissman, J. and Harrison, R. (1998), “Impact of 44 000-kg (97,000-lb) Six-Axle Semitrailer Trucks on Bridges on Rural and Urban U.S. Interstate System“, Transportation Research Record 1624, Structural Analysis and Design: Bridges, Culverts, and Pipes,, Paper No. 98-0481, Transportation Research Board, Washington, DC., 180-183.

76. Wright, P.H. and Dixon, K.K. (2004), *Highway Engineering (7th Edition)*, John Wiley and Sons, Inc., Hoboken, NJ.

77. Zhao, J. and Tabatabai, H. (2012), “Evaluation of a Permit Vehicle Model Using Weigh-in-Motion Truck Records”, J. Bridge Eng., 17(2), 389-392.

APPENDIX A: TABLES OF RECOMMENDED DESIGN VALUES

Table of Maximum Moments, Shears and Reactions Simple Spans, One Lane **With** Dynamic Load Allowance AASHTO HL-93 Design Truck/Tandem and Uniform Lane Load

Span (ft)		Moment (kips-ft)	End Shear and End Reaction (k)	Span (ft)		Moment (kips-ft)	End Shear and End Reaction (k)
1	----------	10.7	42.9	26	----------	419.8	70.5
2	----------	21.6	43.2	27	----------	440.7	71.7
3	----------	32.6	43.5	28	----------	461.7	72.8
4	----------	43.8	43.8	29	----------	482.9	74.2
5	----------	55.2	44.2	30	----------	504.3	75.6
6	----------	66.7	46.3	31	----------	525.8	76.8
7	----------	78.4	49.7	32	----------	547.4	78.1
8	----------	90.2	52.4	33	----------	569.2	79.2
9	----------	102.2	54.6	34	----------	591.2	80.4
10	----------	114.4	56.4	35	----------	613.4	81.4
11	----------	126.7	57.9	36	----------	635.7	82.5
12	----------	144.5	59.3	37	----------	658.1	83.4
13	----------	163.1	60.4	38	----------	680.8	84.4
14	----------	181.9	61.5	39	----------	703.6	85.3
15	----------	200.9	62.4	40	----------	726.5	86.2
16	----------	220.0	63.3	42	----------	774.2	87.9
17	----------	239.3	64.1	44	----------	835.8	89.5
18	----------	258.7	64.9	46	----------	898.1	91.1
19	----------	278.3	65.6	48	----------	961.0	92.5
20	----------	298.0	66.3	50	----------	1,024.6	93.9
21	----------	317.9	66.9	52	----------	1,088.8	95.2
22	----------	338.0	67.5	54	----------	1,153.6	96.5
23	----------	358.2	68.1	56	----------	1,219.1	97.7
24	----------	378.6	68.6	58	----------	1,285.2	98.9
25	----------	399.1	69.3	60	----------	1,352.0	100.1

Table of Maximum Moments, Shears and Reactions Simple Spans, One Lane **With** Dynamic Load Allowance AASHTO HL-93 Design Truck/Tandem and Uniform Lane Load

Span (ft)		Moment (kips-ft)	End Shear and End Reaction (k)	Span (ft)		Moment (kips-ft)	End Shear and End Reaction (k)
62	----------	1,419.4	101.2	160	----------	5,506.0	141.4
64	----------	1,487.4	102.3	170	----------	6,009.4	144.9
66	----------	1,556.1	103.3	180	----------	6,528.8	148.4
68	----------	1,625.4	104.4	190	----------	7,064.2	151.9
70	----------	1,695.4	105.4	200	----------	7,615.6	155.3
72	----------	1,766.0	106.4	210	----------	8,183.0	158.7
74	----------	1,837.3	107.4	220	----------	8,766.4	162.1
76	----------	1,909.1	108.3	230	----------	9,365.8	165.5
78	----------	1,981.7	109.3	240	----------	9,981.2	168.8
80	----------	2,054.8	110.2	250	----------	10,612.6	172.2
82	----------	2,128.6	111.1	260	----------	11,260.0	175.5
84	----------	2,203.1	112.0	270	----------	11,923.4	178.8
86	----------	2,278.1	112.9	280	----------	12,602.8	182.2
88	----------	2,353.9	113.8	290	----------	13,298.2	185.5
90	----------	2,430.2	114.6	300	----------	14,009.6	188.8
92	----------	2,507.2	115.5	350	----------	17,806.6	205.2
94	----------	2,584.9	116.3	400	----------	22,003.6	221.5
96	----------	2,663.1	117.2	450	----------	26,600.6	237.8
98	----------	2,742.1	118.0	500	----------	31,597.6	254.0
100	----------	2,821.6	118.8	550	----------	36,994.6	270.1
110	----------	3,229.0	122.8	600	----------	42,791.6	286.3
120	----------	3,652.4	126.7	700	----------	55,585.6	318.5
130	----------	4,091.8	130.5	800	----------	69,979.6	350.6
140	----------	4,547.2	134.2	900	----------	85,973.6	382.8
150	----------	5,018.6	137.8	1000	----------	103,567.6	414.9

Table of Maximum Moments, Shears and Reactions Simple Spans,

One Lane **With** Dynamic Load Allowance

AND the Magnification Factor for the **Proposed Military Live Load**

Use for AASHTO Strength Condition I instead of HL-93 Values

Span (ft)		Moment (kips-ft)	End Shear and End Reaction (k)	Span (ft)		Moment (kips-ft)	End Shear and End Reaction (k)
1	----------	17.4	64.8	26	----------	684.3	106.5
2	----------	35.2	65.2	27	----------	718.3	108.3
3	----------	53.1	65.7	28	----------	752.6	109.9
4	----------	71.4	66.1	29	----------	787.1	112.0
5	----------	90.0	66.7	30	----------	822.0	114.2
6	----------	108.7	69.9	31	----------	857.1	116.0
7	----------	127.8	75.0	32	----------	892.3	117.9
8	----------	147.0	79.1	33	----------	927.8	119.6
9	----------	166.6	82.4	34	----------	963.7	121.4
10	----------	186.5	85.2	35	----------	999.8	122.9
11	----------	206.5	87.4	36	----------	1,036.2	124.6
12	----------	235.5	89.5	37	----------	1,072.7	125.9
13	----------	265.9	91.2	38	----------	1,109.7	127.4
14	----------	296.5	92.9	39	----------	1,146.9	128.8
15	----------	327.5	94.2	40	----------	1,184.2	130.2
16	----------	358.6	95.6	42	----------	1,261.9	132.7
17	----------	390.1	96.8	44	----------	1,362.4	135.1
18	----------	421.7	98.0	46	----------	1,463.9	137.6
19	----------	453.6	99.1	48	----------	1,566.4	139.7
20	----------	485.7	100.1	50	----------	1,670.1	141.8
21	----------	518.2	101.0	52	----------	1,770.8	143.8
22	----------	550.9	101.9	54	----------	1,872.1	145.7
23	----------	583.9	102.8	56	----------	1,974.0	147.5
24	----------	617.1	103.6	58	----------	2,076.4	149.3
25	----------	650.5	104.6	60	----------	2,179.4	151.2

Table of Maximum Moments, Shears and Reactions Simple Spans,

One Lane **With** Dynamic Load Allowance

AND the Magnification Factor for the **Proposed Military Live Load**

Use for AASHTO Strength Condition I instead of HL-93 Values

Span (ft)		Moment (kips-ft)	End Shear and End Reaction (k)	Span (ft)		Moment (kips-ft)	End Shear and End Reaction (k)
62	----------	2,283.0	152.8	160	----------	7,884.6	198.2
64	----------	2,387.0	154.5	170	----------	8,497.3	200.5
66	----------	2,491.6	156.0	180	----------	9,114.2	202.7
68	----------	2,596.7	157.6	190	----------	9,734.5	204.8
70	----------	2,702.5	159.2	200	----------	10,357.2	206.5
72	----------	2,808.7	160.6	210	----------	10,981.6	208.2
74	----------	2,915.4	162.1	220	----------	11,606.7	209.8
76	----------	3,022.6	163.6	230	----------	12,231.8	211.1
78	----------	3,130.2	165.0	240	----------	12,855.8	212.4
80	----------	3,238.4	166.4	250	----------	13,478.0	213.5
82	----------	3,347.0	167.8	260	----------	14,097.5	214.5
84	----------	3,456.2	169.1	270	----------	14,713.5	215.3
86	----------	3,565.7	170.5	280	----------	15,325.0	216.1
88	----------	3,675.8	171.8	290	----------	15,931.3	216.6
90	----------	3,786.3	173.0	300	----------	16,531.4	217.1
92	----------	3,897.2	174.4	350	----------	19,409.2	236.0
94	----------	4,008.6	175.7	400	----------	22,003.6	254.8
96	----------	4,120.4	176.9	450	----------	26,600.6	273.4
98	----------	4,232.6	178.2	500	----------	31,597.6	292.1
100	----------	4,345.3	179.4	550	----------	36,994.6	310.7
110	----------	4,914.5	183.2	600	----------	42,791.6	329.2
120	----------	5,493.2	186.8	700	----------	55,585.6	366.3
130	----------	6,080.4	190.0	800	----------	69,979.6	403.2
140	----------	6,675.3	193.0	900	----------	85,973.6	440.2
150	----------	7,277.0	195.7	1000	----------	103,567.6	477.1

Table of Maximum Moments, Shears and Reactions Simple Spans,

One Lane **With** Dynamic Load Allowance

AND the Magnification Factor for the **Louisiana Bridge Design (LADV-11)**

Use for AASHTO Strength Condition I instead of HL-93 Values

Span (ft)		Moment (kips-ft)	End Shear and End Reaction (k)	Span (ft)		Moment (kips-ft)	End Shear and End Reaction (k)
1	----------	13.9	55.8	26	----------	545.7	91.7
2	----------	28.1	56.2	27	----------	572.9	93.2
3	----------	42.4	56.6	28	----------	600.2	94.6
4	----------	56.9	56.9	29	----------	627.8	96.5
5	----------	71.8	57.5	30	----------	655.6	98.3
6	----------	86.7	60.2	31	----------	683.5	99.8
7	----------	101.9	64.6	32	----------	711.6	101.5
8	----------	117.3	68.1	33	----------	740.0	103.0
9	----------	132.9	71.0	34	----------	768.6	104.5
10	----------	148.7	73.3	35	----------	797.4	105.8
11	----------	164.7	75.3	36	----------	826.4	107.3
12	----------	187.9	77.1	37	----------	855.5	108.4
13	----------	212.0	78.5	38	----------	885.0	109.7
14	----------	236.5	80.0	39	----------	914.7	110.9
15	----------	261.2	81.1	40	----------	944.5	112.1
16	----------	286.0	82.3	42	----------	1,006.5	114.3
17	----------	311.1	83.3	44	----------	1,086.5	116.4
18	----------	336.3	84.4	46	----------	1,167.5	118.4
19	----------	361.8	85.3	48	----------	1,249.3	120.3
20	----------	387.4	86.2	50	----------	1,332.0	122.1
21	----------	413.3	87.0	52	----------	1,415.4	123.8
22	----------	439.4	87.8	54	----------	1,499.7	125.5
23	----------	465.7	88.5	56	----------	1,584.8	127.0
24	----------	492.2	89.2	58	----------	1,670.8	128.6
25	----------	518.8	90.1	60	----------	1,757.6	130.1

Table of Maximum Moments, Shears and Reactions Simple Spans,

One Lane **With** Dynamic Load Allowance

AND the Magnification Factor for the **Louisiana Bridge Design (LADV-11)**

Use for AASHTO Strength Condition I instead of HL-93 Values

Span (ft)		Moment (kips-ft)	End Shear and End Reaction (k)	Span (ft)		Moment (kips-ft)	End Shear and End Reaction (k)
62	----------	1,845.2	131.6	160	----------	7,157.8	183.8
64	----------	1,933.6	133.0	170	----------	7,812.2	188.4
66	----------	2,022.9	134.3	180	----------	8,487.4	192.9
68	----------	2,113.0	135.7	190	----------	9,183.5	197.5
70	----------	2,204.0	137.0	200	----------	9,900.3	201.9
72	----------	2,295.8	138.3	210	----------	10,637.9	206.3
74	----------	2,388.4	139.6	220	----------	11,396.3	210.7
76	----------	2,481.9	140.8	230	----------	12,175.6	215.1
78	----------	2,576.2	142.0	240	----------	12,975.6	219.4
80	----------	2,671.2	143.3	250	----------	13,708.0	222.4
82	----------	2,767.2	144.4	260	----------	14,450.3	225.2
84	----------	2,864.0	145.6	270	----------	15,202.4	228.0
86	----------	2,961.6	146.8	280	----------	15,963.5	230.8
88	----------	3,060.0	147.9	290	----------	16,733.6	233.4
90	----------	3,159.3	149.0	300	----------	17,512.0	236.0
92	----------	3,259.4	150.1	350	----------	21,516.3	248.0
94	----------	3,360.3	151.2	400	----------	25,670.9	258.4
96	----------	3,462.1	152.3	450	----------	29,925.7	267.5
98	----------	3,564.7	153.4	500	----------	34,230.8	275.1
100	----------	3,668.1	154.4	550	----------	38,536.1	281.4
110	----------	4,197.7	159.6	600	----------	42,791.6	286.3
120	----------	4,748.1	164.7	700	----------	55,585.6	318.5
130	----------	5,319.3	169.7	800	----------	69,979.6	350.6
140	----------	5,911.4	174.5	900	----------	85,973.6	382.8
150	----------	6,524.2	179.1	1000	----------	103,567.6	414.9

APPENDIX B: DATA FILES ASSOCIATED WITH FIGURES AND TABLES

FIGURES [1,2] (see page vii for location of the figure in text)

Figure 5-3	Appendix C. Max Moment Location Calculations
Figure 5-4	Appendix C. Max Moment Location Calculations
Figure 5-5	Appendix C. Max Moment Location Calculations
Figure 5-6	Appendix C. Max Moment Location Calculations
Figure 5-7	Appendix C. Max Moment Location Calculations
Figure 5-8	Appendix C. Max Moment Location Calculations
Figure 5-9	Appendix C. Max Moment Location Calculations
Figure 5-10	Appendix C. Max Moment Location Calculations
Figure 5-11	Appendix D. STANAG vs. Calculations Comparison.xlsx
Figure 5-12	Appendix D. STANAG vs. Calculations Comparison.xlsx
Figure 5-13	Appendix D. STANAG vs. Calculations Comparison.xlsx
Figure 5-14	Appendix D. STANAG vs. Calculations Comparison.xlsx
Figure 5-15	Appendix D. STANAG vs. Calculations Comparison.xlsx
Figure 5-16	Appendix D. STANAG vs. Calculations Comparison.xlsx
Figure 5-17	Appendix D. STANAG vs. Calculations Comparison.xlsx
Figure 5-18	Appendix E. Axle at Midspan Calculations.xlsx
Figure 5-19	Appendix E. Axle at Midspan Calculations.xlsx
Figure 5-20	Appendix E. Axle at Midspan Calculations.xlsx
Figure 5-21	Appendix E. Axle at Midspan Calculations.xlsx
Figure 5-22	Appendix F. Various HET Vehicles.xlsx
Figure 5-23	Appendix F. Various HET Vehicles.xlsx
Figure 5-24	Appendix F. Various HET Vehicles.xlsx
Figure 5-25	Appendix F. Various HET Vehicles.xlsx
Figure 5-26	Appendix E. Axle at Midspan Calculations.xlsx
Figure 5-27	Appendix E. Axle at Midspan Calculations.xlsx
Figure 5-28	Appendix E. Axle at Midspan Calculations.xlsx
Figure 5-29	Appendix G. Multiple MLC100W Vehicles Single Span.xlsx
Figure 5-30	Appendix G. Multiple MLC100W Vehicles Single Span.xlsx
Figure 5-31	Appendix G. Multiple MLC100W Vehicles Single Span.xlsx
Figure 5-32	Appendix E. Axle at Midspan Calculations.xlsx
Figure 5-33	Appendix E. Axle at Midspan Calculations.xlsx
Figure 5-34	Appendix E. Axle at Midspan Calculations.xlsx
Figure 5-35	Appendix E. Axle at Midspan Calculations.xlsx
Figure 5-36	Appendix E. Axle at Midspan Calculations.xlsx
Figure 5-37	Appendix E. Axle at Midspan Calculations.xlsx
Figure 5-38	Appendix E. Axle at Midspan Calculations.xlsx
Figure 5-39	Appendix E. Axle at Midspan Calculations.xlsx
Figure 5-40	Appendix E. Axle at Midspan Calculations.xlsx
Figure 5-41	Appendix E. Axle at Midspan Calculations.xlsx
Figure 5-42	Appendix E. Axle at Midspan Calculations.xlsx

Figure 5-43	Appendix E. Axle at Midspan Calculations.xlsx
Figure 6-4	Appendix I. Reliability Analysis.xlsx
Figure 6-5	Appendix I. Reliability Analysis.xlsx
Figure 6-6	Appendix I. Reliability Analysis.xlsx
Figure 6-7	Appendix I. Reliability Analysis.xlsx
Figure 6-8	Appendix I. Reliability Analysis.xlsx
Figure 6-9	Appendix I. Reliability Analysis.xlsx
Figure 6-10	Appendix I. Reliability Analysis.xlsx
Figure 6-11	Appendix I. Reliability Analysis.xlsx
Figure 6-12	Appendix I. Reliability Analysis.xlsx
Figure 6-13	Appendix I. Reliability Analysis.xlsx
Figure 6-14	Appendix I. Reliability Analysis.xlsx
Figure 6-15	Appendix I. Reliability Analysis.xlsx
Figure 6-16	Appendix I. Reliability Analysis.xlsx
Figure 6-17	Appendix I. Reliability Analysis.xlsx
Figure 6-18	Appendix I. Reliability Analysis.xlsx
Figure 6-19	Appendix I. Reliability Analysis.xlsx
Figure 6-20	Appendix I. Reliability Analysis.xlsx
Figure 6-21	Appendix I. Reliability Analysis.xlsx
Figure 7-1	Appendix E. Axle at Midspan Calculations.xlsx
Figure 7-2	Appendix E. Axle at Midspan Calculations.xlsx
Figure 7-3	Appendix E. Axle at Midspan Calculations.xlsx
Figure 7-4	Appendix E. Axle at Midspan Calculations.xlsx

TABLES [2,3,4]

Table 5-1	Appendix C. Max Moment Location Calculations.xlsx
Table 5-2	Appendix C. Max Moment Location Calculations.xlsx
Table 5-3	Appendix C. Max Moment Location Calculations.xlsx
Table 5-4	Appendix D. STANAG vs. Calculations Comparison.xlsx Appendix E. Axle at Midspan Calculations.xlsx
Table 5-5	Appendix D. STANAG vs. Calculations Comparison.xlsx Appendix E. Axle at Midspan Calculations.xlsx
Table 5-6	Appendix E. Axle at Midspan Calculations.xlsx Appendix F. Various HET Vehicles.xlsx
Table 5-7	Appendix G. Multiple MLC100W Vehicles Single Span.xlsx
Table 5-8	Appendix G. Multiple MLC100W Vehicles Single Span.xlsx
Table 5-9	Appendix E. Axle at Midspan Calculations.xlsx Appendix G. Multiple MLC100W Vehicles Single Span.xlsx
Table 5-10	Appendix E. Axle at Midspan Calculations.xlsx Appendix H. Special Permit Vehicles.xlsx
Table 5-11	Appendix E. Axle at Midspan Calculations.xlsx Appendix H. Special Permit Vehicles.xlsx
Table 6-1	Appendix I. Reliability Analysis.xlsx
Table 7-1	Appendix E. Axle at Midspan Calculations.xlsx

B.1 APPENDIX B END NOTES

1. See page vii for location of the figure in text

2. All files names begin with prefix “WP Parker 2019 UNO MSCE”

3. See page xvii for location of the table in text

4. The source data for these tables was consolidated and formatted into the tables that are included in an Microsoft Excel 2013 file entitled “WP Parker 2019 UNO MSCE Appendix J. Consolidated Tables 5.1-5.11 and 7.1.”

APPENDIX C: MAXIMUM MOMENT CALCULATIONS

File Name: WP Parker 2019 UNO MSCE Appendix C. Max Moment Location Calculations

Contents (worksheets/tab names included in the Excel workbook are): Page

APPENDIX D: APPENDIX D: STANAG/FM VS. CALCULATIONS COMPARISON

File Name: WP Parker 2019 UNO MSCE Appendix D. STANAG vs. Calculations Comparison.xlsx

Contents (worksheets/tab names included in the Excel workbook are): Page

APPENDIX E: AXLE AT MIDSPAN CALCULATIONS

File Name: WP Parker 2019 UNO MSCE Appendix E. Axle at Midspan Calculations.xlsx

Contents (worksheets/tab names included in the Excel workbook are): Page

APPENDIX F: VARIOUS HEAVY EQUIPMENT TRANSPORT (HET) VEHICLES

File Name: WP Parker 2019 UNO MSCE Appendix F. Various HET Vehicles.xlsx

Contents (worksheets/tab names included in the Excel workbook are): Page

APPENDIX G: MULTIPLE MLC 100W VEHICLES ON A SINGLE SPAN

File Name: WP Parker 2019 UNO MSCE Appendix G. Multiple MLC100W Vehicles Single Span.xlsx

Contents (worksheets/tab names included in the Excel workbook are): Page

APPENDIX H: SPECIAL PERMIT VEHICLES CALCULATIONS

File Name: WP Parker 2019 UNO MSCE Appendix H. Special Permit Vehicles.xlsx

Contents (worksheets/tab names included in the Excel workbook are): Page

APPENDIX I: RELIABILITY ANALYSIS CALCULATIONS

File Name: WP Parker 2019 UNO MSCE Appendix I. Reliability Analysis.xlsx

Contents (worksheets/tab names included in the Excel workbook are): Page

APPENDIX J: CONSOLIDATED TABLES

File Name: WP Parker 2019 UNO MSCE Appendix J. Consolidated Tables 5.1-5.11 and 7.1.xlsx

Contents (worksheets/tab names included in the Excel workbook are): Page

VITA

Walter P. Parker was born in 1965 in Greenville, South Carolina., the son of Mr. and Mrs. Charles Larkin Dean Parker, Sr. He graduated from Wade Hampton High School in 1983, and from Clemson University with a Bachelor of Science degree in Mechanical Engineering in 1987. Following three years of employment as a Design Engineer at Newport News Shipbuilding, Mr. Parker volunteered for military service and was commissioned into the United States Marine Corps in December 1991. During an assignment to New Orleans in the mid-1990's, then Captain Parker enrolled in the Graduate Program in the College of Engineering at the University of New Orleans pursuing a degree of Master of Science in Engineering, but was unable to complete his degree due to re-assignment by the United States Marine Corps. In 2000, Captain Parker graduated from the University of Missouri-Rolla (now known as the Missouri University of Science and Technology) with a Master of Science degree in Engineering Management. In 2011, Major Parker retired from the military following twenty years of active duty service as a combat engineer officer, including the command of Engineer Support Company, 7th Engineer Support Battalion and two combat tours in Iraq. In 2011, Mr. Parker returned to the Graduate Program at the University of New Orleans, and has been engaged in continued studies since that time. Mr. Parker is a licensed professional engineer in the State of Louisiana and a member of the Tau Beta Pi engineering honor society, the Golden Key international honour society, and the American Society of Civil Engineers. He is married to the former Ms. Elizabeth L. Reynaud of New Orleans, Louisiana.